THE ROLE OF VOLATILE SPECIES IN THE SOFTENING OF BLAST FURNACE BURDEN

by

Mohamed Mohamed Abo El Saadat, B.Sc M.Sc

Thesis submitted to the Council for National Academic Awards for the Degree of Doctor of Philosophy. Sponsored by Sheffield City Polytechnic in collaboration with British Steel Corporation, Scunthorpe.

March 1979

PREFACE

This thesis is submitted for the degree of Doctor of Philosophy of the Council for National Academic Awards, the research work described having been carried out in the Metallurgy Department of Sheffield City Polytechnic. No part of the work described has ever been submitted for the award of any other degree.

In addition to the research, the following Courses were attended:

(1) Process Metallurgy

(2) Advanced Thermodynamics

(3) Numerical Methods and Programming

The author is indebted to Dr.A.W.D.Hills and Dr.R.Acheson for their supervision.

Sincere thanks to Mr.E.W.Nixon of the British Steel Corporation for his valuable discussion from time to time.

The personal recommendations and friendly advice of Dr.G.Briggs are also gratefully acknowledged.

From time to time the author received a great deal of support, both technical and personal from his research colleagues and from Technical Officers of the Polytechnic. It is not possible to list all the names but sincere thanks are expressed to each of them especially to Mr.D.Latimer and Mr.B.Lewis for their ever ready support.

Abo. Saadat

March 1979

SYNOPSIS

Considerable controversy exists concerning the mechanism involved in the softening of the burden within the iron blast furnace and in particular the role played by volatile species in this process. This laboratory investigation was undertaken in order to develop a better understanding of the fundamental processes involved in the softening of the iron bearing components of the blast furnace burden and in particular the contribution of sulphur and alkali metal vapours in this process.

The experimental technique developed involved the encapsulation of the test material inside a sealed silica tube containing a gas phase of known composition. The test material was moulded into the form of a Seger cone and the behaviour of the cone at elevated temperatures was used to monitor the softening of the material. This technique was used to study the effect of sulphur and alkali metals on the softening behaviour of both chemical reagents and a commercial iron ore. High temperature observation of the cones was supplemented by optical and scanning electron microscopy after testing.

The results showed that the softening behaviour of the ferrous constituents of the blast furnace burden was influenced by the mass fraction of liquid formed within the sample and by the viscosity of this liquid. Vapour borne sulphur plays an important role in the softening process in the blast furnace through the formation of ferrous sulphide which melts and acts as a lubricant between the solid particles and the more viscous liquid oxide mixtures formed. Alkalis play a less important role in the chemistry of softening in the blast furnace and they may delay softening at low oxygen potentials.

C O N T E N T S

The softening behaviour of the burden inside the shaft of the blast furnace is of equal importance to its reducibility. It is generally considered that a high softening start temperature and a restricted range of sticky fusion are favourable, because, on the one hand, they depress to the lower part of the bosh level the position at which the material begins to melt and, on the other, they accelerate the transition from sticky to fluid melting. With these conditions, the pressure drop in the bosh is lowered and risks of hanging are decreased, resulting in smooth operation of the furnace and yielding iron of consistent composition.

The softening of the burden materials is closely related to the behaviour of these multiphase solids at their liquidus temperature under the specified gas phase conditions existing within the blast furnace. Several authors have already attempted to develop laboratory softening tests and have studied some of the factors affecting softening. The influence of the nature of the gangue, the degree of reduction and the effect of some physical properties of the ore have been studied. Unfortunately, the conclusions reached are not always entirely consistent and numerous problems are still being encountered. As there is a considerable conflict both with respect to the data and the theory describing the mechanisms and rate controlling steps of burden softening in the iron blast furnace it was decided that a major investigation into the fundamental mechanisms involved was required.

2.1 The Blast Furnace Process

2.1.1 Introduction

Figure 2-1 shows a cross sectional view of a typical blast furnace.

The top and bottom sections of the blast furnace are cylindrical. The bottom section is an inverted frustrum of a cone of quite rapid outward angle, and this in turn is surmounted by a frustrum of an upright cone of a much slower inward convergent angle. This shape has been adopted since it gives a uniform ascent velocity to the gases in the furnace.

Iron ore, after suitable preparation, and coke are charged into the furnace by a double bell and hopper system. Air, pre-heated to about 1000^{o}C, is blown into the lower part of the furnace through a number of tuyeres at a gauge pressure of about 2.4 atmospheres. In the race way in front of the tuyeres, carbon monoxide is formed by combustion with coke. Thus iron ore and coke pass downwards counter-current to a stream of hot reducing gases. In the upper part of the furnace, counter-current heat and mass transfer occur, whilst in the lower part reduction is completed and the gangue and added fluxes react to form slag. Both slag and iron melt and form separate layers in the well below the tuyere level, from which they are periodically tapped by opening the slag and metal tap-holes. In this way the blast furnace performs the functions of

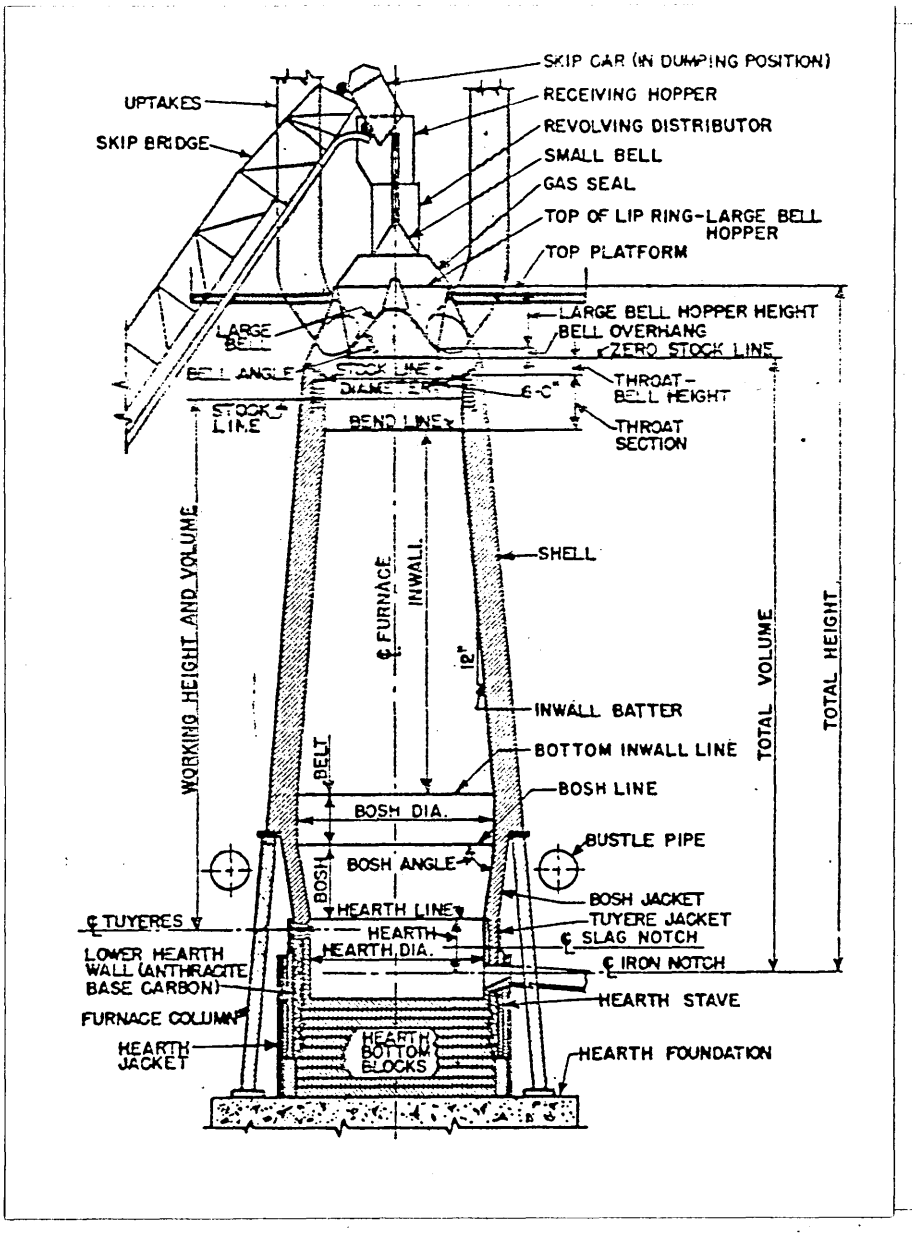

Figure 2-1: A cross sectional view of a typical blast furnace.

gas producer as well as of a high and low temperature reducer. The spent gases are collected from the top of the furnace by off-takes and are cleaned. Part of the gas is used to pre-heat the air for the furnace and the remainder is used as a fuel around the steel works.

From an energy view point a consumption of 370 kg of coke per tonne of molten metal is a normal figure in advanced practices. In order to be competitive, a direct reduction process would have to produce iron at 50% of the cost of iron produced by the blast furnace route[1], since the product in this case is a solid.

Clearly in the foreseeable future, the blast furnace will continue to be the most efficient method for iron making. For producing 15,000 tonnes of hot metal per day, the blast furnace has no competitors.

Eketorp[1] has compared the energy required for steel making via different methods and concludes that the smelting - reduction alternative is the only method which can achieve lower figures for energy requirements after the blast furnace - basic oxygen furnace route. But, so far, the difficult problem of heating a reducing bed or bath without at the same time oxidising it has not been solved technically, so the smelting reduction process is still not applicable on an industrial scale.

2.1.2 Temperature Gradients in the Blast Furnace

The upward stream of blast furnace gases leave the race way at about 2000°C but the spent gases leave the furnace with a temperature of about 200°C. The temperature isotherms through a section of the furnace are shown in Figure 2-2.

The shape and the distribution of the temperature contour lines differ from one blast furnace to another. They are closely related to the permeability of the blast furnace charge column. In spite of the enormous efforts made to obtain a uniform burden distribution by using automatic charging equipment, probing the gas composition and temperature, the use of movable armour, the use of models to simulate the conditions in the blast furnace and the use of a movable chute instead of the bell, temperature gradients with variations across the furnace still occur.

Sarkisyants[2] has estimated that over the entire height of the blast furnace the average difference in temperature between the gas and the burden is roughly 300°C.

Kitaev[3] observed that the thermal capacity of the flowing gas does not vary over the height of the furnace. Considerable changes do, however, occur in the thermal capacity

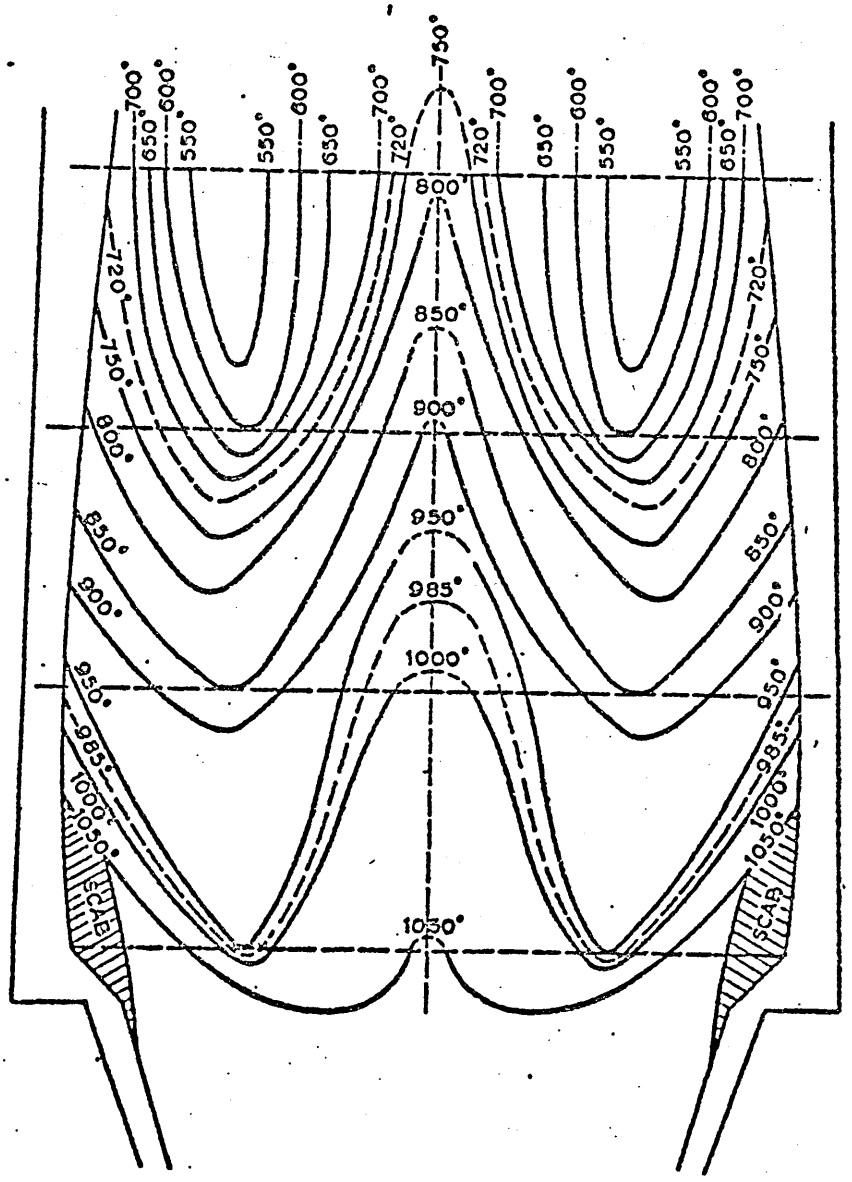

Figure 2-2: Temperature isotherms in a blast furnace.

of the burden. He[3] noted that in the upper part of the shaft - the ratio of the thermal capacity of the burden to that of the gases fluctuated around 0.8. In the lower part of the furnace, the bosh, the ratio of the thermal capacity of the burden to that of the gases increased up to a value of 3.2. The rate of heat transfer from the gas to the burden therefore decreased with distance from the throat to the centre of the stack and also with distance from the hearth to the centre of the stack. Thus the maximum gas-burden temperature difference is at the tuyeres and is about 400-500°C, the next largest is at the stock line about 200°C, and the smallest difference is in the stack, 10-20°C.

In the opinion of Lazarev, et al.[4] the lower heat exchange zone in the blast furnace consists of two parts, as shown in Figure 2-3;

(i) An upper region where direct reduction processes occur - the apparent thermal capacity of the charge, C_{ch}, becoming greater than that of the gas, C_g.

(ii) A lower region where the amount of unreduced iron decreases and C_{ch}/C_g ratio can change, becoming in certain cases less than unity.

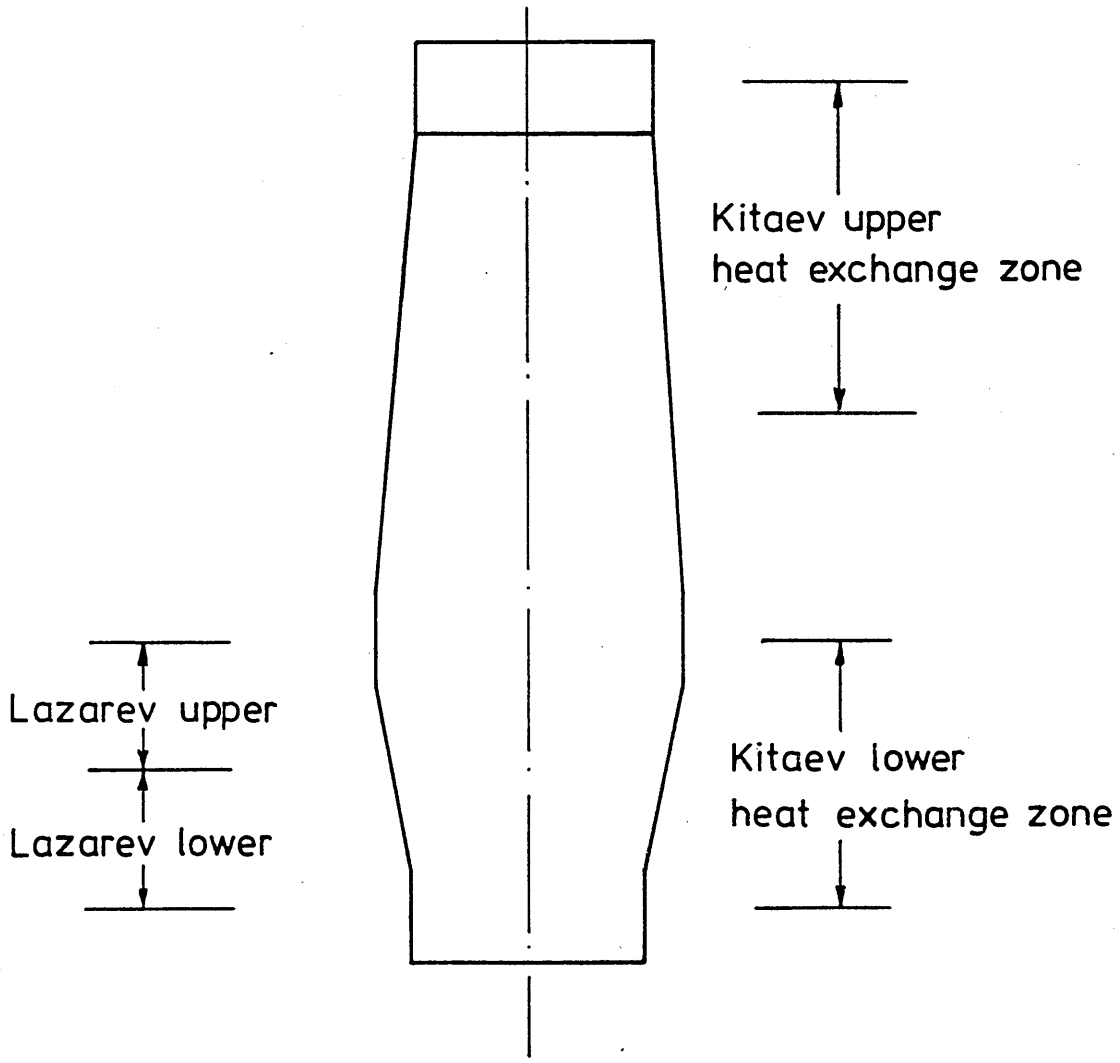

FIG.2-3 Heat exchange phenomena in blast furnace

Laventrev, et al.[5] explained the existence of the latter of these heat exchange regions in the lower half of the furnace by the evolution of a large quantity of heat arising from the reoxidation of pig iron in the oxidizing zone of the furnace. This results in a considerable decrease in the apparent thermal capacity of the charge. They[5] related the existence of the second part of the lower heat exchange zone in the blast furnace, in which the molten products heat up quickly and reach a temperature 100-200°C below that of the combustion zone, to the basis of the theory that each heat exchange step has a characteristic value of C_{ch}/C_g ratio, determined by the laws governing blast furnace operation at different levels.

2.1.3 The Isothermal Zone in the Blast Furnace

Kitaev[3] has reported the existence of an isothermal zone in the blast furnace stack, with a temperature difference between the ascending gas and descending charge of only 20°C. Measurements on experimental[3] and large blast furnaces have shown that a characteristic temperature profile exists over the height of the furnace as shown in Figure 2-4. The temperature along a given vertical column within the blast furnace stack is nearly constant over a substantial height.

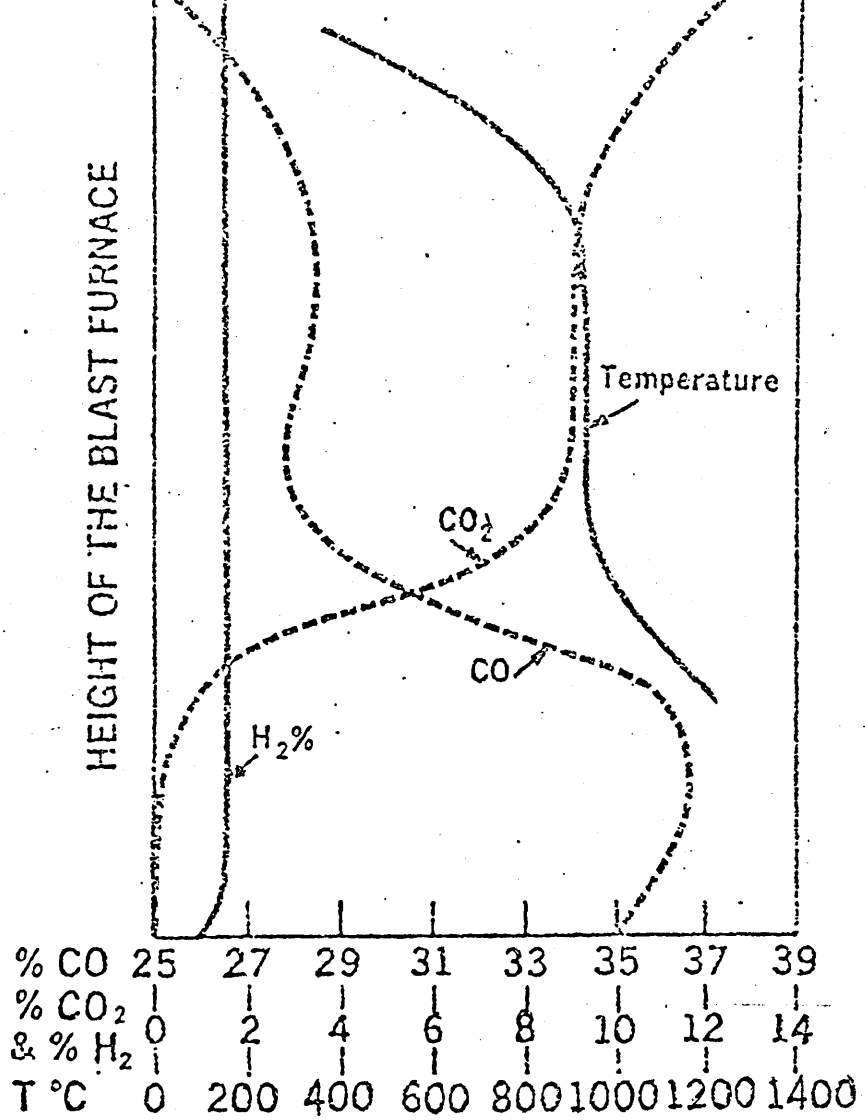

Figure 2-4: Variation of temperature and composition of gases over the height of a blast furnace, (after Kitaev[3]).

Poos[6] has reported that in the thermal reserve zone the temperature of the gas and the burden are substantially equal. He[6] claimed that most of the indirect reduction of iron oxides by carbon monoxide took place in this zone and that although reactions were slightly exothermic, the heat produced was only just sufficient to compensate that lost through the walls of the furnace.

Meyer, et al.[7] reported the existence of a zone of small temperature difference between the gas and the solids giving rise to the "pinch point" on the Reichardt diagram[8]. They[7] also suggested that the indirect reduction that took place had little thermal effect on the system and that contrary to earlier suggestions, the carbon deposition reaction did not occur to any appreciable extent.

Kanbara, et al.[9] reported the existence of a thermal reserve zone and attributed it to the attainment of a balance between the exothermic reduction of FeO to metallic iron and the endothermic carbon solution reaction between 1000-1100^{o}C.

Apasin, et al.[10] have reported the existence of a critical zone, which governs the coke consumption in the blast furnace in the temperature range 900-1000^{o}C. This zone was characterized by slow heat exchange between the charge and the furnace gases. They[10] defined the distinguishing

features of the isothermal zone as being constancy of temperature, or the existence of a gradient of not more than 10 degrees per metre of height, and the existence of a CO_2/CO ratio close to equilibrium for the reduction of ferrous-oxide by carbon monoxide at the corresponding temperature.

Girard, et al.[11] have observed the existence of a thermal reserve zone extensive enough to keep the burden materials at a constant temperature for time periods well in excess of two hours. In such time periods, temperatures and chemical composition even at high driving rates come to equilibrium.

Loginovita[12] observed that at temperatures in the range 800-900°C, there was no change in the FeO content of the charge. He[12] suggested that the rate of formation of ferrous oxide by the reduction of higher oxides was the same as the rate of reduction of ferrous oxide to iron in this zone of the furnace.

Hills[13] has suggested that softening of the burden begins in the isothermal zone. As the melting process causes the effective specific heat capacity of the burden to increase, so the burden temperature in the bosh changes much more slowly than the gas temperature. In the stack, however,

it is the burden temperature that changes more rapidly. The gas and burden temperature must thus approach very closely to each other between the two regions, reducing the driving force for heat transfer and giving rise to a plateau in the temperature profile within the furnace. He[13] concluded that melting starts at this temperature plateau.

2.1.4 Thermodynamic Considerations

The iron oxide in ores may be present either as hematite (Fe_2O_3) or magnetite (Fe_3O_4) or limonite, goethite and hydrogoethite (hydrated hematites). In a reducing atmosphere the removal of oxygen from the oxide takes place either by the sequence:

$$Fe_2O_3 \rightarrow Fe_3O_4 \rightarrow Fe \quad \text{below } 570^{\circ}C$$

or

$$Fe_2O_3 \rightarrow Fe_3O_4 \rightarrow FeO \rightarrow Fe$$

at temperatures above 570°C at which wustite (Fe_xO, where $x = 0.95$) is the stable reduced oxide phase. Darken and Gurry[14] have established the equilibrium diagram for the iron-oxygen-carbon system at one atmosphere pressure as shown in Figure 2-5a. Dotted lines indicate metastable equilibria. Similar equilibrium diagrams have been[14] established between iron-oxygen and hydrogen as shown in Figure 2-5b. The iron may be considered to exist in a

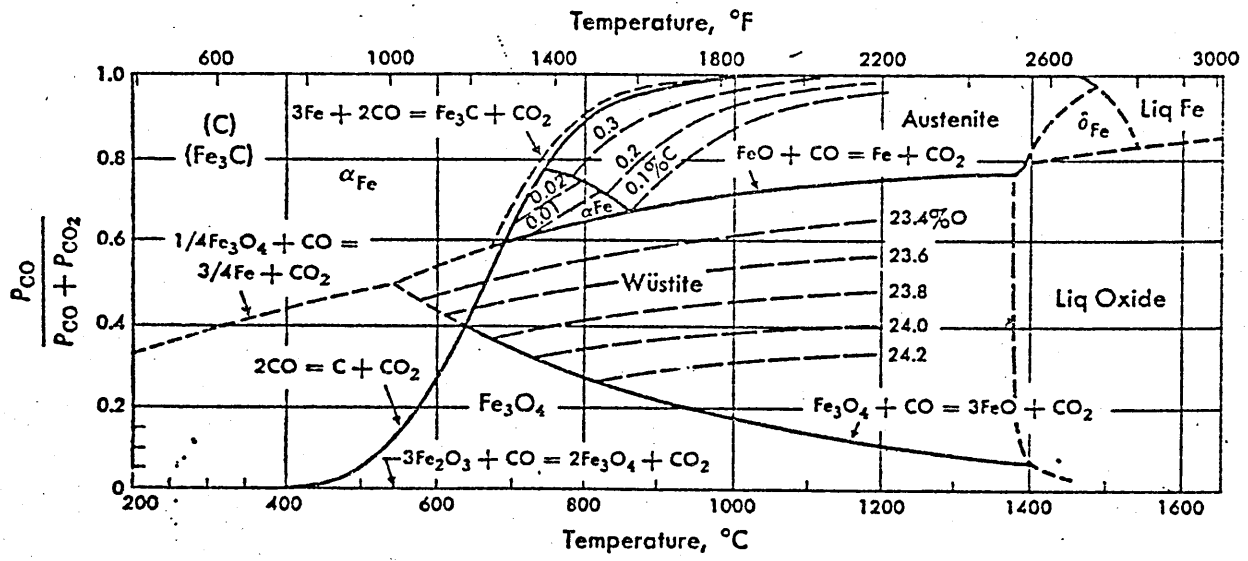

Figure 2-5a: Equilibrium of iron-oxygen-carbon system at 1 atmosphere.

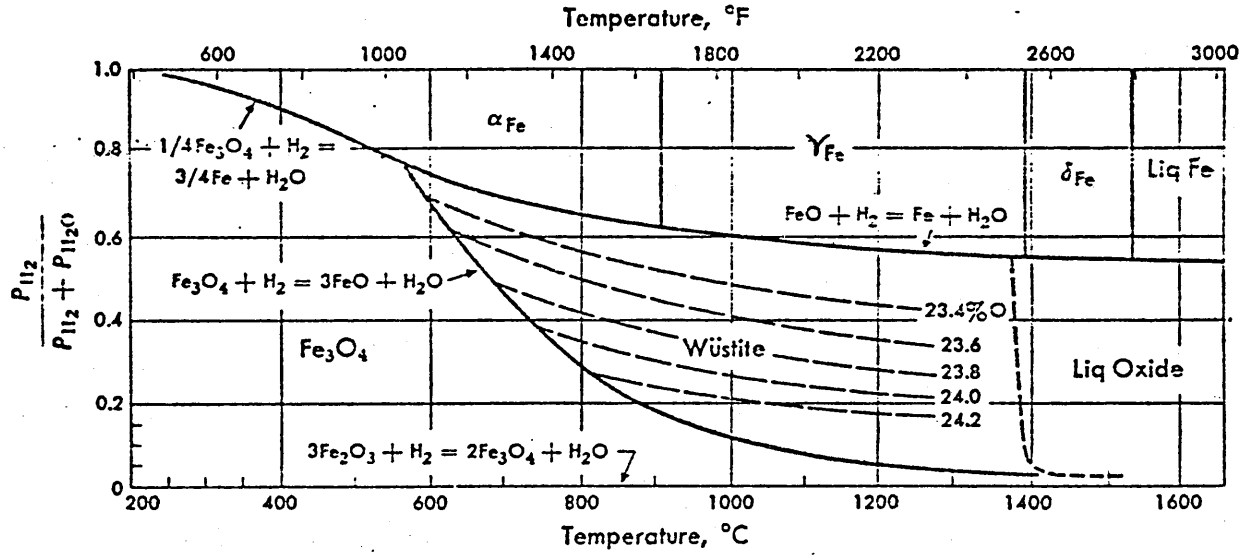

Figure 2-5b. Equilibrium of iron-oxygen-hydrogen system at 1 atmosphere.

substantially pure state, as the solubility of hydrogen in iron at ordinary pressures is negligibly small. In the blast furnace both H_2 and CO act as a reducing gas, so the P_{CO}/P_{CO_2} equilibrium with the solid phase must be considered in conjunction with the equilibrium with a definite composition of H_2-H_2O in the gas phase according to the water-gas reaction:

$$CO_2 + H_2 = CO + H_2O$$

Also two other reactions may take place

$$2CO + 2H_2 = CO_2 + CH_4$$

$$C + 2H_2 = CH_4$$

2.1.5 The Bosh Region of the Blast Furnace

The bosh zone of the blast furnace is the region where the highest temperatures and steepest temperature gradients prevail, and the most rapid changes in the physical state of materials take place. The physical conditions inside this part of the furnace render it very difficult to insert and maintain probes for direct observations.

The gases CO and CO_2 are the primary products of the heterogeneous reaction between carbon and oxygen in front of the tuyeres. The ratio of CO to CO_2 increases quickly with rising temperature. It is thought that the nature of the carbon surface may also affect the CO to CO_2 ratio.

Thermodynamic considerations indicate that the bosh gases are not comprised solely of CO, CO_2, H_2 and N_2. The currently accepted data lead to the prediction that there are significant partial pressures of S, K, Na, CS, CS_2, P, COS, Mn, Cr, Fe, SiO and Si. The partial pressures of all these evaporating species varies through the height of the bosh, all of them trying to establish equilibrium with the solids present, despite the very high speed of the gas column flow. Supporting this view, Richardson and Jeffes[15] in their excellent work on the topic, reported that the phosphorus pentoxide in the slag was reduced in the bosh by the coke or by CO in the gas to produce phosphorus vapour. This vapour then dissolved in the iron in a cooler region of the furnace. Also, Decker, et al.[16] claimed that silicon monoxide could form during the combustion of coke and be further reduced to silicon either by the CO in the gas or by the carbon in the melt. Tsuchiya, et al.[17] studied the distribution of Si, Mn and C in a quenched blast furnace and reported that the silicon content in molten iron began to increase rapidly from the upper or middle level of the bosh, reaching a value of about 3 mass % at the tuyere level. They found that the position of peak Mn content was slightly lower than that for silicon. They[17] also concluded that Si was transferred to the metal by a gas metal reaction.

2.2 The Softening Behaviour of Iron Bearing Minerals in the Blast Furnace Charge

2.2.1 Methods for Determining the Softening Behaviour of Different Iron Bearing Materials

Kortmann, et al[18], have investigated the softening of pellets in a cylindrical furnace equipped with a pressure ram for applying a mechanical load, at the start of the test, to a known mass of the pellets to be tested. The pellets were heated in a neutral atmosphere according to a well defined temperature programme up to 1050°C. After that the sample was reduced by a gas mixture of 40 parts CO and 60 parts N_2 by volume. During the course of the test, the loss of mass of the sample, the pressure drop across the bed, and the change in height of the sample were continuously recorded. The pressure drop across the pellet bed at constant gas flow provided a measure of the behaviour of pellets during reduction.

Burghardt and Grebe[19] in their work described a method for determining the softening temperature of different forms of iron bearing feed. The technique was based on the fact that disintegration or early plastic deformation and softening of a charge must lead to compaction in a predetermined space and hence produced a change in the pressure difference across the charge.

The C.N.R.M. laboratories[20] have developed an apparatus in

which material of known state of reduction is packed into a heat resistant steel crucible, which is placed inside an electric furnace under a given pressure. The test materials are heated in a neutral atmosphere according to a well-defined temperature programme. The softening start and finish temperatures are conventionally defined as those corresponding to shrinkages of 3 and 25% respectively, of the initial height of the specimen.

Nakamura, et al.[21] measured the deformation of various iron bearing constituents of the blast furnace burden by a creep test at elevated temperatures. They[21] applied a correlation between the deformation and the apparent viscosity of various blast furnace iron bearing burdens at the softening temperatures.

2.2.2 Experimental Observation

The softening behaviour of the burden materials varies as a result of both the intrinsic differences in the characteristics of the materials involved and also as a result of changes taking place during reduction. The temperature interval between the start of plastic deformation and the onset of softening can also vary from burden to burden. The softening range determines the extent of plastic deformation of the compacted burden layers in the blast furnace and hence influences the gas penetration of the burden column of the blast furnace. A wide softening temperature

range increases the pressure drop in the bosh region, so the risks of hanging are increased, resulting in irregular descent of the burden with frequent slipping, causing unreduced burden to reach the hearth well. The net result will be fluctuation in the physical and chemical state of the pig iron produced, lower pig iron production and higher coke rate. A similar effect can occur when the ferrous constituents of the burden have a low softening temperature, which causes the formation of the sticky zone at a higher level in the furnace.

The temperature at which plastic deformation starts is a function of the degree of reduction. Potebnya, et al[22] has shown that the progressive reduction of ferruginous minerals to wustite, at varying degrees of reduction from 10% to 30%, lowers the initial softening temperature. Replacement of wustite by metallic iron at degrees of reduction from 30% to 70% did not affect the softening behaviour, but at greater than about 70% reduction a lowering of the initial softening temperature was observed due to a rapid increase in the plasticity of the metallic shell.

Lecomte, et al[23] investigated the factors affecting the softening start (T_1) and finish (T_2) temperatures of sinters, and established the following relationships:

$$T_1 = 685 + 1.23 \text{ Mass Fe} + 280 \frac{\text{at.O}}{\text{at.Fe}} + 70.3 \frac{\text{Mass CaO}}{\text{Mass SiO}_2}$$

$$T_2 = 733 + 299 \frac{\text{at.O}}{\text{at.Fe}} + 91.5 \frac{\text{Mass CaO}}{\text{Mass SiO}_2}$$

Where T_1 and T_2 in ^{o}C are those corresponding to shrinkages of 3 and 25% of the initial height of the tested sample and the ratio at. O to at. Fe is the initial state of sinter oxidation. Lecomte, et al[23] also established a relationship between the degree of reduction, P, expressed as a percentage, corresponding to the minimum softening temperature for a particular sinter and the total iron content of the sinter expressed as a mass fraction.

$$P = 162.4 - 2.01 \text{ (Mass fraction Fe)}$$

Some workers[24,25,26] studying the softening temperature as a function of the degree of reduction, R, have noted that for some types of burden constituent the softening temperature is practically independent of the degree of reduction. For other types the softening temperature decreased rather sharply as the degree of reduction increased and reached a minimum value for reductions ranging from 35 to 70%.

For sinter, it is considered that the phase composition and texture and microstructural features have a substantial effect on the initial softening temperature. Potebnya et al[22] have investigated the structural transformations of

sinter during softening and related these to the degree of reduction. They[22] claimed that the initial softening temperature of unreduced or slightly reduced (up to 10%) sinters was governed by the softening temperature of the glass, the silicate phases, the monocalcium ferrite and the low melting point eutectics which were present along the periphery of sinter fragments. On increasing the degree of reduction there were changes in the qualitative and quantitative relationship between the phases present and the softening temperature.

For iron ores[27] the structure of the gangue including its porosity and its texture may play a role, in addition to the overall effect of chemical composition of the softening behaviour.

For pellets the softening behaviour is affected by the phases present and the extent of swelling. Heinrich/Kortman et al.[18] claimed that pellet strength could be adversely affected by loosening of the grain structure due to swelling as well as plastic deformation of the constituents forming the pellets.

2.3 Softening in the Blast Furnace

According to the work of Kanfer, et al.[28] the softened masses first appear in the zone of existence of wustite and metallic iron in the blast furnace. This zone appears after the disappearance of magnetite.

Orlov, et al.[29] observed that softened masses appeared in quantities of 6-12 mass %, together with up to 5 mass % of slag in samples removed from the bosh parallel, mainly in the peripheral and axial zones.

Balon, et al[30] claimed that the region of sintered and softened materials stretch from the middle of the stack to the bosh. At the furnace walls it finishes near the bosh parallel, in the intermediate zone it finishes near the bottom of the bosh, and in the central zone it finishes near the blast tuyeres region.

Kanfer, et al.[28] concluded that the appearance of softened masses started in the peripheral zone at 70% reduction, in the central zone at 95% reduction, and in the intermediate zone at 38% reduction. Also according to them[28] the appearance of the softening masses started at the 1100°C isothermal line, and this was followed by the appearance of pseudo-wollastonite slags at the 1250°C isothermal line.

Kanbara, et al.[9] stated that the ore layers which were in the temperature range between the start of softening and melting down formed the softening-melting zone in the blast furnace. Accordingly, their structure changed continuously from that of the ores to a semi molten state where the metal and slag phases began to separate from each other. They[9] added that the softening-melting layers were uniformly distributed corresponding to the temperature profile in the furnace, and their formation was around 1100°C.

Sasaki, et al.[31] defined the softening-melting layer as an iron ore layer which started with light sintering of considerably reduced iron ore granules and ended with the formation of liquid phases which trickled down through the bed. Figure 2-6 is taken from the work of Sasaki, et al.[31] and shows the structure of the softening-melting layers. Below the half-molten portion, the metallic iron extends like hollow "icicles" into the voids in the coke layer, small slag droplets remaining on the inner and outer surfaces of the "icicles".

Nekrasov, et al.[32] have investigated the reduction processes in the stack of the blast furnace and have reported that, at the middle of the stack only solid materials were found. Softened material was found in amounts of about 10 mass %, only in samples taken from the central part of the furnace, where

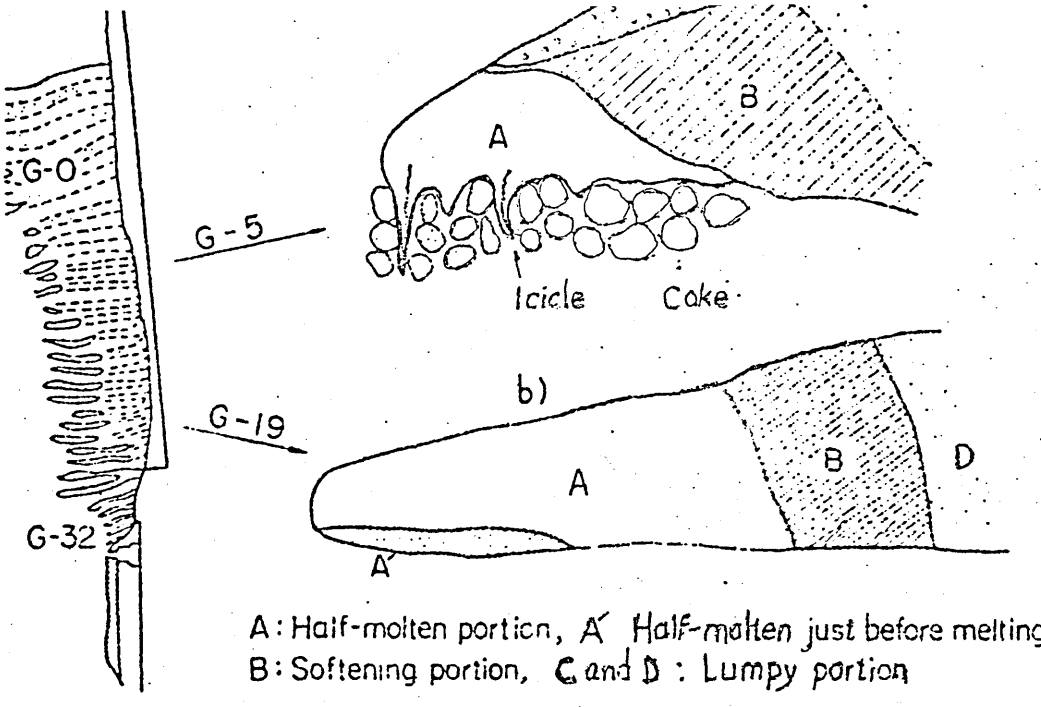

Figure 2-6a The structure of softening-melting layer in a blast furnace (after Sasaki[31]).

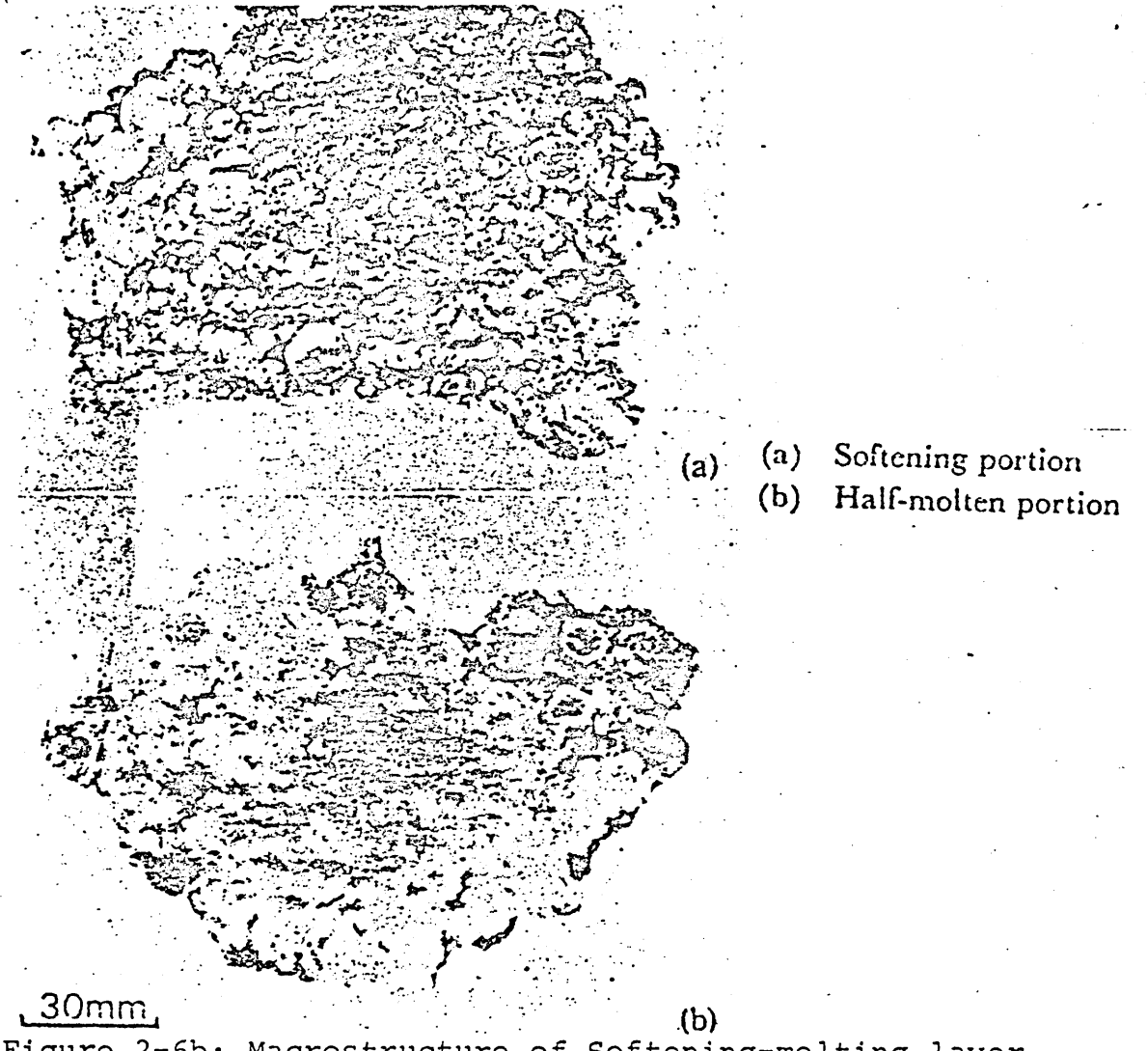

Figure 2-6b: Macrostructure of Softening-melting layer. (after Sasaki[31]).

the temperature exceeded 1000°C. Very small quantities of metal and slag were found at the lowest level of the stack and softened material reached 20 mass % in some of the samples. In the bosh parallel the softened materials started to decrease while the slag and metal in the sample taken reached 16 mass %.

2.4 Primary Slag

2.4.1 Primary Slag Formation

According to Balon, et al.[30] the first slag and metal appears in the middle of the stack. It is believed that the primary slag is more basic, has a higher-melting point, and is more viscous than hearth slags. Some workers[27] claim that primary slag formation begins with the fusion of clay minerals or other low melting point compounds present in the gangue of the ferrous component in the burden or as impurities in the limestone.

Orlov, et al.[29], as a result of their investigation of the smelting process in a blast furnace of 2000 m^3 capacity, claimed that the formation of the primary slag was preceded by the formation of sintered masses from fine fractions (1.00 - < 1.0mm) of partly reduced sinter and coke.

Luganin and Lugania[33] have put forward a different mechanism for the formation of primary slag. They[33] consider the primary slags to be formed by the action of double carbonates. For each per cent of K_2O and Na_2O, 2.5% and 3.3% respectively of double carbonates can form; enough to impregnate the whole charge. The double carbonates melt at 780-800^oC and the melt can dissolve quartz and hematite to form alkali metal silicates and ferrites. The presence of molten double carbon-

and the nature of dissolved impurities since they normally decompose at a temperature of 800-820°C.

Muravev, et al.[34] carried out a petrographic investigation of slag taken from a nitrogen quenched blast furnace, and reported[34] that slag in the sintered and softened charge was present mainly in the form of local centres inside it, or in the form of various precipitates (drops, slivers, hollow bubbles) on its surface. Later, separation of slag and metallic melt occurred. They[34] concluded that the primary slags formed at 1100-1200°C from the silicate binder in the sinter and pellets and the gangue in the iron and manganese ore.

Other workers[35] have reported that droplets of molten coke ash entrained by the rising bosh gas may play a significant role by attaching themselves to either gangue or lime. Silica or lime, as the case may be, will then dissolve in the liquid phase.

It can be concluded that after the formation of a pasty mass, the formation of the primary slag starts. The primary slag formation starts first at the periphery of the middle zone of the stack. As the high temperatures extend towards the furnace axis, the region where slag formation starts broadens. In the lower part of the stack it already embraced not only the peripheral but also the intermediate zone, and in the bosh the central zone as well.

2.4.2 Primary Slag Composition

According to Balon, et al[30] the first slags appearing in the middle of the stack (peripheral zone), have a composition mainly of $(Fe_{1-x}\ Ca_x)\ Si\ O_4$. This primary slag also contained wustite, in the form of residual solid inclusions of the ore components in the free form, together with smaller quantities of melilite [a continuous solid solution of $Ca_2\ Mg\ Si_2\ O_7$, $Ca_2Al\ (Si, Al)\ O_7$] and wollastonite $[Ca_{1-x}(Fe,Mn)_x]\ Si\ O_3$ of variable composition $(x = 0.0 - 0.2)$.

Muravev, et al[34] have reported that the primary slags in the blast furnace are derived from the melting and decomposition of the gangue minerals of the sinter, pellets and manganese and iron ores. The primary slags formed consisted of single mineral slags of the wollastonite $[Ca_{1-x}\ (Fe, Mn)_x]\ Si\ O_3$ $(x = 0.0 - 0.2)$ and monticellite $[(Mn_{1-x}\ Ca_x)\ Si\ O_4]$ $(x = 0.0 - 0.2)$.

Volovik[36] has reported that the initial slag formed from semi-reduced portions of the charge, containing much ferrous oxide, silica and lime, with a fairly high sulphur content.

Sasaki, et al[31] have evidence that limestone does not participate in the slagging process in the softening melting layer. They[31] also added that this was the same with olivines, some of which were found in an unslagged state even in dropped materials at lower levels.

Balon, et al[30], as a result of their investigation, reported that samples taken from the peripheral zone and axis of the furnace, despite the big difference in the height of location of the slag formation levels, were similar in composition and developed similarly as they moved into the furnace hearth.

2.4.3 Slag Compositional Changes

As the primary slag moves into the lower part of the stack it completely loses its wustite component, while the total quantity of $(Fe_{1-x}\ Ca_x)\ Si\ O_4$ and $(Mn_{1-x}\ Ca_x)\ Si\ O_4$ of variable composition ($x = 0.0 - 0.2$) and (MnS) on the contrary - increases. New slag constituents appear, e.g. $Ca_3\ Si_2\ O_7$ and $Ca\ SiO_3$. Within the boundaries of the bosh parallel both the $(Fe_{1-x}\ Ca_x)\ Si\ O_4$ and $(Mn_{1-x}\ Ca_x)\ Si\ O_4$ disappear, $Ca_3\ Si\ O_7$ and $\left[Ca_{1-x}\ (Fe,Mn_x)\right]Si\ O_3$ contents of the slag reach a maximum, the content of $(Mn_{1-x}\ Ca_x)\ Si\ O_4$, $Ca\ Si\ O_3$ and (Mn S) continues to increase and Ca_2SiO_4 appears.

Muravev, et al[34] observed that in samples of sintered material adjoining the region where materials are in the solid state, the mineral phase having the composition $Ca_{1-x}\ (Fe, Mn_x)\ SiO_3$ contained 20% $FeSiO_3$. Further, from the solid materials region towards the region of rapid increase in sintered and softened charge materials, the wollastonite $\left[Ca_{1-x}\ (Fe,\ Mn_x)\right]SiO_3$ was fairly "pure" i.e. ($\beta\ CaSiO_3$). Also according to Balon et al[30] $Ca_{1-x}\ (Fe,\ Mn_x)\ SiO_3$ transformed to α Ca Si O_3 and a continuous solid solution of

Ca_2 Mg Si_2 O_7, Ca_2 Al (Si Al) O_7 through continuous assimilation of lime, magnesia and alumina entering from the fluxes and coke ash.

2.5 The Softening Mechanism in the Blast Furnace Iron Bearing Burden

Generally softening begins from the periphery of a fragment of the iron bearing material when the free energies of the solid and liquid forms of phases present at the surface are equal. For any system, in order for the change of a constituent from the solid state to the plastic state to occur the following must be satisfied:

1. The fusion temperature must be obtained.
2. The latent heat of fusion must be supplied or removed.

It is logical to consider that the softening process starts as soon as the formation of solid/liquid mixtures and 'pastes' in which certain constituents in a multi-constituent mixture melt. The softening range depends on the difference in softening temperature of the various phases.

Benz, et al[37] reported that iron is carburised by carbon monoxide with consequent lowering of the solidus temperature in accordance with the familiar iron-carbon phase diagram.

Sasaki, et al[31] investigated the carbon content in the half-molten portions in a water quenched blast furnace and reported the carbon content in the metallic iron to be

approximately 0.2 mass % in the upper part of the half-molten portion and 0.5 mass % in the lower part. Clearly in the softening layer the carbon content must be less than 0.2 mass %. The melting point of this metal (~ 1500°C) is significantly higher than the temperatures actually prevailing and hence it is unlikely to contribute to the softening processes occurring.

Hills[13] has suggested that the theory relating the initial molten iron phase formed in the blast furnace to the carburisation of solid iron by the furnace gas is not correct. He[13] points out that the presence of wustite in the region where melting occurs will maintain a fairly high oxidising potential, too high for any appreciable degree of carburisation to occur. Even if carburisation of solid iron were to take place, it is unlikely to be rapid enough to be responsible for melting since its rate would be limited by solid state diffusion.

According to Lecomte, et al[23] the first component to melt is FeO,CaO,SiO_2. From the FeO-CaO-SiO_2 diagram, Figure 2-7 (a), they[23] concluded that the minimum temperature of fusion lies near the 1100°C isotherm in the case of the following composition: FeO = 46%, SiO_2 = 37% CaO = 17%. Also they[23] examined the softening of the burden using the Fe_2O_3 - CaO - SiO_2 ternary diagram, Figure 2-7 (b). They[23] showed that the softening of SFCA Compounds (Calcium and

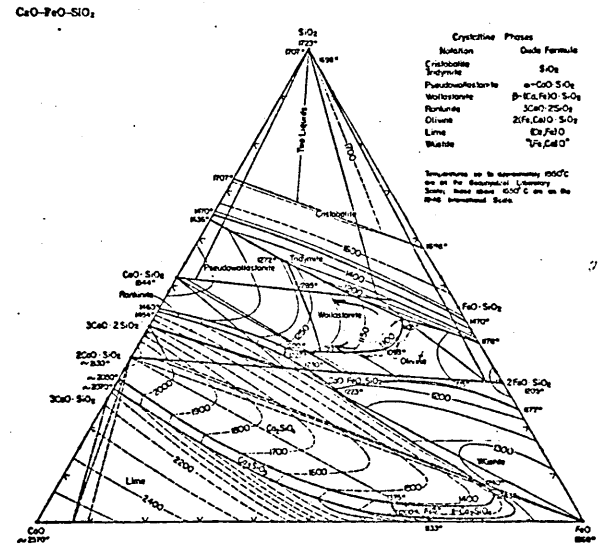

Figure 2-7(a): CaO-FeO-SiO_2 phase diagram[67].

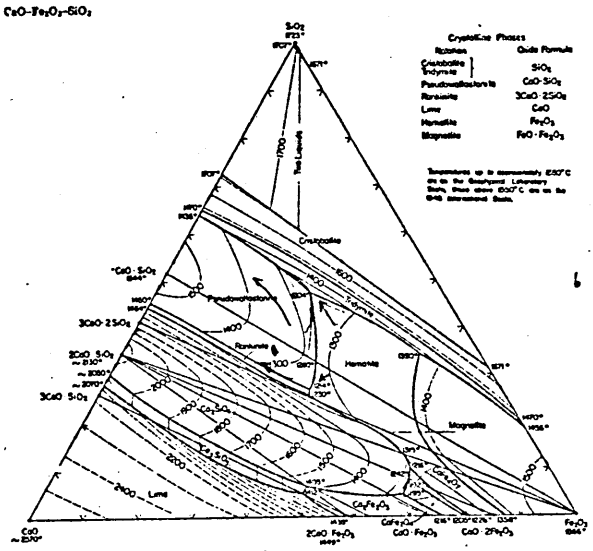

Figure 2-7(b): CaO-Fe_2O_3-SiO_2 phase diagram[67].

alumina silico-ferrites) occurred at temperatures near to the 1250^{o} isotherm.

Hills[13] has suggested the possibility of the formation of an initial melt phase, resulting from the reaction between the furnace gases and one of the solid phases in the burden and the subsequent dissolution of the other solid phases in this initial molten phase as the temperature of the burden rises. He[13] suggested that the initial melting process in the iron blast furnace involved the formation of iron sulphide by reaction between the sulphur-containing furnace gases and solid iron or iron oxide, and related the processes occurring to the Fe - O - S ternary phase diagram. The formation of the initial liquid Fe - S - O ternary eutectic, was followed by further dissolution of iron and wustite during its journey to the tuyere zone, until the temperature of the melt reached 1345^{o}C. It would then meet an immiscibility gap where the liquid splits into two conjugate liquid phases as shown in Figure 2-8. The composition of one liquid phase moves towards the iron rich corner of the ternary diagram representing the initial liquid iron formed, while the other liquid phase moves towards the Fe - O side forming an FeO-FeS binary which dissolves SiO_2 to form an FeO-FeS-SiO_2 slag phase.

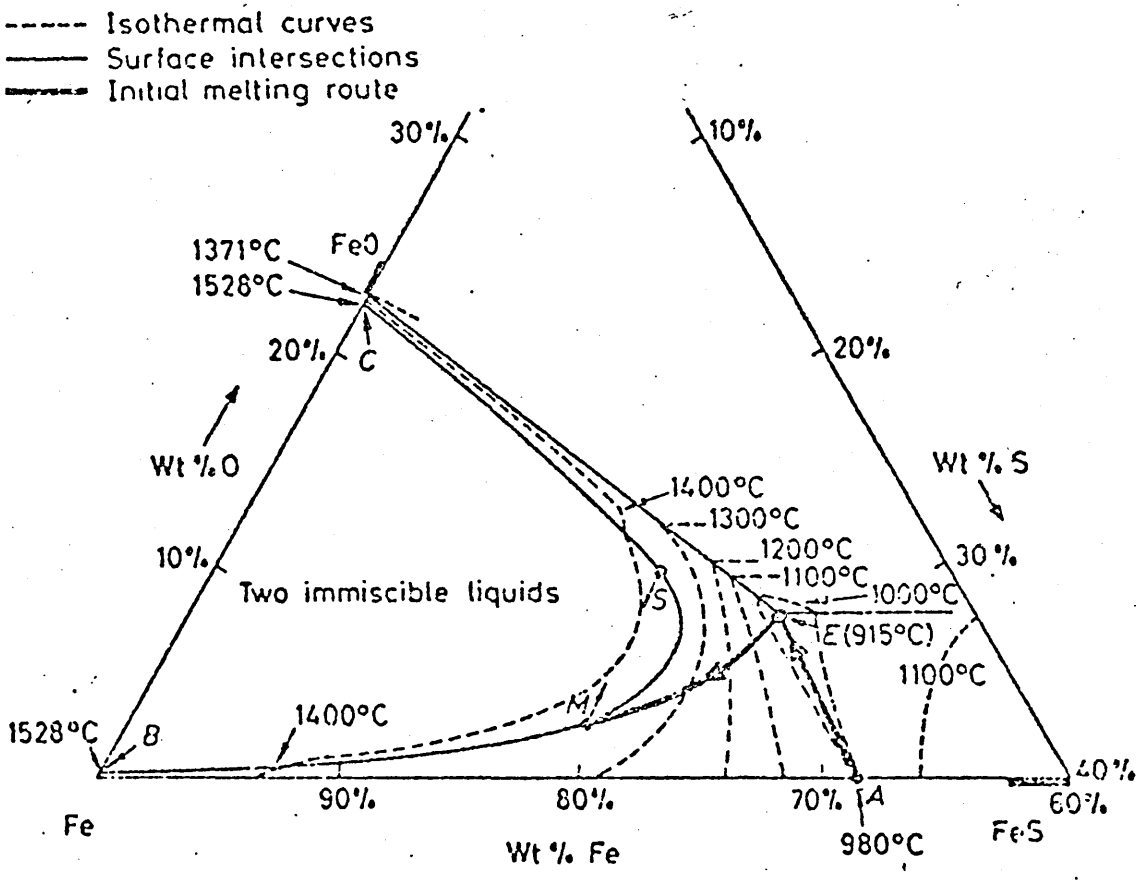

Figure 2-8: Iron corner of Fe-O-S ternary phase diagram (After Hills[13]).

In support of this theory, Volovik,[36] reported that the primary slag is saturated with sulphur.

2.6 The Behaviour of Sulphur in the Blast Furnace

2.6.1 The Behaviour of the Sulphur in the Coke in the Blast Furnace

Volovik[36] has reported that there is no change in the sulphur content of the coke until the bosh is reached. From the bosh to the tuyeres the coke retains about 60% of the original sulphur present. He[36] noted that the specific gravity of lumps of coke from the hearth reached 1.8 Mg/m^3 which was double that of samples taken from the bunkers. He[36] attributed this increase in specific gravity to slag grains which penetrated the coke pores and grains of metallic inclusions found on the coke surface. The slag grains themselves were of $Ca_{1-x}(Fe, Mn)_x SiO_3$ ($x = 0.0 - 0.2$) enriched with calcium sulphides, and the metallic grains were mainly iron sulphide.

According to the data of Pokryshkin[38] the coke loses about 28% of its sulphur in the stack, and half before the tuyere level. Analysis of individual lumps of tuyere coke showed that the inside of a piece of coke contained 10 - 15% more sulphur than did the surface layers.

Borts, et al[39] have investigated the behaviour of sulphur throughout the entire furnace. They[39] reported that the sulphur content of the coke ash rose from 0.56 to 1.7 mass % as a result of sulphur absorption from the dust filling

the open pores of the coke lumps, which covered the coke lumps with a 5 mm layer. They[39] added that this dust consisted mainly of iron oxides (14.4 mass % FeO - 40.1 mass % Fe_2O_3 and 14.4 mass % CaO).

2.6.2 Behaviour of Sulphur in Blast Furnace Iron Bearing Component

Volvik[36] has reported that the processes of sulphur transfer from the gas phase into the solid continue from the bosh parallel down to the tuyere level up to the moment of separation of the metal and slag. He[36] also noted that over the whole height of the furnace the sulphur absorption capacity of lime is greater than that of the iron.

Kodama, et al[40] as a result of their investigation on a water quenched blast furnace reported that the amount of sulphur present in the iron ore increased from the 800°C level and reached 0.04 to 0.1 mass % just before melting.

Hills[13] in his analysis of transport phenomena taking place in the blast furnace has shown that in the bosh region, the slag phase is picking up sulphur, while the iron phase is losing sulphur. He[13] concluded that the iron must pick up sulphur from the gas phase at some level higher in the furnace.

Borts, et al[39] reported the sulphur content in sinter rises from 0.21 to 0.47 mass % as it descends through the stack

Metal started to appear in the bosh region in the form of a porous sponge and iron "icicles", see Figure 2-6, containing 0.3 mass % sulphur. In the region of the tuyeres the metal contained 3 to 6 times more sulphur than in the final pig iron. Petrographic analysis of samples taken from a nitrogen quenched blast furnace showed that the slag phase was located among skeletons of spongy uncarbonised metal. They[39] added that the sulphur in the samples investigated was in the form of sulphides of the $(Fe, Ni)_6 S_8$ type. They[39] attributed the very high sulphur content in the slag in the lower bosh to the absorption of sulphur from the gas phase and dissolution of ferrous sulphide from the sponge iron. The decrease in the slag sulphur content in the tuyere zone was due to the oxidation of primary slag sulphur.

Shinomura, et al[41], investigated the distribution of sulphur in a quenched blast furnace and reported that ores in the lumpy and softening zones absorbed sulphur as they contacted the gas. The observed sulphur distribution is shown in Figure 2-9.

Sasaki, et al[31] reported a sulphur content of 0.2 mass % in metal immediately separated from the softening melting layer. This sulphur content gradually decreased until at tuyere level it approached the tapping value of the pig iron. In their[31] investigation no definite conclusion was obtained for the behaviour of sulphur in the slag parts of dropped materials immediately separated from the softening

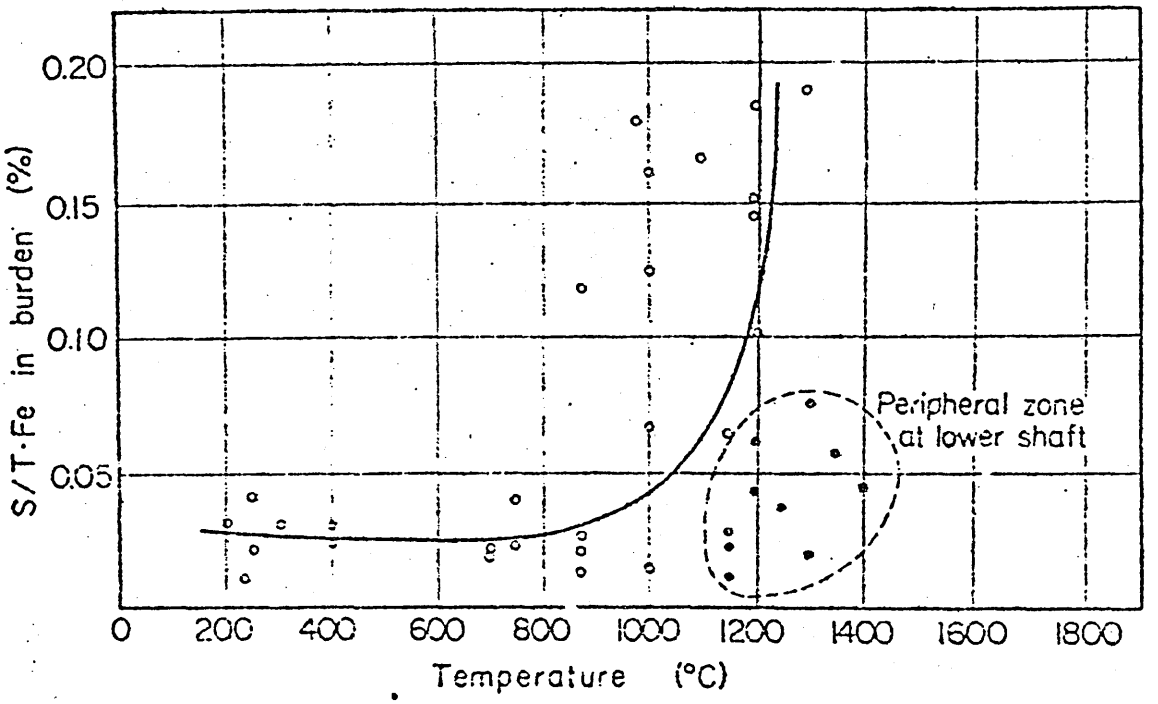

Figure 2-9: Sulphur distribution in the ferrous constituents of blast furnace burden along a vertical section. (After Shimomura[41]).

melting layer. Some results showed that the sulphur content did not greatly increase towards the tuyere level, in others a gradual increase was observed.

Grip et al [42] reported that the pressure drop across a bed containing only pellets in a batch reactor used to simulate conditions in the bosh region of the blast furnace, rose very rapidly between 1150-1200°C. They[42] concluded that this was due to molten iron sulphide.

Balon, et al.[43] have investigated the sulphur distribution in a quenched blast furnace and claimed that films of sulphides (FeS) formed because of their lower melting point. They[43] suggested that the fragmentation of the burden, started the fusion process during the journey to the tuyere zone.

2.6.3 The Behaviour of Sulphur in the Blast Furnace Gas

Volovik, et al.[44] have reported that the volatilised sulphur from the coke and smelting products on entering the oxidizing zone reacts to form SO_2, according to the equation:

$$\tfrac{1}{2} S_2 + O_2 = SO_2$$

The rise in temperature along the oxidizing zone produced a sharp drop in the gas SO_2 content and its complete disappearance in the maximum temperature zone. As the blast moved away from the tuyere zone, the following reaction

took place:

$$2C + SO_2 = 2CO + \tfrac{1}{2} S_2$$

At a temperature of 1267°C, dynamic equilibrium was established between the sulphur dioxide and free sulphur. H_2S formed at high temperature was completely decomposed at 1690°C. Below 1727°C free sulphur will clearly predominate in the gas.

Blomster, et al.[45], studied the thermodynamic equilibrium in the system C - S - O at temperatures between 750-1100°C by the use of gas analyses and thermodynamic equilibrium calculations and reported[45] a yield of elementary sulphur in excess of 90% with a carbon/oxygen ratio in the gas 0.5.

Tsuchiya, et al.[46], investigated the mechanisms of mass transfer via the gas phase at the melting zone in the blast furnace and reported[46] that sulphur is transferred by the gas phase to the ferrous constituents of the blast furnace burden. They[46] also added that even the desulphurization by metal-slag reaction is probably unlikely, as they[46] observed a high percentage of FeO in the slag (FeO)>~ 5-6%, suggesting[46] that sulphur in the metal was removed from the molten iron to the gas phase as S_2 or CS_2, etc., and to the slag phase as sulphides by gaseous alkali or alkaline earth metals produced in high temperature zone.

2.6.4 Phase Equilibrium Involving Sulphur in the Blast Furnace

Wustite (FeO) has the NaCl type crystal structure and is stable over a wide range of compositions on the oxygen - rich side of the stoichiometric FeO composition. This range of non stoichiometry which can be accounted for by vacancies on the iron cation sublattice, is a function of temperature and oxygen partial pressure. The diffusion coefficient of iron in FeO increases with temperature and deviation from stoichiometry.

Magnetite (Fe_3O_4) has a structure very similar to that of FeO but with differences in the number and location of Fe^{3+} cations. Fe_3O_4 exists over a wide range of compositions at elevated temperatures which is believed to be due to the presence of vacant iron cation sites.

Pyrrhotite (FeS) is stable over a wide range of compositions between stoichiometric FeS and $FeS_{1.23}$. This nonstoichiometry is due to the presence of iron vacancies and is a function of temperature and sulphur partial pressure. The diffusivity of iron in FeS is very high and orders of magnitude greater than that of sulphur.

Turkdogan, et al.[47] have studied the Fe-O-S ternary system and established a ternary eutectic point at about 915°C

where solid iron, FeO, and FeS coexist with a liquid oxysulphide.

Kor and Turkdogan[48] have reported the solid solubility of sulphur in FeO to be 140 ppm at 1250°C and suggest that sulphur may form a substitutional solution relative to the oxygen sites.

Leonard and St.Pieree[49], have reported the solubility of sulphur in FeO in equilibrium with Fe_3O_4 to be 420ppm at 1100°C.

Hauffe et al.[50] and Meussner, et al.[59] have studied the sulphidation of iron to FeS in sulphur vapour. The reaction obeyed the Wagner parabolic rate law with the rate determining step being the diffusion of iron through the FeS layer.

McCormick, et al.[51] have studied diffusion - limited sulphidation of wustite and reported an initially rapid sulphidation rate that decreased continuously with time. They noted that during the initial period, an intermediate layer of Fe_3O_4 was formed between the FeO core and the external FeS layer. The kinetics of the sulphidation process followed a non-parabolic rate law. After the compositions of the various phases at the FeO/Fe_3O_4 and Fe_3O_4/FeS inter-

faces became invariant, the parabolic rate law became operative.

According to the report by Neuhause, et al.[52], sulphurising conditions rapidly worsened as the atmosphere became more acidic due to an increase in the $\frac{CO_2}{CO + CO_2}$ ratio.

According to data[53] on sulphur solubility in ferrous oxide and liquid iron, the sulphur content falls by 71-78 mass % if reduced iron is melted and carburized at temperatures of 1200-1400°C.

In general it is to be expected that the impregnation of the iron-bearing material with sulphur depends upon the sulphur content in the gas phase, the specific surface area available for reaction, the size and nature of the pores and the amount of reduced iron.

2.7 The Behaviour of Alkalies in the Blast Furnace

2.7.1 Introduction

Alkalies enter the blast furnace as complex silicates or chlorides in the ore, the sinter, the pellets, the flux and the coke. Of the alkalies entering the furnace, a part goes out in the slag, some leaves as dust in the flue gas, another part is absorbed by the refractory lining and the rest circulates within the furnace. Except that part which goes out in the slag, all the rest can create problems in varying degrees of intensity.

The alkali compounds of interest which are present under blast furnace operating conditions are the oxides, carbonates, cyanides, silicates and sulphates.

Richardson and Jeffes[15] pointed out that potassium and sodium compounds would be reduced to the metallic vapours in the melting zone. They[15] also added that as the gases ascended the stack and their temperature fell, it would become possible for the metal vapours to combine with CO_2 in the gas to form carbonates, or if free silica was present, to form silicates.

Vidal et al.[54], in their investigation of the reactions taking place in the bosh of an experimental blast furnace at Liege, confirmed that alkali circulation occurred.

Sasaki et al.[31], have reported that the alkali distribution agreed well with the profile of the softening melting layers and that the alkali concentration sharply increased in the softening melting layer. They[31] related their results to the absorption of alkali from the highly concentrated alkali containing gas. They[31] noted that the alkali content started to decrease at the tips of the iron "icicles" and alkaline reduction was considered to proceed up to a point immediately before their separation.

2.7.2.(a) Alkali Oxides

Na_2O melts at 1132°C and K_2O sublimes above 881°C in air. But in the blast furnace the CO/CO_2 ratio is such that in the presence of excess carbon, strongly reducing conditions result. From the standard free energies of formation of carbonates[55] shown in Figure 2-10, pure potassium oxide is reduced above 815°C to give potassium vapour. A temperature of 1000°C can be estimated for a similar reduction of sodium oxide resulting in sodium vapour.

2.7.2. (b) Alkali Carbonates

Sodium and potassium carbonates melt at 850°C and 901°C respectively in air. K_2CO_3 can be considered to be stable below 900°C. From Figure 2-10 it is seen that the pure alkali carbonates are not reduced in the blast furnace to give alkali vapour at 1 atmosphere pressure until a temperature of about 1200°C is reached. At 800°C, with a CO/CO_2

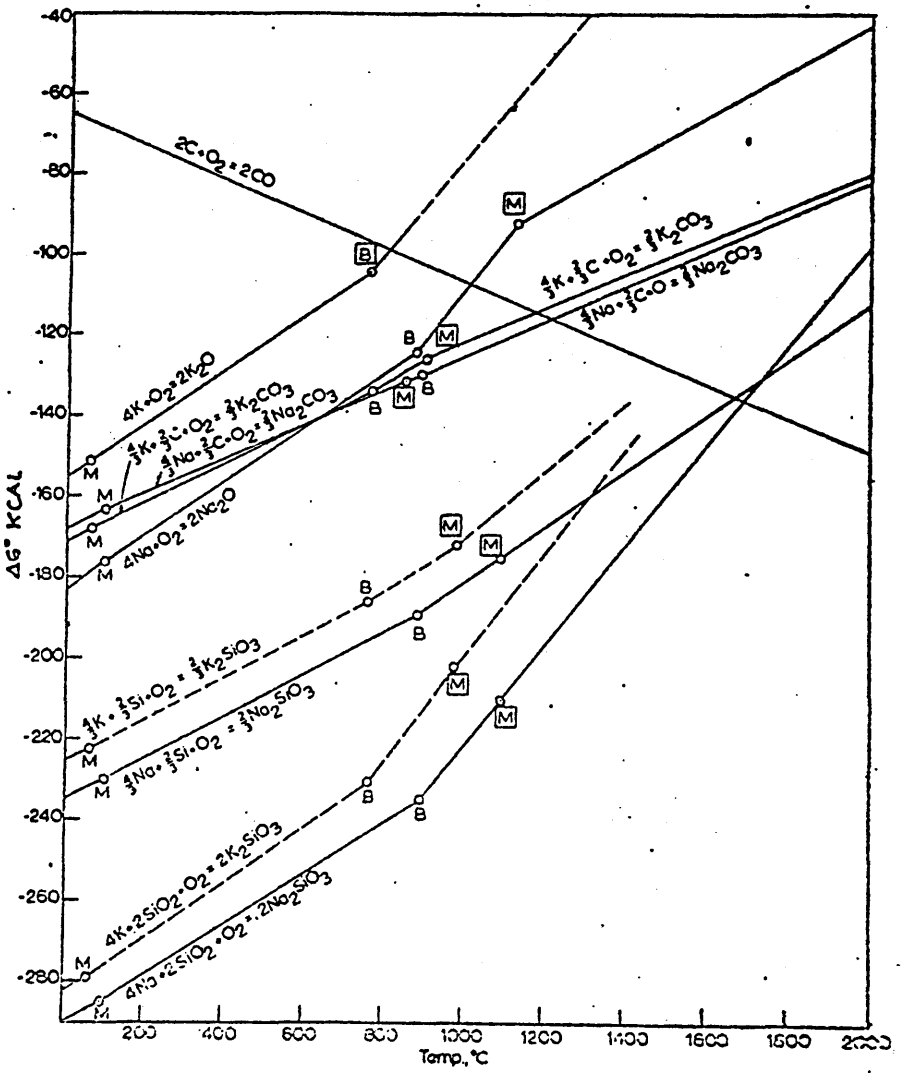

Figure 2-10: Standard free energies of formation of oxides, carbonates and silicates of sodium and potassium.

ratio of 2.8 (see Figure 2-10) in the blast furnace, the partial pressure of potassium vapour is estimated to be about 1×10^{-5} atmosphere. This value is so low that K_2CO_3 can be considered to be quite stable below 900°C in the blast furnace. Richardson and Jeffes[15] estimated that both potassium and sodium carbonates could be formed from the respective vapour under conditions prevailing in the shaft of the furnace at temperature below 900°C. Since the solid carbonates are formed directly from the gas phase, they will be finely divided. A portion of the carbonate formed will be deposited on the burden and are returned to the high temperature reduction zone.

2.7.2 (c) Alkali Cyanides

Potassium cyanide melts at 622°C and boils at 1625°C, where as sodium cyanide melts at 562°C and boils at 1530°C[55]. Alkali cyanides therefore, exist as liquids in the temperature range 900-1200°C. In the softening zone in the blast furnace KCN will be oxidized to the more stable potassium carbonate which is a solid below 900°C. Although the silicate is more stable still, its formation is by a heterogeneous reaction involving a silica surface and may not take place to any appreciable extent. Thus the cyanide is formed directly from the gas phase and the carbonate is formed by the subsequent oxidation of the cyanide droplets. The carbonate formed exists mostly in the form of fumes.

2.7.3 The Behaviour of Alkalies in the Thermal Reserve Zone

In the thermal reserve zone, wustite is in equilibrium with the gas phase according to the equation:

$$FeO + CO_{(g)} \rightarrow Fe + CO_{2(g)}$$

As the alkali metals enter the blast furnace as silicates in the ore, the sinter, the pellets, the flux and the coke, its reduction follows the equation:

$$2\ K_2\ Si\ O_3 + 2\ Fe \rightarrow 4\ K_{(g)} + 2\ SiO_2 + 2\ FeO$$

or

$$2\ Na_2\ Si\ O_3 + 2\ Fe \rightarrow 4\ Na_{(g)} + 2\ SiO_2 + 2\ FeO$$

From the standard free energy change for the above reaction[55], the equilibrium vapour pressure of potassium at 1000°C is found to be 10^{-5} atmospheres. A correction to the above vapour pressure values must be made if the alkali silicates exist in the furnace as complex silicates. Similar calculations carried out with the data on sodium silicate show that at 1000°C, the equilibrium vapour pressure of sodium is 1.8×10^{-6} atmospheres.

Richardson and Jeffes[15] have reported values of 0.002 atmospheres for potassium and 0.001 atmospheres for sodium in the stack of the blast furnace, but as the gases are moving at high velocity, this equilibrium vapour pressure will be some lower value.

2.7.4 Influence of Alkalies on Blast Furnace Operation

Alkali compounds are known to accelerate iron-oxides reduction especially in the early stages of reduction.

Nekrasov, et al.[56] have investigated the effect of alkalies on the blast furnace charge and reported that, in the case of pellets, an increase in the degree of reduction from 22% to 48% was observed when alkali compounds were present in the gas phase. The porosity of the charges studied rose linearly with increasing degree of reduction up to 80% reduction, after which it either did not change or decreased. The distribution of alkali elements[56] was non-uniform although compounds tended to be concentrated at the periphery, seldom at the centre.

Abraham, et al.[57] have claimed that alkalies in addition to causing pellets to exhibit catastrophic swelling, caused disintegration of coke, hanging in the furnace and higher than normal fuel requirements by transferring heat to the shaft as a result of their circulation.

Bleifuss[65] has investigated the effect of alkali compounds on the swelling of pellets. He[65] reported that 0.5 mass % Na_2CO_3 caused maximum swelling, while with K_2CO_3 expansion was more uniform. With NaCl and KCl, pellets underwent uniform slow deformation. He[65] related this catastrophic swelling not to massive growth of metallic iron filaments but to non topochemical reduction of wustite during metallisation.

CONCLUSION

From the literature survey, it is clear that the methods developed to investigate the softening behaviour of ferrous constituents in the blast furnace charge have not studied the effect of different gas phase constituents in the blast furnace. As the softening is the result of the effect of the temperature increase on the state of the sample - degree of reduction, phase composition, texture and microstructural features, etc. - a marked relationship is likely to exist between the composition of the gas phase and the softening behaviour.

In considering the softening mechanism two views have been postulated to explain the effect of the gas phase. One relates the softening to the carbonization of the reduced iron by CO/CO_2 gas. It can be considered that this view did not cause the established range of softening temperature. As can be seen from Figure 2-5a, a maximum of 0.6 mass %C will dissolve in the iron. Consulting the Fe-C phase diagram the liquid phase starts to appear at temperatures over 1400^{o}C. The second view considers that sulphur vapour reacts with Fe or FeO producing FeS as a start of the softening.

In this work a method for investigation of the softening behaviour of ferrous bearing material under controlled gas phase composition, without applying any load to the sample, was developed.

3.1 Purpose of the Investigation

The main purpose of this investigation was to attempt to develop a laboratory method for studying the effect of gas composition on the softening behaviour of the ferrous constituents of blast furnace burden materials. By studying the softening behaviour of these materials it was hoped that a correlation between the behaviour of the various materials tested and the smoothness of blast furnace operation could be obtained.

The experimental method adopted involved a modified Seger cone technique. Samples of synthetic burden materials and partially reduced ores were moulded into the form of a cone and the softening behaviour of this cone studied in various gaseous atmospheres. In the initial experiments, the effect of sulphur, in the form of iron sulphide, on the softening characteristics of various mixtures of pure FeO, Fe and SiO_2 in inert atmospheres, was investigated. In the later experiments the softening behaviour of a particular iron ore was investigated in gaseous atmospheres containing various amounts of sulphur or alkali metals.

3.2 Materials Used

FeO

FeO was prepared from ferrous oxalate supplied by the British Drug Houses Limited. Its maximum limit of impurities was 0.5%. Table 3-3 gives its chemical analysis. The ferrous oxalate was heated in a platinum crucible, covered by a tight platinum lid, to a temperature of 1200°C for two hours in order to ensure complete dissociation according to the chemical reaction:

$$(COO)_2 \, Fe \, H_2O \rightarrow FeO + CO + CO_2 + H_2O$$

The platinum crucible was then removed from the furnace and rapidly cooled in a stream of air from a hair drier. Magnetic separation of Fe_3O_4 was carried out, but in general very little was produced.

Fe_2O_3

Calcined ferric oxide supplied by Hopkin and Williams was used.

FeS

Ferrous sulphide supplied by Hopkin and Williams was used. Table 3-1 lists the impurities in the ferrous sulphide used.

SiO_2

Pure precipitated silica supplied by Hopkin and Williams was used.

Table 3-1: The impurities in ferrous sulphide

Element	Concentration	Element	Concentration
Silicon	~ 10 ppm	Lead	~ 10 ppm
Nickel	~ 50 ppm	Copper	~ 20 ppm
Magnesium	~ 2 ppm	Aluminium	~ 10 ppm
Chromium	10 ppm	Molybdenum	10 ppm

Table 3-2: Chemical analysis of Bahira Iron Ore

Element	Mass %	Element	Mass %
FeO	0.917	V_2O_5	0.120
Fe_2O_3	73.94	Total S as SO_2	0.44
SiO_2	6.4	Acid soluble Na_2O	1.145
Al_2O_3	2.8	Water soluble Na_2O	0.705
CaO	0.952	Acid soluble K_2O	Nil
MgO	0.311	Water soluble K_2O	Nil
MnO	0.993	Soluble chlorides	0.738
P_2O_5	0.405	Moisture at 150°C	1.3
BaO	0.021	Loss on ignition at 900°C	10.22
TiO_2	0.22		
PbO	0.024		
ZnO	0.165		

Table 3-3: Ferrous oxalate impurities

Impurities	Mass %	Impurities	Mass %
Chloride (Cl)	0.005	Sulphate (SO_4)	0.05
Nitrate (NO_3)	0.01	Fe	0.5

Table 3-4: Potassium carbonate specification

Constituent	Mass %	Constituent	Mass %
K_2CO_3	>99	Iron (Fe)	<0.004
Chloride (Cl)	<0.04	Sulphate (SO4)	<0.03

Table 3-5: Sodium carbonate impurities

Impurities	Mass %	Impurities	Mass %
Insoluble matter	<0.01	Sulphate (SO4)	<0.0025
Chloride (Cl)	<0.002	Calcium group	<0.013
Nitrate (NO_3)	<0.002	Heavy metal (Pb)	<0.0005
Phosphate (PO_4)	<0.001	Loss at 300°C	<1

Iron Ore

Bahira iron ore was used in this work and comes from an Egyptian deposit. The ore is brown to yellowish in colour and consists of hydrated ferric oxide with gangue minerals such as quartz, barite and halite. Table 3-2 gives the chemical analysis of this ore.

Sulphur

Sulphur supplied by Hopkin and Williams Limited was used.

Potassium

Potassium metal supplied by Fisons Scientific Apparatus Limited was used.

Potassium Carbonate

Anhydrous potassium carbonate supplied by Hopkin and Williams Limited was used. It contained a minimum of 99% K_2CO_3 in dried material. Table 3-4 gives its specification.

Sodium Carbonate

Anhydrous sodium carbonate supplied by British Drug Houses Limited was used. Table 3-5 gives its specification.

Ammonium Chloride

Ammonium chloride supplied by J. Preston Limited was used.

3.3 Cone Preparation Technique

3.3.1 Determination of the Optimum Particle Size for the Preparation of the Cones

Preliminary experiments were carried out to determine the optimum particle size for the preparation of the test cones. A sample of Bahira iron ore was ground in a ball mill, screened and -60 + 100, -100 + 150, -150 + 200 and -200 mesh size fractions separated. Three cones were produced from each size range of particles, dried at 200°C for 24 hours and fired at 1050°C for two hours to check their stability. The -60 + 100 mesh size range particles were found to collapse during drying, while the -150 + 200 and -200 size range particles were found to collapse during firing. The -100 mesh size range particle were found to give the most satisfactory result.

3.3.2 The Binding Agent

Starch was initially tested as a binding agent but this proved to be unsatisfactory. During firing to 1050°C the cones collapsed and also water vapour was produced inside the furnace which made it difficult to observe the cone's behaviour.

The use of ammonium chloride as a binding agent was shown to give satisfactory results. The optimum amounts of ammonium chloride required to act as a binding agent was determined as follows.

Bahira iron ore of -100 mesh size, was used to produce cones with different proportions of ammonium chloride ranging from 5 mass % to 10 mass %. After the cones were dried at 200°C for 24 hours, they were fired at 1050°C for two hours. The addition of 6 mass % of ammonium chloride as the binding agent was found to give the most stable cones.

3.3.3 Basic Cone Preparation Technique

After weighing out the appropriate amounts of cone components, 6% by mass of ammonium chloride was added to the mixture. The powder was mechanically mixed and then alcohol was added to produce a paste.

A two piece, brass, Seger Cone mould (shown in Plate 3-1) was employed to produce the cones used in this work. This particular mould produced a cone with a height of 2.6cm and with an equilateral triangular base of side 0.84cm, as shown in Figure 3-1. A proprietry mould release fluid supplied by A. W. Chesterton and Co. was applied to the inner wall of the mould before casting the pasty mixture. After removal from the mould, each cone was dried for 24 hours at 200°C. For cones produced from FeO or reduced Fe_2O_3, drying was carried out under argon at a positive pressure in order to avoid reoxidation. For cones containing partially reduced Fe_2O_3 as one of its constituents firing to 1050°C was carried out at the rate 10°C/min under argon at positive pressure.

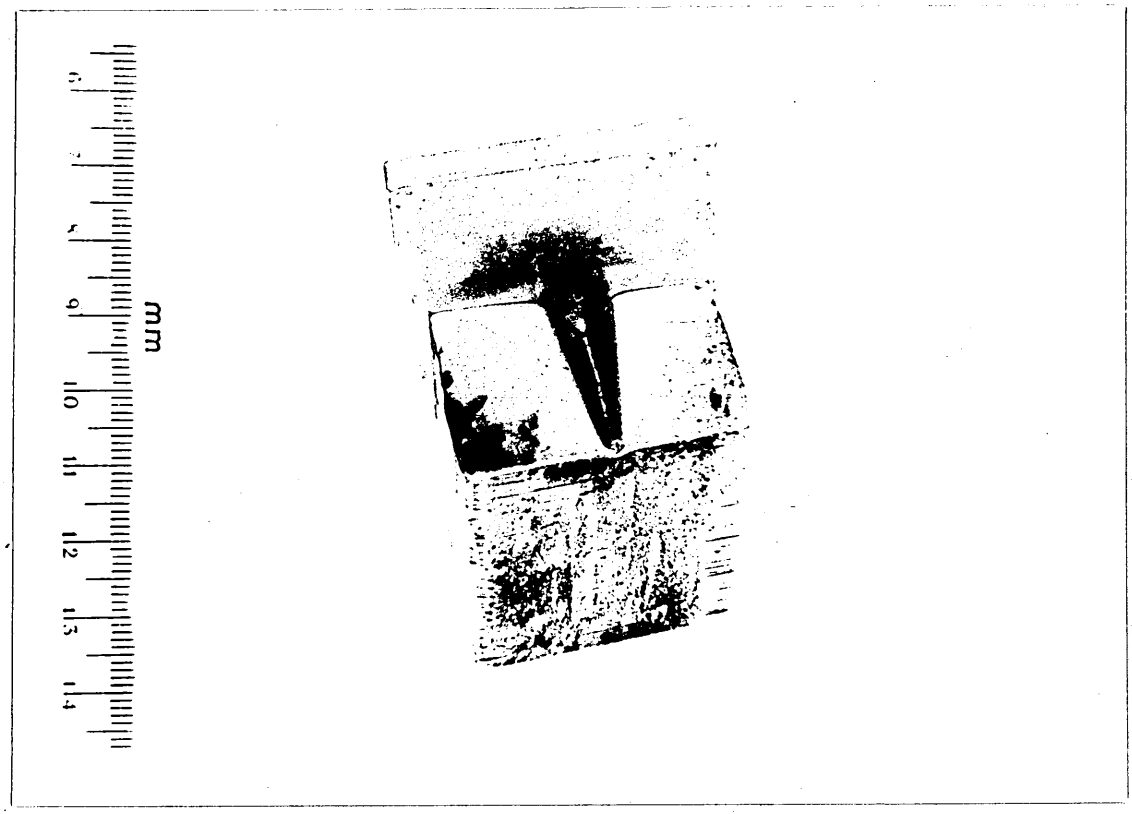

Plate 3-1: A two piece brass mould used to produce tested cones.

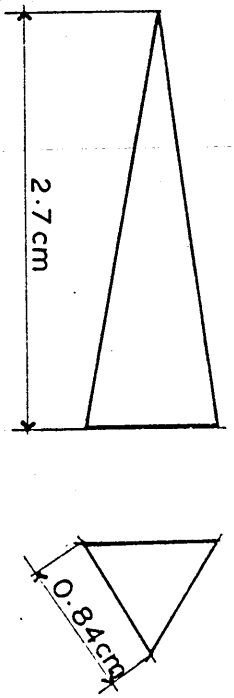

SCALE 1:2

FIG. 3.1 CONE DIMENSIONS

The chemical analysis of a number of representative cones was carried out to determine the percentage of ammonium chloride remaining after drying. This amounted to 0.67 mass %.

In certain runs using cones having a composition of 50 mass % FeS, 50 mass % SiO_2, the cones were weighed before and after the softening test and so the mass loss could be obtained.

3.3.4 Cone Enrichment with Alkali Additives

A series of experiments was carried out with Na_2CO_3 as one cone constituent, in order to investigate its effect on the softening of the test cones. Na_2CO_3 representing 2 mass % of the test cone was added before shaping the cone. As the melting point of Na_2CO_3 is 850°C the cones were fired to 840°C instead of 1050°C as described in section 3.3.2. The cones fired at 840°C were fragile and many collapsed during handling.

It was therefore found necessary to use an impregnation technique. In this technique a known mass of unhydrated Na_2CO_3 was dissolved in a predetermined quantity of distilled water. Thus an aqueous solution of known strength was obtained. A fired cone was weighed and then immersed into the aqueous solution under vacuum for 1 hour. It was then dried at room temperature in a dessicator for 24 hours and then heated to 300°C for half an hour in the

furnace described in section 3.4.2, according to the procedure in section 3.4.3. The cone was weighed, the difference in mass giving the amount of Na_2CO_3 in the cone.

3.4 The Experiments Conducted to Determine the Softening Behaviour of the Base Components in the Blast Furnace Charge in an Inert Atmosphere

3.4.1 Introduction

In the first series of experiments, the softening behaviour in an inert atmosphere of the pure base components of the blast furnace charge, ie FeO, SiO_2, FeS and mixtures of these was studied. Cones of these materials were prepared and their softening behaviour studied in a horizontal tube furnace.

3.4.2 Apparatus

A horizontal, alumina tube furnace, heated by silicon carbide elements was used. The alumina tube was provided with gas tight seals on each end. The ends were water cooled and provided with gas inlet and outlet ports and a quartz disc through which the cone could be observed during the experiments. The temperature was measured using a Pt/Pt - 13 mass % Rh thermocouple which was placed within 1cm of the test cone. The extent of the hot zone was determined and was found to be 2cm long. The argon flow rate was measured by an argon flow meter supplied by M.F.G. Co. Ltd., and the gas pressure inside the furnace was determined by a "Slim Jim" manometer supplied by Air Flow Developments Limited.

3.4.3 Procedure

The cones were introduced into the hot zone of the hori-

zontal tube furnace in which the softening test was to be carried out. Seger standard cones were introduced within 1cm of the test cones to confirm the accuracy of the temperature indicated by the Pt/Pt - 13 mass % Rh thermocouple. The argon flow rate was about 200cm^3/minute, while the gas pressure inside the furnace was on average 130mm H_2O. The temperature of the furnace was raised at a rate of 10°C/minute during each run until cone softening occurred or the maximum temperature of the furnace was attained. For the investigation of the softening of cones containing 50 mass% FeS and 50 mass % SiO_2, a special regime was applied, in which the cones behaviour was examined at temperatures from 900°C to 1400°C at intervals of 100°C.

A microscopic examination was carried out on each cone after the softening test. Chemical analysis of certain cones after testing was carried out.

At temperatures over 1000°C an optical pyrometer supplied by Foster Instrument Company Limited was used to confirm the accuracy of the measured temperature.

3.5 The Test Regime for the Study of the Softening Behaviour of a Commercial Iron Ore

3.5.1 Introduction

The Bahira iron ore deposit represents the main source of iron ore in Egypt and contains reserves of 400 million tons. Table 3-2 shows the high percentage of both sodium and chlorides which amounts to 1.145 mass % Na_2O and 0.738 mass % soluble chlorides. Industrial processing of the Bahira iron ore has shown that 50% of the Na_2O and 70% of the chlorine are removed during the sintering process. The balance charged to the blast furnace can give rise to irregular operations, decreased production and relatively high coke consumption.

The purpose of this series of experiments was to investigate the softening behaviour of cones produced from this iron ore and to relate this softening behaviour with its behaviour in the blast furnace.

3.5.2 The Experimental Method for the Partial Reduction of Iron Ore Cones

3.5.2(a) Apparatus

A horizontal tube furnace employing silicon carbide rods as the heating elements was used. Temperature control was by hand through a Variac. The alumina tube was provided with two gas sealed ends and Apiezon was used to ensure

complete sealing of the system from the surrounding atmosphere. The gas sealed ends were furnished with gas inlet and outlet ports and a water cooling system.

The reducing gas flow was measured by means of a calibrated rotameter. High purity argon was used to flush the reaction tube during heating and cooling. Hydrogen was used as the reducing agent, any moisture present being removed by a drying system consisting of anhydrous magnesium perchlorate, followed by a molecular sieve.

To obtain better sealing of the reduction apparatus, the reduction temperature was measured by a thermocouple attached to the outer wall of the furnace tube in the hot zone. A calibration curve between the temperature of the hot zone inside the furnace and the reading of the outer thermocouple was set up. The thermocouples used were Pt/Pt - 13 mass % Rh, the millivoltage output being monitored by a continuous balance potentiometer recorder.

The cone to be reduced was supported on a C60 alumina cement mould in an alumina boat.

3.5.2.(b) The Procedure for the Partial Reduction of Iron Ore Cones

The cone to be reduced was weighed on an automatic balance and placed in the alumina boat. This was then introduced

into the furnace and positioned in the region of the furnace hot zone. After sealing the system, the air was purged out of the furnace tube using argon and then a flow of argon left on to ensure a positive pressure within the furnace tube until the sample had reached the required temperature. When the required temperature was reached, 700°C the argon was turned off and hydrogen introduced into the tube. After the required time, the hydrogen flow was stopped and the furnace tube was again purged with argon. The furnace was switched off and allowed to cool with a positive pressure of argon in the furnace tube. Cooling to room temperature took about 6 hours. The cone could then be removed and weighed.

Throughout these experiments the percentage reduction has been defined as:

$$\frac{\text{Mass of oxygen lost}}{\text{Total mass of oxygen initially present}} \times 100,$$

where the total mass of oxygen initially present is that which is in combination with iron.

3.5.3 The Study of the Softening Behaviour of the Partially Reduced Cones in Inert Atmosphere

The apparatus and method used are essentially the same as for the earlier experiments described in section 3.4.2 and 3.4.3, except that a calibrated nitrogen rotameter was used for the softening test in nitrogen. The inert gas

flow rate was 1 dm^3/minute. A stainless steel boat was used in some of the softening tests instead of C60 alumina cement boat to ensure that no reaction took place between the base and the test specimen.

3.5.4 The Effect of Alkalis on the Softening of Bahira Iron Ore

3.5.4(a) Apparatus

Softening tests were carried out in a furnace with an A.I.S.I. 371 stainless steel, (18 mass % Cr, 10.5 mass% Ni), tube 90cm long by 5cm in diameter, provided with water cooled gas sealed ends. The gas sealed ends were furnished with a quartz disc through which cone observation was possible. A furnace supplied by Carbolite was used.

3.5.4(b) Procedure

Potassium metal contained in a nickel boat was positioned at a predetermined distance from the gas inlet end as determined by the temperature profile shown in Figure 3-2, to obtain the required potassium vapour pressure according to Figure 3-3. The test cone was positioned in the hot zone of the furnace in a nickel boat. Care was taken to keep the reacting cones 300-400^{o}C hotter than the potassium metal source while heating up to the temperature of the experiment so that there was no danger of potassium distilling over on to the cones and condensing there. On

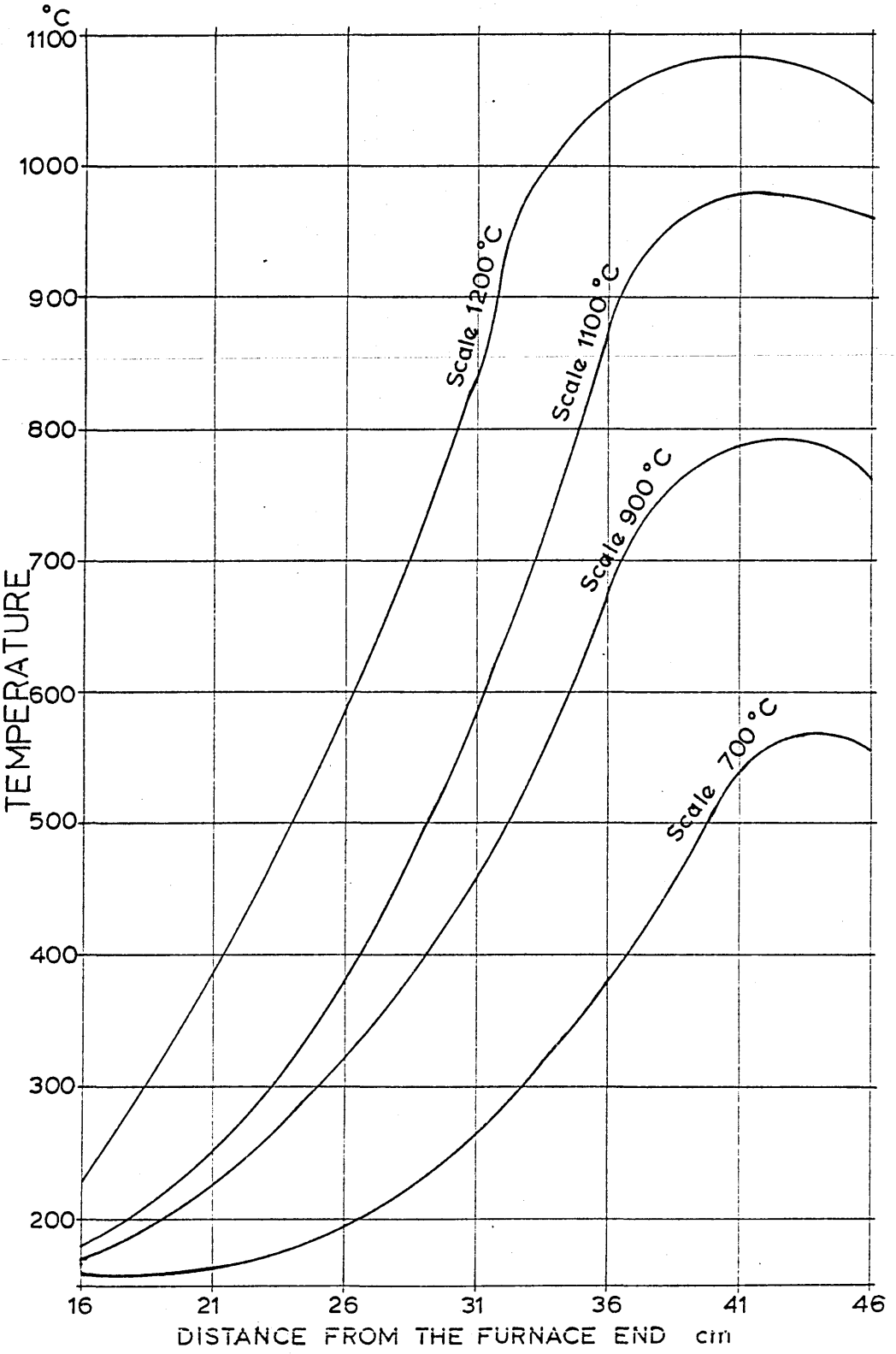

FIG. 3.2 TEMPERATURE GRADIENT INSIDE THE STAINLESS STEEL TUBE FURNACE AT DIFFERENT SCALE TEMPERATURE

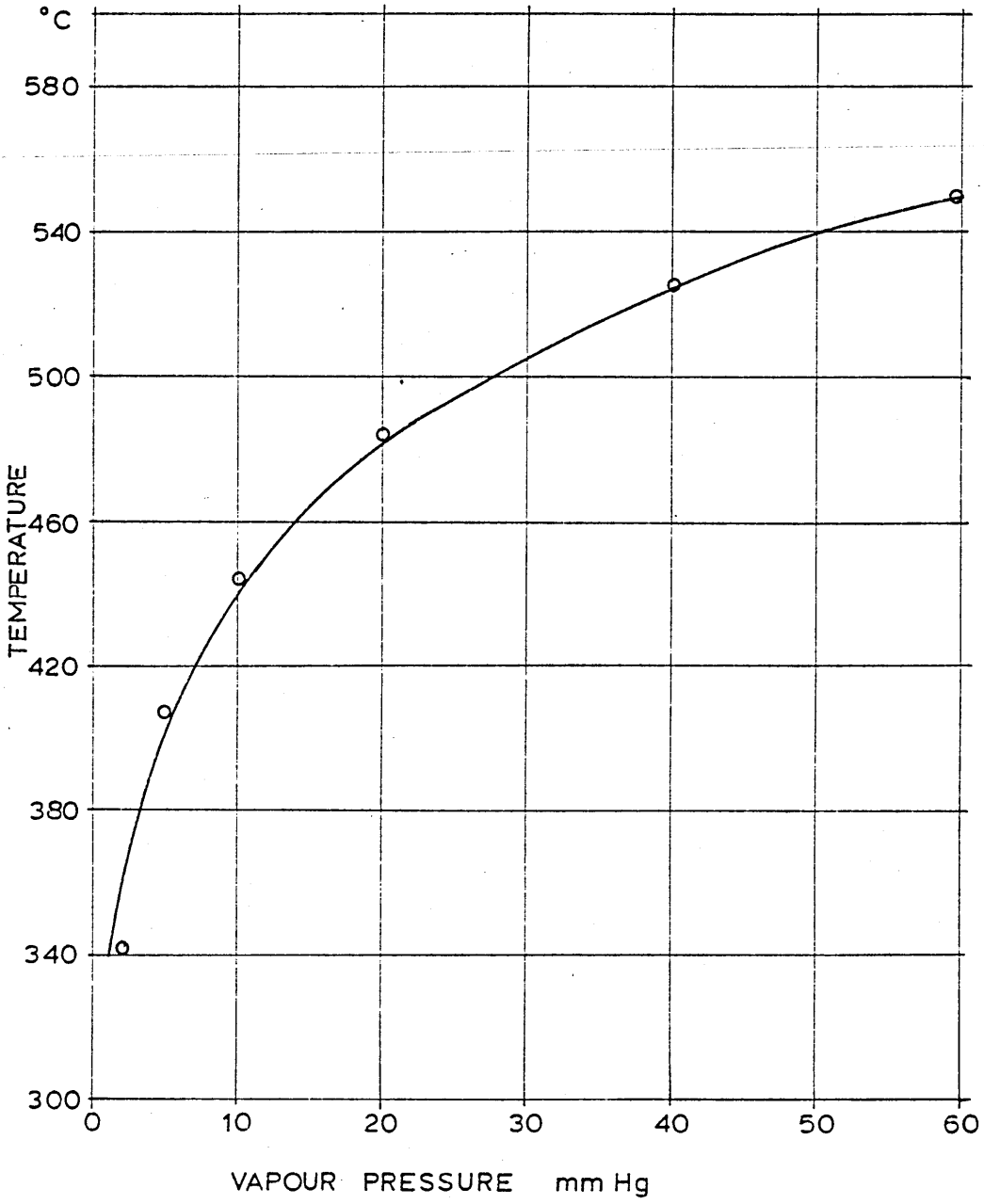

FIG. 3·3 THE VAPOUR PRESSURE OF POTASSIUM AT VARIOUS TEMPERATURES

cooling, the hot zone containing the would be expected to remain hotter than the potassium s e, and the rapid cooling of the source would ensure t he potassium partial pressure dropped very rapidl The argon flow was maintained during cooling so that t oo would help to reduce the potassium vapour pressur

3.5.4(c) Technique

The softening behaviour of Bahira ore cones reduced to different degrees was investig at different potassium vapour pressures.

3.6 The Sealed Tube Experiments

3.6.1 Introduction

In the earlier 'open' tube experiments difficulties had been encountered in retaining volatile components within the test cone and in controlling the composition of the gaseous atmosphere surrounding the cone. The purpose of this work was to try to develop a new method by which the softening behaviour of different ores in various controlled atmospheres could be studied.

3.6.2 General Description of the Sealed Tube System

A diagram of the sealed tube apparatus is shown in Figure 3-4.

Cones were prepared as described in section 3.3.3, and pre-reduced as described in section 3.5.2(b).

The base upon which the cone stands in the silica tube was made from C60 alumina cement. This base was made using a brass mould. Vaseline was used to prevent the cement from sticking to the brass mould. After the cement had been allowed to set it was fired in a furnace at 1000^{o}C to ensure that no water remained within.

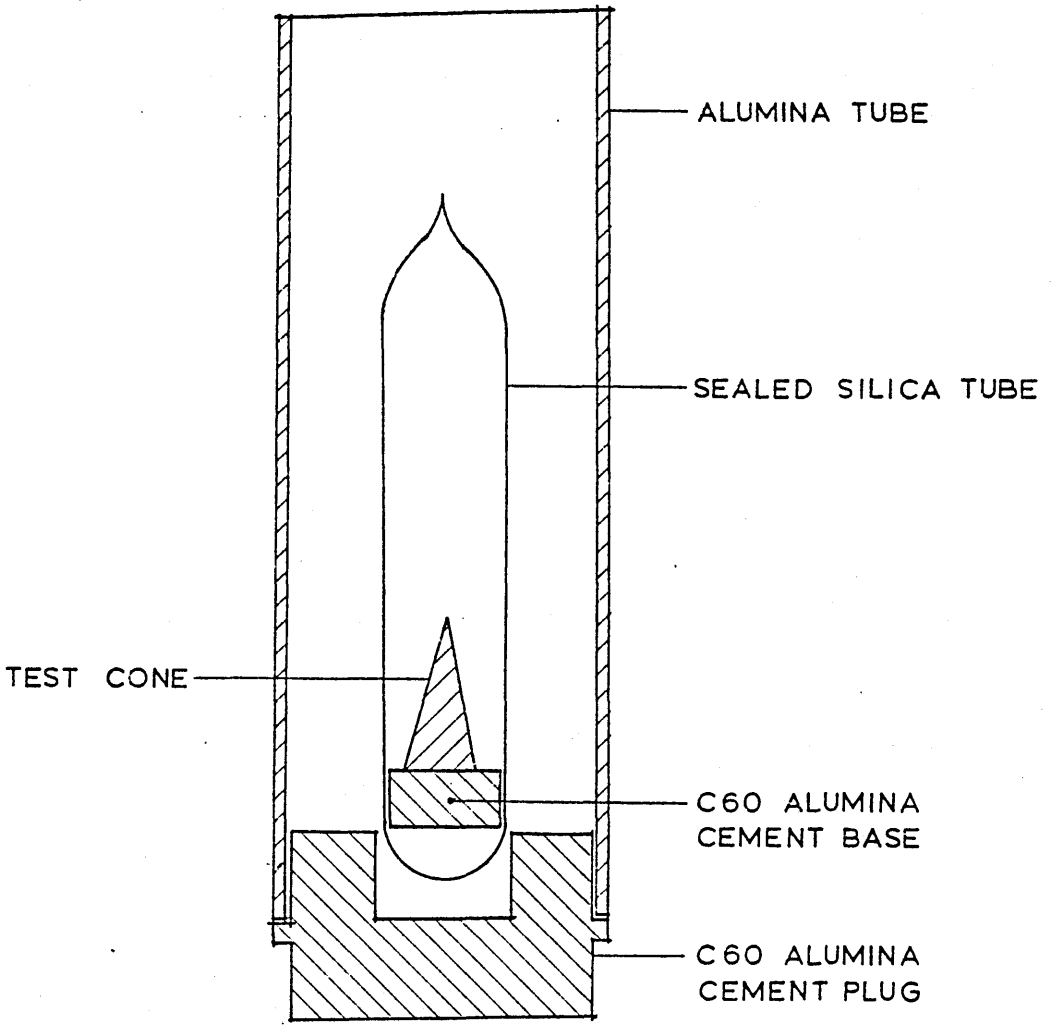

FIG. 3.4 A DIAGRAM OF THE SEALED SILICA TUBE APPARATUS

The cone was fixed to the base with a little C60 alumina cement, introduced into a furnace and heated to 1000°C in an argon atmosphere. This was carried out to ensure that the cone and cement were thoroughly dry before being sealed in a silica tube. In later experiments the cone was supported on stainless steel (18% mass % Cr, 8 mass % Ni) wire fixed in the C-60 alumina cement base to prevent any reaction between the cone and the base.

A 1.7cm diameter silica tube of length about 9cms was used to encapsulate the cone on its cement base. After encapsulation the silica tube was supported on an alumina plug surrounded by a short length of alumina tube and the whole assembly introduced into a vertical tube furnace.

3.6.3 The Encapsulation Technique

After sealing one end of a length of silica tube, using an intense oxidising oxy-acetylene flame, the pre-reduced iron ore cone fixed to the cement base was introduced into it so that the base rested at the sealed end of the tube. A narrow neck was drawn down at a distance of about 9cm from the sealed end using an intense oxidising oxy-acetylene flame. The silica tube was then connected to a vacuum system which was also connected to a gas supply. (Argon or nitrogen according to the gas phase required in the sealed silica tube). A vacuum was applied to the silica

tube until the vacuum gauge reading indicated 0 mm of mercury pressure. The argon or nitrogen was then allowed to fill the silica tube to a pressure of 760mm of mercury. This cycle of evacuating and filling with the required gas was repeated three times to ensure complete flushing. The silica tube was finally filled with inert gas at a pressure of 100mm of mercury. At 1200^{o}C this produced a pressure of one atmosphere inside the tube. A neutral low intensity oxy-acetylene flame was applied to the narrow neck, thus sealing the tube and permitting it to be separated from the remaining length of tube.

In some sets of experiments, elemental sulphur was introduced into the silica tube before introducing the cone to be tested. This was carried out as follows. A known mass of elemental sulphur was introduced into the tube using a long steel spoon, with the sulphur held in a paper container. The container holding the sulphur was emptied at the sealed end of the silica tube and removed, thus ensuring that no sulphur was spilled.

In other sets of experiments a pre-determined amount of an alkali metal compound was introduced in a stainless steel crucible into the silica tube. After introducing the test cone on its base a neck was drawn down about 2cm above the tested cone. The crucible was introduced so that it was supported in the upper half of the silica tube by the neck.

The tube was sealed under a pre-determined gas pressure as described before. Plate 3-2 illustates a sealed silica tube with a crucible of alkali metal compound within it.

3.6.4 The Furnace Used in the Sealed Tube Experiments

As shown in Figure 3-5, a vertical tube furnace heated by silicon carbide elements was used. The temperature of the silica tube was measured using two Pt/Pt-13 mass % Rh thermocouples. The upper plug was provided with two holes to introduce the two thermocouples. The lower plug served as a holder for the sealed silica tube. The plugs were cast from C60 alumina cement using a wooden mould. The sealed silica tube was enclosed in an alumina tube, 13cm in length, to minimise the development of a temperature gradient inside the sealed silica tube. The 13cm alumina tube was connected to a 15cm alumina tube by means of the lower plug. The lower alumina tube was connected to an A.I.S.I.304 stainless steel, (18 mass % Cr-10 mass % Ni), tube by another cement plug. The stainless steel tube was used because it was found that repeated heating and cooling of a single alumina tube lea to severe spalling.

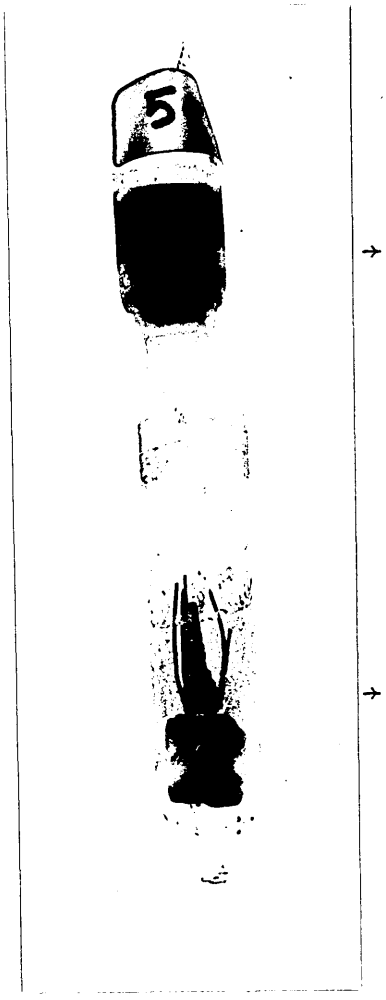

Plate 3-2: Sealed silica tube having test cone and alkali metal container.

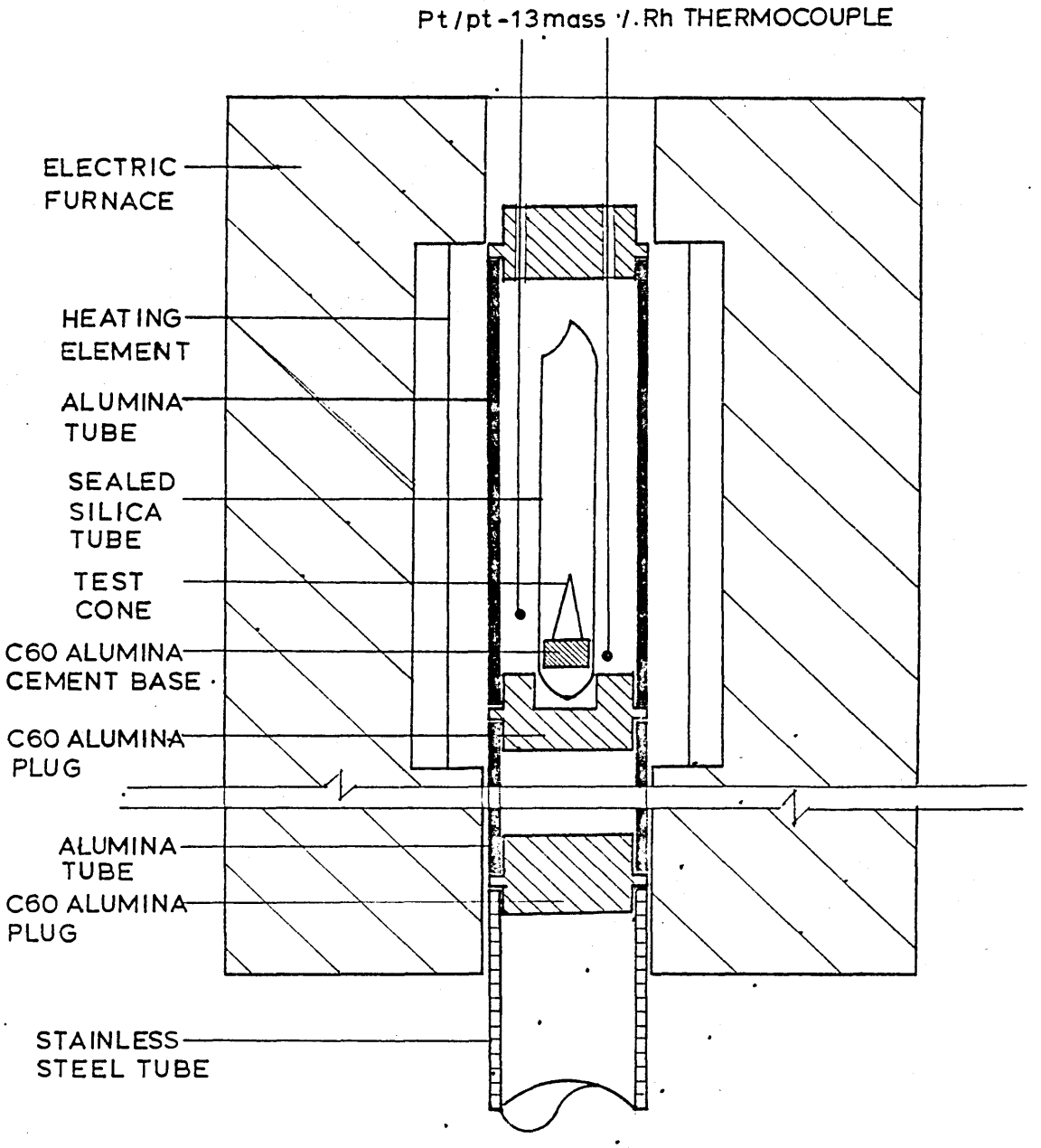

FIG. 3·5 A DIAGRAM OF THE APPARATUS ASSEMBLED USED FOR THE SOFTENING TEST OF THE SEALED SILICA TUBE TECHNIQUE

3.6.5 Procedure

The extent of the hot zone in the furnace used was determined. The hot zone was found to begin 26cm from the end of the furnace and was 9cm in length.

The progress of a typical experiment was as follows. The sealed silica tube was fixed vertically in the alumina plug and the parts of the apparatus assembled as shown in Figure 3-5. The power for the furnace could then be switched on. When the temperature of the silica tube reached 1000^{o}C, the power for the furnace was switched off and the furnace allowed to cool. When the temperature of the silica tube had fallen to 200^{o}C the stainless steel tube was pushed up to a pre-determined position so that the 13cm long alumina tube protruded out of the furnace. The state of the cone inside the sealed silica tube could then be examined.

This procedure was repeated for a temperature of 1030^{o}C and so on at 30^{o}C intervals until either one of the five softening criteria was observed (section 3.9.1) or 1230^{o}C was reached. 1230^{o}C was considered to be the maximum possible operating temperature allowable for the silica tube. Once the softening temperature had been identified within a 30^{o}C range the test was again repeated at 10^{o}C intervals until softening of the sample within the sealed silica tube became visible.

3.7 The Development of Sealed Tube Technique

3.7.1 Initial Experiments

It was initially planned to investigate the softening behaviour of pure Fe_2O_3 cones reduced to various degrees. Fe_2O_3 powder was reduced to the required degree, mechanically mixed/binding agent with the and then moulded into a cone using the method described in section 3.3.3. The cones were fired to 1100°C in a horizontal tube furnace in a flowing stream of pure argon. Each cone was then attached to a C60 cement base as described in section 3.6.2. Each cone was encapsulated in a silica tube at a pre-determined gas pressure and composition as described in section 3.6.3. Softening tests were then carried out in the vertical furnace, described in section 3.6.4.

It was noted that a red deposit tended to form on the inner wall of the silica tube in the proximity of the iron oxide cone during softening tests at temperatures greater than 1050°C. At the same time, a white deposit tended to form on the inner wall of the silica tube above the red deposit. This is illustrated in Plate 3-3. Qualitative chemical analysis of the white deposit showed it to be predominantly an oxide of silicon, probably SiO_2. Traces of iron, nickel, aluminium and calcium were also detected. The aluminium

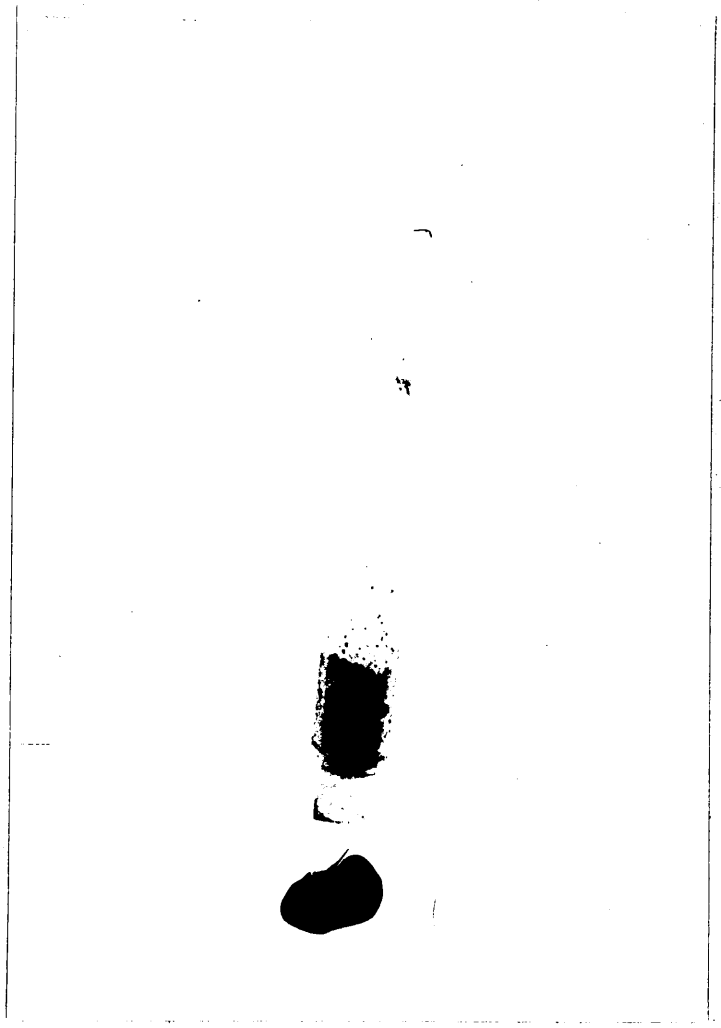

Plate 3-3: The red deposit in the proximity of the test cone in sealed silica tube.

and calcium probably originated from the binding material in the cement base. The red deposit was analysed using the scanning electron microscope. This confirmed the existence of iron, aluminium, silicon and sodium as constituents of the red deposit.

It was suggested that the red deposit might be due to a temperature gradient inside the tube which developed during the cooling period, causing constituents to evaporate from the cone and cement base and to condense on the inner wall of the silica tube. Another possibility was that infra-red radiation from the heating element made the cone hotter than the wall of the silica tube, causing evaporation from the cone and condensation on the wall of the silica tube.

It was therefore, decided to try and determine what temperature gradients existed within the tube and to modify the apparatus so that these temperature gradients would be minimised.

3.7.2 Determination of the Temperature Distribution in the Silica Tube System

The object of this exercise was to determine the temperature distribution throughout the silica tube and to obtain a correlation between the temperature of the outside of the silica tube and the actual temperature of the tested cone. Three thermocouples were arranged as follows. The first thermocouple was inserted inside the lower third of the tested cone. The second thermocouple was inserted inside the C60 alumina cement base. The third thermocouple was attached by a platinum wire to the outer surface of the silica tube. The upper end of the silica tube was left open. The thermocouples used were Pt/Pt-13 mass % Rh. For each temperature measurement a correction for the compensating leads was added. A Northrup Speedomax WA multipoint chart recorder was employed to monitor the thermocouple outputs. The required temperature was produced by different control positions on the temperature recorder. Five minutes was allowed before each measurement to ensure temperature stabilisation. The arrangement of the thermocouples is shown in Figure 3-6. Table 3-6 presents the temperature readings observed.

In a second experiment the temperature distribution was determined with the thermocouples in the same position as

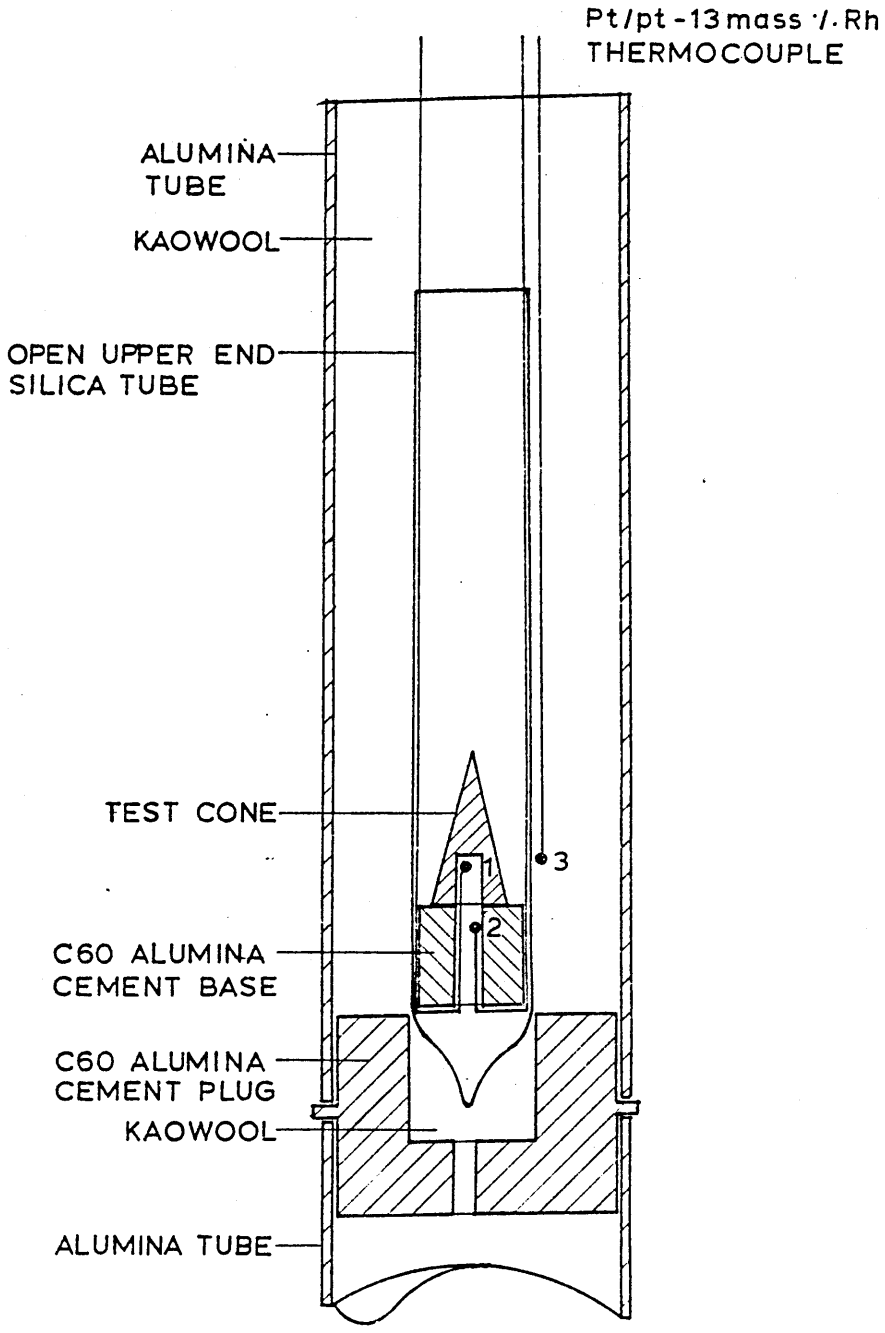

FIG. 3.6 A DIAGRAM SHOWING THE ARRANGEMENT OF THERMOCOUPLE IN THE OPEN SILICA TUBE

Table 3-6: Temperature reading at the different points in silica tube system °C - open tube

Temp. Inside the Cone	Temp. Inside the Cement Base	Temp. Outside Silica Tube	Temp. Inside the Cone	Temp. Inside the Cement Base	Temp. Outside Silica Tube
758	757	760	1167	1154	1172
764	760	766	1180	1163	1183
864	856	868	1182	1164	1184
981	979	985	1194	1166	1196
991	990	992	1194	1166	1196
1069	1049	1072	1200	1161	1201
1111	1096	1113	1200	1161	1201
1111	1106	1115	1204	1163	1206
1144	1129	1145	1210	1161	1210
1148	1134	1157	1210	1161	1211
1156	1156	1157	1211	1170	1211

before but with the upper end of the silica tube sealed. Figure 3-7 shows the difference in temperature between the inside of the test cone, the inside of the cement base and the outside wall of the silica tube. Table 3-7 gives the results of these measurements. From these measurements a temperature difference of up to 18°C was sometimes recorded between the test cone and the outside wall of the silica tube.

3.7.3 The Enclosure of the Silica Tube in a Graphite Block

In an attempt to obtain a more uniform temperature throughout the system, the silica tube was enclosed in a graphite block. Graphite was chosen because of its high thermal conductivity.

A mould was shaped from a graphite rod. The inner diameter of the carbon mould was 1.8cm whilst its outer diameter was 3.8cm. The outer diameter of the silica tube was 1.7cm and the inner diameter of the alumina tube was 3.9cm.

The end of the silica tube was sealed with C60 alumina cement. The lower third of the iron ore cone was hollowed out. A thermocouple was inserted in the lower third of the cone. In addition to measuring the temperature, this thermocouple also served as a support for the cone. A second

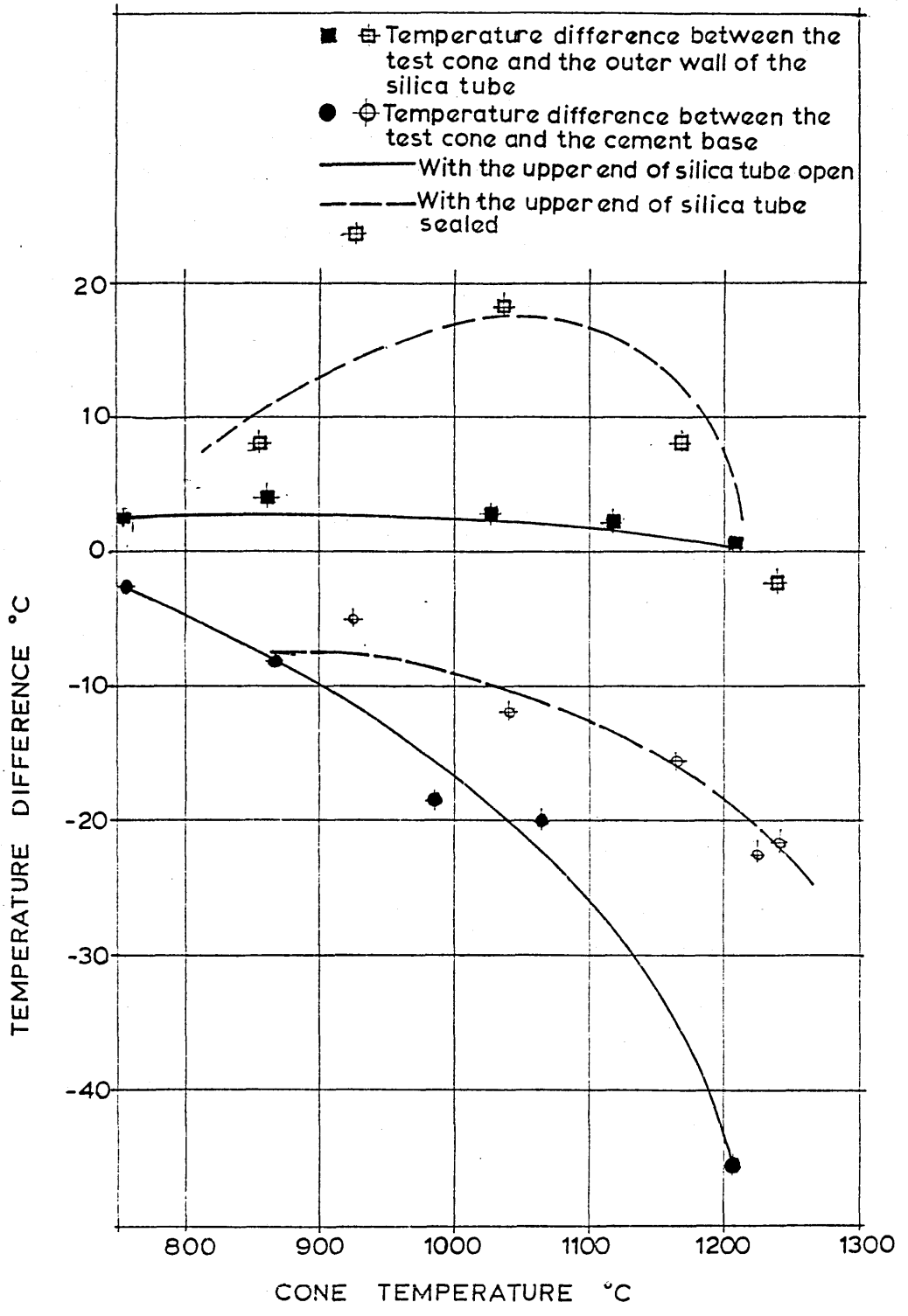

FIG. 3.7 THE TEMPERATURE DIFFERENCE BETWEEN THE INSIDE OF THE TESTED CONE, THE CEMENT BASE AND THE OUTER WALL OF THE SILICA TUBE

Table 3- 7: Temperature reading at the different points in silica tube system in ^{o}C - closed tube

Temp. Inside the Cone	Temp. Inside the Cement Base	Temp. Outside the wall of Silica Tube	Temp. Inside the Cone	Temp. Inside the Cement Base	Temp. Outside the wall of Silica Tube
854	844	862	1056	1039	1061
854	844	862	1166	1153	1178
854	848	862	1174	1154	1179
900	898	937	1172	1154	1179
917	908	946	1172	1155	1179
928	927	950	1172	1157	1179
937	931	956	1164	1153	1179
937	929	956	1225	1200	1227
931	927	956	1229	1204	1229
1013	1013	1043	1232	1215	1233
1032	1017	1050	1240	1220	1237
1050	1033	1068	1240	1216	1237
1050	1039	1069			

thermocouple was inserted between the inner wall of the graphite mould and the outer wall of the silica tube. The top of the alumina tube containing the graphite mould was sealed with Kaowool. A Northrup Speedomax WA multi-point millivolt recorder was used to monitor the output from the thermocouples. Figure 3-8 shows the arrangement of the system. The temperatures indicated by the thermo-couples are given in Table 3-8.

A temperature difference of up to 135^{o}C was recorded which is much greater than in the absence of the graphite mould.

A trial to minimise this temperature difference by increas-ing the air gap between the silica tube and the graphite mould to 0.25cm was carried out. Table 3-9 gives the temperature recorded with an air gap of 0.25cm.

Comparing the results in Tables 3-8 and 3-9 it is clear that increasing the air gap increases the temperature diff-erence between inside of the cone and the outside wall of the silica tube.

A further experiment was carried out to determine the mag-nitude of the temperature drop across the air gap between the silica tube and the graphite mould. One thermocouple was fastened to the outer surface of the silica tube while

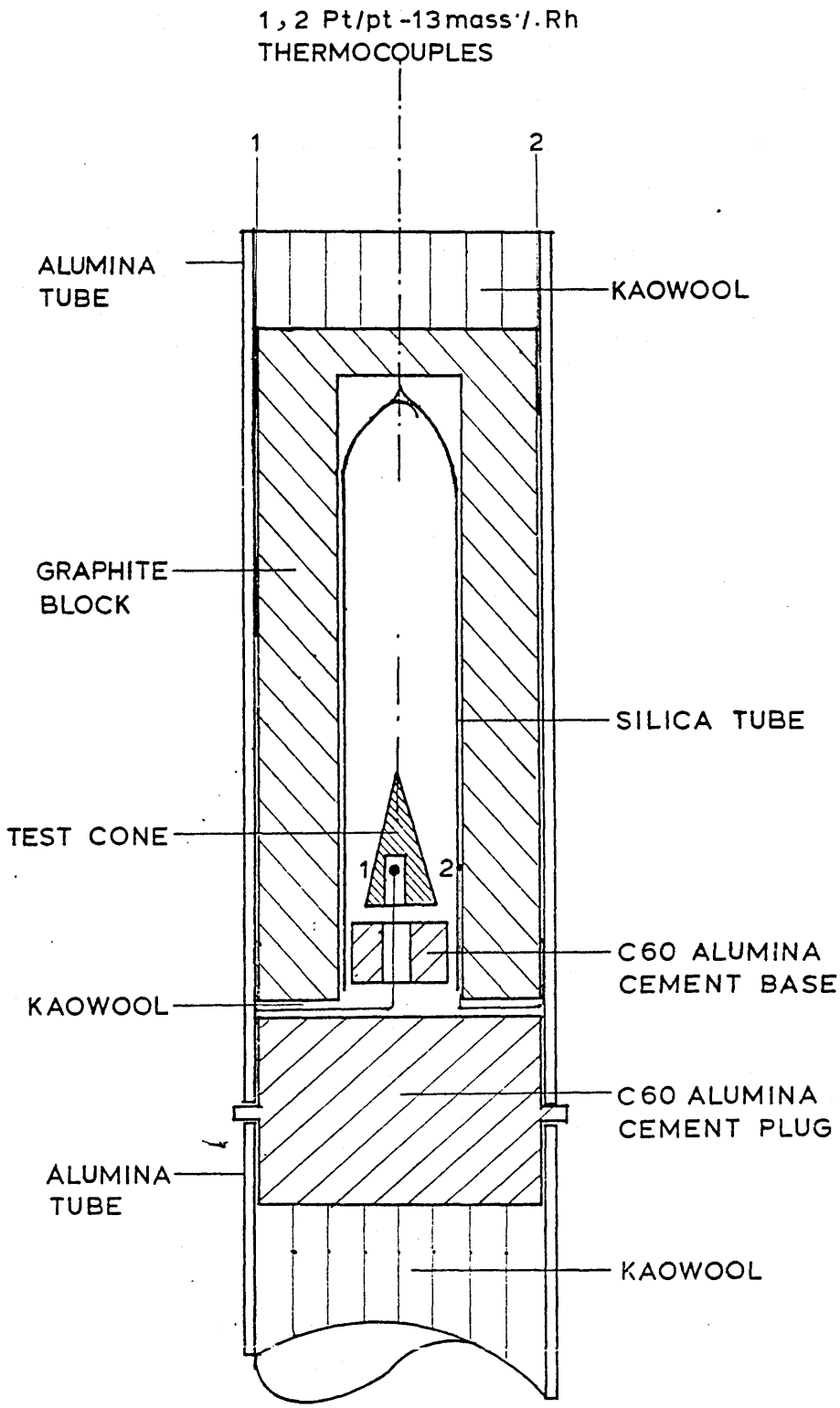

FIG. 3.8 DIAGRAM SHOWS THE ARRANGEMENT OF THERMOCOUPLES IN SILICA TUBE SYSTEM ENCLOSED IN A GRAPHITE BLOCK

Table 3-8: Temperature differences betwe[illegible]de of the test cone and the outside wa[illegible]ilica tube in °C - silica tube enclosed[illegible]ite block

Temp. Inside the Cone	Temp. Outside the Silica Tube	Temperature Differences	Temp. Inside [illegible] Cone	[illegible]. [illegible] Si[illegible] the Tube	Temperature Differences
710	762	52	955	07	152
711	770	59	1007	28	121
779	863	84	108[illegible]	215	135
776	856	80	108	214	126
789	862	73	10[illegible]	160	97

Table 3- 9: Temperature readin[illegible]ins[illegible]he cone and outside the silica tube wi[illegible]a[illegible]p 0.25cm between the silica tube and t[illegible]aph[illegible]ould in °C

Temp. Inside the Cone	Temp. Outside the Silica Tube	Temperature Differences	[illegible]emp [illegible]de Cor[illegible]	Temp. Outside the Silica Tube	Temperature Differences
783	927	144	014	1187	173
813	963	150	016	1206	190
898	1066	168	101	1203	186
910	1077	167	102	1203	183
924	1078	154	10[illegible]	1202	183

a second thermocouple was placed in the air gap. Figure 3-9 shows the thermocouple arrangement used and Table 3-10 gives the temperature readings obtained.

From Table 3-10 a temperature difference up to 44^{o}C was established between the outer surface of the silica tube and the air gap between the carbon mould and the silica tube.

Other experiments were also carried out. The upper end of the carbon mould was left unsealed, except for a layer of Kaowool. The sealed end of the silica tube was placed upwards whilst its lower end was sealed with Kaowool, as shown in Figure 3-10. One thermocouple was inserted inside the lower third of the cone, a second thermocouple was attached to the inner sealed end of the silica tube and a third thermocouple was suspended free in the air space between the carbon mould and the silica tube. Table 3-11 gives the temperature measurements obtained.

From the above experiments it is clear that an unacceptable temperature gradient was developed in the silica tube system when enclosed in a graphite mould even though graphite has a high thermal conductivity.

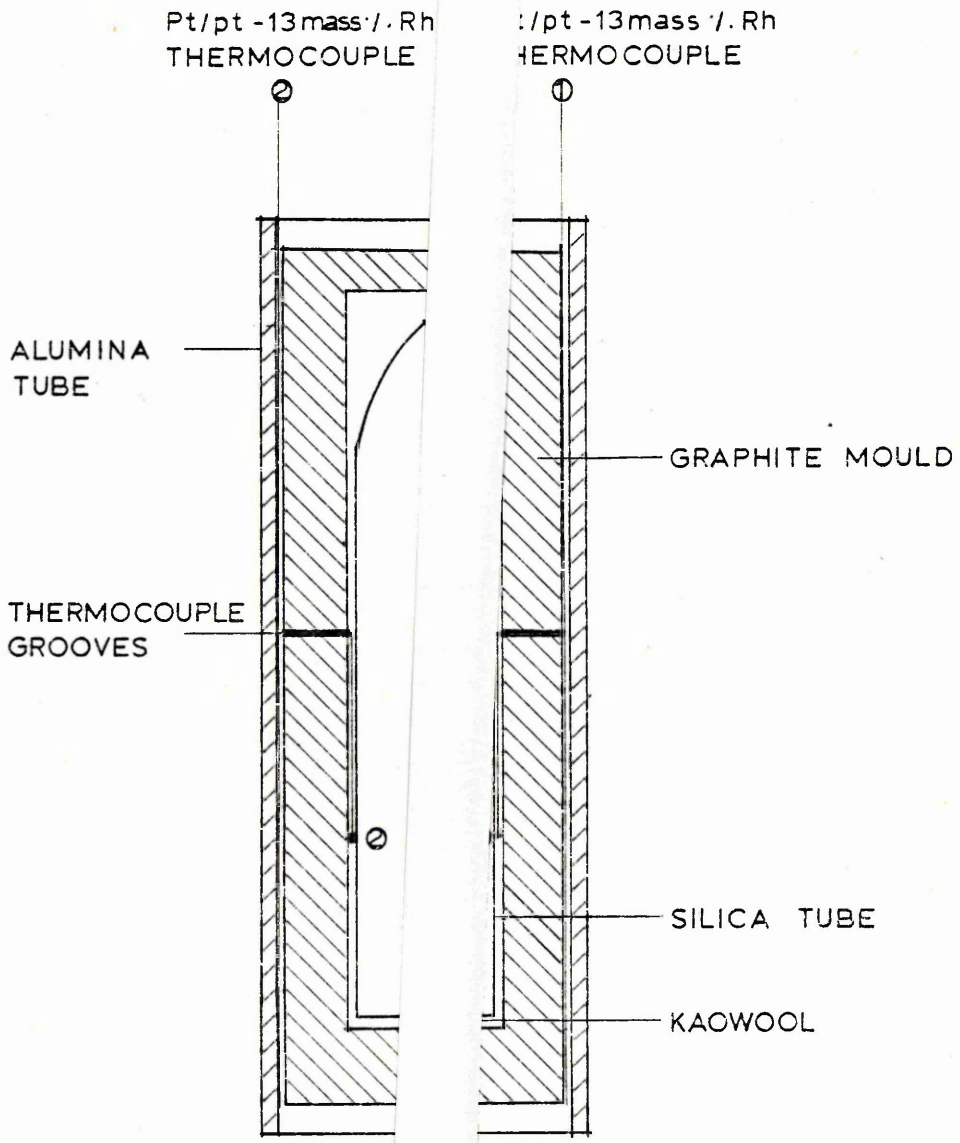

FIG. 3·9 A DIAGRA F THE SILICA TUBE
ENCLOSED GRAPHITE MOULD

graphite mould and the silica tube in °C

Reading of Free Thermo-couple in Air Gap	Temp. of Outer Wall of Silica Tube	Temp. Differ-ences	Reading of Free Thermo-couple in Air Gap	Temp. of Outer Wall of Silica Tube	Temp. Differ-ences
836	833	3	1043	1003	40
837	835	2	1049	1011	38
926	908	18	1053	1020	33
938	914	24	1053	1022	31
944	928	16	1125	1082	43
945	930	15	1127	1093	34
955	935	20	1125	1096	29
1017	982	35	1197	1154	43
1038	989	49	1198	1154	44

Table 3-11 Temperature reading at the different points in silica tube system °C

Temp. Inside the Cone	Temp. Inside the Silica Tube	Temp in Space between Carbon Mould, Silica Tube	Temp. Inside the Cone	Temp. Inside the Silica Tube	Temp. in Space between Carbon Mould, Silica Tube
840	840	840	1029	1147	1152
843	845	847	1088	1205	1211
935	941	946	1092	1210	1214
938	958	951	1093	1210	1214
1028	1146	1148			

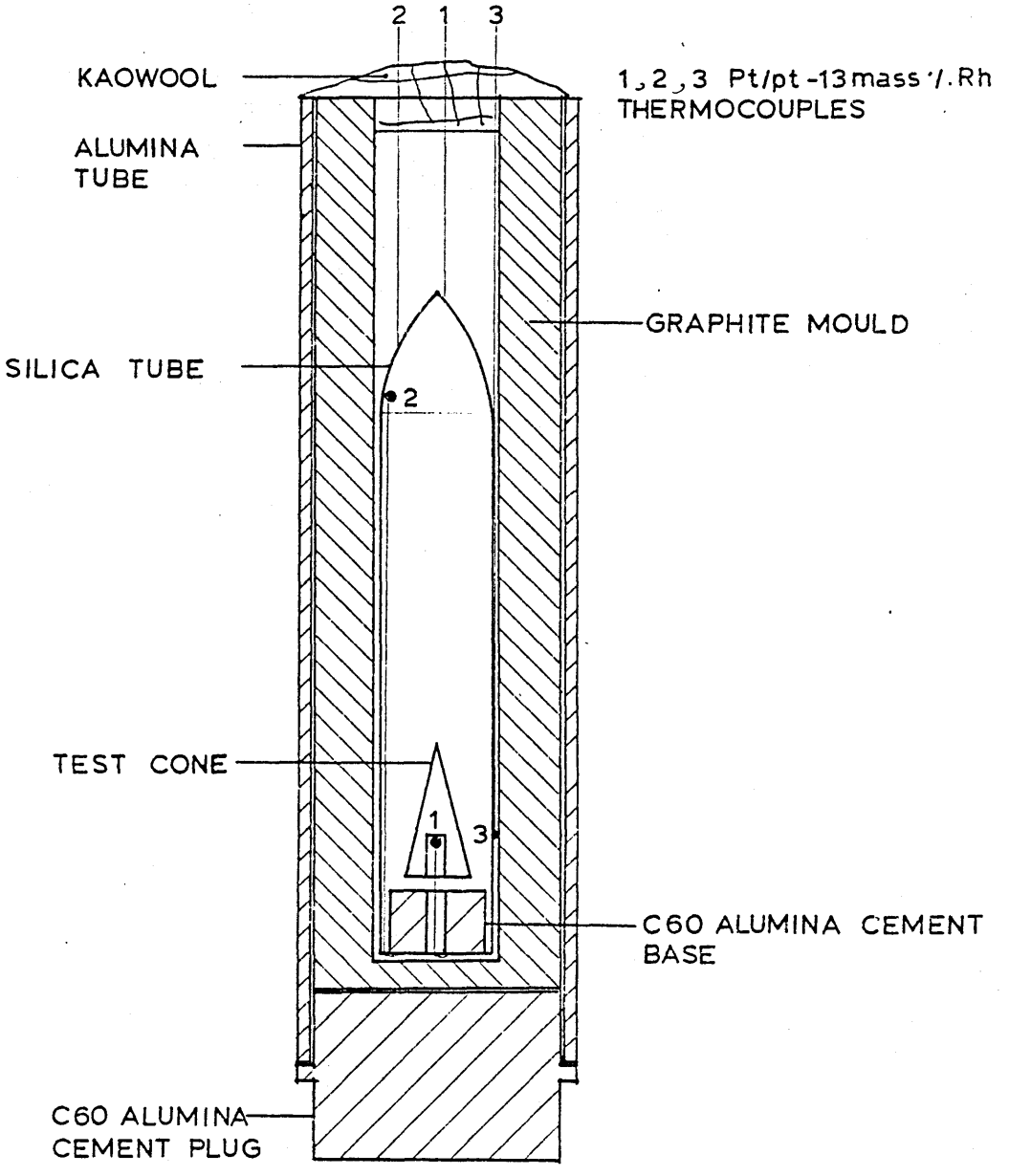

FIG. 3.10 A DIAGRAM SHOWING THE ARRANGEMENT OF THERMOCOUPLES IN SILICA TUBE SYSTEM ENCLOSED IN AN UPPER END OPEN GRAPHITE BLOCK

In order to demonstrate the effect of the graphite mould, an experiment was conducted using the thermocouple arrangement shown in Figure 3-10 but with the graphite mould removed. The results obtained are shown in Table 3-12 and plotted in Figure 3-11. It is clear from the figure that a maximum temperature difference of no more than 15°C was observed, much less than in the presence of the graphite mould.

3.7.4 The Enclosure of the Silica Tube in a Bed of Hollow Alumina Beads

Since the high conductivity graphite mould did not provide an even temperature distribution, an alternative strategy was tried in which the silica tube was enclosed in a bed of hollow alumina beads of very low thermal conductivity. Figure 3-12 shows the arrangement that was used. In the test experiment, three thermocouples were used to measure the temperature of the inside of the cone, the inner upper end of the silica tube, and the outer surface of the silica tube. The temperatures recorded are shown in Table 3-13, which shows that a temperature difference of less than 2°C was recorded between the inside of the cone and the outer surface of the silica tube.

It was therefore, decided to carry out the softening tests in the vertical furnace, using the alumina beads as a enclosure medium for the silica tube and to determine the test temperature by subtracting 2°C from recorded temperature.

in silica tube system in °C

Temp. Inside The Cone	Temp. Inside Upper End of Tube	Temp. Outside of Silica Tube	Temp. Inside The Cone	Temp. Inside Upper End of Tube	Temp. Outside of Silica Tube
776	771	770	1080	1070	1075
780	779	781	1072	1065	1071
850	842	845	1144	1132	1141
854	853	862	1150	1147	1162
862	859	864	1158	1153	1165
959	954	963	1214	1204	1217
961	957	956	1216	1205	1220
962	956	965	1217	1207	1222
1086	1083	1096	1219	1208	1222

Table 3-13 Temperature reading at the different points in silica tube system enclosed in a bed of hollow alumina beads in °C

Temp. Inside the Cone	Temp. Upper End of Silica Tube	Temp. Outside Surface of Silica Tube	Temp. Inside the Cone	Temp. Upper End of Silica Tube	Temp. Outer Surface of Silica Tube
896	896	906	1194	1192	1197
903	903	908	1237	1237	1240
1097	1096	1102	1237	1235	1241
1097	1096	1102	1224	1224	1225
1097	1096	1100	1224	1224	1225
1193	1191	1196	1225	1224	1226

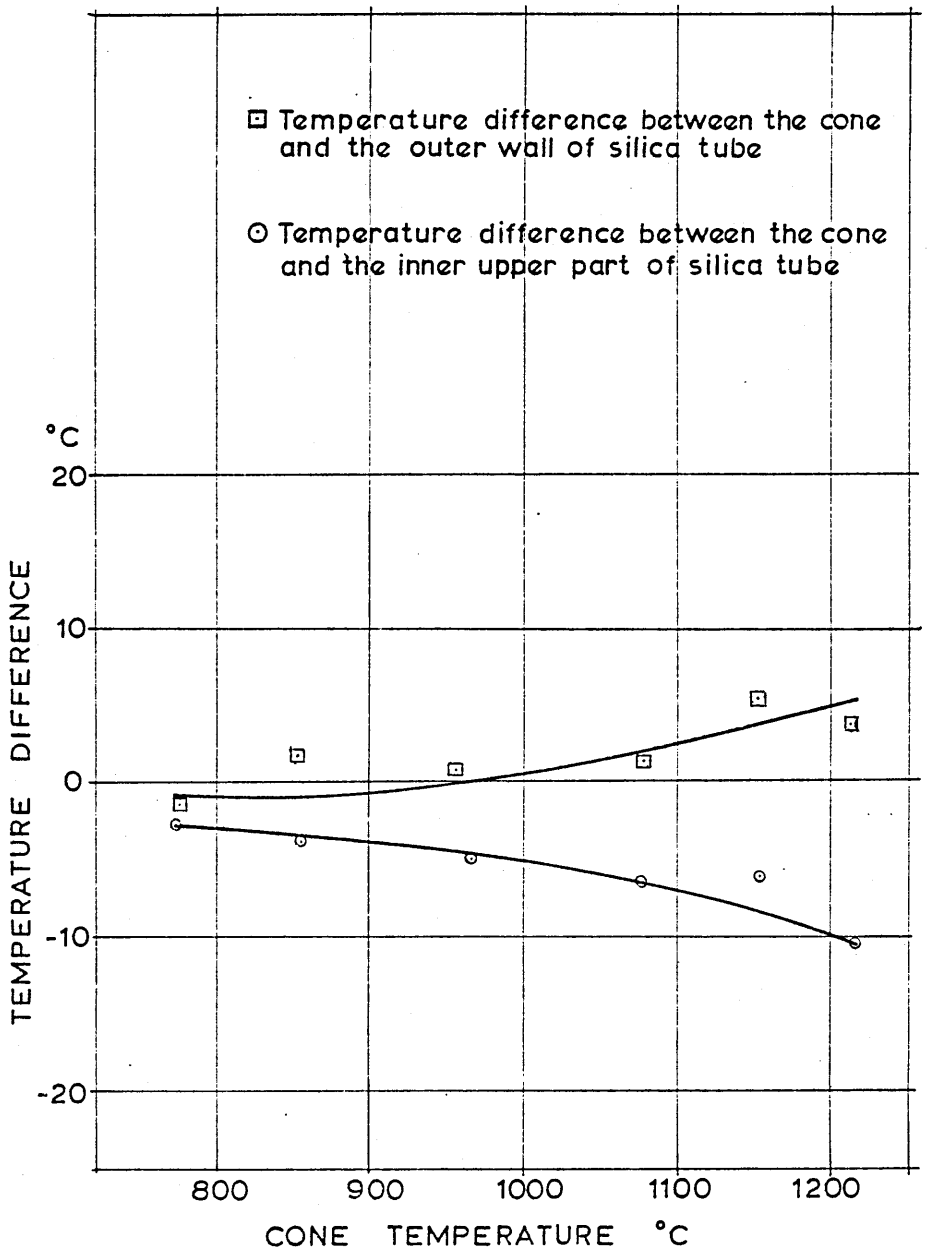

FIG. 3.11 TEMPERATURE DIFFERENCE BETWEEN THE INSIDE OF THE TESTED CONE, THE INNER UPPER END OF THE SILICA TUBE AND THE OUTER WALL OF THE SILICA TUBE AFTER REMOVAL OF THE CARBON MOULD

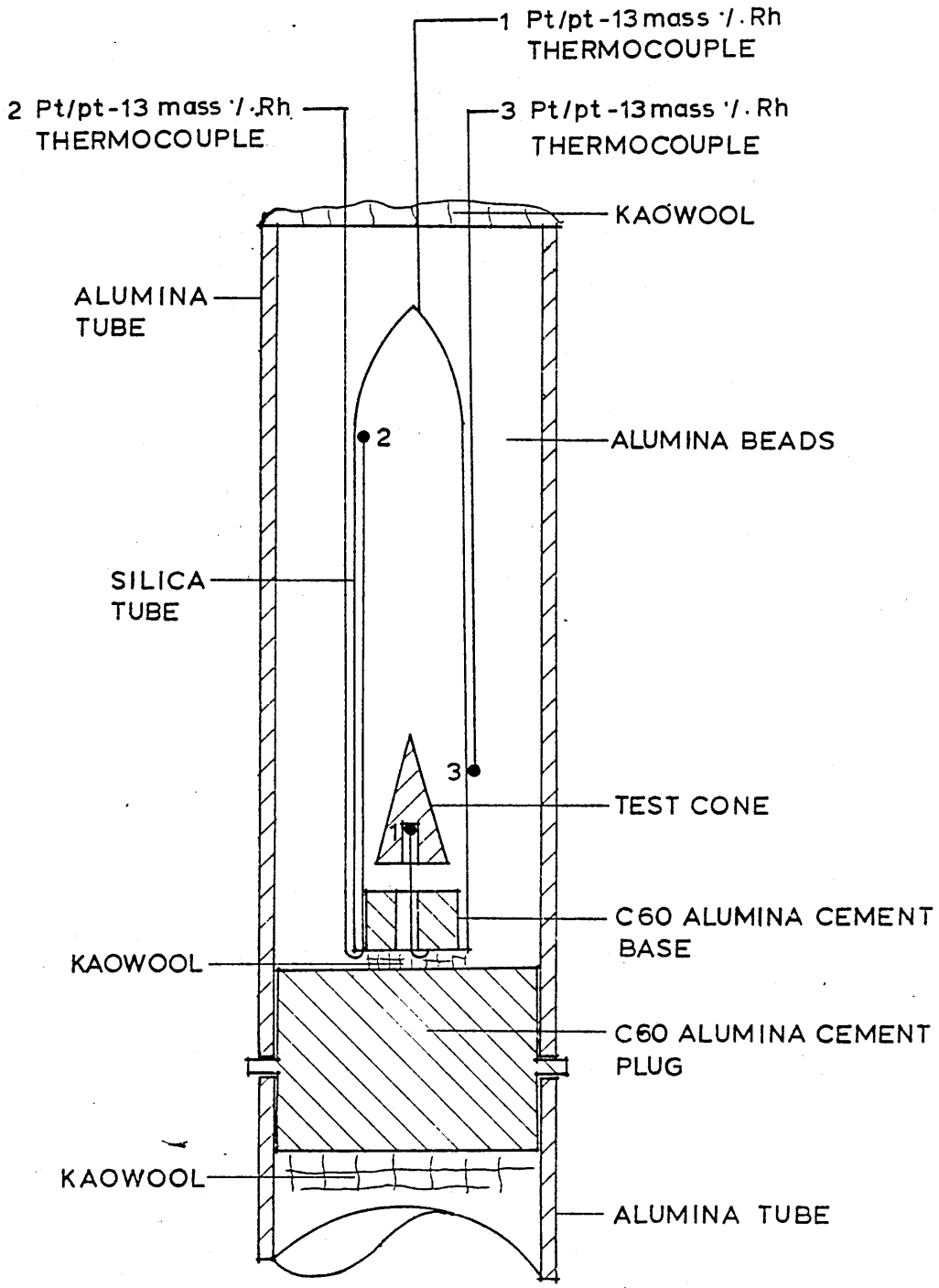

FIG. 3-12 A DIAGRAM OF THE SILICA TUBE ENCLOSED IN HOLLOW ALUMINA BEADS

3.8 Metallographic Examination

3.8.1 Zeiss Photomicroscope

A Zeiss microscope was used to examine and photograph the test cones. Photographs were taken on 35mm F.P.4 film using automatic exposure.

The samples to be photographed were mounted in a cold setting S.P.701 P.A resin using Metset hardener. The samples were vacuum impregnated by means of a vacuum dessicator connected to a single stage rotary pump, vacuum being applied for a maximum of 30 seconds.

Scratches were removed from the surface by rubbing down on 200, 400, 600 silicon carbide papers. Kerosene was used as a cooling agent. The samples were then polished on a 6μ, 1μ, 1/4μ diamond paste wheel until all the scratches were removed. Care was taken to thoroughly wash and dry the samples between each polishing operation.

3.8.2 The Scanning Electron Microscope

Scanning electron micrographs were obtained using a Philips PSEM Scanning Electron Microscope 500 operating at an accelerating voltage of 25kV.

The samples were attached to aluminium specimen stubs by colloidal silver, a vacuum dessicator being used to speed the drying of the colloidal silver.

In order to have a conducting surface the samples were initially coated with gold. However, the energy levels M_α for gold and K_α for sulphur overlap making resolution between the two elements difficult. Carbon coating of the samples was tried as an alternative and was found to give satisfactory results.

The Edax("Energy dispersive analysis of X-rays")which uses energy levels to detect elements down to atomic number 11, i.e. sodium, was used.

The distribution of particular elements was investigated by X-ray mapping by the selection of the energy level of the element being considered e.g. sulphur: 2,307 keV. This map was recorded on film producing a photographic negative.

3.9 Visual Observation of the Softened Cones and Precision of the Assessment of the Softening Temperature

3.9.1 Visual Observation

The softening temperature was assessed by visual observation of the cones. This observation was carried out continuously for the cones heated in the open tube experiments. For the closed tube experiments, the observation was made after the cone had been cooled from the test temperature.

Five different states of the cones were recognised and are shown in Plate 3-4, as indicated in Table 3.14 below.

Table 3.14

State	Run Number
Not softened	90, 91, 89, 120, 116.
Softened	107, 108, 92, 117, 2, 39,44.
Over softened	109, 118, 28, 33.
Melted	3, 40.
Not softened but melt formed	22, 37.

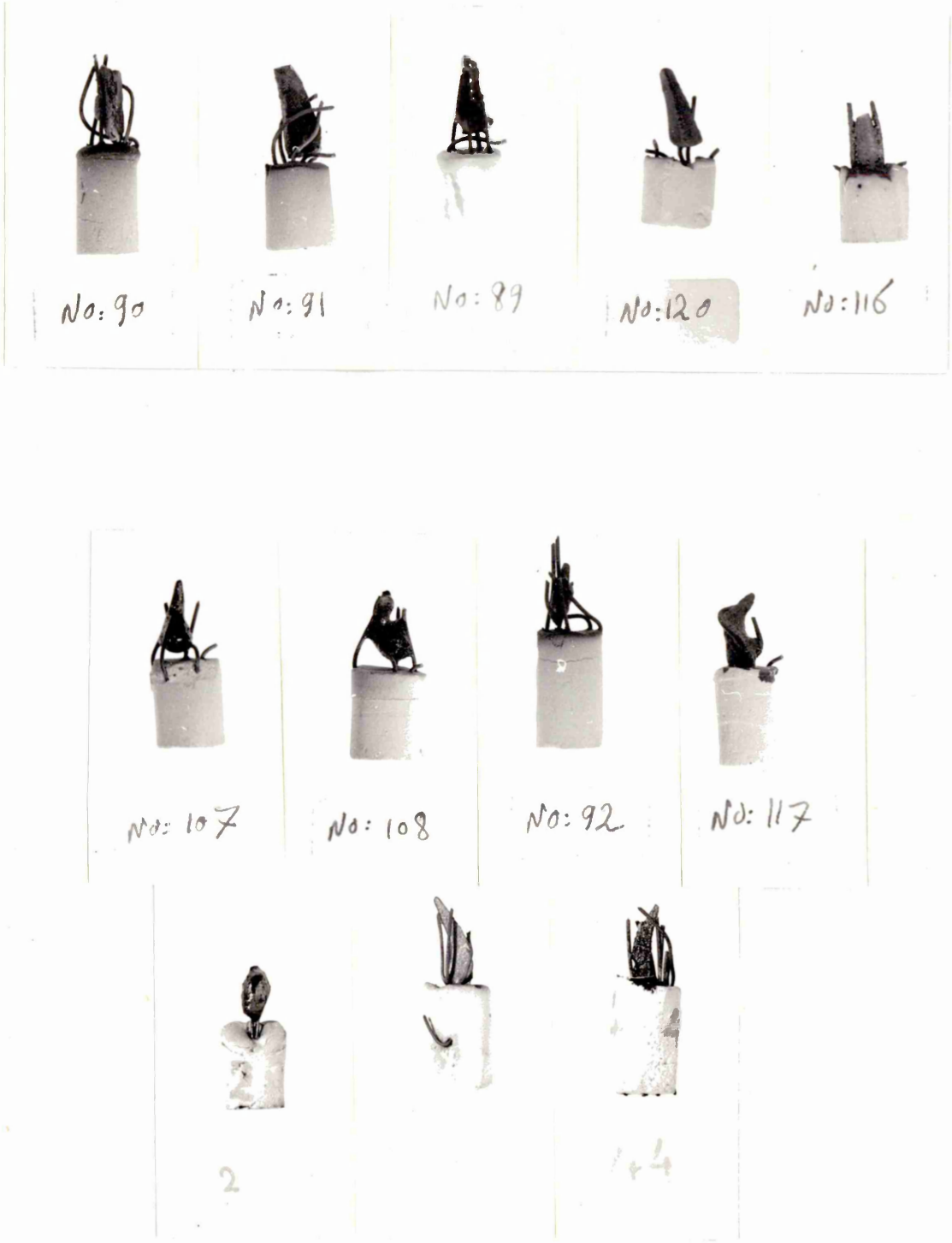

Plate 3-4: Visual observations of the tested cones.

Plate 3-4 continued

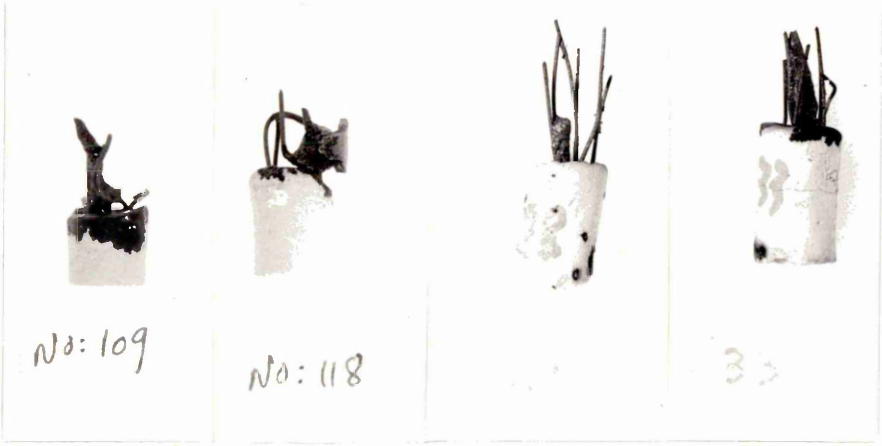

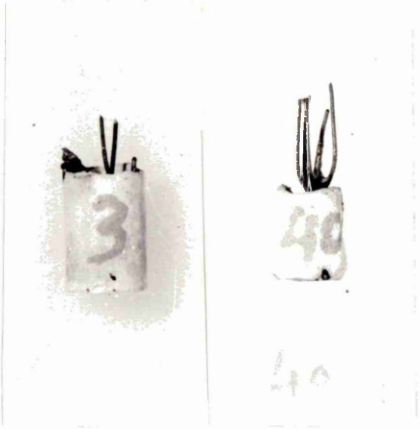

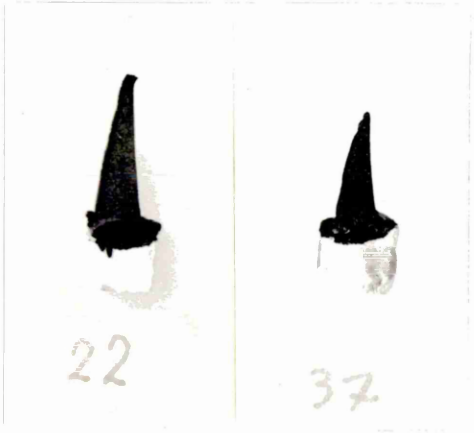

3.9.2 Precision of Assessment of Softening Temperature

The precision that can be allotted to the assessed softening temperature has been estimated by comparing the state of the otherwise identical cones after they had been heated to different temperatures in the softening range for the same period of time. The results of these estimates are shown in Plate 3.4.

The ratio of the mass of iron contained in the cones to the mass of silica was 3.12 except for cones 22 and 37 which were made from iron ore. The additional compositions of the cones, their degrees of reduction, the temperatures to which they had been heated and their assessed states are listed in Table 3.15.

Cones 107 and 108 were heated to the same temperature, within the degree of experimental error and their appearances are almost identical. Cones 91 and 92 respectively showed no softening and softening, the difference between their test temperature being 15°C. Cones 89 and 109 show, respectively, no softening and over softening their respective test temperatures being 1152°C and 1182°C. However cone 109 had been previously heated to 1168°C after which its appearance corresponded to the softened state.

Similarly cones 120 and 118 respectively show softening and over softening after heating to test temperatures 20°C apart, but cone 118 had shown a softening appearance after

Table 3.15

Cones	Additional Composition	Deg. Red.	Test Temp.	Assessed State
107	1.75 mass % Na_2CO_3	49.7%	1161°C	Softened
108	1.735 mass % Na_2CO_3	49.7%	1162°C	Softened
90	2 mass % Na_2CO_3	7.3%	1189°C	Not Softened
91	2 mass % Na_2CO_3	7.3%	1213°C	Not Softened
92	2 mass % Na_2CO_3	7.3%	1228°C	Softened
89	2 .35 mass % Na_2CO_3	49.7%	1152°C	Not Softened
109	2.37 mass % Na_2CO_3	49.7%	1182°C	Over Softened
120	1.87 mass % Na_2CO_3	71%	1153°C	Not Softened
118	1.9 mass % Na_2CO_3	71%	1173°C	Over Softened
116	1.3 mass % Na_2CO_3	71%	1157°C	Not Softened
117	1.3 mass % Na_2CO_3	71%	1173°C	Softening
2		32%	1214°C	Softening
3		32%	1228°C	Melting
28		7.3%	1237°C	Over Softening
40		7.3%	1236°C	Melting
39		7%	1186°C	Softened
44		7%	1190°C	Softened
33		7%	1204°C	Over Softened
22	Bahira Iron Ore	4%	1217°C	Not Softened but melt formed
37	Bahira Iron Ore	52%	1200°C	Not Softened but melt formed

being heated to the intermediate temperature of 1163°C. Cones 116 and 117, heated to 1157°C and 1173°C, show no softening and softening whereas cones 2 and 3, heated respectively to 1214°C and 1228°C, show softening and melting. Cones 28 and 40, heated virtually to the same temperature again, showed over-softening and complete melting. Cones 39, 44 and 33 were of identical composition and degree of reduction. They had been heated to 1186°C, 1190°C and 1204°C respectively under sulphur vapour pressure of one atmosphere. Cones 39 and 44 showed virtually identical states of softening whereas cone 33, heated to a temperature 14°C above cone 44, showed the beginning of an over softened state.

The results do not provide a precise value of the precision with which the softening temperature has been determined, but do show that it is likely to be no worse than $\pm 5^{\circ}C$. This degree of precision, then, has been allotted to all the softening temperatures presented in the results section of the thesis. Cones 22 and 37 showed a state that occurred on rare occasions. The cone had not softened and still retained its sharp edges. However a melt phase had formed that was sufficiently fluid to run out of the cone and form a pool of liquid on the cement base.

The precision of $\pm 5^{\circ}C$ allotted to the measurement of softening temperature is certainly in keeping with the use of Seger cones. Standard Seger[61] cones can be obtained that soften at 10°C intervals, so that the precision allotted to their softening temperatures is certainly better than $\pm 5^{\circ}C$.

4.1 OPEN TUBE RESULTS

4.1.1 The Softening Behaviour of Wustite in Argon

According to the data given in Table 4-1 the mean softening point of a wustite cone in argon is 1379°C, while the theoretical melting temperature of wustite is 1370°C.[14] The softening temperature is taken to be the temperature at which the cone bends completely as shown Plate 4-1.

4.1.2 The Softening Behaviour in Argon of Pure Fe_2O_3 Reduced to Various Degrees

Table 4-2 shows that cones produced from pure Fe_2O_3 reduced to different degrees showed no evidence of softening even when heated to temperatures in excess of 1250°C, the maximum limit of the furnace used. Since no softening was observed in these initial experiments, a series of experiments was carried out with a view to establishing the validity of studying softening using cones of blast furnace burden constituents. The cones used in these experiments all contained varying amounts of FeS.

4.13 The Softening Behaviour of Cones Containing FeS

4.1.3 (a) The Softening Behaviour of Ferrous Sulphide Cones in Argon

According to the data in Table 4-3 the mean softening point of a ferrous sulphide cone in an inert atmosphere (argon) was 1023°C, while the theoretical melting point of ferrous sulphide is 1190°C.[14]

Table 4-1 The Softening Behaviour of Wustite in Argon

Sample No.	Test Temperature ^{o}C	Observation
1	1220	A decrease in the height of the cone was noticed.
	1300	More noticeable decrease in the height of the cone.
	1370	Softening.
2	1220-1300	0.4cm decrease in the height of the cone.
	1300-1340	Another 0.3cm decrease in the height of the cone.
	1385	Softening.
3	1200-1320	0.4cm decrease in the height of the cone.
	1380	The cone started to bend.
	1382	Softening.

Plate 4.1: The softening of a tested cone.

Table 4-2 The Softening Behaviour of Partially Reduced Fe_2O_3 Cones in Argon

Sample No.	Degree of Reduction	Test Temperature °C	Observation
1	3%	1220	No Softening
2	16.9%	1220	No Softening
3	42.1%	1227	No Softening
4	55.4%	1220	No Softening
5	70.2%	1234	No Softening
6	85.3%	1229	No Softening
7	100%	1234	No Softening

Table 4-3 The Softening Behaviour of Ferrous Sulphide Cones in Argon

Sample No.	Test Temperature °C	Observation
1	1010	Decrease of the cone height
	1030	Softening.
2	980	The cone begins to collapse
	1020	Softening
3	1020	Softening

4.1.3 (b) The Softening Point of FeS-Fe Cones

(FeS: 32 mass%; Fe: 68 mass %)

From Table 4-4, it can be seen that no softening occurred for these FeS-Fe cones up to the maximum available temperature, 1380°C, at which the furnace could be operated. Chemical analysis carried out on the FeS-Fe cones tested at 1380°C showed 2.45 mass % sulphur content. Plate 4-2 shows these cones after testing.

4.1.3 (c) The Softening Behaviour of FeS-FeO Cones

(FeS: 57 mass%; FeO: 43 mass %)

According to the data in Table 4-5, the mean softening point of FeS-FeO cones containing 57 mass % FeS and 43% mass % FeO is 982°C in argon. This is a little bit above the melting temperature of the ternary Fe-O-S eutectic which is 915°C[14].

4.1.3 (d) The Softening Behaviour of FeS-SiO_2 Cones

(FeS: 50 mass %; SiO_2: 50 mass %)

The investigation of the softening of FeS-SiO_2 (50 mass % - 50 mass %) cones at a constant argon flow rate of 2 dm^3/minute, at a constant furnace pressure of 60mm water gauge and at constant heating rate, showed that no softening occurred at temperatures up to 1400°C. This indicated that no reaction occurred between SiO_2 and FeS under these cond-

Table 4-4 The Softening Behaviour of FeS-Fe Cones

(FeS:32 mass % - Fe: 68 mass %)

Sample No.	Test Temperature °C	Observation
1	1380	No Softening
2	1380	No Softening
3	1380	No Softening

Table 4-5 The Softening Behaviour of FeS-FeO Cones in Argon (FeS: 57 mass % - FeO: 43 mass %)

Sample No.	Test Temperature °C	Observation
1	980	Softening
2	985	Softening
3	980	Softening

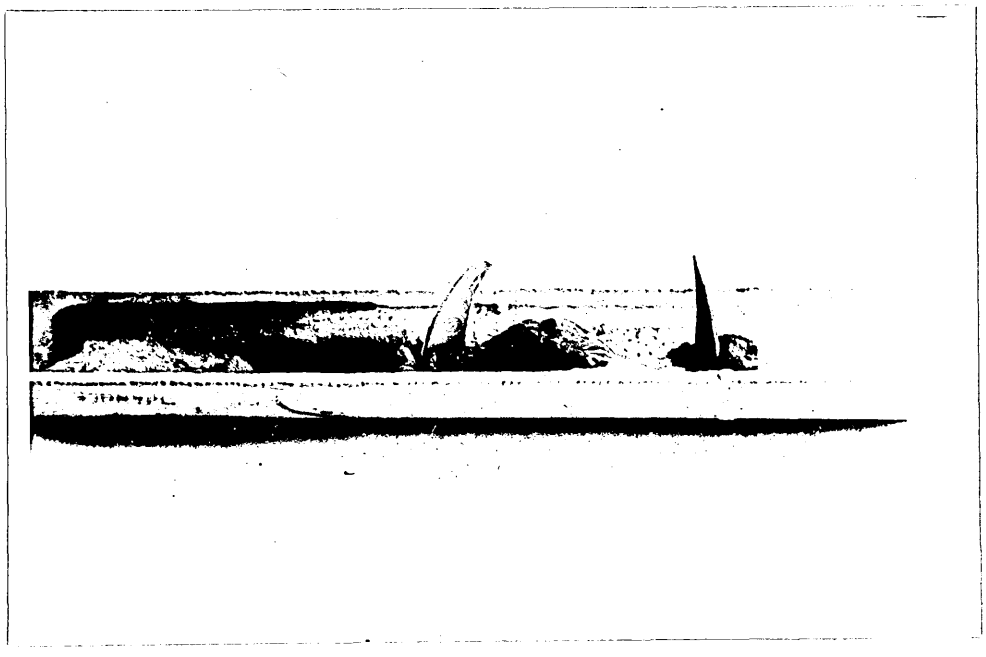

Plate 4.2: The tested cone (FeS:32 mass %; Fe:68 mass %) is to the right and to the middle and the left are Seger standard cones.

itions. The results of these investigations are shown in Table 4-6, which shows that the percentage mass loss for all these cases is abnormally high. The results of a chemical analysis carried out on the cones tested at 1400°C is given in Table 4-7. The analysis shows that sulphur is the only element lost in the softening tests which agrees with the results of C.L.McCobe et al[58].

4.1.3 (e) Photo Micrographs of $FeS-SiO_2$ Cones

(FeS: 50 mass %; SiO_2: 50 mass %)

Plate 4-3 shows a polished section of an $FeS-SiO_2$ cone (FeS: 50 mass %; SiO_2: 50 mass %) after testing at 900°C. The photomicrograph shows a brown silicate matrix with ferrous sulphide particles having a yellow lustre, distributed within it.

Plate 4-4 shows a polished section of an $FeS-SiO_2$ (50 mass % - 50 mass %) cone tested at 1000°C in an argon atmosphere. The photomicrograph is similar to that shown in Plate 4-3 except that the yellow phase is surrounded by trace of a grey boundary, which may be wustite.

Plate 4-5 is a polished section of an $FeS-SiO_2$ (50-50 mass %) cone tested at 1100°C in an argon atmosphere. The photomicrograph is similar to those in Plates 4-3 and 4-4 except that the dark grey areas, which are considered to be wustite, are considerably more pronounced.

Table 4-6 The Softening Behaviour of $FeS-SiO_2$ Cones in Argon

(FeS: 50 mass % - SiO_2: 50 mass %)

Run No.	Test Temperature °C	Observation	Average Mass Loss
1	900	No Softening	9.91%
2	1000	No Softening	12.85%
3	1100	No Softening	15.5%
4	1200	No Softening	17.4%
5	1300	No Softening	19.26%
6	1400	No SOftening	28.82%

Table 4-7 Chemical Analysis of $FeS-SiO_2$ (50-50 mass %)

Cones Tested for Softening Behaviour at 1400°C

Cone Constituents	Percentages of Initial Mass in the Cone	Percentages of Constituents after Test	
		Cone A	Cone B
Silica	50 mass %	53.2 mass %	52.5 mass %
Sulphur	18.18 mass %	0.171 mass %	0.11 mass %
Iron	31.82 mass %	36.0 mass %	36.65 mass %

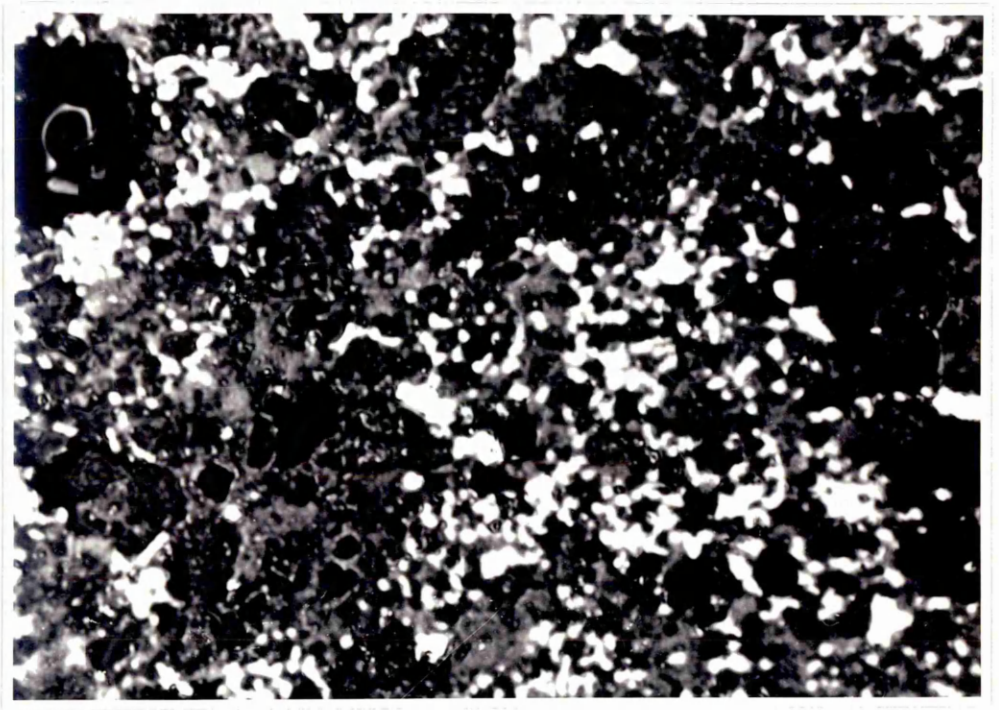

Plate 4.3: A polished section of FeS-SiO_2 (50 mass % - 50 mass %) cone tested for softening at 900°C in an argon atmosphere. The photo micrograph shows a silicate matrix (brown) with ferrous sulphide particles distributed within it (yellow lustre). Magnification 180 X.

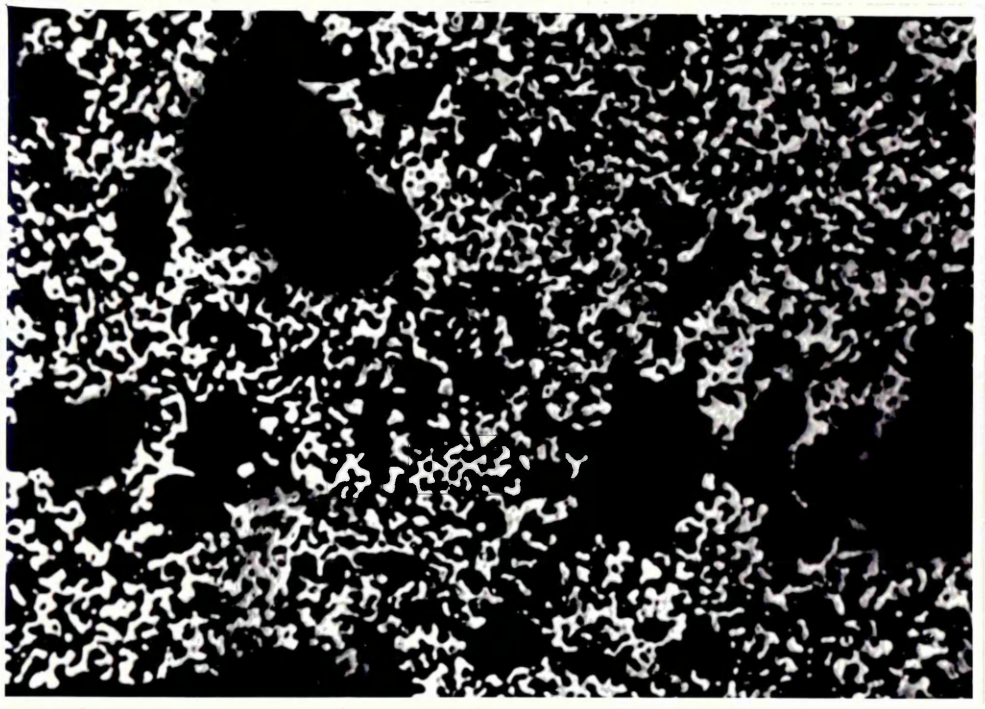

Plate 4.4: A polished section of $FeS-SiO_2$ (50 mass % - 50 mass %) cone tested for softening at 1000°C in an argon atmosphere. The photo-micrograph shows a brown matrix with yellow lustre inclusions which can be identified as silica and ferrous sulphide respectively. The yellow phase is surrounded by traces of grey boundary, which may be wustite. Magnification 180 X.

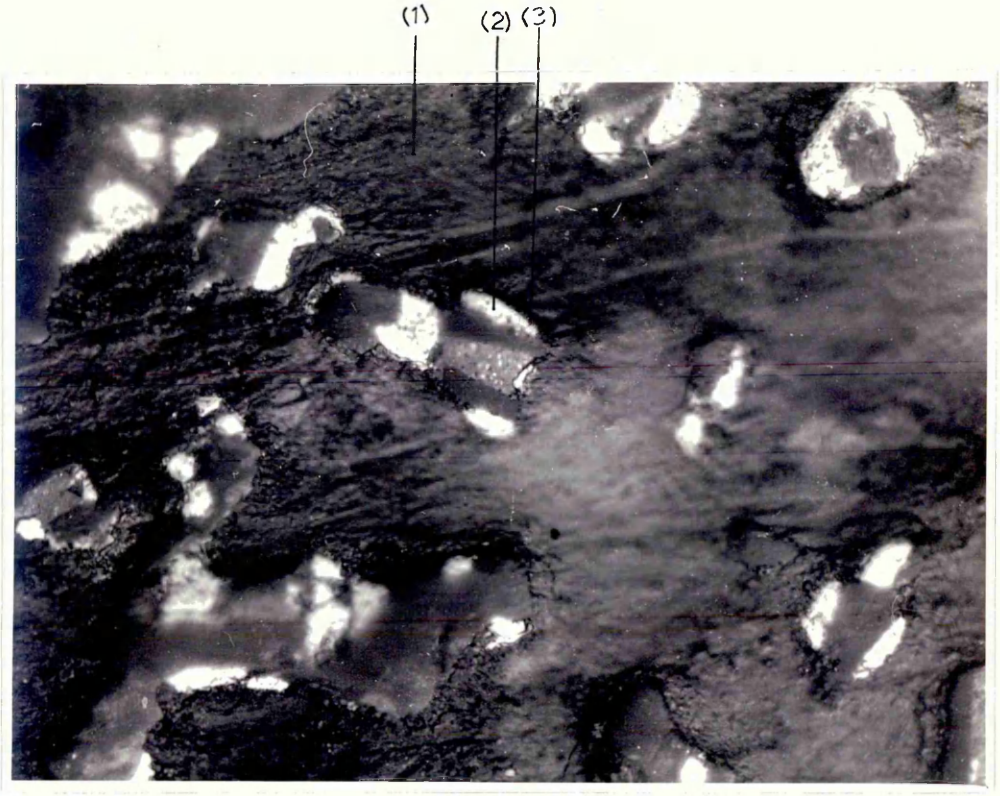

Plate 4.5: A polished section of $FeS-SiO_2$ (50 mass % - 50 mass %) cone tested for softening at 1100°C in an argon atmosphere. The photo-micrograph shows a coarse silicate matrix(1)(brown) with yellow lustre inclusions of ferrous sulphide(2) surrounded by a dark grey boundary of possibly wustite(3). Magnification 200 X.

Plate 4-6 shows a polished section of an $FeS-SiO_2$ (50 mass % - 50 mass %) cone tested for its softening behaviour at 1200°C in an argon atmosphere. Once again, the photomicrograph shows a brown matrix but the yellow lustre inclusions of FeS are not so apparent, although they are still surrounded by grey boundaries. White particles of metallic iron are also visible.

Plate 4-7 shows a polished section of an $FeS-SiO_2$ (50 mass % - 50 mass %) cone tested at 1300°C in argon atmosphere. The photomicrograph shows a silicous frame work (brown) with a few yellow inclusions of ferrous sulphide. The yellow inclusions are surrounded by narrow bands of a grey phase (wustite or magnetite). A few particles of metallic iron are also present.

Plate 4-8 shows a polished section of an $FeS-SiO_2$ (50 mass %- 50 mass %) cone tested at 1400°C in an argon atmosphere. The photomicrograph shows a brown skeleton of silica with a few yellow inclusions of FeS. There is a light grey phase around the boundary of the yellow inclusions.

4.1.4 The Softening Behaviour of a Commercial Iron Ore

4.1.4 (a) The Softening Behaviour of the Ore in Argon

Table 4-8 gives the softening temperatures of the cones reduced to varying degrees and tested in argon.

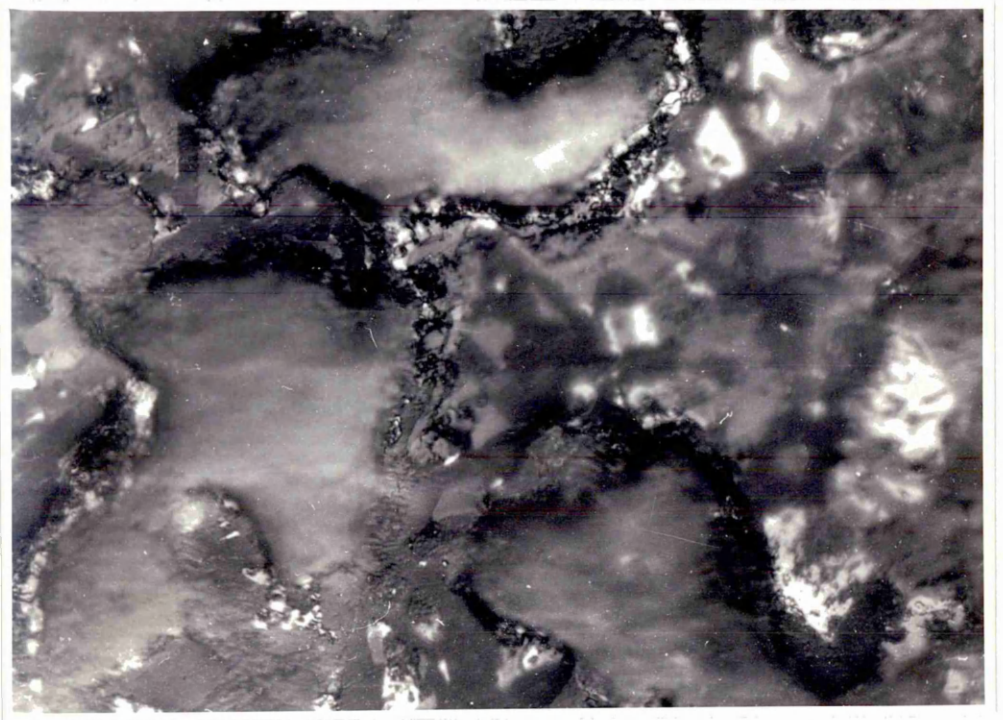

Plate 4.6: A polished section of an FeS-SiO_2 (50 mass % - 50 mass %) cone tested for softening at 1200°C in an argon atmosphere. The photo-micrograph shows a brown matrix with less clear yellow lustre inclusions of FeS surrounded by a grey boundary. There are also some white particles of metallic iron. Magnification 200 X.

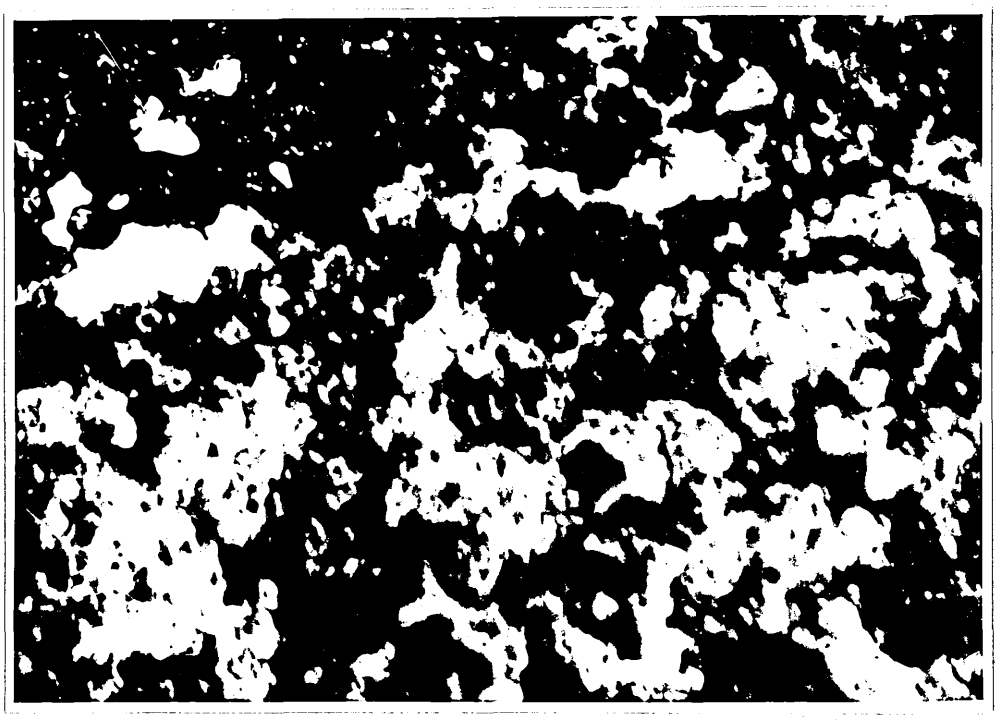

Plate 4.7: A polished section of $FeS-SiO_2$ (50 mass% - 50 mass %) cone tested for softening at 1300°C in an argon atmosphere. The photo-micrograph shows a silicous framework (brown), with a few yellow inclusions of ferrous sulphide. The yellow inclusions are surrounded by a narrow band of a grey phase (wustite or magnetite). A few particles of metallic iron are also present. Magnification 200 X.

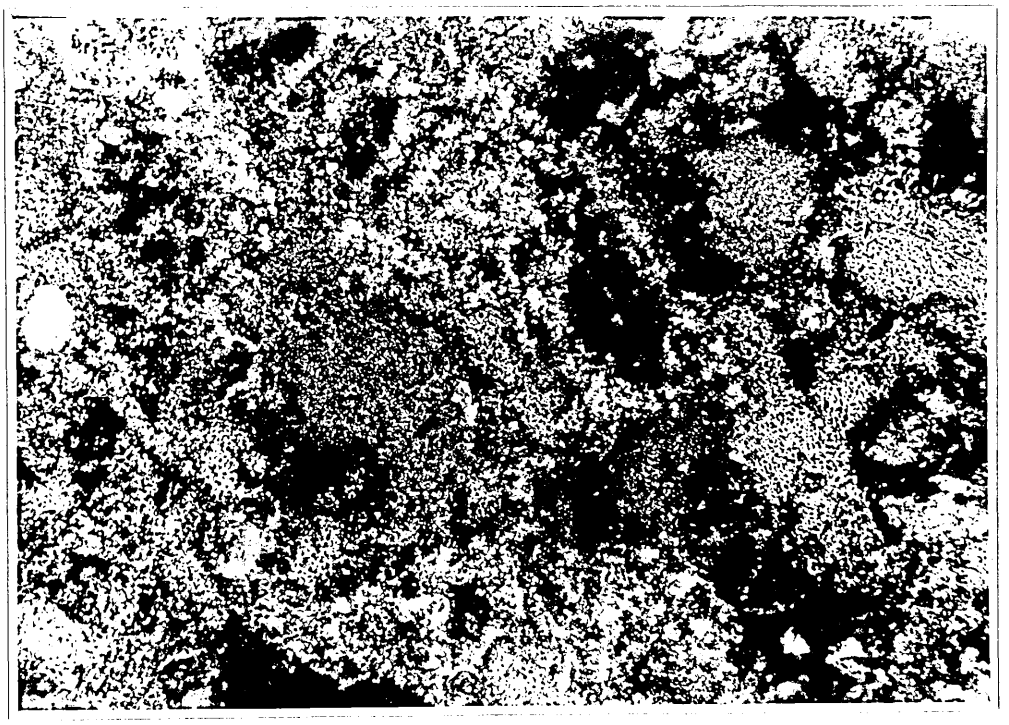

Plate 4.8: A polished section of $FeS-SiO_2$ (50 mass % - 50 mass %) cone tested for softening at 1400°C in an argon atmosphere. The photo-micrograph shows a brown skeleton of silica with a few yellow inclusions of FeS. There is a light grey phase around the boundary of the yellow inclusion. Magnification 200 X.

Table 4-8 The Softening Behaviour of Iron Ore Cones in Argon

Degree of Cone Reduction	Inert Gas Pressure	Inert Gas Flow Rate	Test Temperature °C	Test Result
0%	120mm H_2O	200 cc/min	1180	No Softening
23.86%	130mm H_2O	200 cc/min	1120	Softening
39.79%	130mm H_2O	200 cc/min	1075	Softening
47.29%	140mm H_2O	200 cc/min	1117	Softening
66.23%	140mm H_2O	200 cc/min	1140	Softening
89%	140mm H_2O	200 cc/min	1170	Softening
99%	140mm H_2O	200 cc/min	1174	No Softening
100%	140mm H_2O	200 cc/min	1190	No Softening

Table 4-9 The Softening Behaviour of Iron Ore Cones in Nitrogen

Degree of Cone Reduction	Inert Gas Pressure	Inert Gas Flow Rate	Test Temperature °C	Test Result
0%	120mm H_2O	200 cc/min	1170	No Softening
22.9%	130mm H_2O	200 cc/min	1080	Softened
37.4%	130mm H_2O	200 cc/min	1047	Softened
48.8%	140mm H_2O	200 cc/min	1060	Softened
66.9%	140mm H_2O	200 cc/min	1110	Softened
92.47%	140mm H_2O	200 cc/min	1150	No Softening
100%	140mm H_2O	200 cc/min	1170	No Softening

4.1.4 (b) The Softening Behaviour of the Ore in Nitrogen

Table 4-9 gives the softening temperature of the tested cones reduced to varying degrees and tested in nitrogen.

4.1.4 (c) Effect of Potassium Vapour on the Softening Behaviour of Iron Ore

As shown in Table 4-10 no softening occurred when partially reduced iron ore cones were tested in argon containing potassium vapour.

4.1.4 (d) Metallographic Examination

Plate 4-9 shows a polished section of an iron ore cone reduced 5% in a hydrogen atmosphere, and then exposed to a 43mm potassium vapour pressure at 1150°C. The photomicrograph shows coarse crystals of hematite (white) with an associated slag phase (dark grey).

Plate 4-10 shows a polished section of a cone which has been given a 57.8% reduction in hydrogen and then exposed to a 43mm of potassium vapour pressure at 1150°C. The photomicrograph shows a slag phase (dark grey, a grey phase may be wustite and white crystals may be iron).

Table 4-10 Effect of Potassium Vapour on the Softening Behaviour of Iron Ore

Potassium Vapour Pressure	Pressure of the System	Degree of Cone Reduction	Cone Temperature ^{o}C	Observation
33mm Hg	100mm H_2O	0%	1150	No Softening
33mm Hg	100mm H_2O	10%	1150	No Softening
33mm Hg	100mm H_2O	34%	1150	No Softening
33mm Hg	100mm H_2O	51.4%	1150	No Softening
43mm Hg	100mm H_2O	57.1%	1150	No Softening
43mm Hg	100mm H_2O	83%	1150	No Softening
43mm Hg	100mm H_2O	100%	1150	No Softening

Plate 4.9: A polished section of iron ore cone which has been given a 5% reduction in hydrogen atmosphere, and then exposed to a 43mm mercury potassium vapour pressure at 1150°C. The photo-micrograph shows coarse crystals of hematite (white) with an associated slag phase (grey). Magnification 180 X.

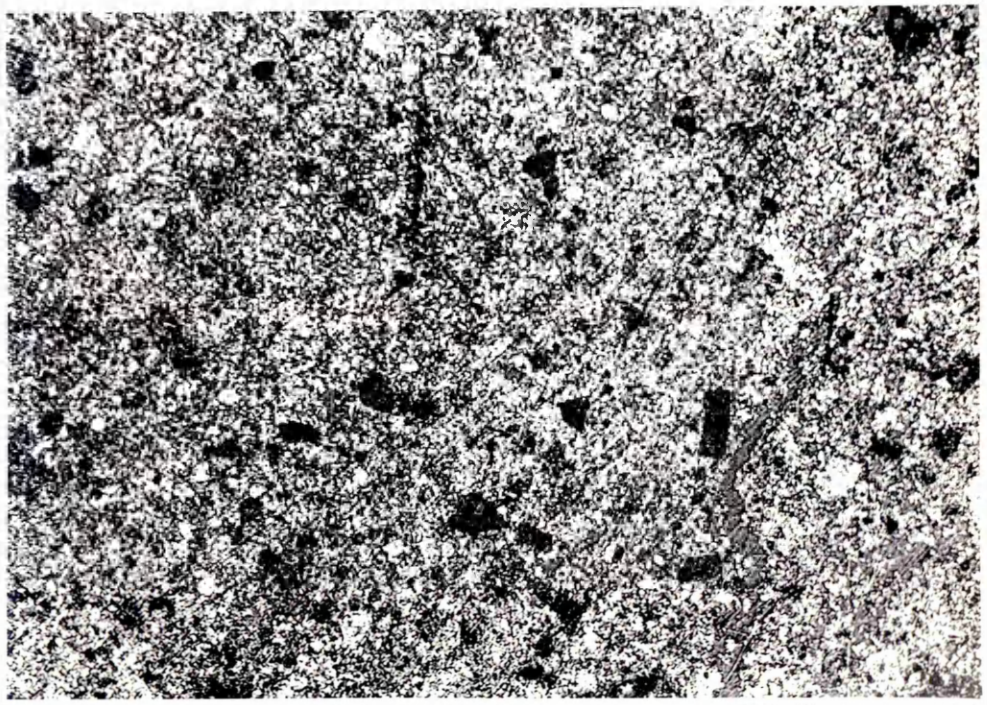

Plate 4.10: A polished section of a cone which has been given a 57.8% reduction in hydrogen and then exposed to 43mm mercury potassium vapour pressure at 1150^{o}C. The photo-micrograph shows iron crystals (white), wustite (grey) and a slag phase (dark grey). Magnification 180 X.

Plate 4-11 shows a polished section of a cone which has been given 83% reduction in hydrogen and then exposed to a 43mm of potassium vapour pressure at 1150^{o}C. The photomicrograph shows wustite (grey), metallic sponge iron (white) and a slag phase (dark grey).

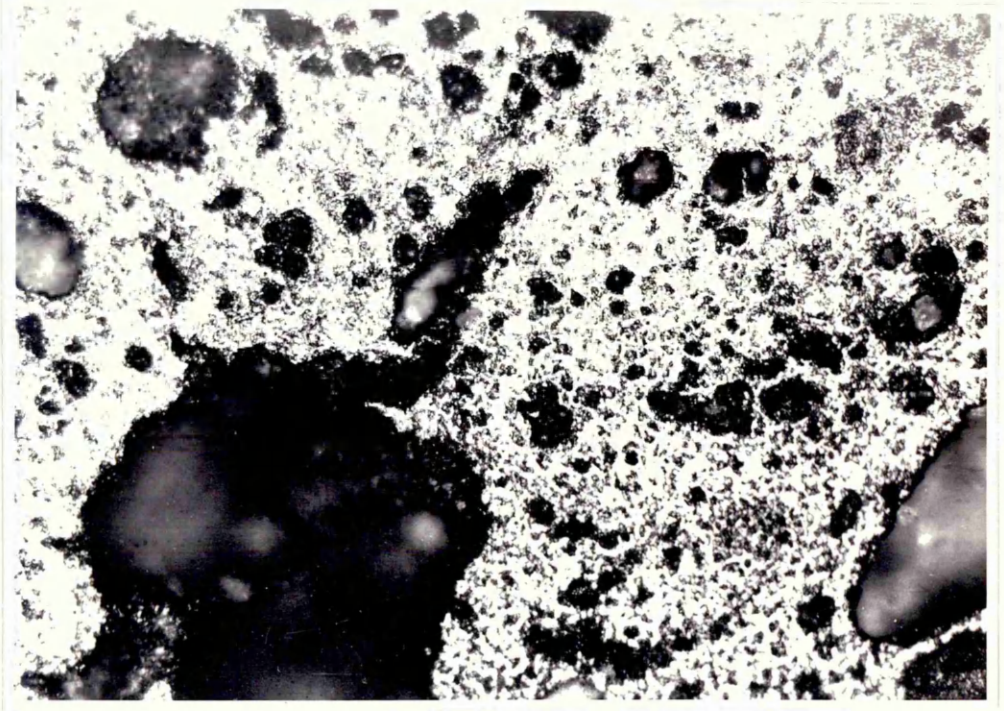

Plate 4.11: A polished section of a cone which has been given an 83% reduction in hydrogen and then exposed to a 43mm mercury potassium vapour pressure at 1150°C. The photo-micrograph shows wustite (grey), metallic or sponge iron (white), and a slag phase (dark grey). Magnification 180 X.

4.2 SEALED SILICA TUBE RESULTS

4.2.1 (a) The Softening Behaviour of Pure/partially reduced Fe_2O_3 Cones in Argon

The results of softening tests on pure Fe_2O_3 cones reduced to different degrees and sealed into silica tubes under argon at a pressure of 180mm at room temperature are shown in Table 4-11. The results show that there are no/cones softening over the ranges of reduction up to the temperatures considered to be the maximum for the silica tube. The silica tube starts to devitrify at higher temperatures. A small amount of liquid flowed from the cones reduced by 22 and 35%, however, the amount was very small.

4.2.1 (b) The Softening Behaviour of Pure/partially reduced Fe_2O_3 Cones in Sulphur Vapour

The introduction of sulphur vapour into the sealed silica tubes resulted in a liquid/being formed at temperatures in the range 1180-1230°C. In most cases, this liquid flow from the cones although some times it merely formed globules on the surface of the tested cone as shown by the results in Table 4-12. Once again, the liquid flow down to the base in thereduction range 28-78.7%, while the formation of globules on the surface of the tested cone occurred at 85.5% reduction.

Table 4-11 The Softening Behaviour of Pure Fe_2O_3 Cones in Argon in a Sealed Silica Tube

Run No.	Degree of Reduction	Test Temperature °C	Observation
1	0%	1205	No Softening
2	22%	1190	No Softening
3	22%	1204	No Softening, Volume Decrease and a Melt on the Base
4	28%	1202	No Softening, a Slight Bending of the Cone
5	35.3%	1208	No Softening, a Melt on the Base
6	41%	1174	No Softening
7	42%	1216	No Softening
8	43%	1197	No Softening
9	58%	1199	No Softening, the Cone Bent and Attached to the Wall of Silica Tube
10	68%	1173	No Softening, but the Cone Bent
11	75.2%	1186	No Softening
12	85.5%	1234	No Softening
13	100%	1226	No Softening

Table 4-12 The Softening Behaviour of Pure Fe_2O_3 Cones in Sulphur Vapour in a Sealed Silica Tube

Run No.	Degree of Reduction	Test Temperature °C	Observation
1	0	1202	No Softening
2	21%	1223	No Softening
3	28%	1183	No Softening but Liquid Flow Down
4	35.3%	1173	No Softening
5	41%	1200	No Softening but Liquid Formation on Surface
6	41%	1252	No Softening, but Liquid Flow Down
7	58%	1207	No Softening but Liquid Flow Sharp Edges Disappear
8	68%	1205	No Softening
9	78.7%	1186	No Softening but Liquid Flow Down to the Base
10	85.5%	1234	No Softening but Liquid Formation on the Surface
11	85.5%	1234	No Softening

4.2.1 (c) Metallographic Examination

The investigation of Fe_2O_3 cones at different degrees of reduction, after testing in sealed silica tubes under argon, indicated that increasing the temperature of the test favoured grain growth as illustrated in Plates 4-12 and 4-13. This suggests that the tested cones were in a pre-softening stage. A comparison between cones tested at the same temperature indicates that increasing degrees of reduction favoured a more uniform distribution of the pores, Plates 4-14 and 4-15.

Investigation of the reduced Fe_2O_3 cones after being tested under a sulphur vapour pressure in sealed silica tubes, indicated the existence of sulphides, (Plates 4-16), but not in sufficient amounts to cause cone softening. Scanning Electron Microscope examination confirmed the start of liquid formation in the boundary of the particles, Plate 4-17.

4.2.2 (a) The Softening Behaviour of Pure Fe_2O_3-SiO_2 Cones with Argon as Gas Phase Inside the Sealed Silica Tube

Cones produced from a mixture of pure Fe_2O_3, with different degrees of reduction, and SiO_2 such that $\frac{\text{Fe mass}}{SiO_2 \text{ mass}} = 3.12$, were investigated for their softening behaviour in sealed silica tubes under a room temperature argon pressure of 180mm mercury. Table 4-13 gives the results of these exper-

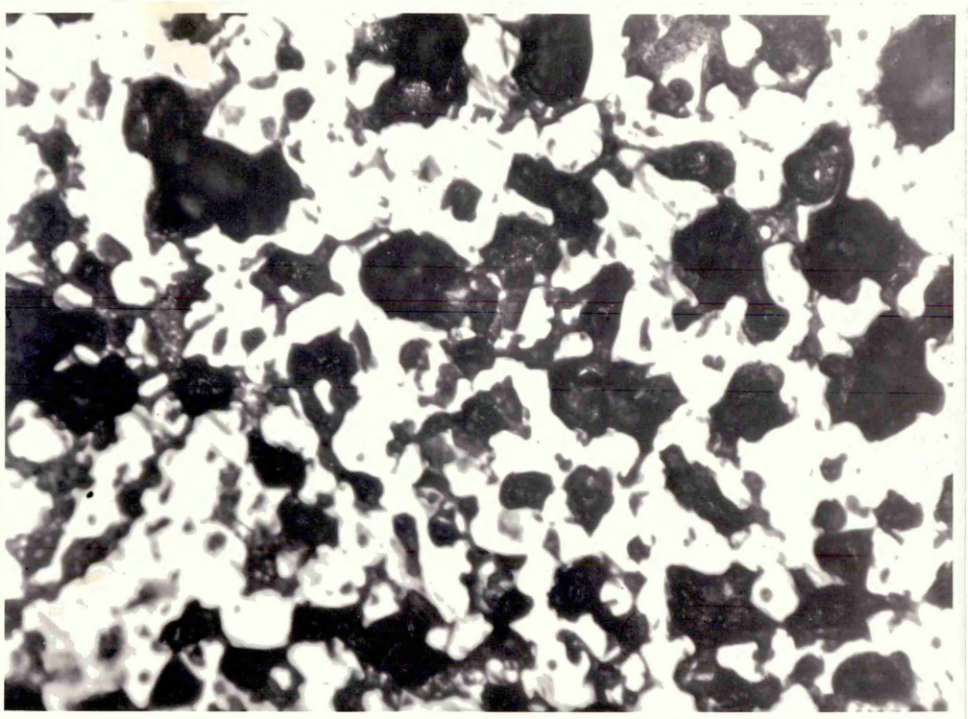

Plate 4-12: A polished section of Fe_2O_3 cone 41% reduced, tested for softening under argon in a sealed silica tube at 1174°C. Light wustite, dark pore.
Magnification: 160X

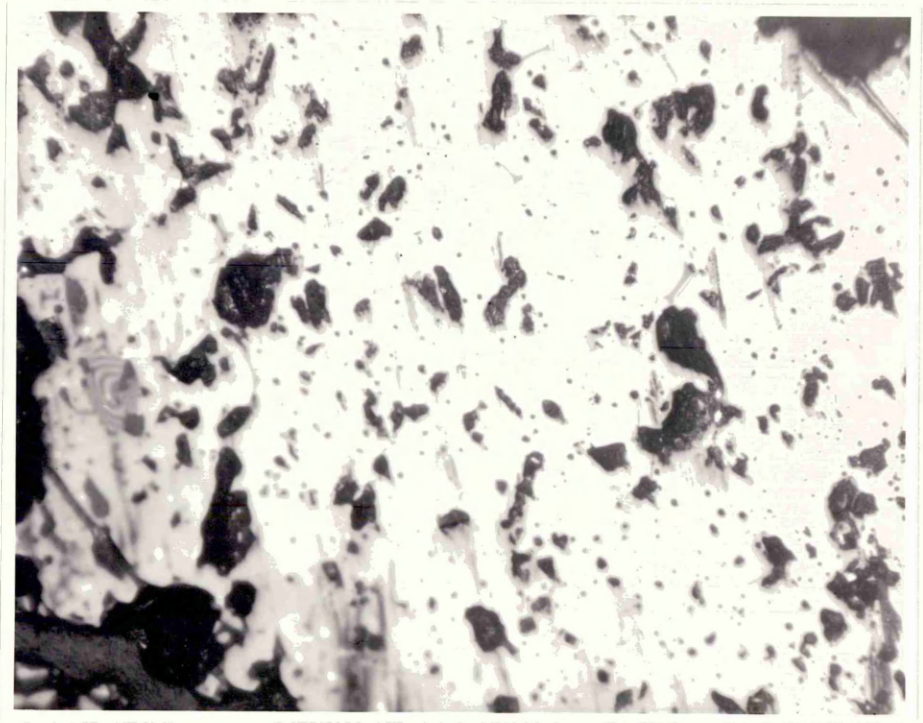

Plate 4-13: A polished section of Fe_2O_3 cone 35.3% reduced, tested for softening under argon in a sealed silica tube at 1208°C. Light wustite, dark pore.
Magnification 160X.

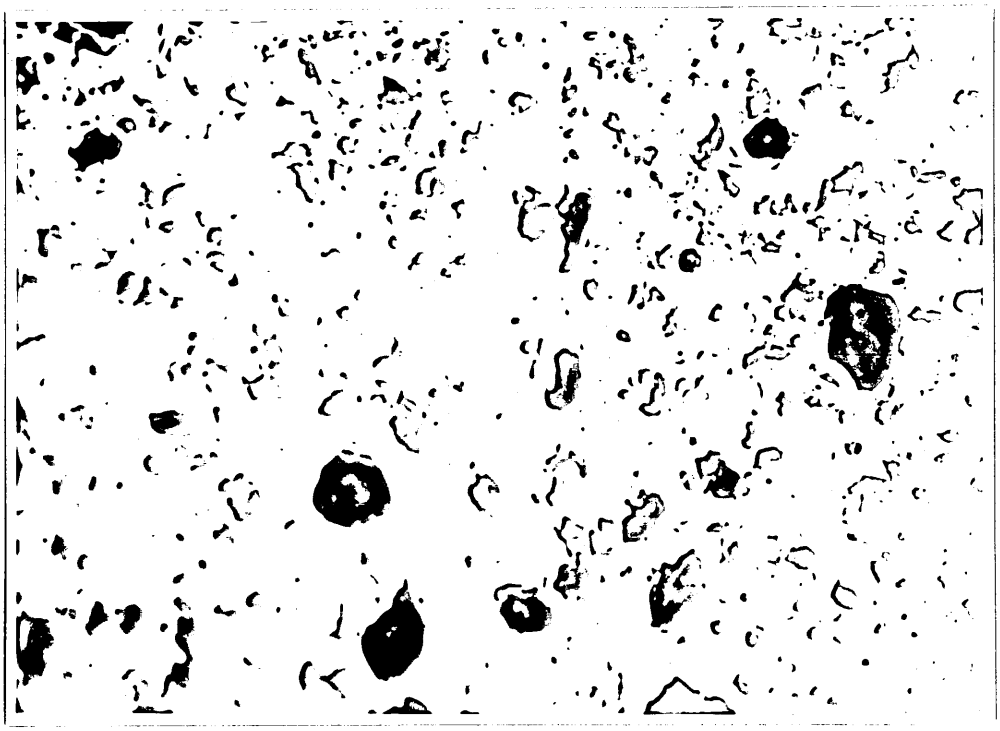

Plate 4-14: A polished section of Fe_2O_3 cone 28% reduced, tested for softening under argon in a sealed silica tube at 1202°C. Light wustite, dark pore.
Magnification 160X.

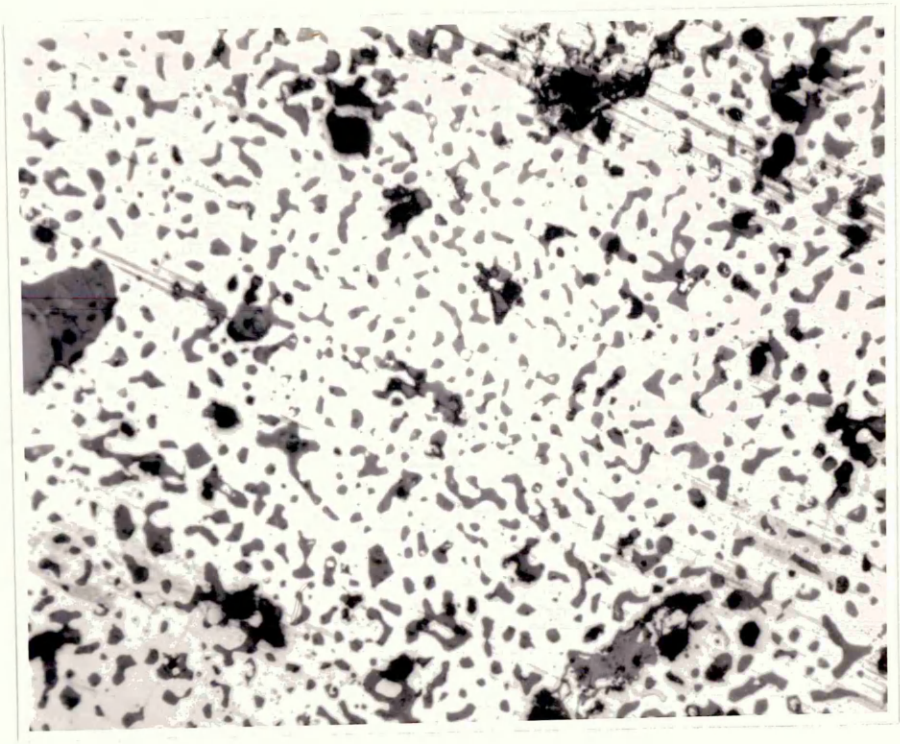

Plate 4-15: A polished section of Fe_2O_3 cone 58% reduced, tested for softening under argon in a sealed silica tube at 1199 °C. Light iron and wustite, dark pore.
Magnification: 160X.

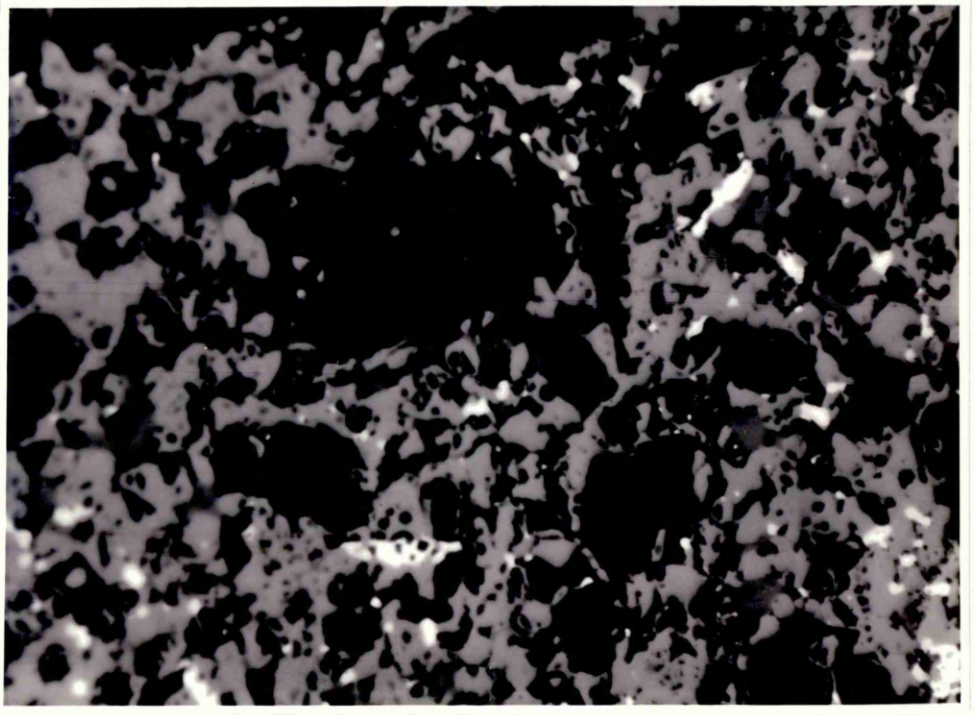

Plate 4-16: A photograph of Fe_2O_3 cone 78.7% reduced. Tested for softening with 0.01 g of sulphur in a sealed silica tube at 1188°C. The white particles are iron sulphides in a darker matrix of iron and wustite. The darker area are pores. Etched in dilute H_2SO_4.
Magnification: 160X.

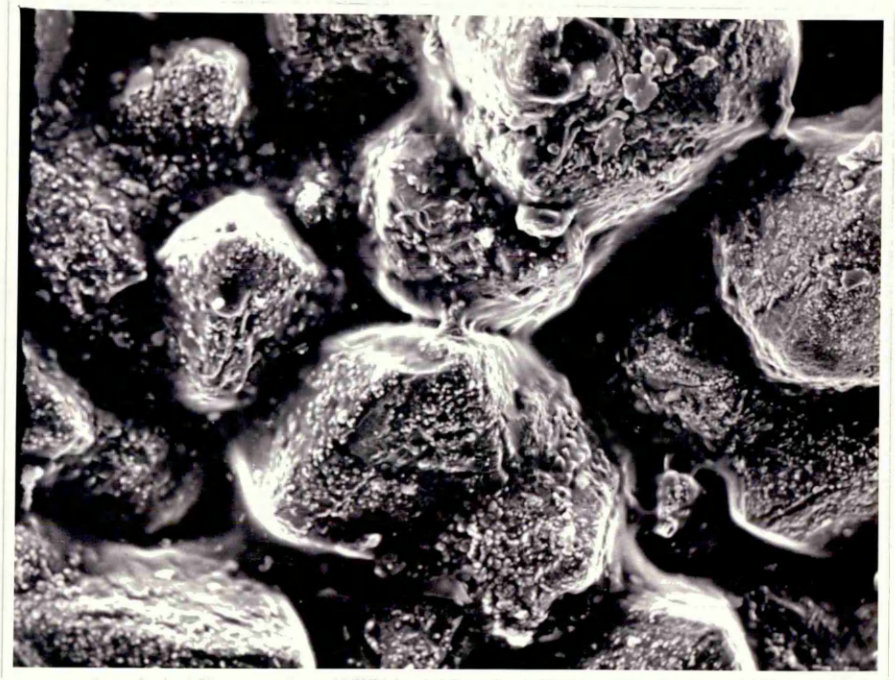

Plate 4-17: Scanning photomicrograph of a cone of Fe_2O_3, 78.7% reduced, tested for softening with 0.01 g of sulphur in a sealed silica tube at 1188°C. Shows the initial development of a neck between the particles.
Magnification: 1200.

Table 4-13 The Softening Behaviour of Pure Fe_2O_3- SiO_2 with Argon as Gas Phase Inside the Sealed Silica Tube

Run No.	Degree of Reduction	Test Temperature °C	Observation
1	0%	1238	No Softening
2	7.3%	1237	Over Softening
3	7.3%	1236	Melting
4	7.3%	1226	Softening
5	22%	1207	Cone Softening
6	28%	1197	Over Softening
7	32%	1228	Melting
8	32%	1214	Cone Softening
9	42%	1201	No Softening
10	42%	1212	Cone Softening
11	42%	1227	Melting
12	49.7	1216	Softening
13	49.7%	1230	Melting
14	57%	1185	No Softening
15	57%	1205	Softening
16	71%	1216	Softening
17	79.3%	1283	Over Softening
18	79.3%	1252	Softening
19	85.5%	1264	Over Softening
20	85.5%	1249	Softening
21	88%	1264	Melting
22	88%	1253	Softening
23	100%	1271	Softening

In all cases the cone comprised of a mixture of partially reduced Fe_2O_3 and SiO_2 such that, $\frac{\text{Mass of Fe}}{\text{Mass of } SiO_2} = 3.12$

iments. Figure 5-3/shows that a lowering of the softening temperature occurred at two levels of reduction, at about 22% reduction and at about 58% reduction. A steep rise in the softening temperature when reduction exceeded 72% can be observed.

4.2.2 (b) The Softening Behaviour of Pure Fe_2O_3-SiO_2 Cones with Sulphur and Argon as Gas Phase Inside the Sealed Silica Tube

Table 4-14 shows the results of investigating the effect of sulphur vapour on the softening behaviour of cones produced from a mixture of pure Fe_2O_3 reduced to different degrees, and SiO_2, with Fe mass/SiO_2 mass = 3.12. Figure 5-3, page 276 shows a comparison between the softening behaviour of the above mentioned cones, in the existence and absence of sulphur vapour. The following observations can be made:

(i) A lowering of the softening temperature of cones produced from mixture of partially reduced Fe_2O_3 and SiO_2 occurred at reductions of about 22% and 58%. This lowering was noticed to shift to reduction values of 28% and 57% in the presence of sulphur vapour as a constituent of the gas phase.

(ii) Generally the presence of sulphur as a constituent of the gas phase depressed the softening temperature to a lower value, the amount depending upon the degree of reduction.

Table 4-14 The Softening Behaviour of Pure Fe_2O_3-SiO_2 Cones with Sulphur as Gas Phase Inside the Sealed Silica Tube

Run No.	Degree of Reduction	Test Temperature ^oC	Observation
1	0%	1190	No Softening
2	7.3%	1205	Over Softening
3	7.3%	1190	Softening
4	7.3%	1186	Softening
5	28%	1161	No Softening
6	28%	1176	Softening
7	33%	1178	Softening
8	42%	1168	No Softening
9	42%	1188	Over Softening
10	42%	1181	Softening
11	57%	1184	Over Softening
12	57%	1165	Softening
13	66%	1177	Softening
14	71%	1172	Softening
15	79%	1156	No Softening
16	79%	1159	No Softening
17	79%	1172	Softening
18	79%	1180	Over Softening
19	85.5%	1173	Over Softening
20	88%	1173	Softening
21	100%	1174	Softening
22	100%	1186	Melting

In all cases the cone comprised of a mixture of partially reduced Fe_2O_3 and SiO_2 such that, $\frac{\text{Mass of Fe}}{\text{Mass of } SiO_2} = 3.12$

4.2.2 (c) The Rate of Cone Softening in the Presence of Sulphur as a Gas Constituent Inside Sealed Silica Tube

To investigate the relation between the softening temperature and the time that a tested cone was held at a particular temperature, the softening temperature of 80 mass % FeO, 20 mass % SiO_2 cones was determined for different testing times. Table 4-15 shows the results of these experiments. From Table 4-15 it can be concluded that a lowering of the softening temperature is obtained by increasing the time of the test up to 60 minutes, but after that increasing the time of softening has no effect on the softening temperature. This result is shown in Plate 4-18.

4.2.2 (d) Metallographic Examination of Partially Reduced Fe_2O_3, SiO_2 Cones Tested Under Argon and Sulphur Vapour

Cones containing Fe_2O_3, reduced to various degrees, and SiO_2 as their constituents with Fe/SiO_2 mass ratio equal to 3.12 were examined metallographically using the Scanning Electron Microscope, after being tested for softening. They showed the formation of liquid matrix surrounding solid particles. By X-ray mapping the solid particles were shown to contain mainly (Fe) while the matrix contained (Fe)

Table 4-15: Softening Test of Fe_2O_3 33% Reduced and SiO_2 Cones, $\frac{Fe\ mass}{SiO_2\ mass}$ = 3.12, with 0.01gm of Sulphur in Sealed Silica Tubes at Various Softening Test Times

(80 mass % FeO - 20 mass % SiO_2)

Run No.	Time of Test	Test Temperature ^oC	Observation
1	15 minutes	1178	Softening
2	30 minutes	1160	Softening
3	45 minutes	1144	Softening
4	60 minutes	1140	Softening
5	75 minutes	1142	Softening

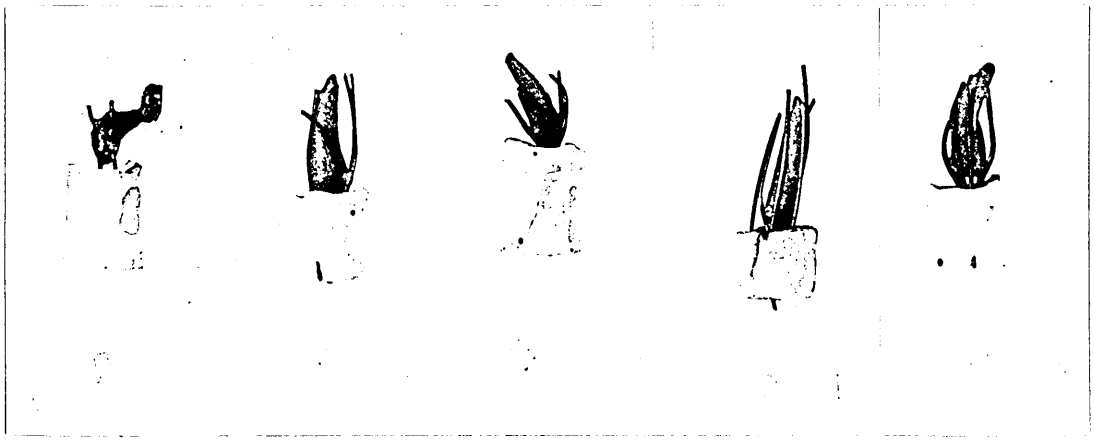

A_1 A_2 A_3 A_4 A_5

Plate 4-18: Cones (33% reduced Fe_2O_3, SiO_2, with (Fe mass/SiO_2 mass = 3.12) after being tested with 0.01g of sulphur in sealed silica tubes for various softening test time. A_1, A_2, A_3, A_4 and A_5 tested for 15, 30, 45, 60 and 75 minutes at 1178, 1160, 1144, 1140 and 1142^{o}C respectively.

and (Si). As an example Plate 4-19 shows a scanning photomicrograph of a cone containing 33% reduced Fe_2O_3 plus SiO_2, with the Fe/SiO_2 mass ratio equal to 3.12, after being tested for softening in a sealed silica tube at 1214°C under argon. X-ray investigation of the dendritic formation showed it to contain (Fe) and (Si) (Plates 4-20 and 4-21). The dendritic areas were estimated to represent about 30% of the investigated area. It can be concluded that softening of a cone containing 33% reduced Fe_2O_3 plus SiO_2, with the Fe/SiO_2 mass ratio equal to 3.12, occurs when the liquid phase formed represents 30% of its volume.

Plate 4-22 shows a photomicrograph of a section in a cone containing 85.5% reduced $Fe_2O_3 + SiO_2$, with the Fe/SiO_2 mass ratio equal to 3.12, investigated for its softening behaviour in a sealed silica tube under argon at 1249°C, while Plates 4-23 and 4-24 shows (Si) and (Fe) distribution.

Cones containing Fe_2O_3 reduced to various degrees and SiO_2 as their constituents, with the Fe/SiO_2 mass ratio equal to 3.12 were examined metallographically by the Scanning Electron Microscope and the Zeiss Microscope after being tested for softening behaviour with 0.01g of sulphur in sealed silica tubes. Examples of the cones investigated are shown in the following Plates.

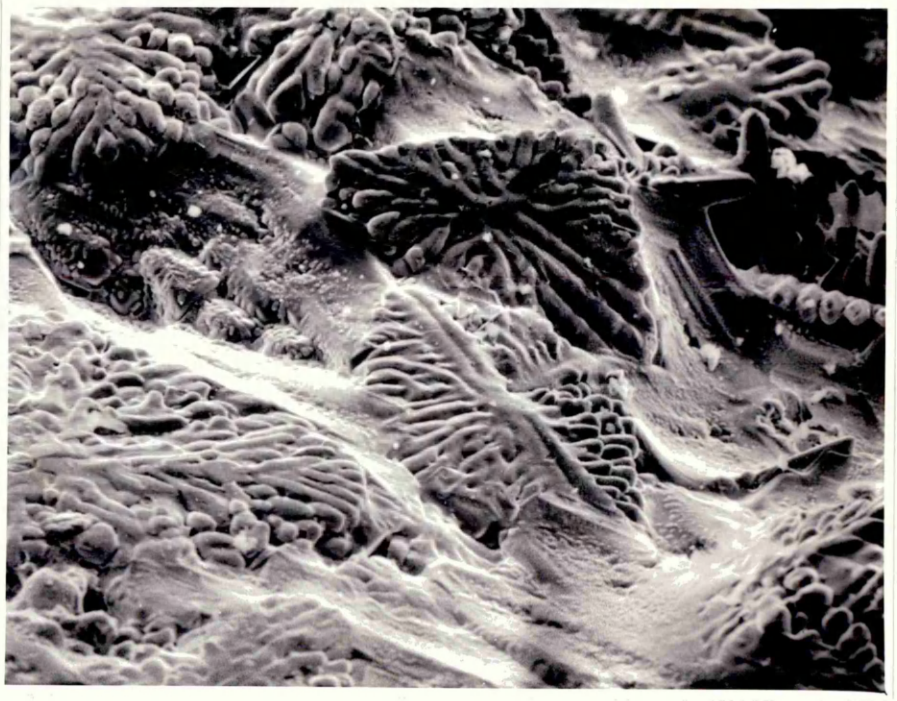

Plate 4-19: A scanning photomicrograph of a cone (33% reduced Fe_2O_3 and SiO_2, (Fe mass/SiO_2 mass = 3.12), after being tested for softening at 1214°C in a sealed silica tube under argon.

Magnification: 200 x 1.2.

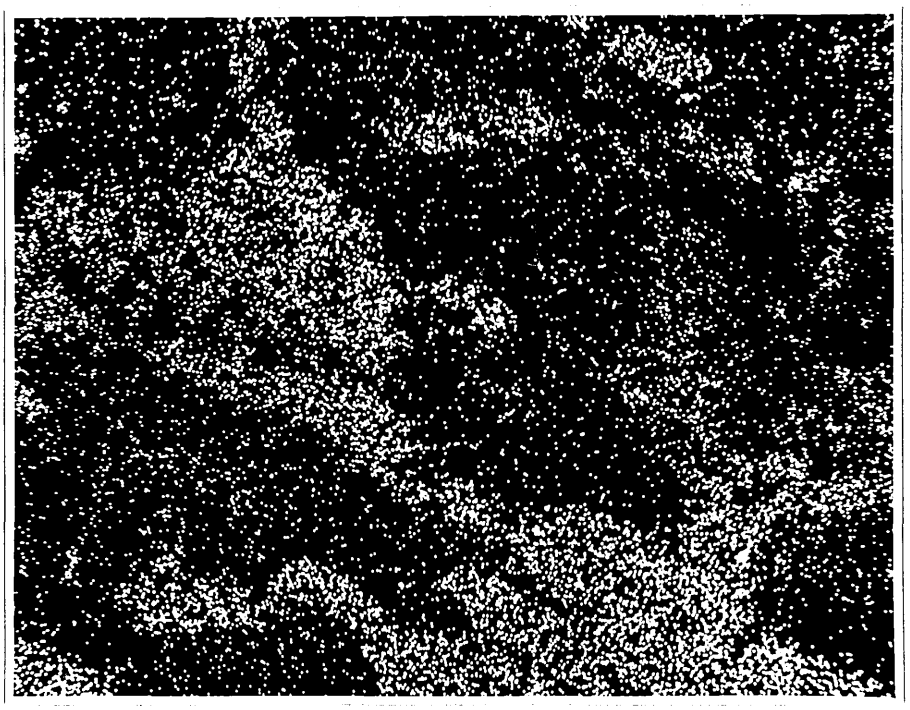

Plate 4-20: Scanning X-ray mapping of (Fe) distribution in the area shown in Plate 4-19.
Magnification: 200 x 1.2.

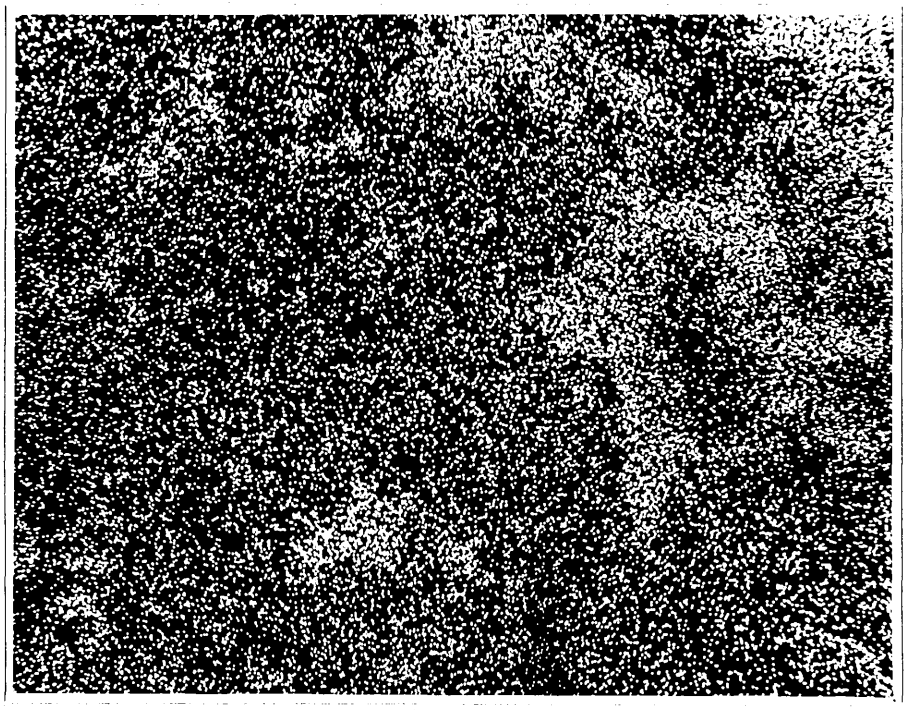

Plate 4-21: Scanning X-ray mapping of (Si) distribution in the area shown in Plate 4-19.
Magnification: 200 x 1.2.

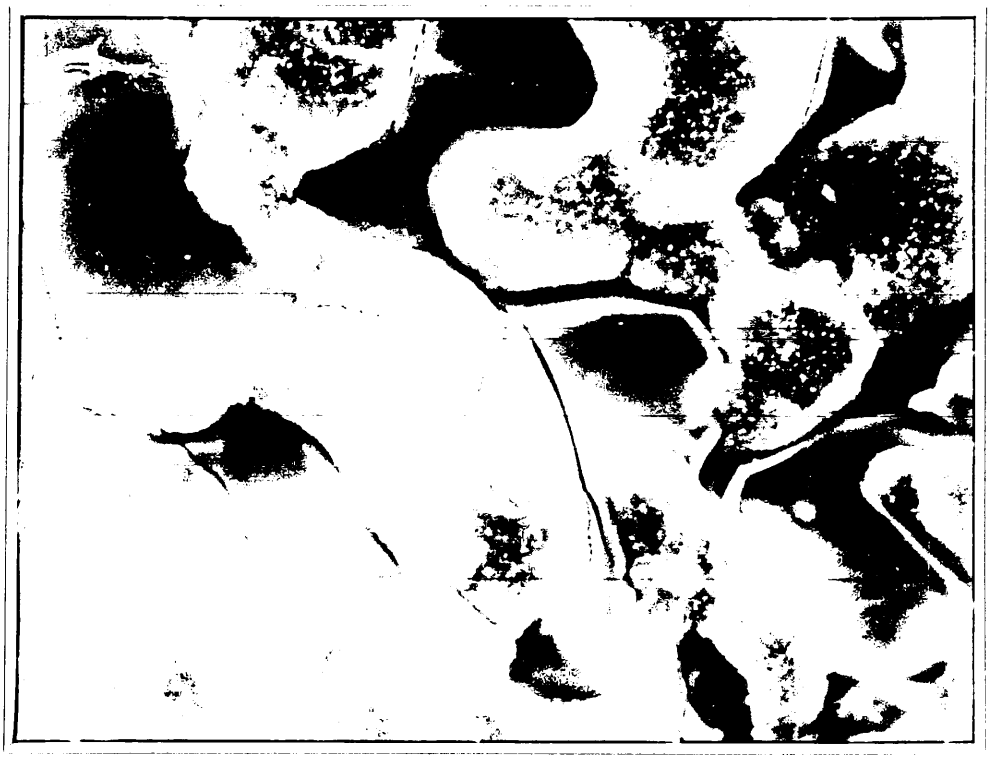

Plate 4-22: A scanning photomicrograph of an 85.5% reduced Fe_2O_3 plus SiO_3 cone, $\frac{\text{Fe mass}}{SiO_2 \text{ mass}} = 3.12$ after being tested for softening at 1249°C in a sealed silica tube under argon.

Magnification: 800 x 1.3.

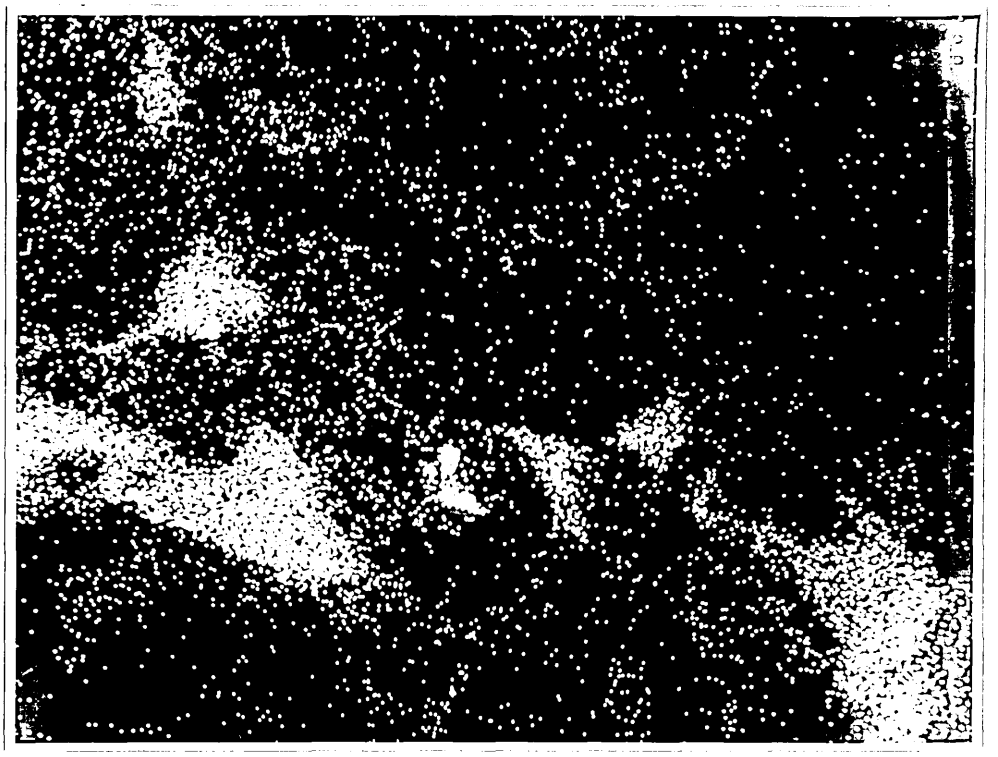

Plate 4-23: Scanning X-ray mapping showing (Si) distribution in the area shown in Plate 4-22.
Magnification: 800 x 1.3.

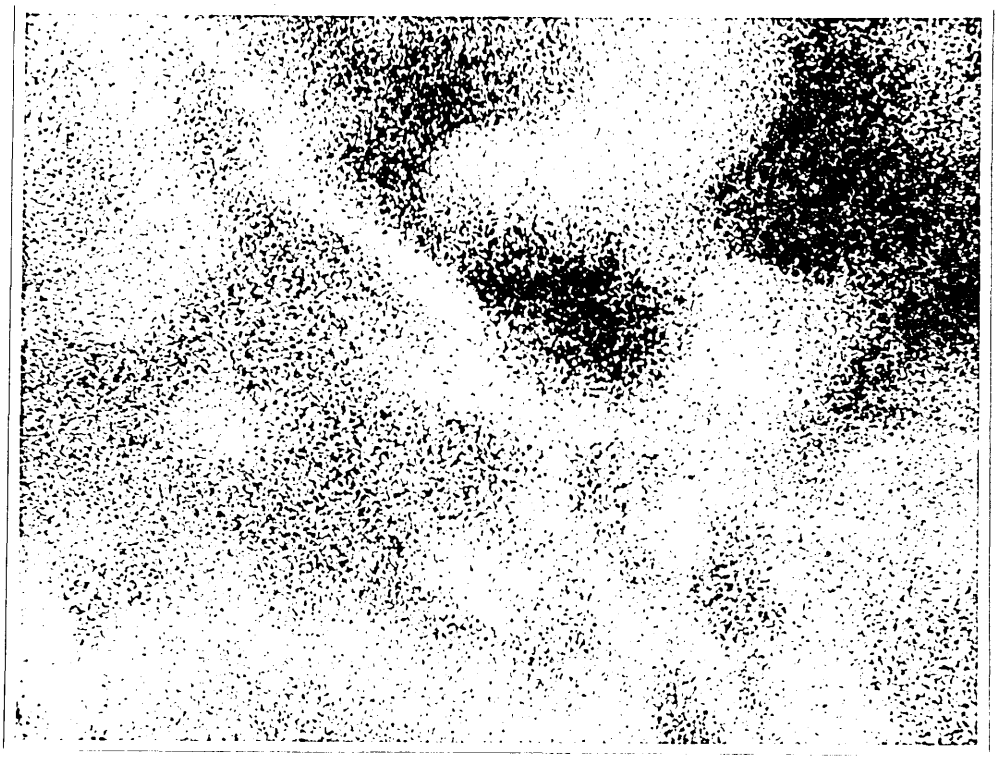

Plate 4-24: Scanning X-ray mapping showing (Fe) distribution in the area shown in Plate 4-22.
Magnification: 800 x 1.3.

Plate 4-25 shows a photomicrograph in a cone containing 7% reduced Fe_2O_3 + SiO_2, Fe/SiO_2 mass ratio equal to 3.12, after being tested for softening at 1190°C for 15 minutes, while Plates 4-26 to 4-28 show X-ray mapping for the distribution of (S), (Fe) and (Si).

Plate 4-29 shows a photomicrograph in a cone composed of 57% reduced Fe_2O_3 + SiO_2, with the Fe/SiO_2 mass ratio equal to 3.12, after being tested for softening at 1165°C with 0.01g of sulphur. X-ray investigation indicated that the liquid formed during the softening test is comprised mainly of (Fe) and (S) with much less (Si), while the area without liquid formation possessed intensive concentrations of (Si). (Fe) was distributed all over the area investigated (Plates 4-30, 31, 32). The area of liquid formation represents about 30% of the area of the section investigated. Plate 4-33 shows another area in the same sample, (Plate 4-29), but at higher magnification, illustrating liquid formation over the particles. X-ray analysis showed the liquid contained (Fe) and (S), the particle in the lower middle contained mainly (Fe) and the particle in the upper left corner contained mainly (Si).

Plate 4-34 shows a photomicrograph in a cone containing 79% reduced Fe_2O_3 with SiO_2, Fe/SiO_2 mass ratio equal to 3.12, after being tested for softening behaviour at 1172°C for 15 minutes.

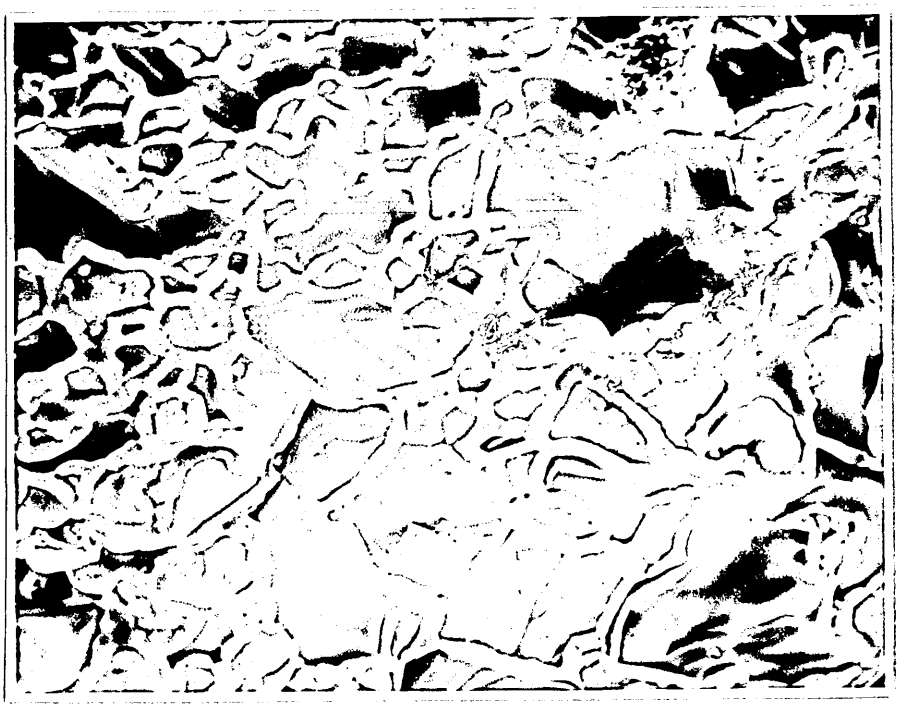

Plate 4-25: Scanning photomicrograph of 7% reduced Fe_2O_3 plus SiO_2 cone after the softening test with 0.01g of sulphur at 1190°C in a sealed silica tube.

Magnification: 640 x 1.3.

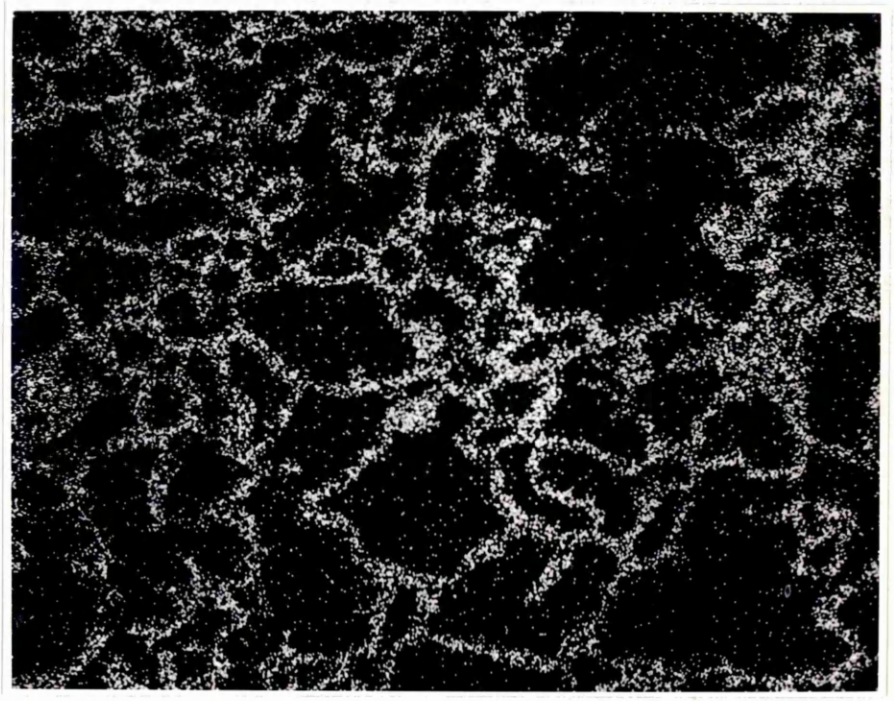

Plate 4-26: Scanning x-ray mapping for (S) distribution in the area shown in Plate 4-25.
Magnification: 640 x 1.3.

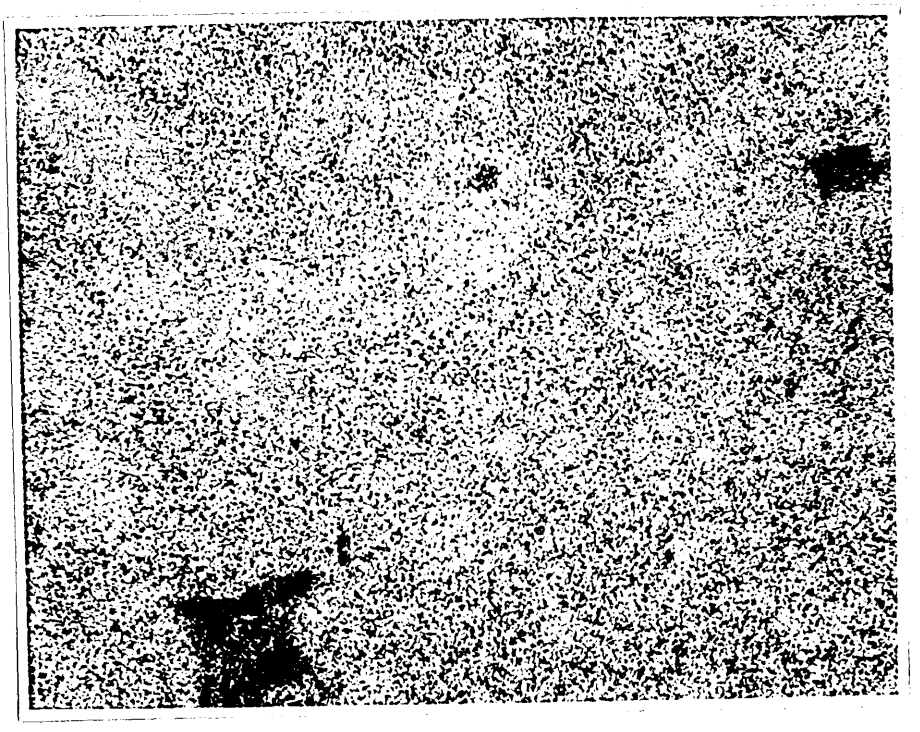

Plate 4-27: Scanning x-ray mapping for (Fe) distribution in the area shown in Plate 4-25.

Magnification: 640 x 1.3.

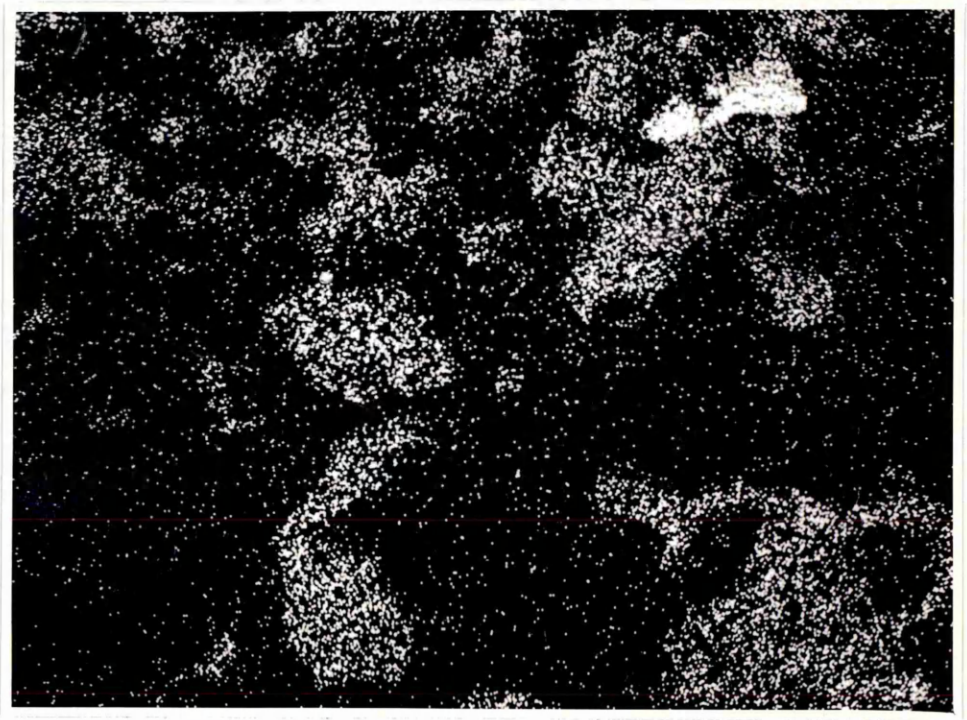

Plate 4-28: Scanning x-ray mapping for (Si) distribution in the area shown in Plate 4-25.
Magnification: 640 x 1.3.

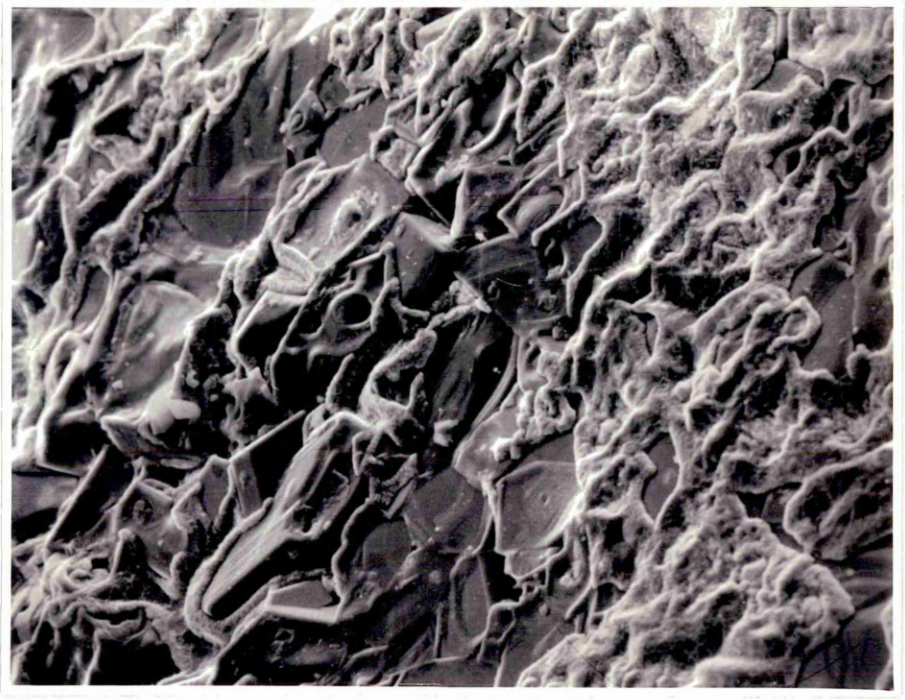

Plate 4-29: Scanning photomicrograph of a cone 57% reduced Fe_2O_3 plus SiO_2, after being tested for softening with 0.01g of sulphur at 1165°C, in a sealed silica tube.

Magnification: 400 x 1.1.

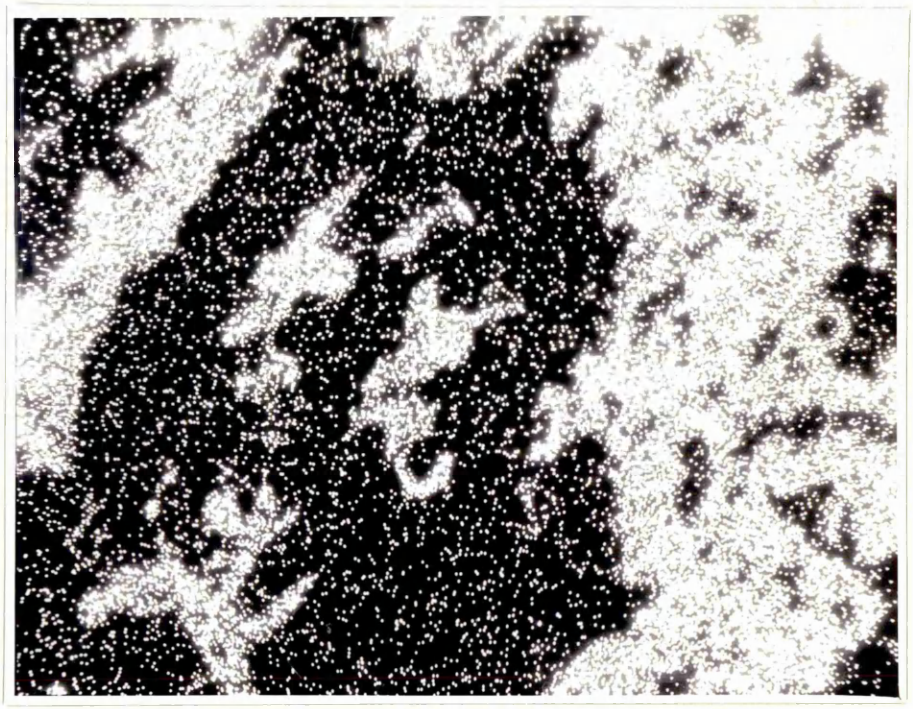

Plate 4-30: Scanning x-ray mapping of (S) distribution in the area shown in Plate 4-29.

Magnification: 400 x 1.1.

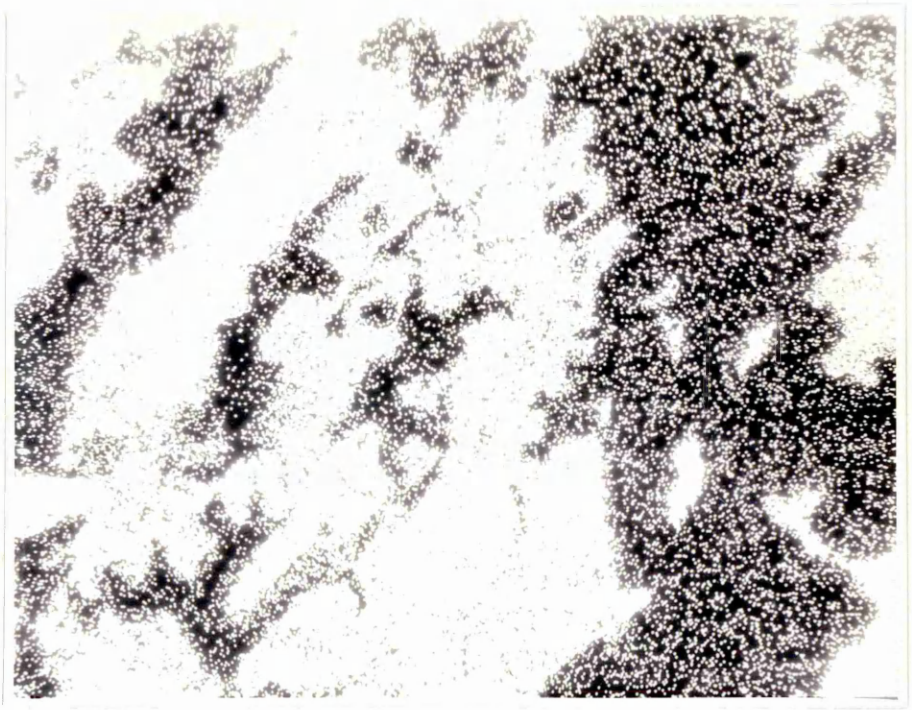

Plate 4-31: Scanning x-ray mapping of (Si) distribution in the area shown in Plate 4-29.
Magnification: 400 x 1.1.

Plate 4-32: Scanning x-ray mapping of (Fe) distribution in the area shown in Plate 4-29.
Magnification: 400 x 1.1.

Plate 4-33: Scanning photomicrograph of a cone 57% reduced Fe_2O_3 plus SiO_2 after being tested for softening with 0.01g of sulphur at 1165°C in a sealed silica tube.
Magnification: 1600 x 1.2.

Plate 4-34: Scanning photomicrograph of 79% reduced Fe_2O_3 plus SiO_2 cone, after softening test with 0.01 g of sulphur at 1172°C in sealed silica tube.

Magnification: 1200 x 1.2.

Plates 4-35 to 4-37 show X-ray mapping for the distribution of (S), (Si) and (Fe) in Plate 4-34

Plate 4-38 shows a photomicrograph of a cone containing 79% reduced Fe_2O_3 with SiO_2 after being tested for softening behaviour at 1180°C for 15 minutes with 0.01g of sulphur, while Plate 4-39 shows the (S) distribution in the photomicrographed area.

The results of the above experiments indicate that formation of liquid occurs in the grain boundary between the solid particles. The components of this liquid are mainly (S) and (Fe). The various samples investigated suggests that with increasing temperature the amount of liquid formation in the grain boundary increases causing more plasticity of the cone until complete melting occurs.

Investigation of the cones after the softening test with 0.01g of sulphur in sealed silica tubes using the Zeiss optical microscope indicated the formation of sulphides, distributed all over the section, as shown in Plate 4-40.

Scanning Electron Microscope investigation of cones having the same composition, 80 mass % FeO, 20 mass % SiO_2, and tested for softening under a sulphur vapour pressure in sealed silica tubes for various testing times, indicated that the amount of liquid formed in the grain boundary was nearly the same, although there was a depression of the softening temperature observed with increasing softening test time.

Plate 4-35: Scanning x-ray mapping of (S) distribution in the area shown in Plate 4-34.
Magnification: 1200 x 1.2.

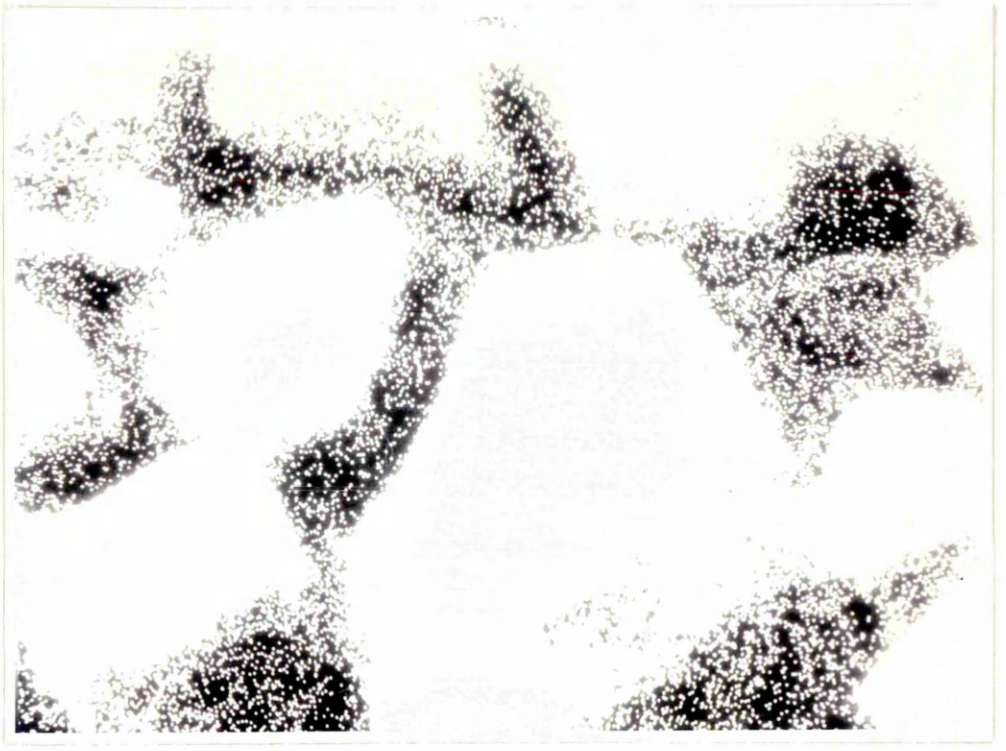

Plate 4-36: Scanning x-ray mapping of (Si) distribution in the area shown in Plate 4-34.
Magnification: 1200 x 1.2.

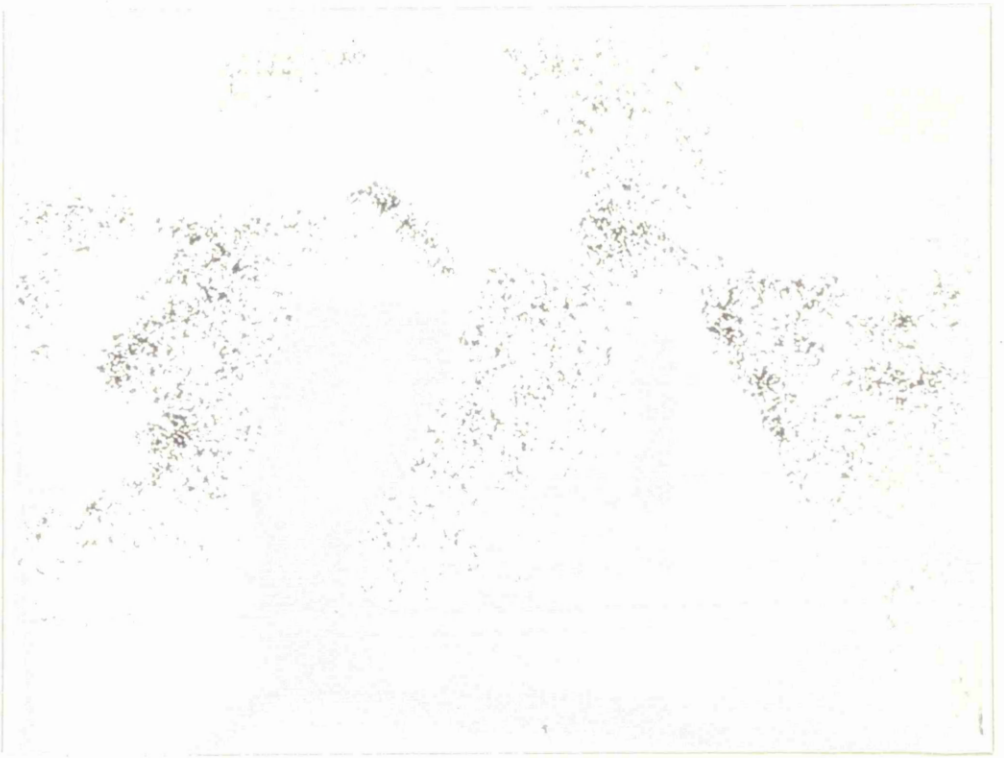

Plate 4-37: Scanning x-ray mapping of (Fe) distribution in the area shown in Plate 4-34.
Magnification: 1200 x 1.2.

Plate 4-38: A scanning photomicrograph of a 79% reduced Fe_2O_3 plus SiO_2 cone, after being tested with 0.01 gm of sulphur for softening at 1180°C.

Magnification: 800 x 1.2.

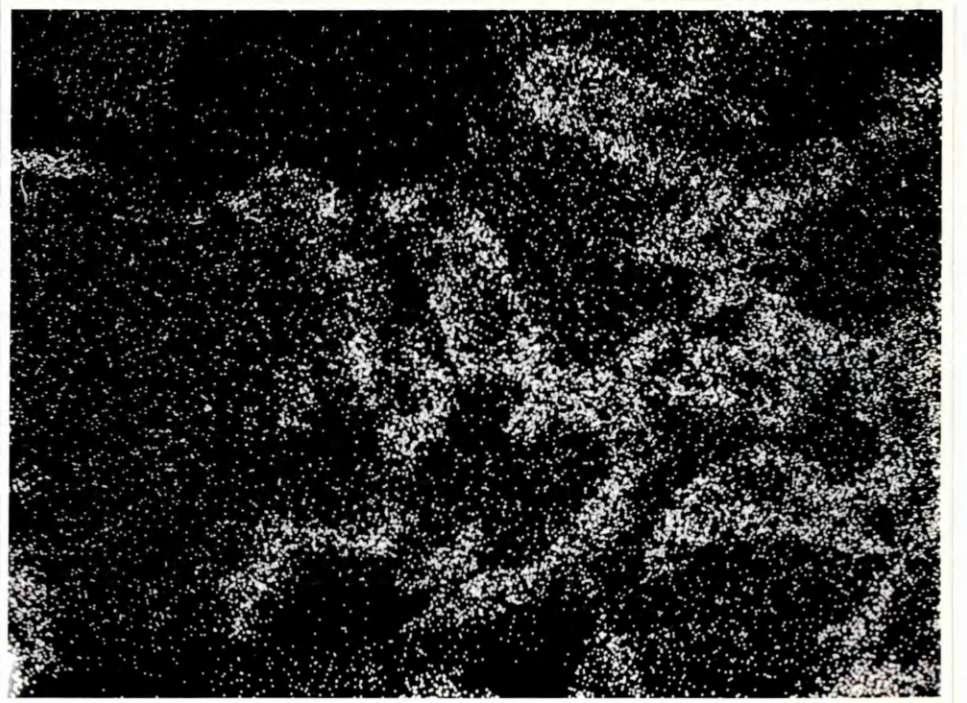

Plate 4-39: Scanning x-ray mapping of (S) distribution in the area shown in Plate 4-38.
Magnification: 800 x 1.2.

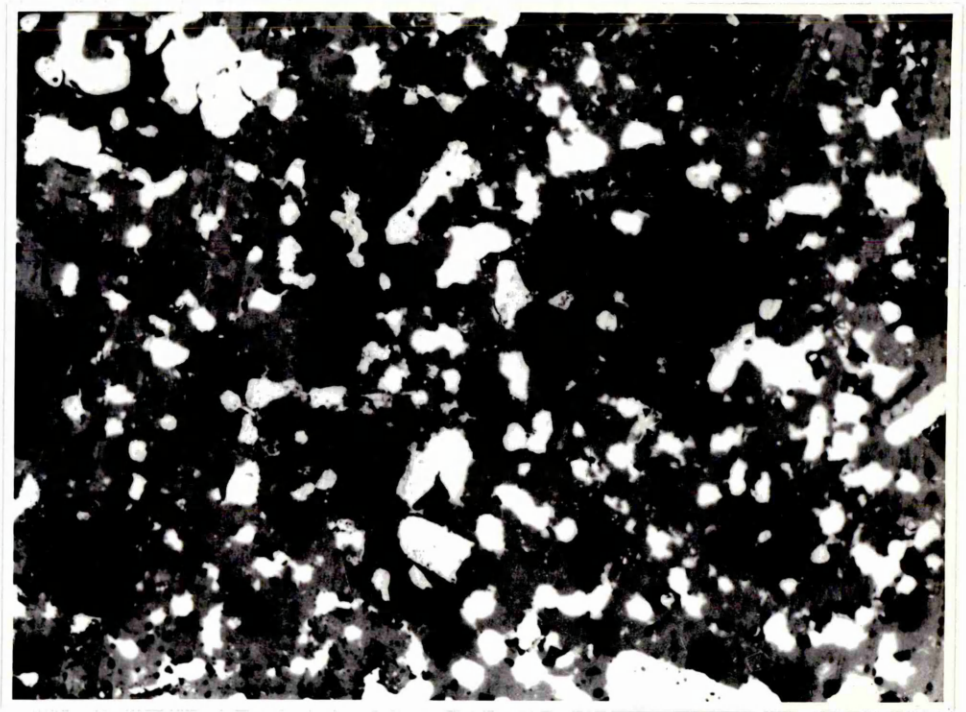

Plate 4-40: A polished section of 79% reduced Fe_2O_3 and SiO_2 cone, Fe mass/SiO_2 mass = 3.12, tested for softening with 0.01gm of sulphur in a sealed silica tube at 1172°C. The yellow lustre particles are iron sulphide inclusions. Magnification: 63X.

4.2.3 (a) The Softening Behaviour of Pure Partially Reduced Fe_2O_3 plus SiO_2 Cones with Potassium Vapour and Argon as the Gas Phase Inside the Sealed Silica Tube

A container holding potassium carbonate and a cone formed from a mixture of partially reduced Fe_2O_3 and SiO_2 mixture ($\frac{\text{mass of Fe}}{\text{mass of } SiO_2} = 3.12$) were sealed in silica tubes under an argon pressure of 50mm of mercury at room temperature (plate 3-2 on page 78), to investigate the softening behaviour of the cone. As shown in Table 4-16, the softening temperature of these cones was 1231°C. From the results in section 4.2.2 (a), the cones having the same composition but sealed in an inert argon atmosphere only, softened at a temperature of 1214°C and completely melted at a temperature of 1228°C. This means that the presence of potassium vapour did not lower the softening temperature of the tested cone. On the contrary, the experiments indicated that the presence of potassium vapour in the amounts shown in Appendix 2 caused hardening of the cones investigated.

4.2.3 (b) Metallographic Examination

Plate 4-41 shows a scanning photomicrograph of a cone tested in a sealed silica tube under a potassium vapour pressure of about 0.2×10^{-4} atmospheres at 1155°C. Investigation of the tested cone by Scanning Electron Microscopy showed that potassium had condensed on the surface. Plates 4-42, 43 and 44 shows the (K), (Fe), and (Si) distribution, x-ray mapping of the section shown in Plate 4-41.

Table 4-16: The Softening Behaviour of Pure $FeO-SiO_2$ Cones Tested with Potassium Carbonate in Sealed Silica Tubes

Run No.	Potassium Carbonate Inside the Silica Tube	Test Temperature °C	Observations
1	0.01g in a container	1155	No softening
2	0.01g in a container	1178	No softening
3	0.01g in a container	1190	No softening
4	0.01g in a container	1225	Not softening but melt formed
5	0.01g in a container	1227	Not softening but melt formed
6	0.01g in a container	1231	Softening

Plate 4-41: Scanning photomicrograph of a cone of 80 mass % FeO - 20 mass % SiO_2 after being tested for softening at 1155°C with 0.01g of K_2CO_3 in a sealed silica tube.
Magnification: 800 x 1.2.

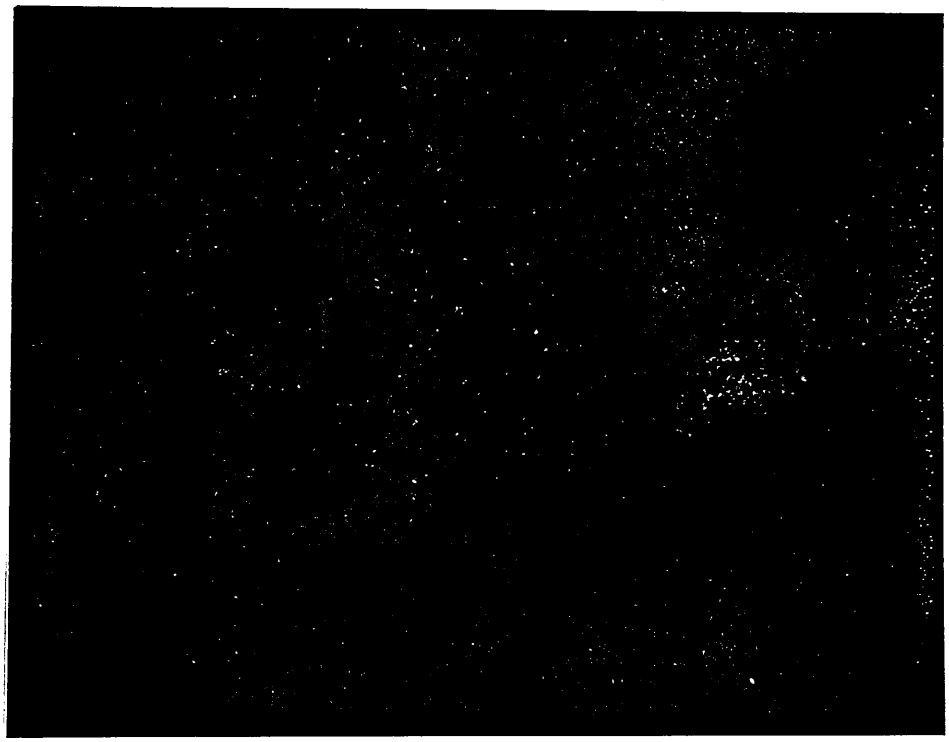

Plate 4-42: Scanning X-ray mapping for (K) distribution in the area shown in Plate 4-41.
Magnification: 800 x 1.2.

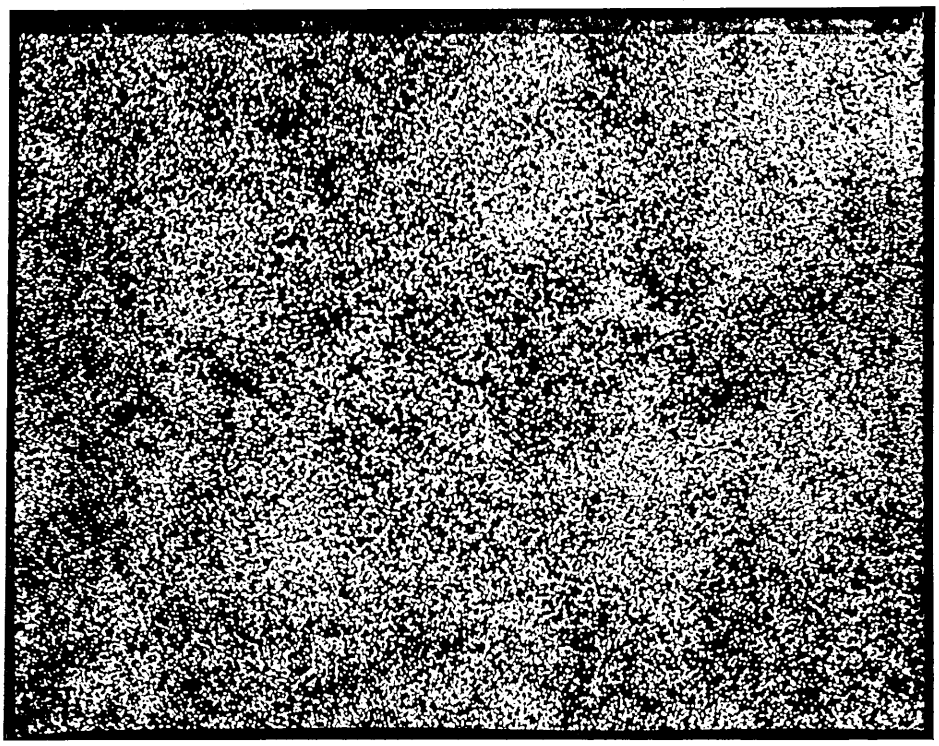

Plate 4-43: Scanning X-ray mapping for (Fe) distribution in the area shown in Plate 4-41.
Magnification: 800 x 1.2.

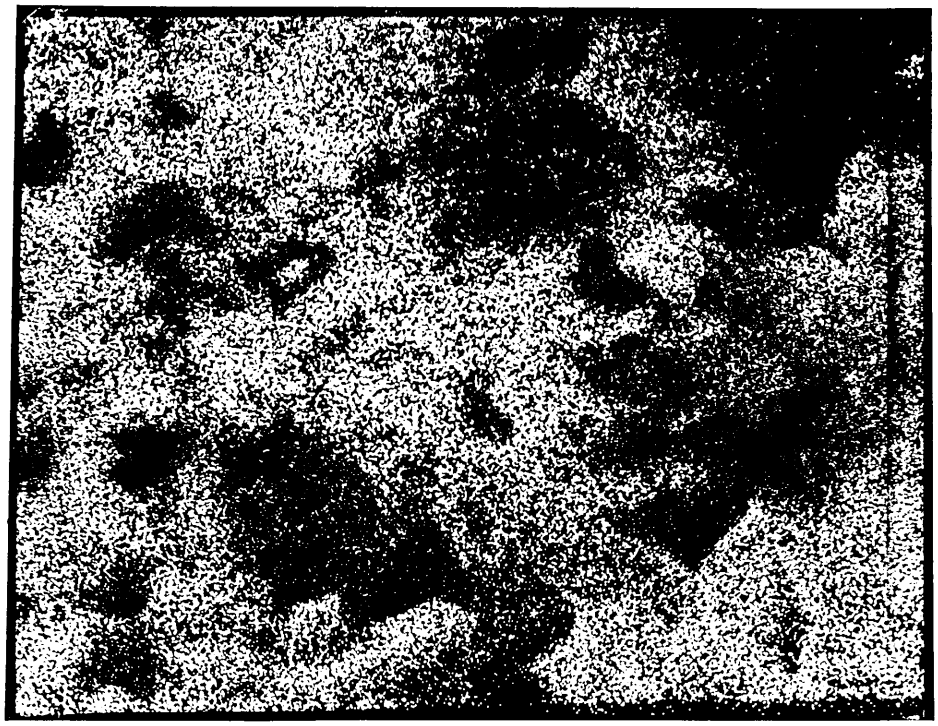

Plate 4-44: Scanning X-ray mapping for (Si) distribution in the area shown in Plate 4-41.

Magnification: 800 x 1.2.

The scanning photomicrograph of a cone tested at 1190°C in a sealed silica tube under a potassium vapour pressure of about 0.2×10^{-4} atmosphere shows a small amount of liquid formation between the grains (plate 4-45).

Plate 4-46 shows a scanning photomicrograph of a cone tested under a potassium vapour pressure of 0.2×10^{-4} atmosphere at 1231°C. This cone softened and on bending fused to the inner wall of the silica tube. Plate 4-46 shows wetting of the grains and the formation of a liquid. X-ray mapping of different areas on the softened cone showed the absence of (K).

4.2.4. (a) <u>The Softening Behaviour of FeO-SiO_2-$Ca\ CO_3$-K_2CO_3 Cones in Sealed Silica Tubes</u>

The softening behaviour of cones having the composition 83 mass % FeO, 10 mass % SiO_2, 5 mass % $Ca\ CO_3$, 2 mass % K_2CO_3 was investigated under an argon atmosphere in sealed silica tubes. The argon pressure inside the silica tube was 50mm of mercury at room temperature. From Table 4-17 softening temperature of 1055°C was observed. However, by increasing the time of the test from 15 minutes, the normal testing time for softening, to 30 minutes, a lowering in softening temperature by 32°C was recorded.

Plate 4-45: Scanning photomicrograph of a cone containing 80 mass % FeO - 20 mass % SiO_2 tested for softening with 0.01g of K_2CO_3 in a sealed silica tube at 1190°C.
Magnification: 800 x 1.4.

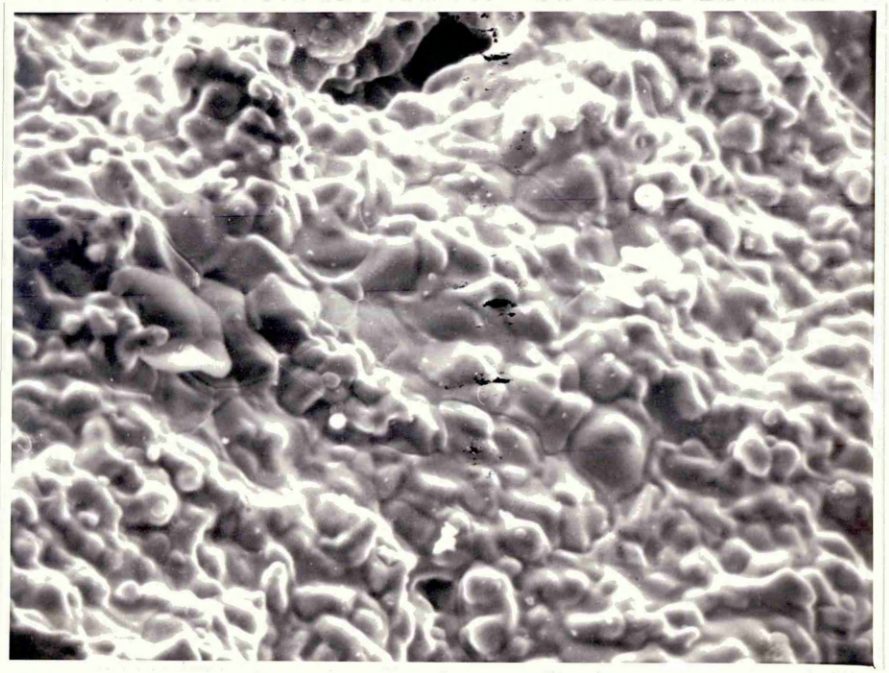

Plate 4-46: Scanning photomicrograph of a cone containing 80 mass % FeO-20 mass % SiO_2 after being tested for softening with 0.01g of K_2CO_3 in a sealed silica tube at 1231°C.

Magnification: 800 x 1.8.

Table 4-17: The Effect of Calcium and Potassium Carbonates in the Softening Behaviour of $FeO-SiO_2$ Cones Inside Sealed Silica Tubes

Run No.	Cone Composition	Test Time Minutes	Test Temp. °C	Observations
1	83 mass % FeO, 10 mass % SiO_2, 5 mass % $CaCO_3$, 2 mass % K_2CO_3	15	1028	No softening
2	83 mass % FeO, 10 mass % SiO_2, 5 mass % $CaCO_3$, 2 mass % K_2CO_3	15	1055	Softening
3	83 mass % FeO, 10 mass % SiO_2, 5 mass % $CaCO_3$, 2 mass % K_2CO_3	15	1085	Over softening
4	83 mass % FeO, 10 mass % SiO_2, 5 mass % $CaCO_3$, 2 mass % K_2CO_3	30	1023	Softening

Table 4-18: The Softening Behaviour of 83 mass % FeO, 10 mass % SiO_2, 5 mass % $CaCO_3$, and 2 mass % K_2CO_3 Cones with 0.01g of Sulphur Inside Sealed Silica Tubes

Run No.	Test Temperature °C	Observation
1	1147	Softening
2	1151	Softening

4.2.4 (b) The Softening Behaviour of $FeO-SiO_2-CaCO_3-K_2CO_3$

Cones having a composition of 83 mass % FeO, 10 mass % SiO_2, 5 mass % $CaCO_3$, 2 mass % K_2CO_3 were investigated for softening behaviour under a sulphur vapour pressure in a sealed silica tube. Softening at about 1149°C was noticed. This softening temperature is much higher than for cones with the same composition but in the absence of sulphur vapour as can be seen by comparing Tables 4-17 and 4-18.

4.2.4 (c) Metallographic Examination of $FeO-SiO_2-CaCO_3-K_2CO_3$ Cones after the Softening Test under Various Gas Phases in Sealed Silica Tubes

Plate 4-47 is a photomicrograph from the Scanning Electron Microscope investigation of a cone having a composition of 83 mass % FeO, 10 mass % SiO_2, 5 mass % $CaCO_3$ and 2 mass % K_2CO_3 after being tested under argon at 1023°C for 30 minutes showing formation of liquid. X-ray mapping of the viewed area in Plate 4-47 indicated that the liquid formed contained mainly (Si) and (K) with very little (Ca) (Plates 4-50, 48 and 49).

Plate 4-51 shows a photomicrograph from the Scanning Electron Microscope examination of a cone with the same composition as the previous one (83 mass % FeO, 10 mass % SiO_2, 5 mass % $CaCO_3$ and 2 mass % K_2CO_3) after being tested in a sealed silica tube with 0.01g of sulphur at 1151°C, which illustrates

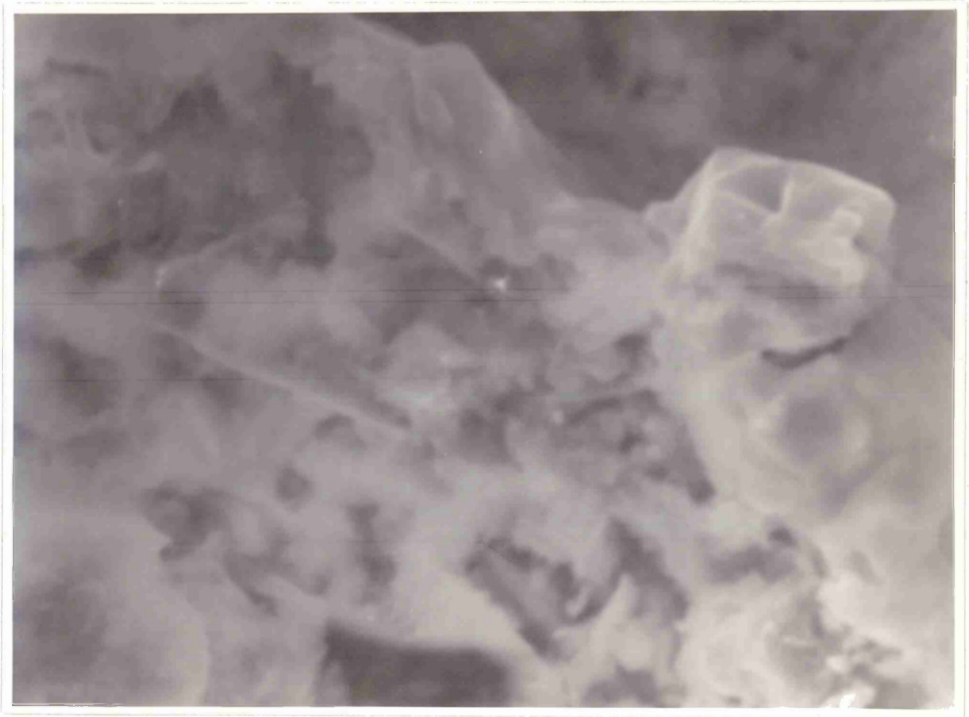

Plate 4-47: Scanning photomicrograph of a cone containing 83 mass % FeO, 10 mass % SiO_2, 5 mass % $CaCO_3$, and 2 mass % K_2CO_3 after being tested for softening under argon in a sealed silica tube at 1023°C for 30 minutes.
Magnification: 800 x 1.3.

Plate 4-48: Scanning x-ray mapping for (K) distribution in the area shown in Plate 4-47.
Magnification: 800 x 1.3.

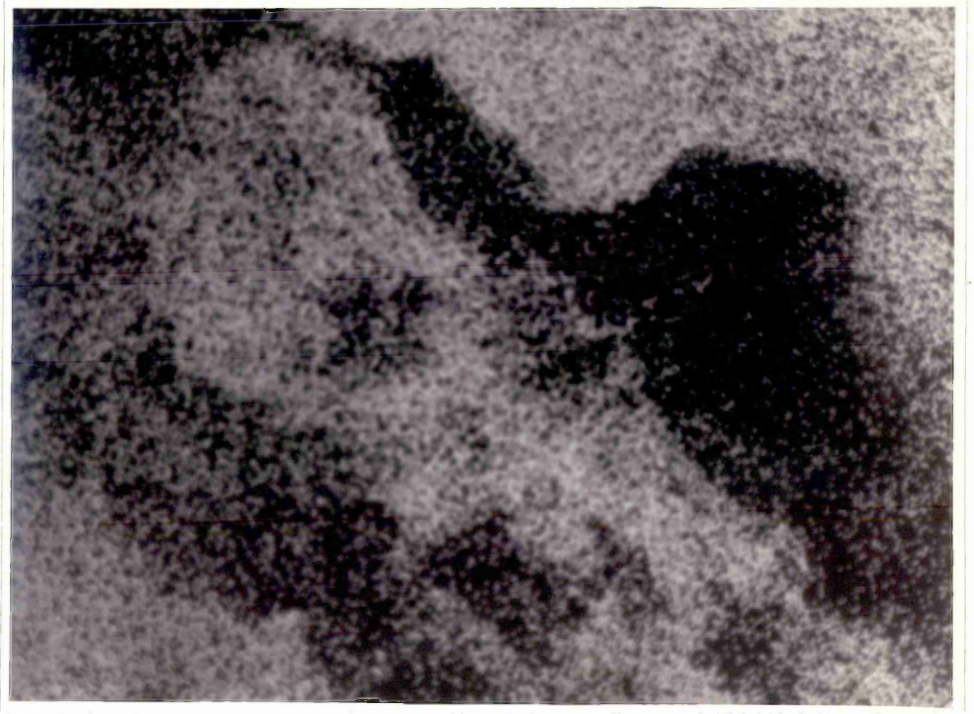

Plate 4-49: Scanning x-ray mapping for (Ca) distribution in the area shown in Plate 4-47.
Magnification: 800 x 1.3.

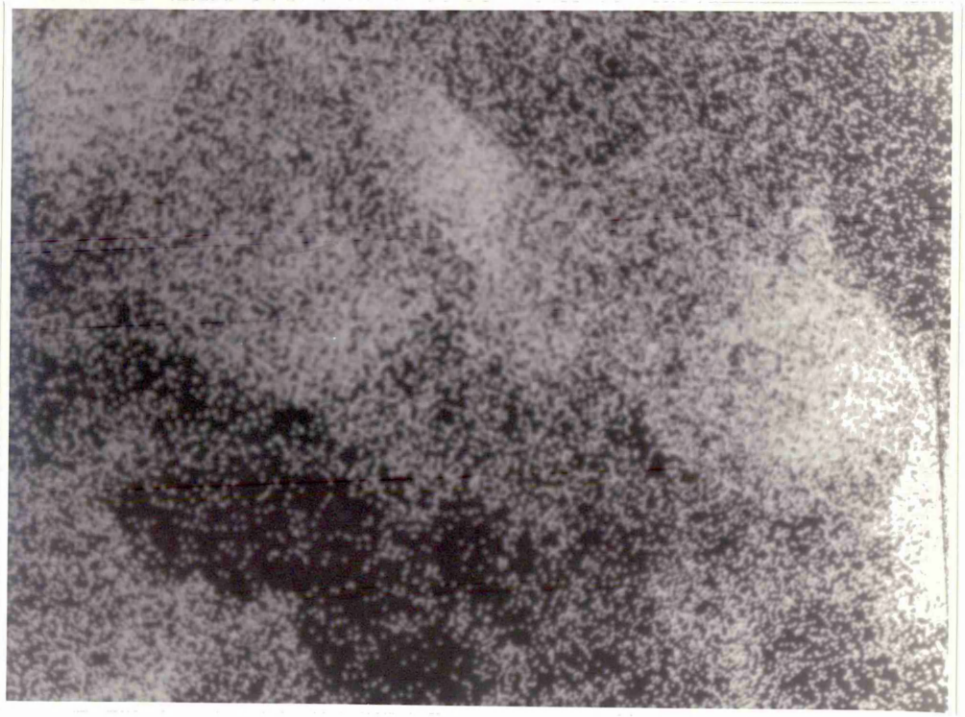

Plate 4-50: Scanning x-ray mapping for (Si) distribution in the area shown in Plate 4-47.
Magnification: 800 x 1.3.

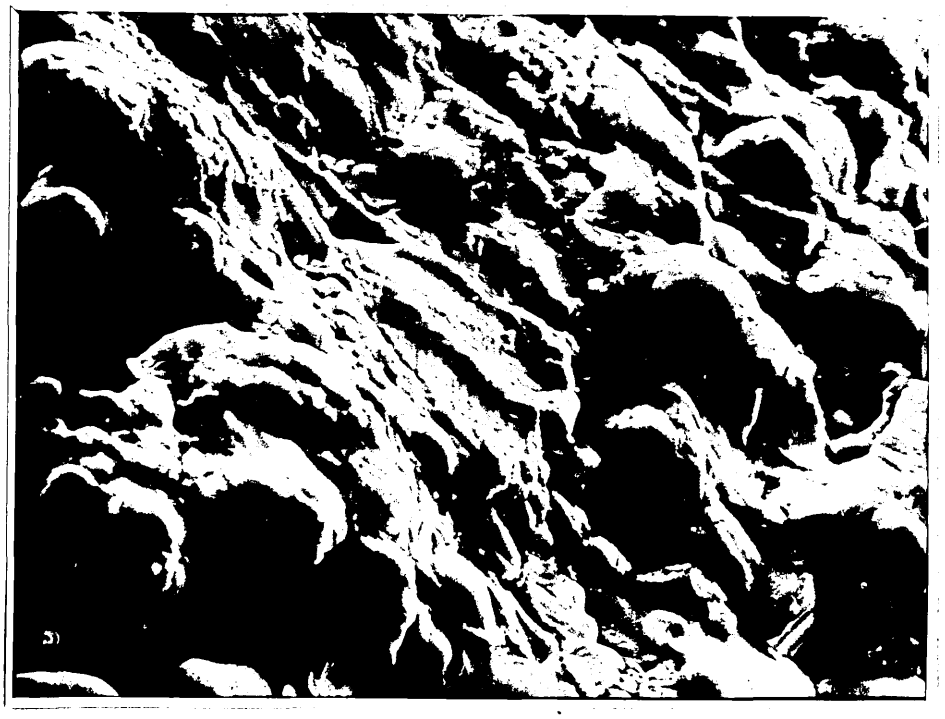

Plate 4-5 1: Scanning photomicrograph of a cone composed of 83 mass % FeO, 10 mass % SiO_2, 5 mass % $CaCO_3$, 2 mass % K_2CO_3 tested for softening with 0.01g. of sulphur in a sealed silica tube at 1151°C. Magnification: 800 x 1.3.

the formation of liquid between the grains and the wetting of other areas by the liquid phase formed during testing of the cone. X-ray mapping, Plates 4-52 to 4-55, indicated that the liquid formed between the grains contained a high concentration of (S). (Fe) was evenly distributed all over the section giving a completely white X-ray mapping image. While X-ray mapping indicated that the liquid was composed mainly of (Ca) and (Si) but considering the extensive presence of (Fe), this may be taken to indicate the presence of a (Fe), (Si), (Ca) and (O) eutectic. The wetted area may also contain a low concentration of (S) and (K). Potassium was uniformly distributed over the tested section except in small regions which showed no signs of liquid formation.

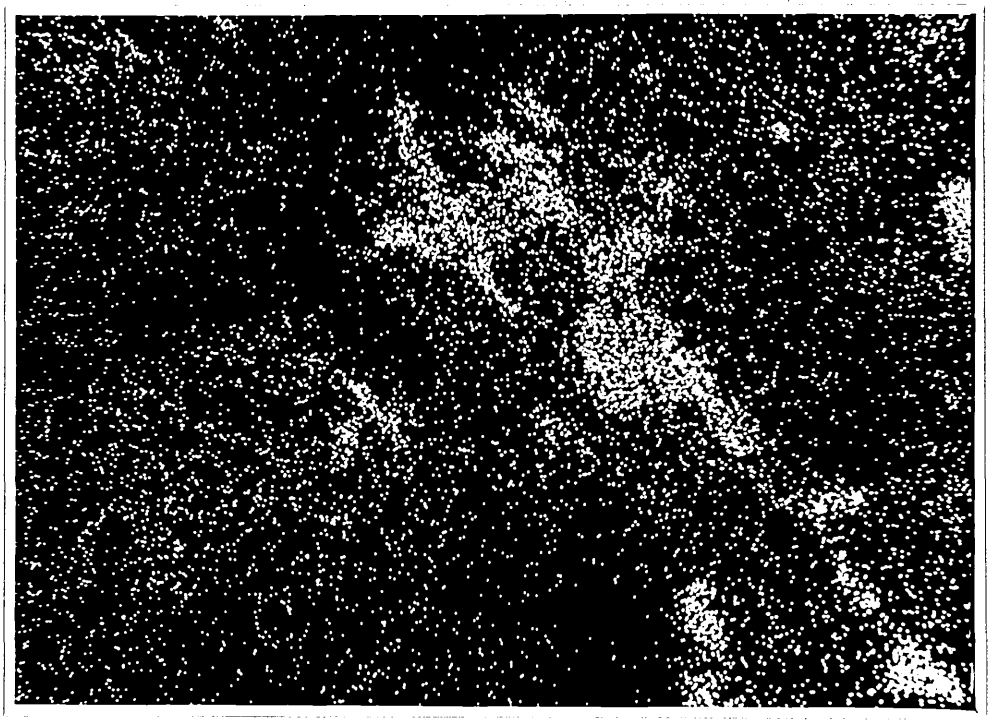

Plate 4-52: Scanning X-ray mapping of (Ca) distribution in the area shown in Plate 4-5$\underline{1}$.

Magnification: 800 x 1.3.

Plate 4-53: Scanning X-ray mapping of (Si) distribution in the area shown in Plate 4-51.
Magnification: 800 x 1.3.

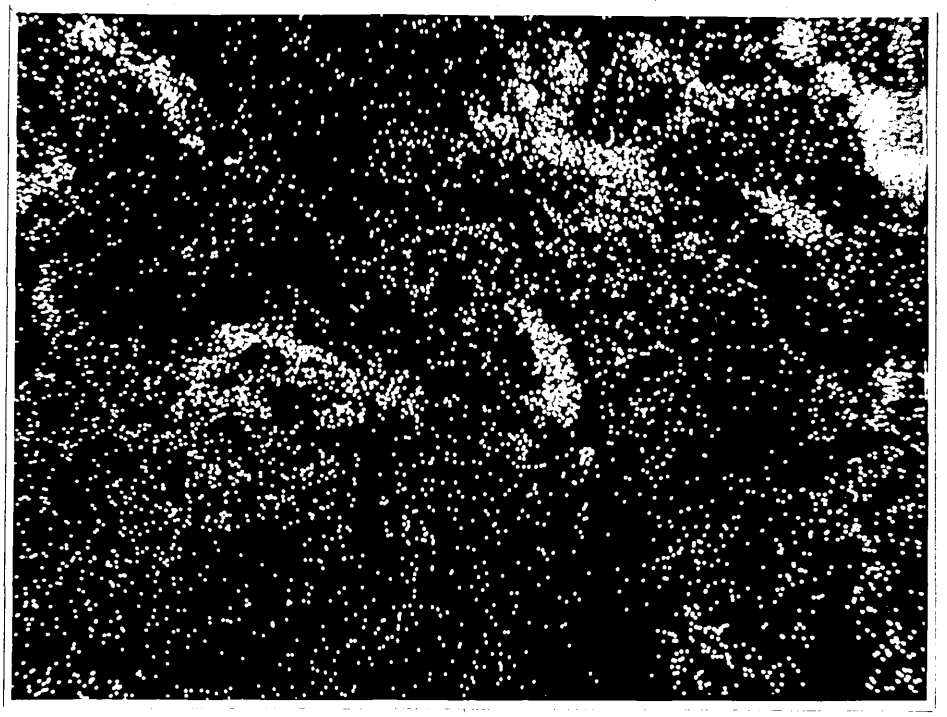

Plate 4-54: Scanning X-ray mapping of (S) distribution in the area shown in Plate 4-51.
Magnification: 800 x 1.3.

Plate 4-55: Scanning X-ray map of (K) distribution in the area shown in Plate 4-51.
Magnification: 800 x 1.3.

4.2.5 (a) The Softening Behaviour of Pure Partially Reduced Fe_2O_3-SiO_2 Cones with Sodium Carbonate in Sealed Silica Tubes

The softening behaviour of reduced Fe_2O_3-SiO_2 cones ($\frac{\text{mass of Fe}}{\text{mass of } SiO_2}$ = 3.12) mixed with different amounts of Na_2CO_3 gave interesting results. Table 4-19 shows the softening behaviour of Fe_2O_3-SiO_2 cones possessing both different degrees of Fe_2O_3 reduction and different percentages of sodium carbonate addition, tested in sealed silica tubes under argon.

Figure 5-1 on page 302, shows the softening behaviour of cones possessing different degrees of Fe_2O_3 reduction enriched with 2 mass % Na_2CO_3. The following observation can be made from this figure:-

(i) A marked lowering in softening temperature occurs after 10% reduction until 30% reduction.

(ii) There is a rise in the softening temperature in the range 30-50% reduction.

(iii) This is followed by a second lowering in the reduction range 60-70%.

(iv) At 100% reduction no softening can be obtained even by raising the test temperature to 1270°C which was considered to be over the reliable working temperature of the silica tube.

TABLE 4-19 - The Effect of Sodium Carbonate on the Softening Behaviour of Partially Reduced Fe_2O_3-SiO_2 Cones in Sealed Silica Tubes

Run No.	Degree of Fe_2O_3 Reduction	Na_2CO_3 Enrichment mass	Test Temperature °C	Observation
1	7.3%	2%	1189	Not Softened
2	7.3%	2%	1213	Not Softened
3	7.3%	2%	1228	Softened
4	22%	0.57%	1188	Softened
5	22%	0.57%	1197	Over Softened
6	22%	0.75%	1178	Softened
7	22%	1.78%	1158	Softened
8	22%	2.2%	1147	Softened
9	22%	3%	1145	Softened
10	22%	3%	1151	Softened
11	41%	2%	1191	Softened
12	49.7%	1.735%	1162	Softened
13	49.7%	1.75%	1161	Softened
14	49.7%	2.35%	1152	Not Softened
15	49.7%	2.37%	1168	Softened
16	49.7%	2.37%	1182	Over Softened

TABLE 4 - 19 Continued

Run No.	Degree of Fe_2O_3 Reduction	Na_2CO_3 Enrichment 'mass'	Test Temperature ^oC	Observation
17	59%	0.2%	1190	Softened
18	59%	1.05%	1201	Softened
19	59%	1.09%	1187	Softened
20	59%	1.48%	1179	Softened
21	59%	2.2%	1156	Softened
22	59%	2.9%	1154	Not Softened
23	59%	2.98%	1163	Softened
24	64.8%	2%	1170	Softened
25	71%	0.98%	1173	Melting
26	71%	1.07%	1193	Over Softening
27	71%	1.05%	1201	Softened
28	71%	1.3%	1157	Not Softening
29	71%	1.3%	1173	Softened
30	71%	1.3%	1188	Over Softened
31	71%	1.5%	1193	Softened
32	71%	1.6%	1207	Softened
33	71%	1.87%	1155	No Softening
34	71%	1.9%	1163	Softened
35	71%	1.9%	1173	Over Softened
36	71%	3%	1173	Softened

Table 4-19 Continued

Run No.	Degree of Fe_2O_3 Reduction	Na_2CO_3 Enrichment mass%	Test Temperature °C	Observation
37	95.5%	0.45%	1223	No Softening
38	95.5%	1.35%	1208	No Softening
39	95.5%	2.2%	1192	No Softening
40	95.5%	3.17%	1201	No Softening
41	95.5%	4.3%	1188	No Softening
42	100%	.86%	1270	No Softening
43	100%	2.1%	1270	No Softening

Figure 5-11, on page 303, shows the effect of the percentage of sodium carbonate enrichment on the softening temperatures of cones possessing the same constitutents and percentages of reduction, investigated under argon in sealed silica tubes. It can be seen that enrichment of the cones with Na_2CO_3 caused a lowering in the softening temperature irrespective of the degree of reduction until a certain percentage of sodium carbonate enrichment was reached. A rise in the softening temperature then occurred, or in other words the sodium carbonate caused hardening of the tested cones at this specified percentage of sodium carbonate enrichment. Again this hardening was followed by a second lowering in the softening temperature. Plate 4-56 shows an example of the effect of the percentage of sodium carbonate enrichment on the softening behaviour. The tubes shown have 71% reduced Fe_2O_3-SiO_2, $\frac{\text{mass of Fe}}{\text{mass of SiO}_2}$ = 3.12, sealed under 50mm of mercury argon pressure and tested at 1173°C for 15 minutes. The enriched cone with 0.98 mass % Na_2CO_3 showed melting. The cone enriched with 1.3 mass % Na_2CO_3 shows indications of softening as it is partially bending. With 1.9 mass % Na_2CO_3 the cone shows over softening at 1173°C. With 3 mass % Na_2CO_3, tested for softening at 1173°C the cone only shows softening. From the results described in section 4.2.2. (b) with no Na_2CO_3 at a test temperature 1173°C no softening occurs and the cone still retains its original shape.

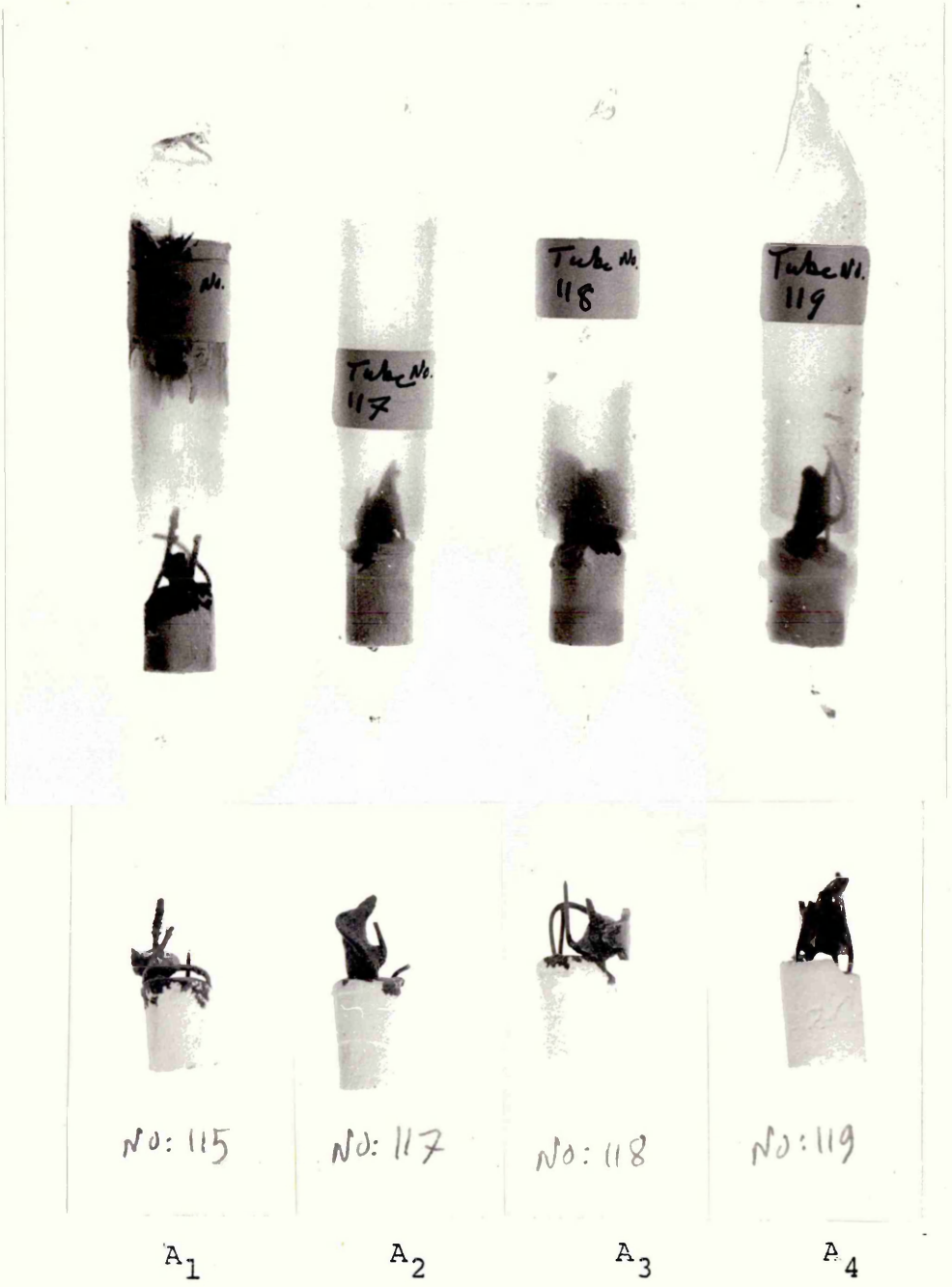

A_1 A_2 A_3 A_4

Plate 4-56: Photo A_1, A_2, A_3, and A_4 are 71% reduced Fe_2O_3-SiO_2 cones having 0.98 mass %, 1.3 mass %, 1.9 mass %, and 3 mass % Na_2CO_3 respectively after being tested for softening behaviour in sealed silica tubes at 1173°C.

Table 4-20 shows results of chemical analysis of cones enriched with sodium carbonates after being tested for softening.

4.2.5 (b) Metallographic Examination of Reduced Fe_2O_3-SiO_2-Cones Enriched with Sodium Carbonate, after the Softening Test

The scanning photomicrograph shown in Plate 4-57, of a cone composed of 59% reduced Fe_2O_3 and SiO_2, $\left(\frac{\text{mass of Fe}}{\text{mass of } SiO_2} = 3.12\right)$ enriched with 0.2% Na_2CO_3 after testing for softening at 1190°C shows that there was liquid formation all over the area examined, which is supported by the observation of a uniform distribution of (Na), (Si) and (Fe), as shown in Plates 4-58, 59 and 60.

Plate 4-61 shows a scanning photomicrograph of a cone composed of 71% reduced Fe_2O_3 and SiO_2, $\left(\frac{\text{mass of Fe}}{\text{mass of } SiO_2} = 3.12\right)$, with 1.9 mass % Na_2CO_3, tested for softening at 1173°C. Plate 4-61 shows that all over the section liquid phase was formed at the test temperature (1173°C). X-ray spot analysis shows the white shapes appearing over the surface are (Na). Plates 4-62, 63 and 64, show X-ray mapping of the (Na), (Si) and (Fe) distribution.

TABLE 4-20: The Percentage of Sodium Oxide in Partially Reduced Fe_2O_3-SiO_2 Cones. Enrichment with Sodium Carbonates after Softening Test in Sealed Silica Tubes

Run No.	Cone Composition	Softening Test Temp. °C	Mass % of Na_2CO_3 Before Softening Test	Mass % of Na_2CO_3 After Softening Test
1	7.3% reduced Fe_2O_3 + SiO_2	1228	2	0.671
2	22% reduced Fe_2O_3 + SiO_2	1178	0.75	0.133
3	22% reduced Fe_2O_3 + SiO_2	1151	3	0.69
4	57% reduced Fe_2O_3 + SiO_2	1140	2	0.784

Chemical analysis carried out on representative, partially reduced Fe_2O_3-SiO_2 cones enriched with 2 mass % Na_2CO_3 after firing and before tested for softening showed 2,07 mass % sodium carbonate content.

In all cases the cone comprised of a mixture of partially reduced Fe_2O_3 and SiO_2 such that, $\frac{\text{mass of Fe}}{\text{mass of } SiO_2} = 3.12$.

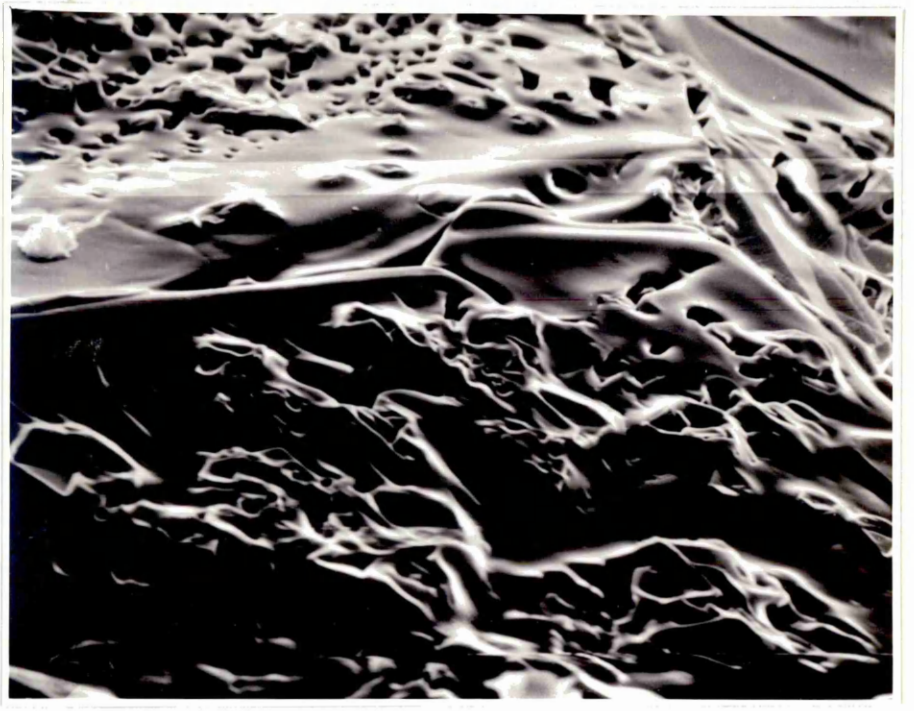

Plate 4-57: Scanning photomicrograph of 59% reduced Fe_2O_3 and SiO_2 cone, $\frac{\text{Fe mass}}{SiO_2 \text{ mass}}$ = 3.12, possessing 0.2 mass % Na_2CO_3. Tested for softening at 1190°C in a sealed silica tube.

Magnification: 800 x 1.4.

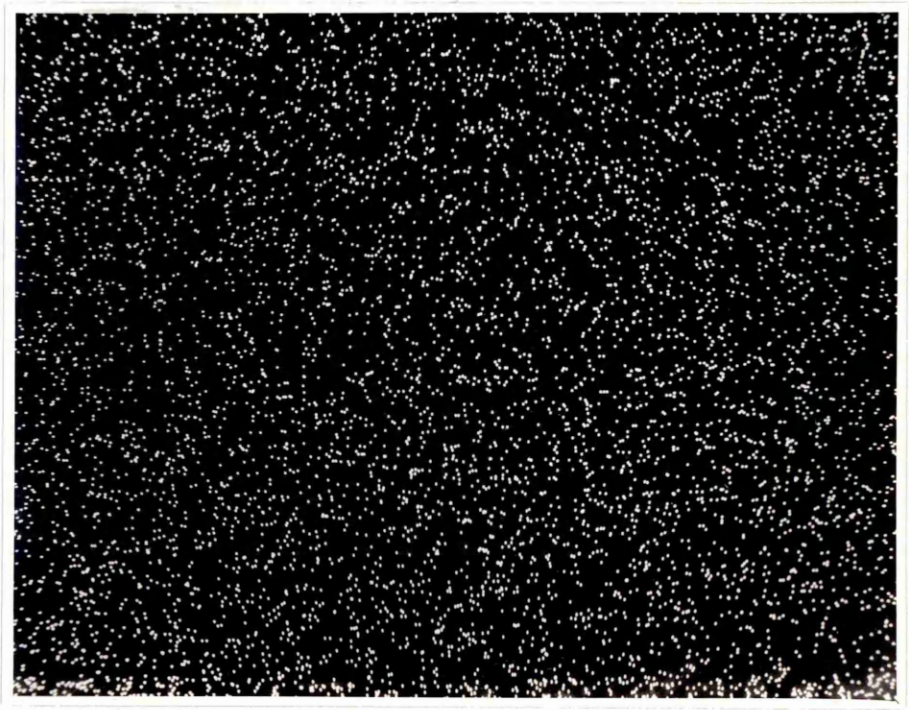

Plate 4-58 Scanning X-ray mapping for (Na) distribution in the area shown in Plate 4-57.
Magnification: 800 xl.4.

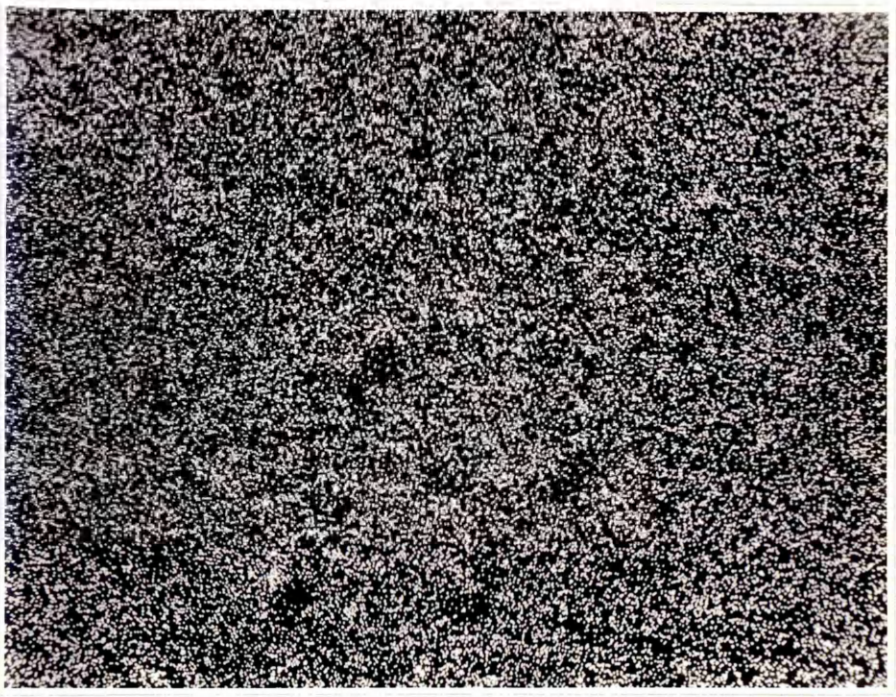

Plate 4-59: Scanning X-ray mapping for (Si) distribution in the area shown in Plate 4-57.
Magnification: 800 x 1.4.

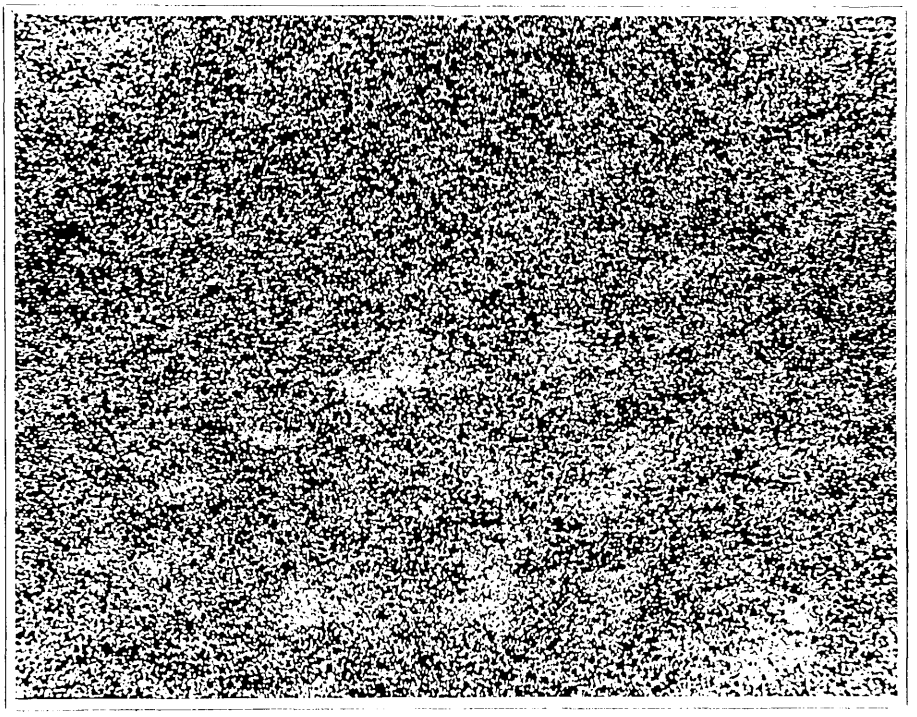

Plate 4-60: Scanning X-ray mapping for (Fe) distribution in the area shown in Plate 4-57.

Magnification: 800 x 1.4.

Plate 4-61: Scanning photomicrograph of 71% reduced Fe_2O_3 and SiO_2 cone, Fe mass/SiO_2 mass = 3.12 with 1.9 mass % Na_2CO_3. Tested for softening at 1173°C in a sealed silica tube.

Magnification: 3200 x 1.2.

Plate 4-62: Scanning X-ray mapping for (Na) distribution in the area shown in Plate 4-61.
Magnification: 3200 x 1.2.

Plate 4-63: Scanning X-ray mapping for (Si) distribution in the area shown in Plate 4-61.
Magnification: 3200 x 1.2.

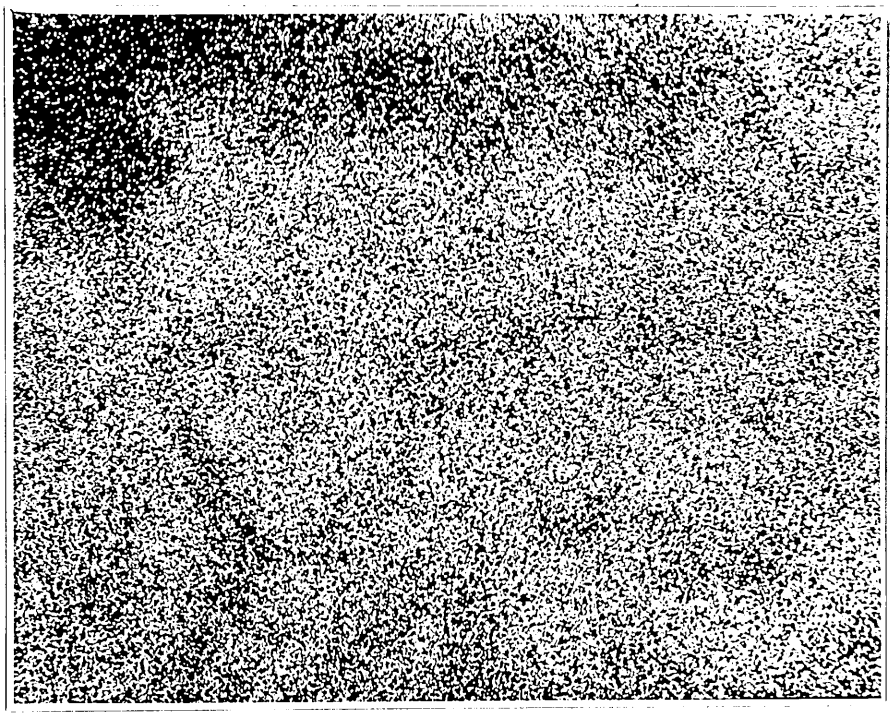

Plate 4- 64: Scanning X-ray mapping for (Fe) distribution in the area shown in Plate 4-61.
Magnification: 3200 x 1.2.

Plate 4-65 shows a scanning photomicrograph of a cone composed of 71% reduced Fe_2O_3 and SiO_2, $\left(\frac{\text{mass of Fe}}{\text{mass of } SiO_2} = 3.12\right)$ with 3 mass % Na_2CO_3, tested for softening at 1173°C. Plate 4-65 shows liquid formation having occurred in the left hand side of the area examined. X-ray investigation (Plate 4-66, 67 and 68) indicates that the liquid constituents were (Na), (Si) and (Fe), while the particles appearing in the right of the photomicrograph (Plate 4-65) possess intensive area of (Fe).

Plate 4-69 shows a scanning photomicrograph of a cone composed of 71% reduced Fe_2O_3 and SiO_2, $\left(\frac{\text{mass of Fe}}{\text{mass of } SiO_2} = 3.12\right)$ with 1.6 mass % Na_2CO_3 tested for softening at 1173°C. Plate 4-69 shows no clear liquid formation. While Plate 4-72 shows the scanning photomicrograph of a softening cone having the same composition as the cone in Plate 4-69 but tested at 1204°C. Plate 4-72 shows a liquid formation represents some 50% of the investigated area. Plate 4-73 shows the same cone in Plate 4-72 but at higher magnification. However x-ray investigation shows the zone of (Na) and the intensive existence of (Fe) all over the surface of the cone.

Plate 4-75 shows a scanning photomicrograph of a cone composed of 95% reduced Fe_2O_3 and SiO_2, $\left(\frac{\text{mass of Fe}}{\text{mass of } SiO_2} = 3.12\right)$, with 4.3 mass % Na_2CO_3, tested for softening at 1188°C. No softening was obtained at this high percentage of Na_2CO_3.

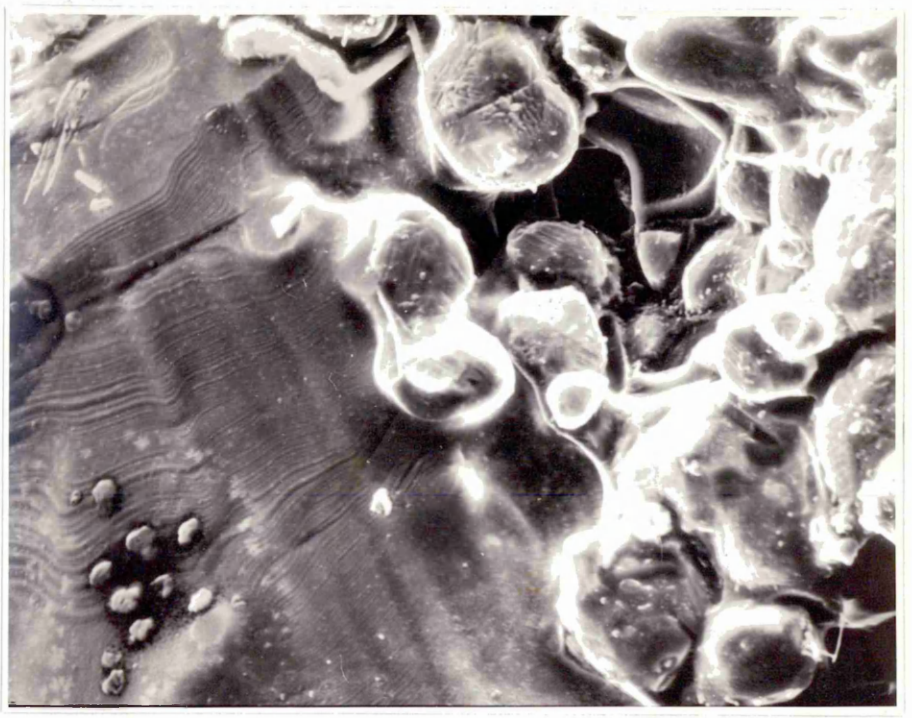

Plate 4-65: Scanning photomicrograph of 71% reduced Fe_2O_3, SiO_2 cone, Fe mass/SiO_2 mass = 3.12, with 3 mass % Na_2CO_3. Tested for softening in a sealed silica tube at 1173°C. Magnification: 800 x 1.4.

enrichment. Although investigation of the tested cone showed evidence of liquid formation on the surface.

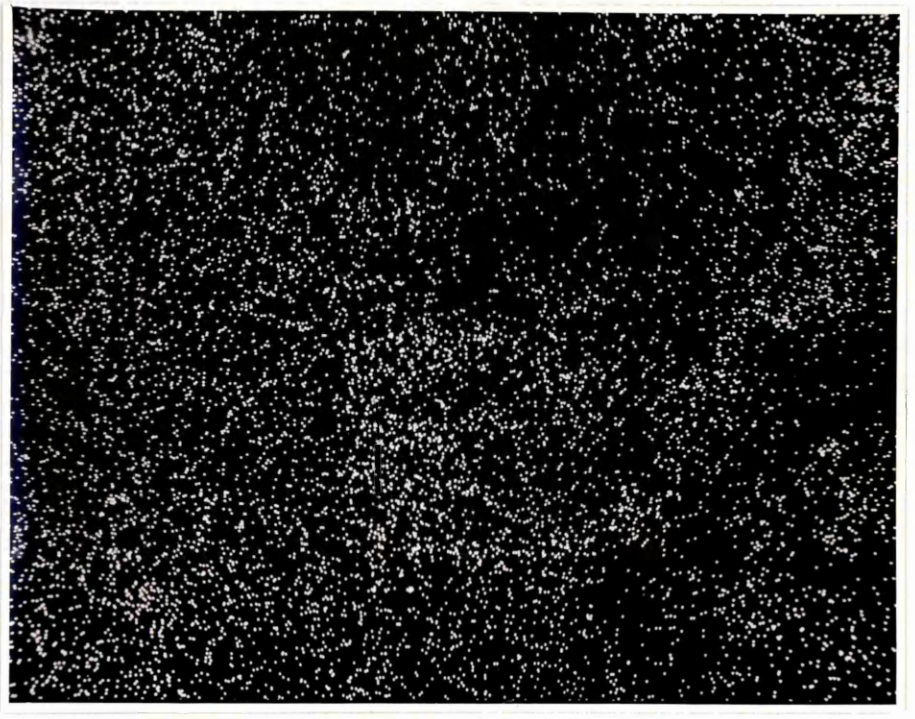

Plate 4-66: Scanning X-ray mapping for (Na) distribution in the area shown in Plate 4-65.
Magnification: 800 x 1.4.

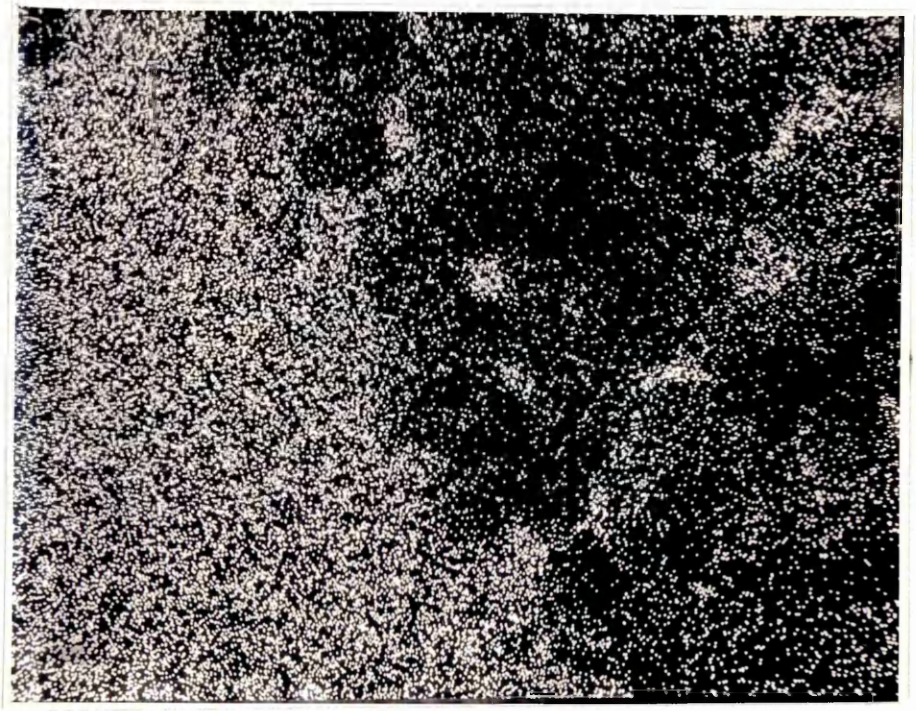

Plate 4-67: Scanning X-ray mapping for (Si) distribution in the area shown in Plate 4-65.
Magnification: 800 x 1.4.

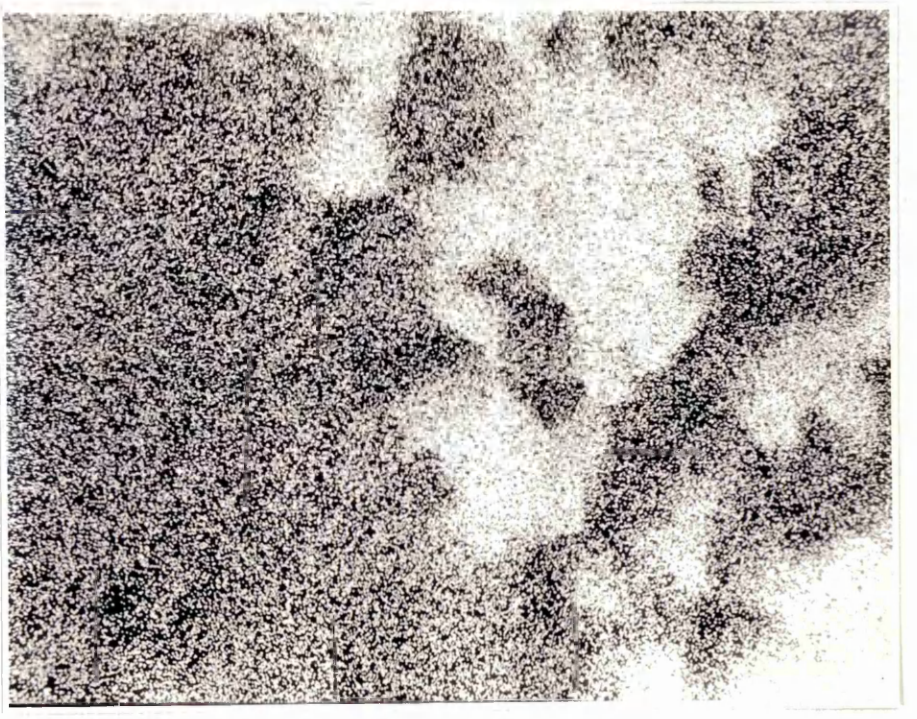

Plate 4-68: Scanning x-ray mapping for (Fe) distribution in the area shown in Plate 4-65.
Magnification: 800 x 1.4.

Plate 4-69: Scanning photomicrograph of 71% reduced Fe_2O_3, SiO_2 cone, Fe mass/SiO_2 mass = 3.12, with 1.6 mass % Na_2CO_3. Tested for softening in a sealed silica tube at 1173°C.
Magnification: 800 x 1.4.

Plate 4-70: Scanning x-ray mapping for (Na) distribution in the area shown in Plate 4-69.
Magnification: 800 x 1.4.

Plate 4-71: Scanning x-ray mapping for (Fe) distribution in the area shown in Plate 4-69.
Magnification: 800 x 1.4.

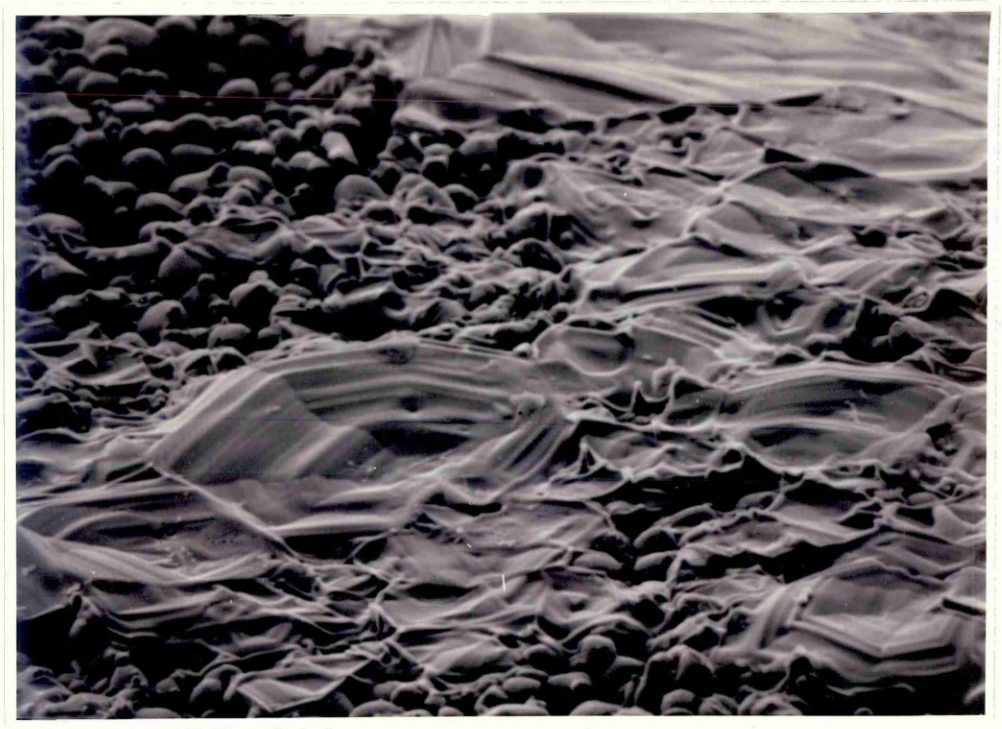

Plate 4-72: Scanning photomicrograph of 71% reduced Fe_2O_3, SiO_2 cone, $\frac{\text{Fe mass}}{SiO_2 \text{ mass}} = 3.12$, with 1.6 mass % Na_2CO_3. Tested for softening in a sealed silica tube at 1204°C.

Magnification: 200 x 1.2.

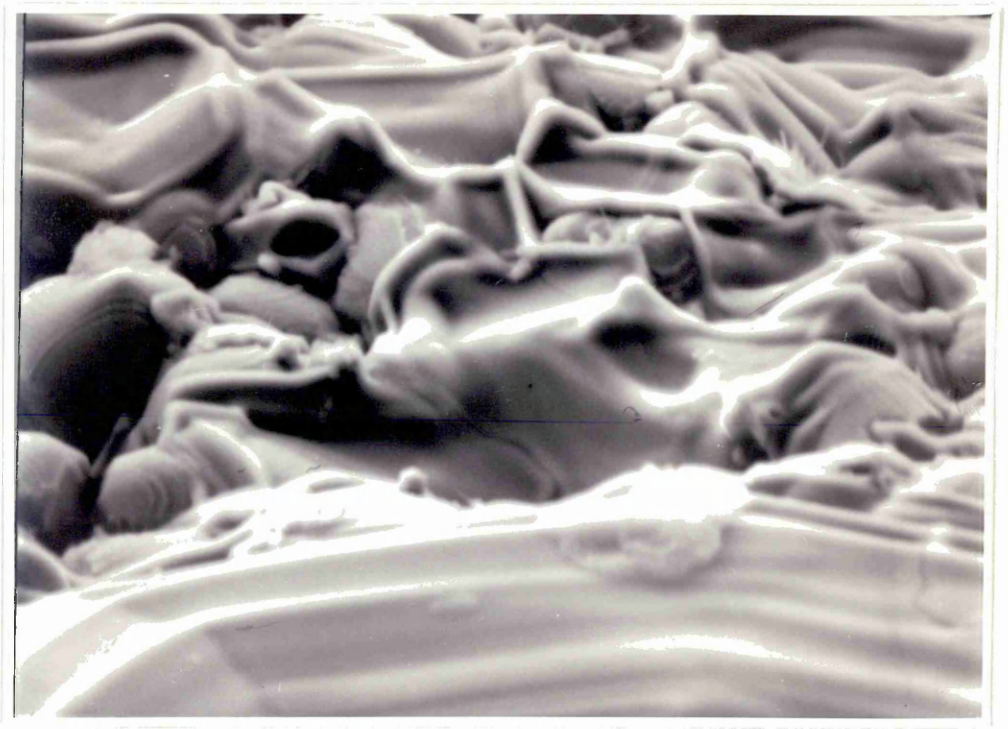

Plate 4-73: Scanning photomicrograph of 71% reduced Fe_2O_3, SiO_2 cone, $\frac{\text{Fe mass}}{SiO_2 \text{ mass}}$ = 3.12, with 1.6 mass % Na_2CO_3. Tested for softening in a sealed silica tube at 1204°C.

Magnification: 800 x 1.2.

Plate 4-74: Scanning x-ray mapping for (Si) distribution in the area shown in Plate 4-73.
Magnification: 800 x 1.2.

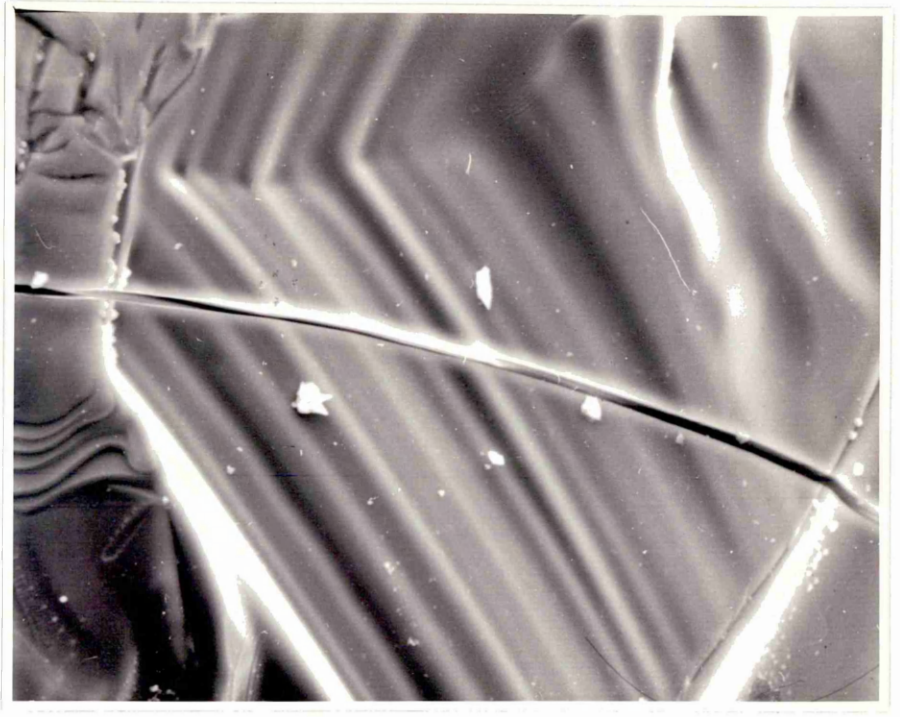

Plate 4-75: Scanning photomicrograph of the surface of a 95% reduced Fe_2O_3, SiO_2 cone, $\frac{\text{Fe mass}}{SiO_2 \text{ mass}} = 3.12$, with 4.3 mass % Na_2CO_3. Tested for softening in a sealed silica tube at 1188°C.
Magnification: 800 x 1.2.

4.2.6 (a) The Softening Behaviour of Iron Ore Cones in an Inert Gas in Sealed Silica Tubes

The softening behaviour of Bahira iron ore was investigated in sealed silica tubes. Cones reduced to different degrees were encapsulated under 180mm of mercury argon pressure. Table 4-21 gives the results of these tests. As shown in Figure 5-13 , on page 312 , a lowering of the softening temperature of this ore occurred in the reduction range 20-70%, followed by a steep increase in softening temperature as the percent of reduction exceeded 70%.

4.2.6 (b) The Softening Behaviour of Iron Ore Cones with 0.01g of Sulphur in Sealed Silica Tubes

Table 4-22 gives the result of these tests. Figure 5-13, on page 312, shows the softening temperature plotted against degree of reduction. It can be seen that there is a lowering of the softening temperature up to about 30% reduction, followed by an increase in softening temperature until 64% reduction, where the softening temperature starts to decrease again, reaching its minimum value at 100% reduction.

The chemical analysis of iron ore cones, showed sulphur up to 1.1 mass % (Table 4-23). Clearly this sulphur was absorbed from the gas phase inside the tube during the softening test.

Silica Tubes with Argon as the Gas Phase

Run No.	Degree of Cone Reduction	Test Temperature °C	Observation
1	0%	1148	Not Softened
2	0%	1208	Softened
3	4%	1215	Not Softening but melt formed.
4	10.7%	1180	Not Softened
5	10.7%	1207	Softened
6	22.75%	1178	Softened
7	29.14%	1166	Softened
8	33.41%	1123	Softened
9	35%	1117	Softened
10	43.2%	1119	Softened
11	48.4%	1163	Softened
12	52%	1198	Not Softening but melt formed.
13	62.7%	1178	Softened
14	77%	1187	Softened
15	89%	1186	Not Softened
16	98.6%	1231	Softened
17	100%	1256	Not Softened
18	100%	1271	Softened

TABLE 4-22 The Softening Behaviour of Egyptian Iron Ore with 0.01g of Sulphur in Sealed Silica Tubes

Run No.	Degree of Cone Reduction	Test Temperature °C	Observation
1	0%	1181	Softened
2	10.7%	1148	Softened
3	16.83%	1168	Softened
4	20.36%	1156	Softened
5	22.4%	1206	Melted
6	27.7%	1148	Not Softened
7	28.2%	1152	Softened
8	34.3%	1148	Softened
9	42.1%	1163	Softened
10	48.5%	1183	Softened
11	52.26%	1203	Softened
12	62%	1164	Softened
13	78.75%	1098	Softened
14	78.75%	1130	Melted
15	90.33%	1078	Softened
16	97.6%	1053	Softened
17	100%	1048	Softened

TABLE 4-23 The Percentage of Sulphur in Iron Ore Cones after the Softening Test with 0.01g of Sulphur in Sealed Silica Tubes

Degree of Cone Reduction	Test Temperature °C	Sulphur in the Cone
20.36%	1156	0.93 mass %
34.3%	1148	0.71 mass %
42.1%	1163	0.53 mass %
48.5%	1183	1.1 mass %
90.33%	1078	0.74 mass %

4.2.6 (c) Metallographic Examination of Bahira Iron Ore Cones

Scanning Electron Microscope investigation of iron ore cones possessing different degrees of reduction after being tested for their softening behaviour under argon vapour pressure in sealed silica tubes illustrated that (Fe) was evenly distributed all over the section. In some areas the first melt phase appeared to form a mixture of (Fe), (Si), (Ca), (Cl), (Na) and (K), while other areas in the cones showed liquid formation involving (Fe), (Al), (Si), (Ca), (Ti) and (Mn) mixtures. As an example, Plate 4-76 shows a scanning photomicrograph of iron ore cone possessing 33.46% reduction tested for softening under argon in a sealed silica tube at 1123°C. Although liquid was formed all over the section, x-ray scanning indicated that the upper left region of Plate 4-76 was comprised mainly of (K), (Si), (Ca), (Al) and (Fe). Spot analysis of points in the matrix indicated the presence of (Ti), (Al), (Si), (K) and (Ca). The area of liquid formation at the right lower edge on spot analysis showed (Ti), (Fe), (Al), (Si), (K) and (Ca) to be present.

Plate 4-77 shows a scanning photomicrograph of 48.4% reduced iron ore cone, tested for softening under argon in a sealed silica tube at 1163°C. Plate 4-81 shows the same area at higher magnification, illustrating solidification shrinkage during cooling.

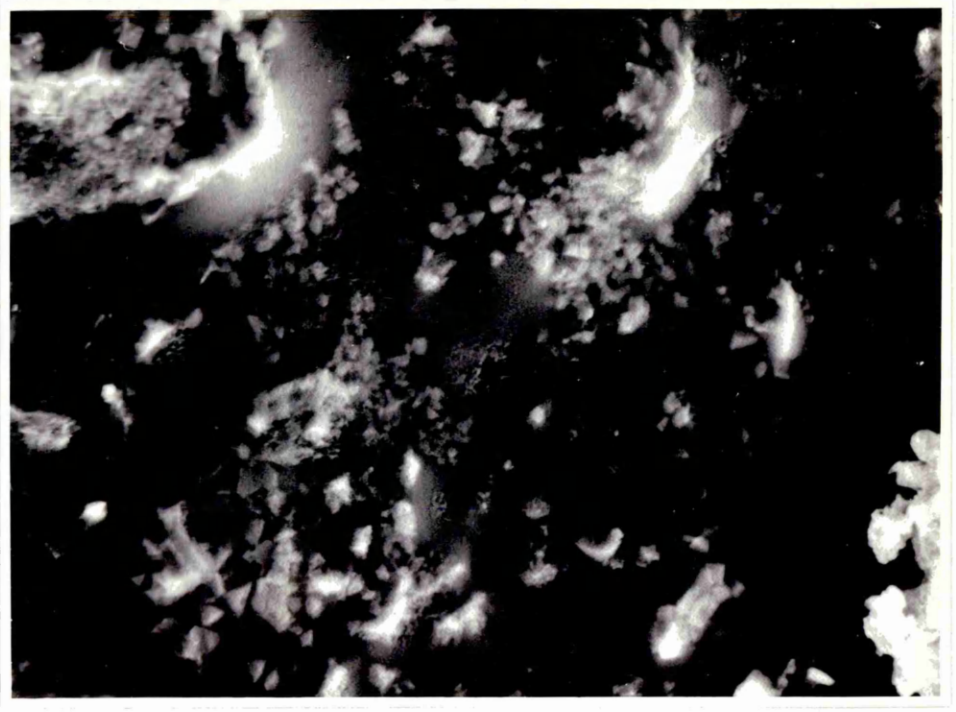

Plate 4-76: Scanning photomicrograph of the 33.4% reduced iron ore cone. Tested for softening under 180mm of mercury argon pressure in a sealed silica tube at 1123^{o}C.
Magnification: 800 x 1.4.

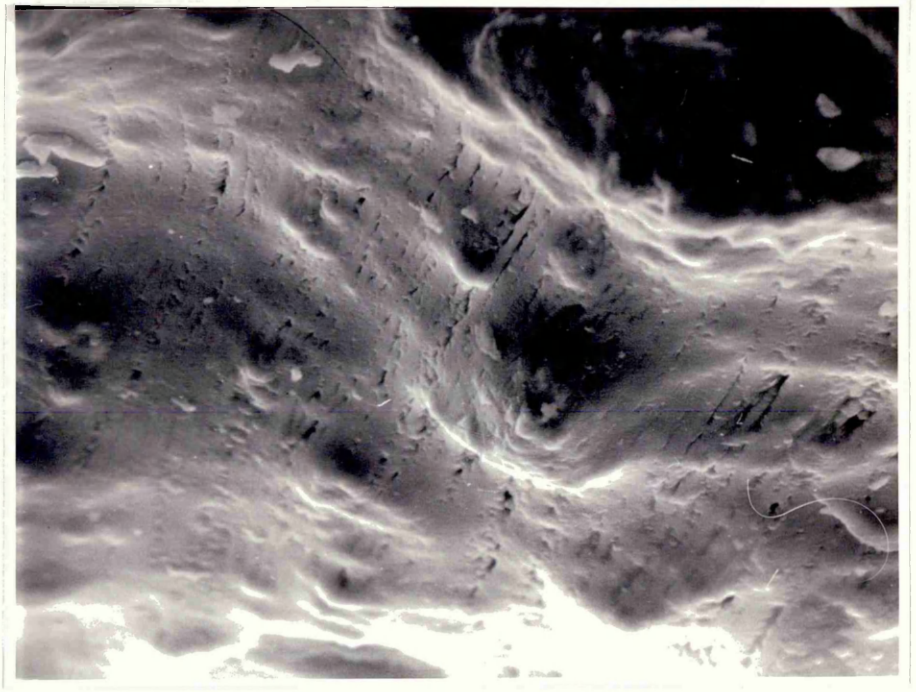

Plate 4-77: Scanning photomicrograph of 48.4% reduced iron ore cone, tested for softening under argon pressure in a sealed silica tube at 1163°C. Magnification: 800 x 1.4.

Although liquid was formed all over the section, x-ray mapping (Plates 4-78, 4-79 and 4-80) indicated that the upper region of Plate 4-77 was comprised mainly of (Al), (Si) and (Fe). Spot analysis of the lower region showed (Fe), (Ti), (Mn) and (Mg) to be present. This suggests that the melt formed during softening is not a uniform liquid, but formed from different groups of constituents.

Plate 4-82 shows a scanning electron photomicrograph of a section of a 100% reduced iron ore cone after the softening test. The softening test was carried out at 1271°C. Although the cone softened, no noticeable liquid formation can be seen. X-ray investigation of distribution of the elements indicated the existence of (Fe) concentrated in the upper half of the tested section. (Ca) and (Si) were evenly distributed. Spot analysis of the lower half of the tested area indicated the presence of (Ti), (Mn), (Mg) and (Ba).

The investigation of iron ore cones possessing different degrees of reduction with 0.01g of sulphur in sealed silica tubes showed a completely different softening mechanism. Liquid formation took place at the grain boundary of the tested cones. X-ray investigation of this liquid at the grain boundary indicated that it was mainly composed of (Fe) and (S). This mechanism of softening is shown in Plate 4-86, which is a photomicrograph of an iron ore cone tested with 0.01g of sulphur at 1181°C. Liquid formation is clearly apparent between the grains. X-ray investigation of (S), (Si) and (Fe) distribution is shown in Plates 4-87, 4-88 and 4-89.

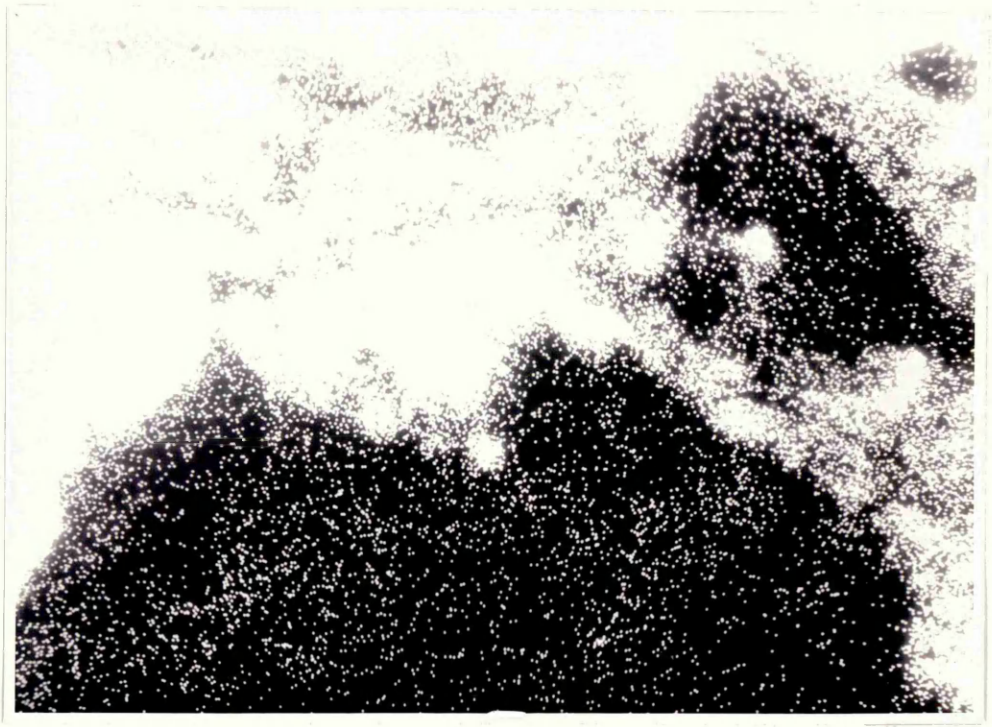

Plate 4-78: Scanning x-ray mapping for (Al) distribution in the area shown in Plate 4-77.
Magnification: 800 x 1.4.

Plate 4-79: Scanning x-ray mapping for (Si) distribution in the area shown in Plate 4-77: Magnification: 800 x 1.4.

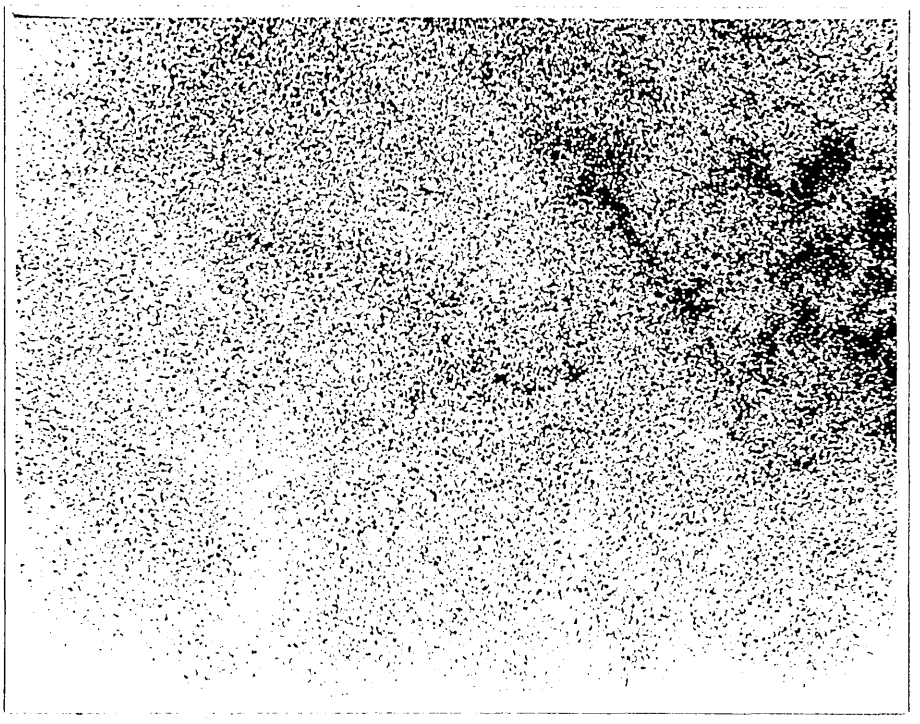

Plate 4-80: Scanning x-ray mapping for (Fe) distribution in the area shown in Plate 4-77.
Magnification: 800 x 1.4.

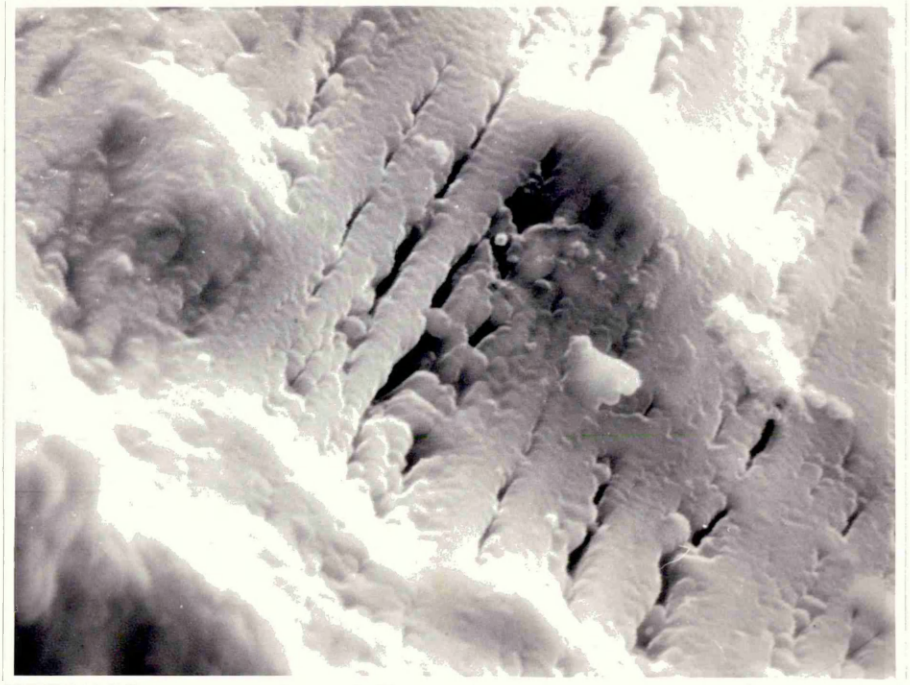

Plate 4-81: Scanning photomicrograph of 48.4% reduced iron ore cone, tested for softening under argon pressure in a sealed silica tube at 1163°C. Magnification: 3200 x 1.4.

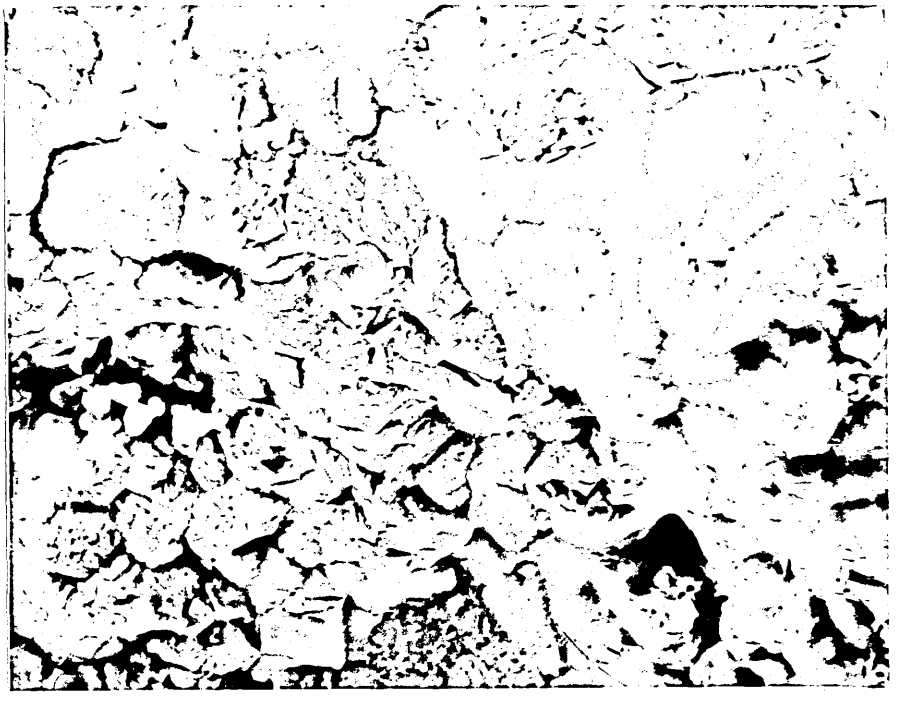

Plate 4-82: Scanning photomicrograph of iron ore cone, 100% reduced, tested for softening under 180mm of mercury argon pressure in a sealed silica tube at 1271°C.
Magnification: 800 x 1.2.

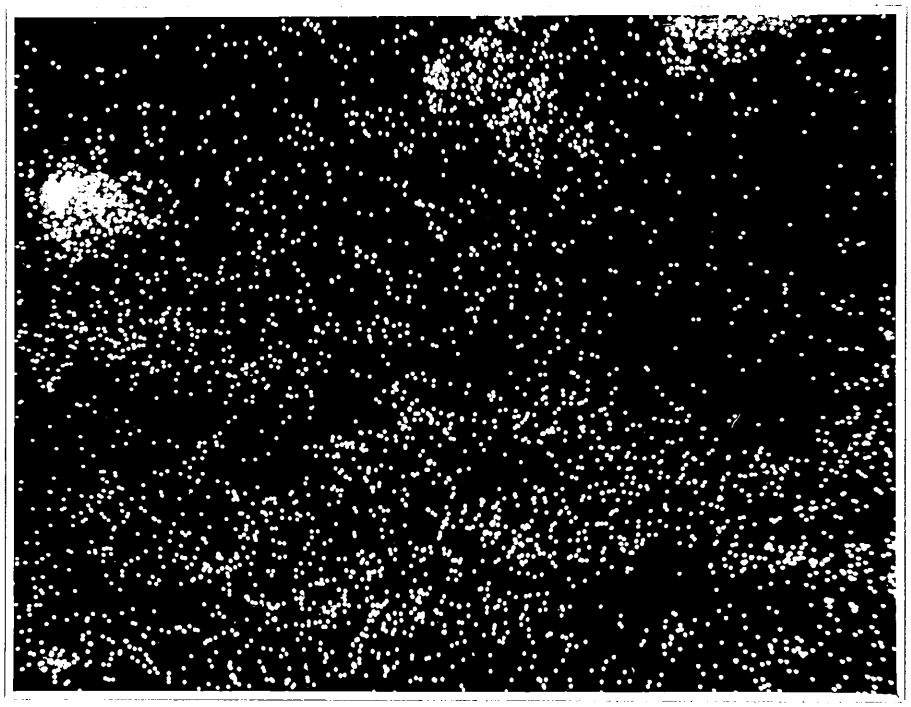

Plate 4-83: Scanning x-ray mapping for (Si) distribution in the area shown in Plate 4-82.
Magnification: 800 x 1.2.

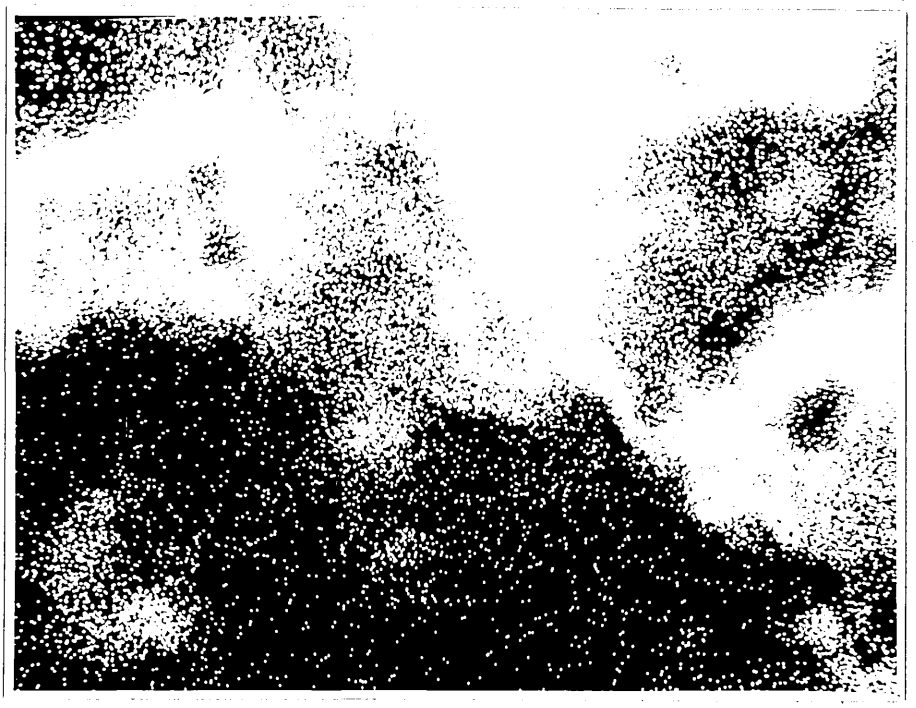

Plate 4-84: Scanning x-ray mapping for (Fe) distribution in the area shown in Plate 4-82.
Magnification: 800 x 1.2.

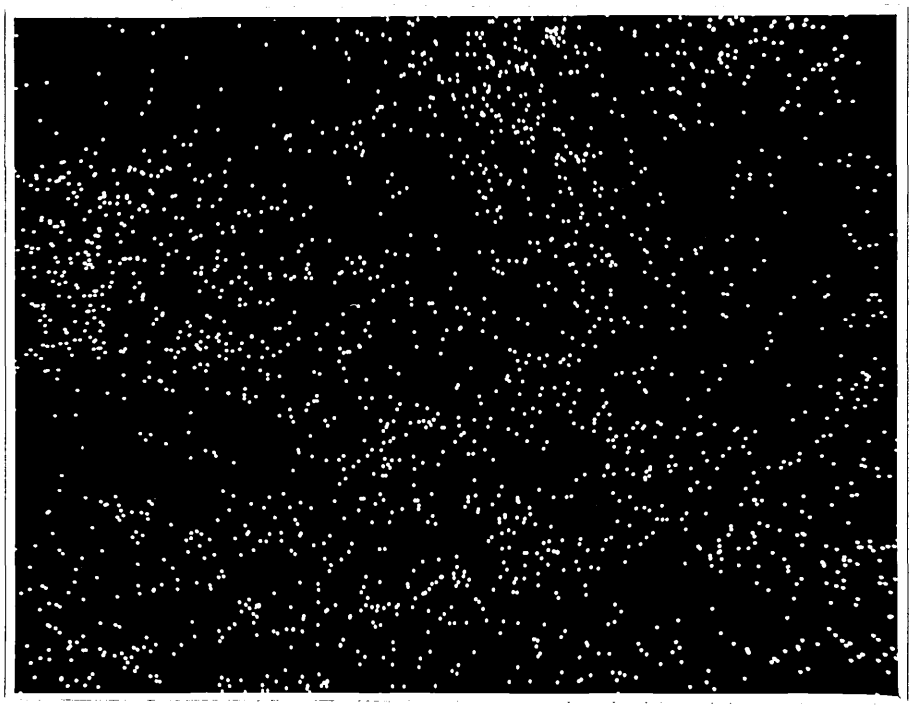

Plate 4-85: Scanning x-ray mapping for (Ca) distribution in the area shown in Plate 4-82.
Magnification: 800 x 1.2.

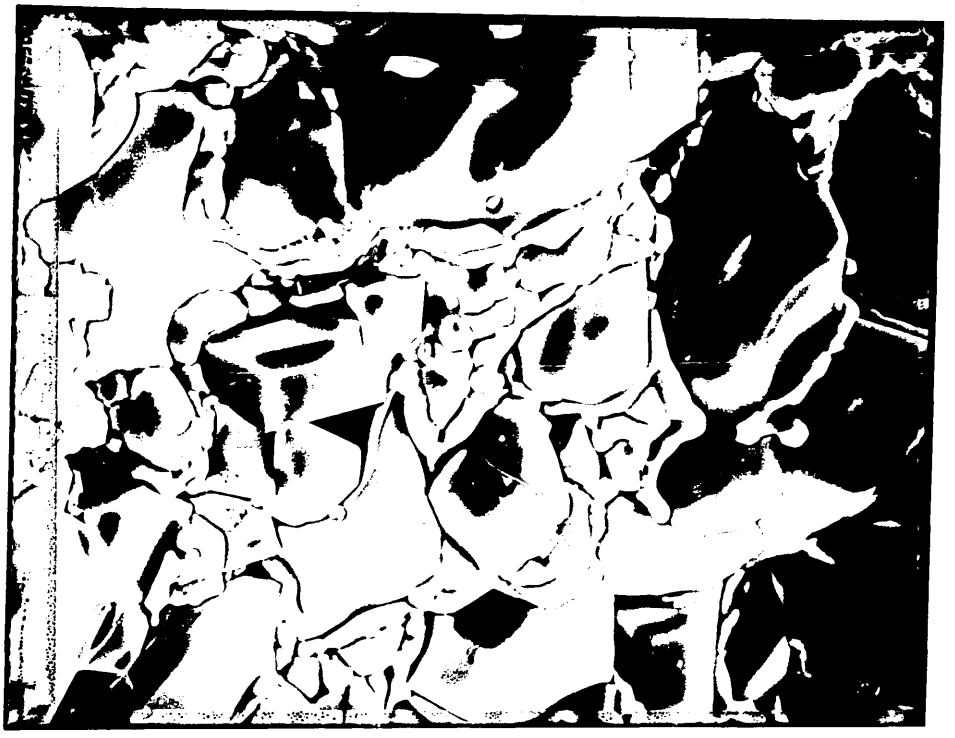

Plate 4-86: Scanning photomicrograph of unreduced iron ore cone, tested for softening with 0.01g of sulphur in a sealed silica tube at 1181°C. Magnification: 800 x 1.2.

plate 4-87: Scanning x-ray mapping for (S) distribution in the area shown in Plate 4-86.
Magnification: 800 x 1.2.

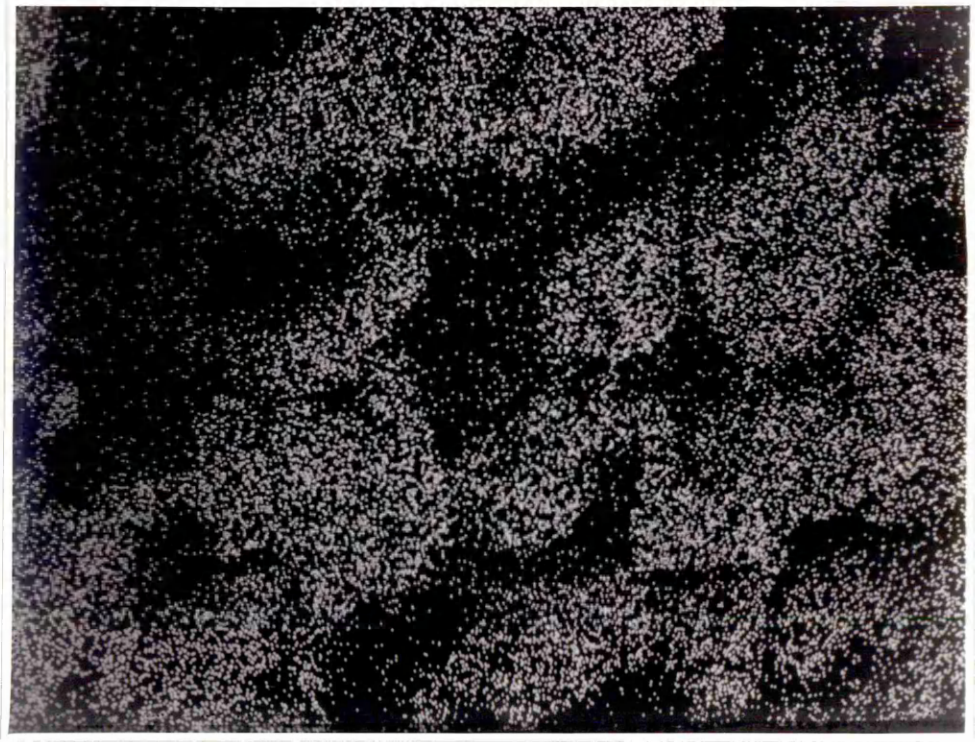

Plate 4-88: Scanning X-ray mapping for (Si) distribution in the area shown in Plate 4-86.
Magnification: 800 x 1.2.

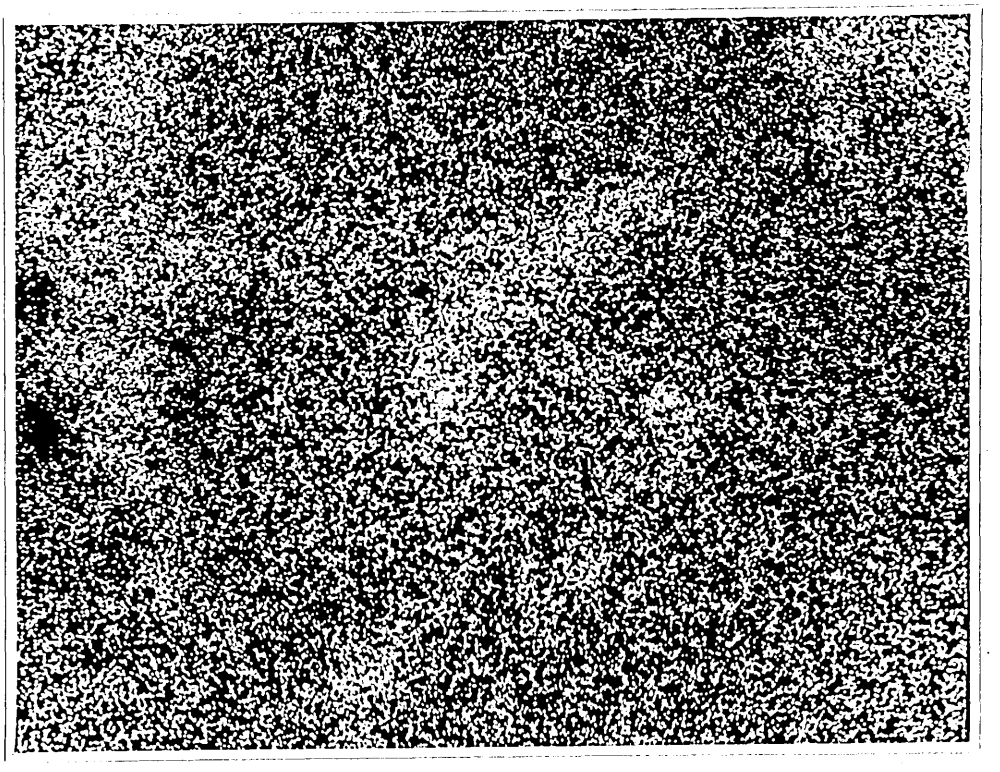

Plate 4-89: Scanning x-ray mapping for (Fe) distribution in the area shown in Plate 4-86.
Magnification: 800 x 1.2.

Figure 5-13 , on page 312, shows an increase in the softening temperature of the iron ore investigated with 0.10g of sulphur in sealed silica tubes in the reduction range from 26% to 60%.

Two samples possessing degrees of reduction in the range from 26% to 60% were investigated after the softening test. Plate 4-90 shows a scanning photomicrograph of 28.2% reduced iron ore cone, tested for softening at 1152°C with 0.01g of sulphur, from which it appears that a limited area of liquid formation occurs through the section investigated. X-ray investigation of (S), (Si), (Fe), (Mn) and (Ti) distribution, Plates 4-91 to 4-95, indicates the existence of local areas of high (S) concentration but generally the (S) is evenly distributed. (Mn) and (Ti) appear to be also evenly distributed over the area under examination.

Plate 4-96 shows a scanning photomicrograph of an iron ore cone, 34.3% reduced, tested for softening with 0.01g of sulphur at 1148°C. X-ray investigation of (S), (Si), (Fe), (Ti) (Ca) and (Mn) distribution, Plates 4-97 to 102 showed that the area of liquid formation possessed (S), (Fe), (Mn) and (Ti).

Plate 4-103 shows a scanning photomicrograph of an iron ore cone, 78% reduced, tested for softening with 0.01g of of sulphur at 1130°C. X-ray investigation of (S), (Na), (Ca),

(Si) and (Mn) distribution is shown in Plates 4-104, 4-105, 4-106, 4-107 and 4-108 respectively.

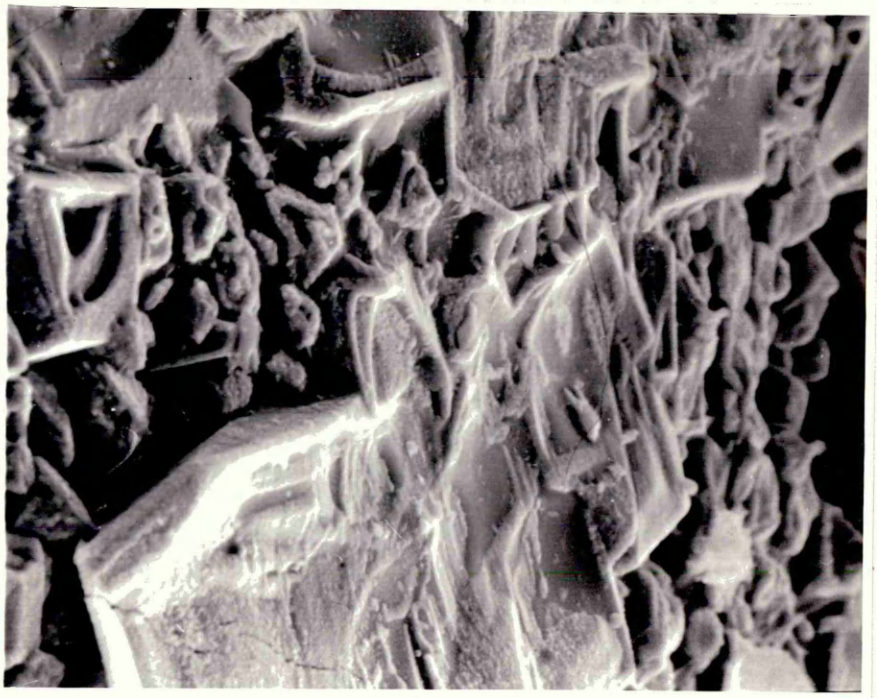

Plate 4-90: Scanning photomicrograph of iron ore cone, 28.2% reduced, tested for softening with 0.01g of sulphur in a sealed silica tube at 1152°C. Magnification: 800 x 1.2.

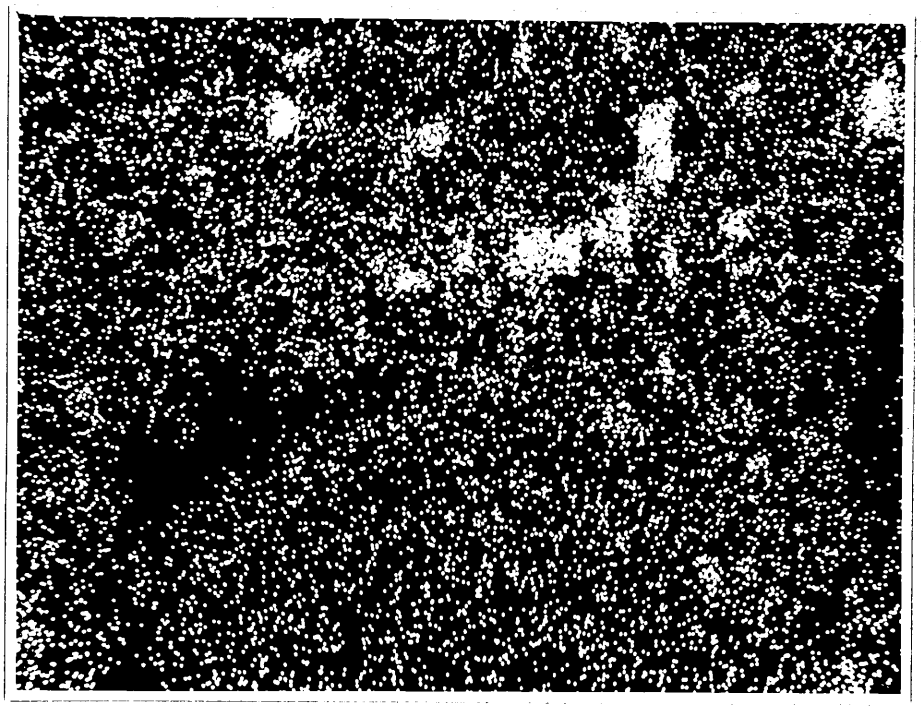

Plate 4-91: Scanning X-ray mapping for (S) distribution in the area shown in Plate 4-90.
Magnification: 800 x 1.2

Plate 4-92: Scanning X-ray mapping for (Si) distribution in the area shown in Plate 4-90.

Plate 4-93: Scanning X-ray mapping from (Fe) distribution in the area shown in Plate 4-90. Magnification 800 x 1.2

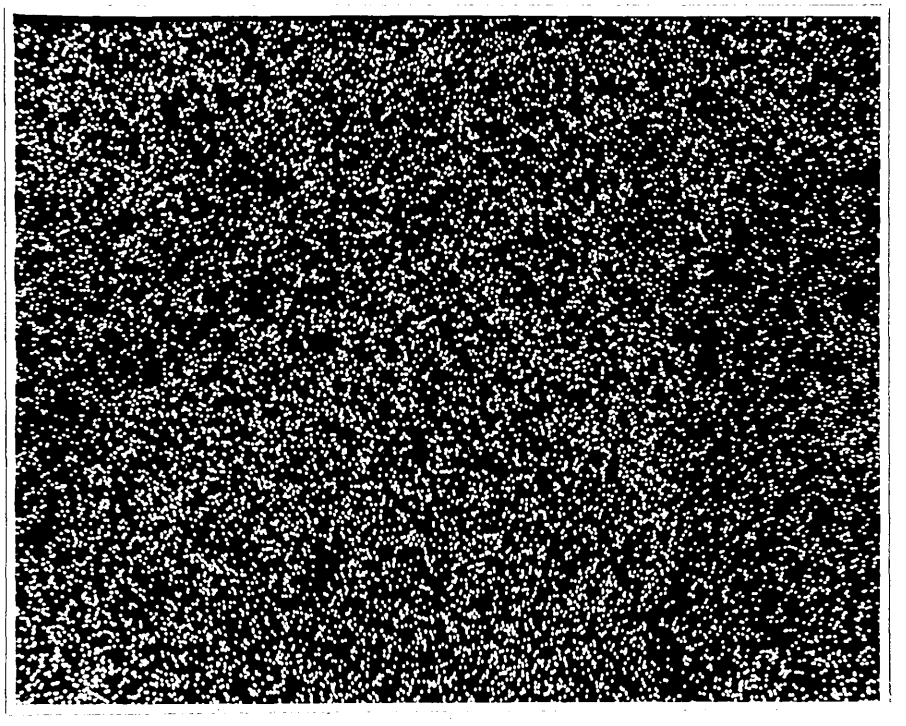

Plate 4-94: Scanning X-ray mapping for (Mn) distribution in the area shown in Plate 4-90.
Magnification: 800 x 1.2

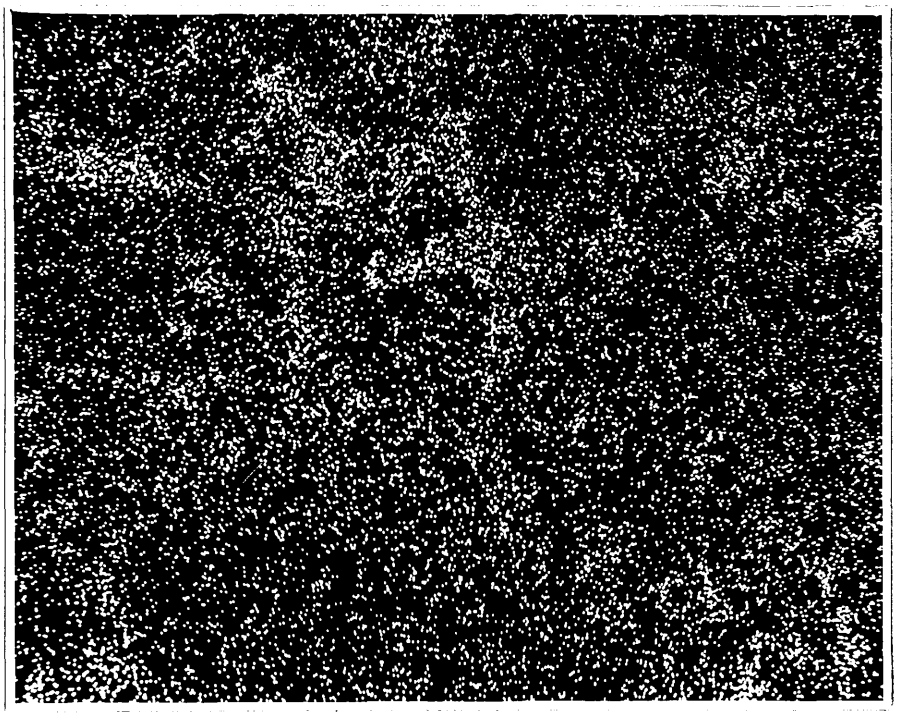

Plate 4-95: Scanning X-ray mapping for (Ti) distribution in the area shown in Plate 4-90.
Magnification: 800 x 1.2

Plate 4-96: Scanning photo micrograph of iron ore cone, 34.3% reduced, tested for softening with 0.01g of sulphur in a sealed silica tube at 1148°C.
Magnification: 800 x 1.2

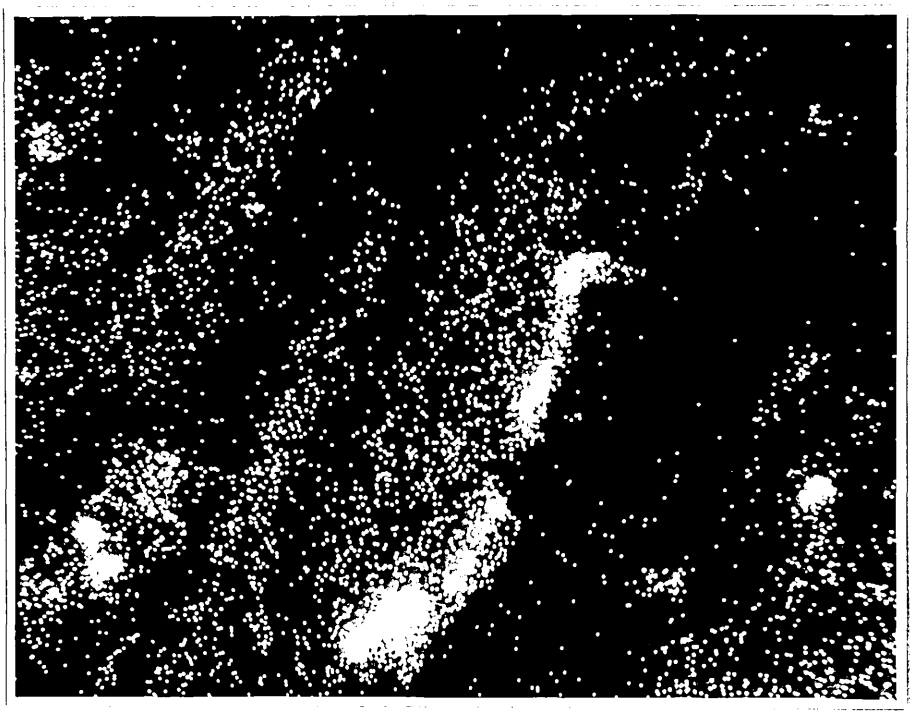

Plate 4-97: Scanning X-ray mapping for (S) distribution in the area shown in Plate 4-96.
Magnification: 800 x 1.2

Plate 4-98: Scanning X-ray mapping for (Si) distribution in the area shown in Plate 4-96.
Magnification: 800 x 1.2

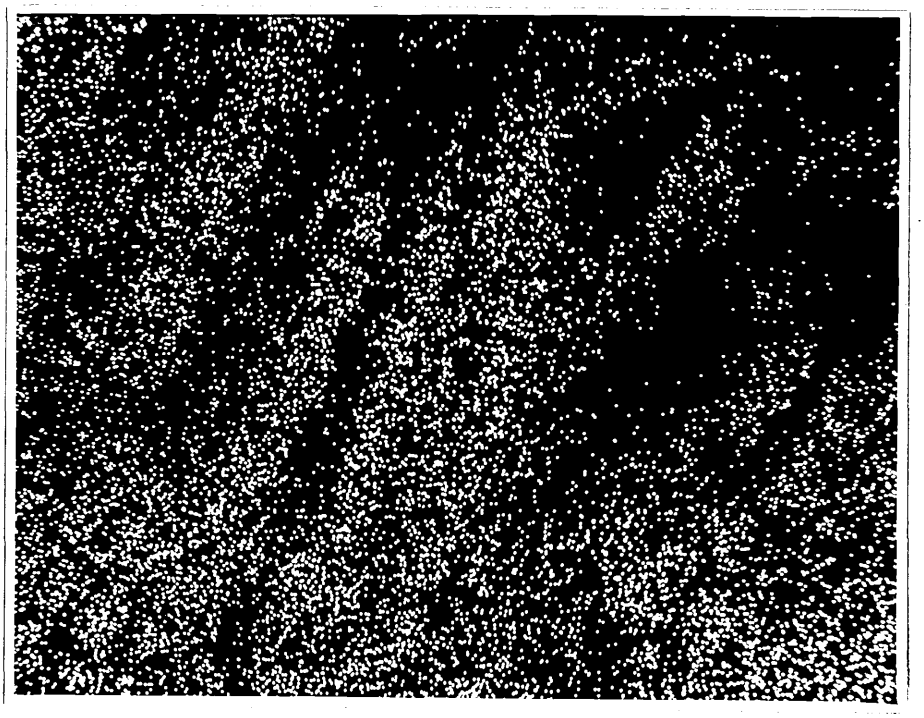

Plate 4-99: Scanning X-ray mapping for (Fe) distribution in the area shown in Plate 4-96.
Magnification: 800 x 1.2.

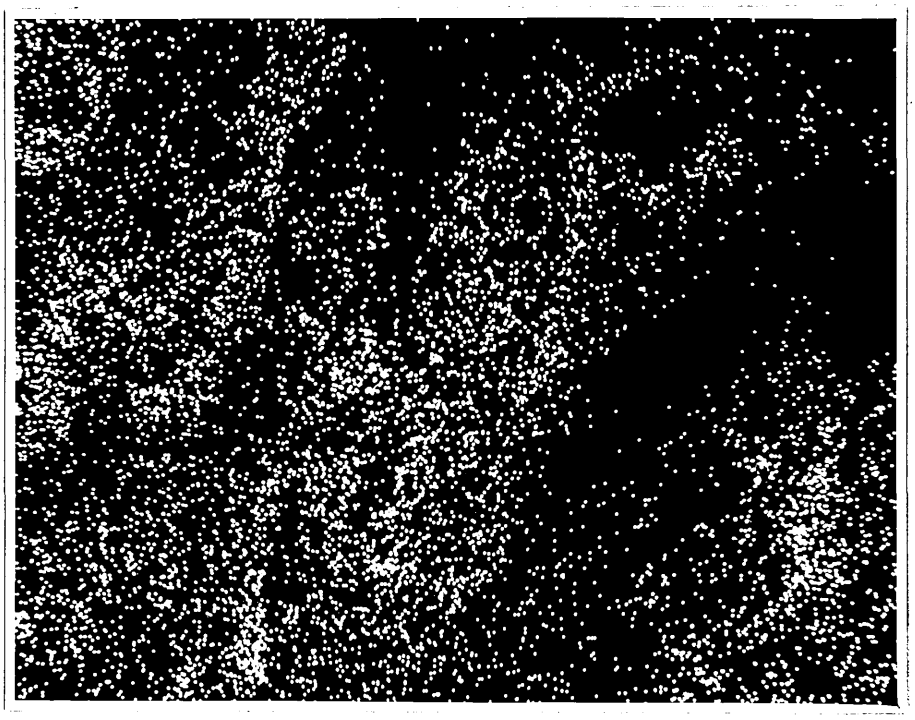

Plate 4-100: Scanning X-ray mapping for (Ti) distribution in the area shown in Plate 4-96. Magnification: 800 x 1.2.

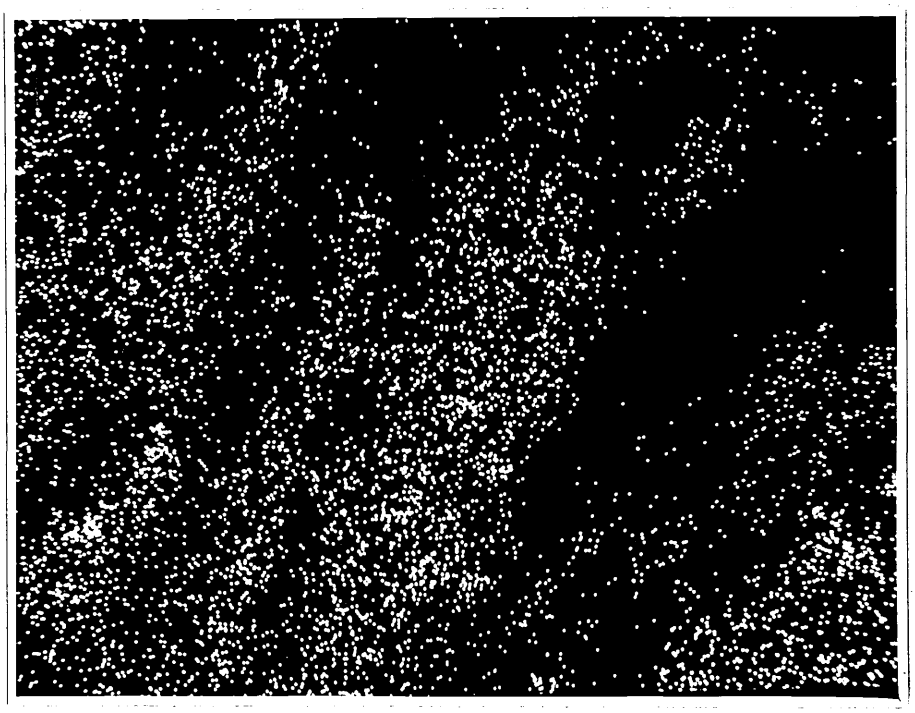

Plate 4-101: Scanning X-ray mapping for (Ca) distribution in the area shown in Plate 4-96.
Magnification: 800 x 1.2

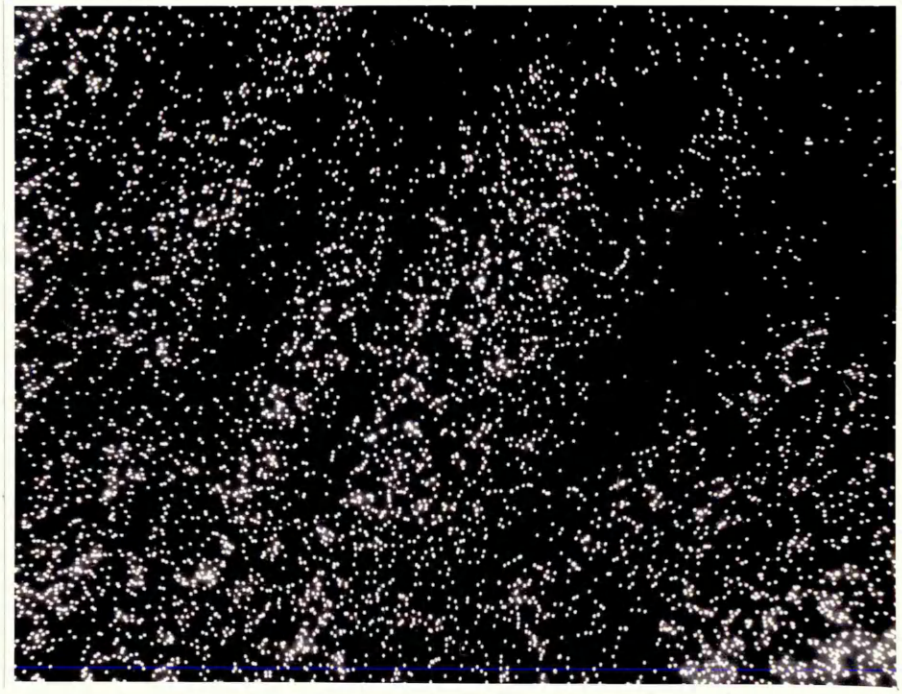

Plate 4-102: Scanning X-ray mapping for (Mn) distribution in the area shown in Plate 4-96.
Magnification: 800 x 1.2.

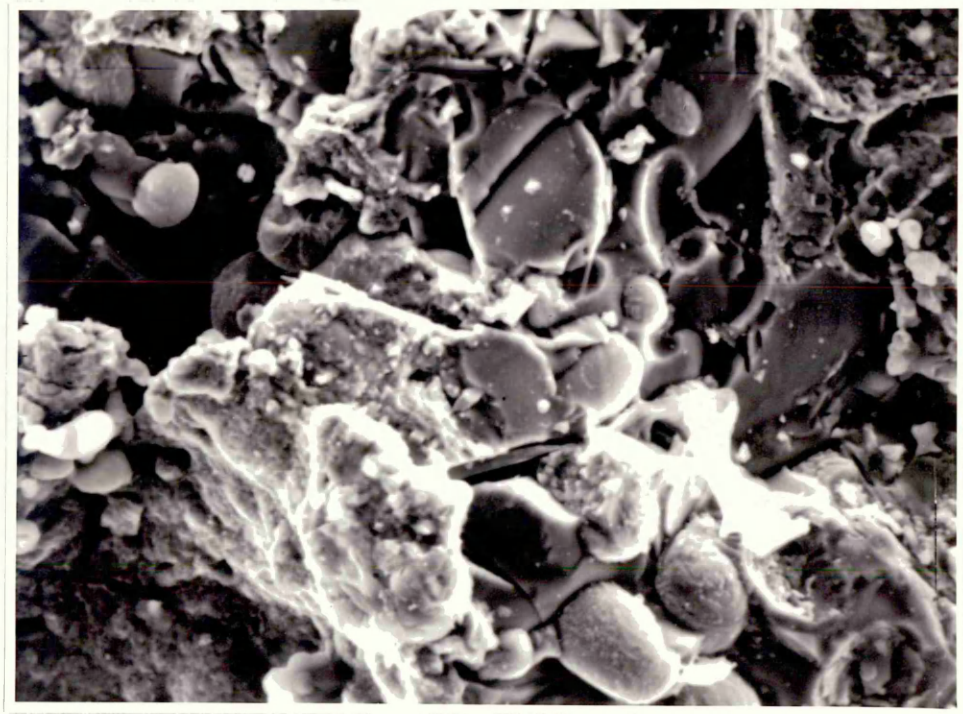

Plate 4-103: Scanning photo micrograph of 78% reduced iron ore cone after being tested with 0.01g of sulphur at 1130^{o}C in a sealed silica tube.
Magnification: 640 x 0.95.

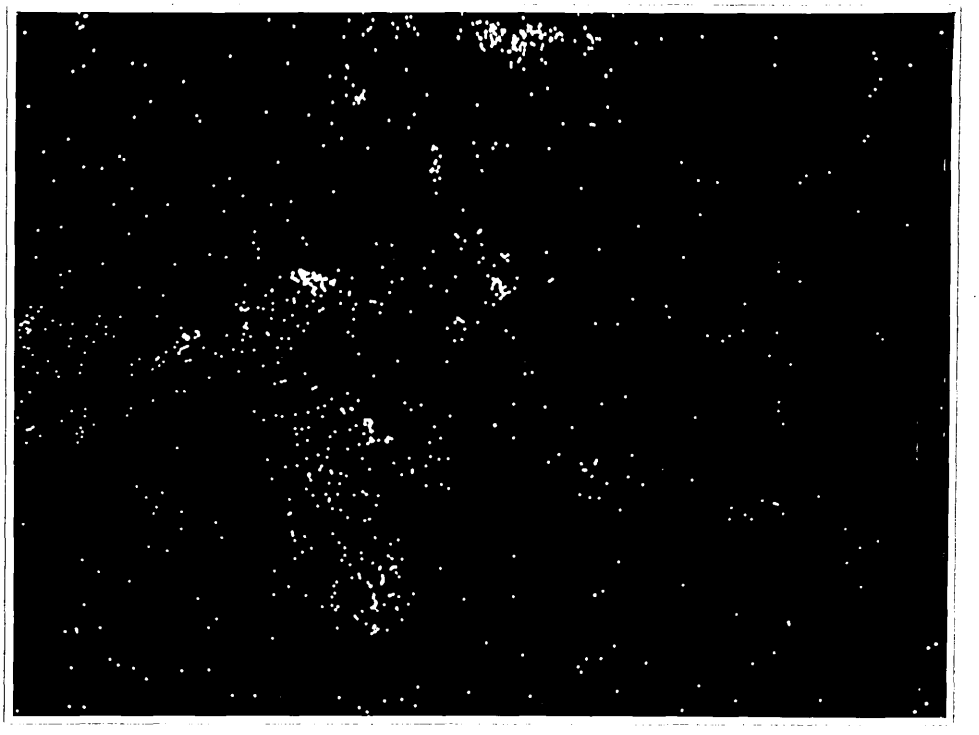

Plate 4-104: Scanning X-ray mapping for (S) distribution in the area shown in Plate 4-103.
Magnification 640 x 0.95.

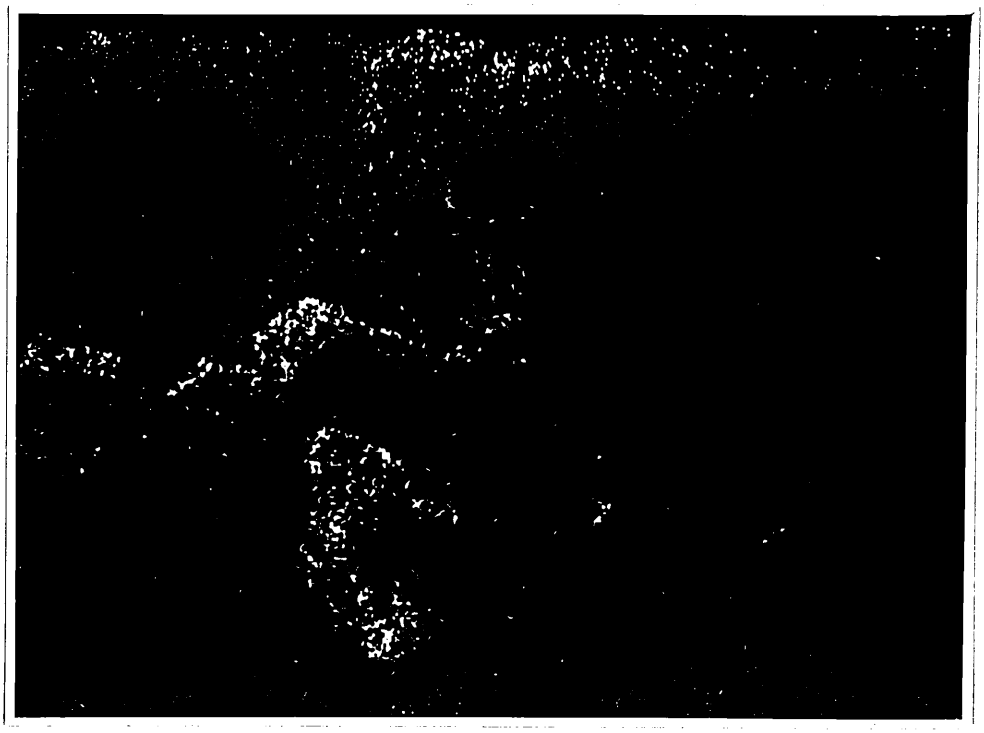

Plate 4-105: Scanning X-ray mapping for (Na) distribution in the area shown in Plate 4-103.
Magnification: 640 x 0.95.

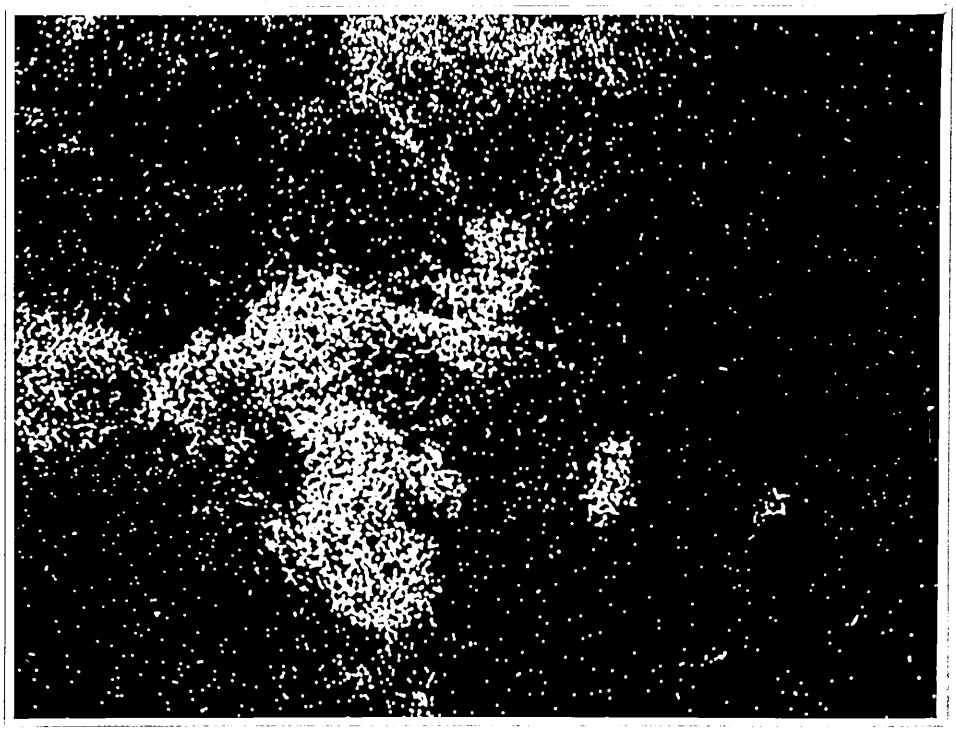

Plate 4-106: Scanning X-ray mapping for (Ca) distribution in the area shown in Plate 4-103.
Magnification: 640 x 0.95.

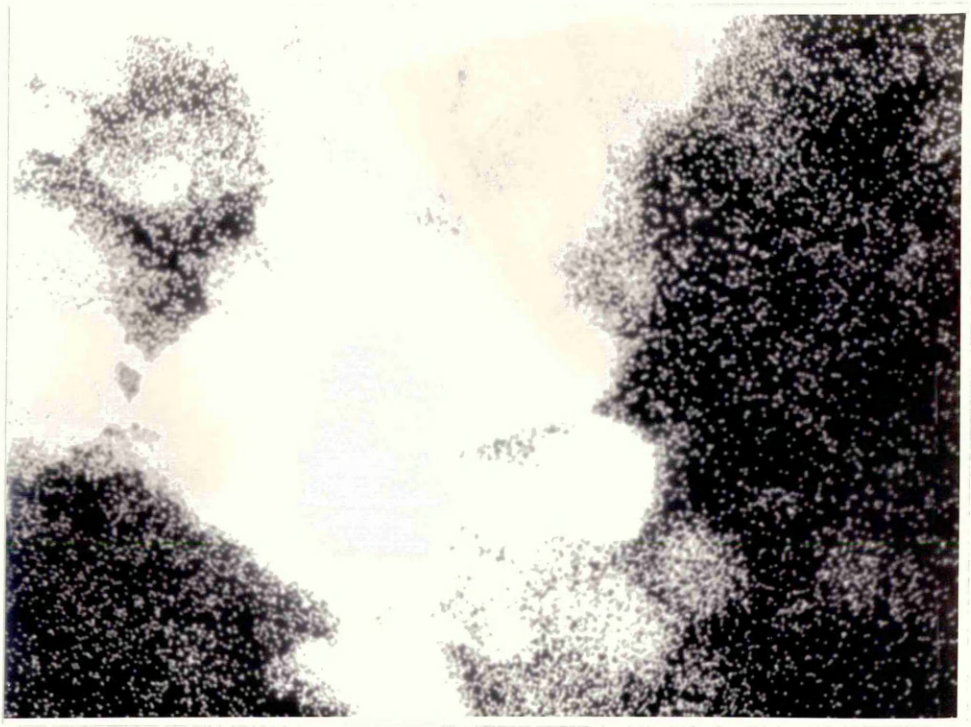

Plate 4-107: Scanning X-ray mapping for (Si) distribution in the area shown in Plate 4-103.
Magnification: 640 x 0.95.

Plate 4-108: Scanning X-ray mapping for (Mn) distribution in the area shown in Plate 4-103.
Magnification: 640 x 0.95

5.1 General Introduction

It is generally accepted that the way in which the burden softens on entering the high temperature zone of a blast furnace has a major influence on the operation of the furnace. The softening zone offers an increased resistance to the flow of furnace gases and has been suggested to contribute up to 60% of the total pressure drop in the furnace[25]. Additionally, the furnace gases are thought to be diverted from the softening zone by its lower permeability[26], and the build up of partially softened material from the walls of the furnace is offered as a fairly general explanation for hanging and scaffold formation phenomena[24].

Softening is due tothe formation of sufficient liquid within the burden, or within individual particles of burden, for the burden to become plastic and to deform under the combined action of burden load, the pressure drop due to gas flow and friction forces due to the relative solid movements. As a result the particles of the burden will deform and reduce the total voidage in the bed. When sufficient liquid has formed to drain out of the burden, however, the voidage of the bed will rise, and the softening regime can be considered to be completed. Softening, then, is associated with the formation of liquid within the individual particles of the burden. The work presented in this thesis, then, will be discussed from the point of view of the factors that

affect the formation of this liquid and its subsequent effect on the properties of blast furnace burden material.

5.2 Choice of Experimental Techniques

5.2.1 Use of Cones

The methods so far used to investigate the softening behaviour of blast furnace burden materials, to obtain information about their behaviour in the high temperature zone of the furnace, depend on one of the following two principles.

(i) The determination of the percentage decrease in volume when pre-reduced samples are heated to temperature under specified loads.

(ii) The determination of the pressure drop across a bed of the pre-reduced sample at temperature, sometimes during its reduction under a specified load.

In methods depending upon both of these two principles, samples reduced to a known degree are tested under specific loads, the loads being applied to plattens constructed from refractory materials such as platinum, alumina or stainless steel.

A fundamentally different approach has been adopted in this work in order to avoid any form of interaction between the sample, the plattens and the atmosphere in which the test is being carried out. This was done because the main aim of the study has been to investigate the effect that different volatile species have on softening behaviour. The

volatile species present in the blast furnace, sulphur, alkali metals etc, are extremely corrosive to most refractory materials so that an apparatus involving the use of plattens to apply specific loads to the material under test would be unlikely to exhibit a useful experimental life.

The use of the softening behaviour of specific mixed oxides in the form of Seger cones to indicate temperature has long been an established practice in the ceramic industry. The technique used in this work is merely a reversal of the information supplied by Seger cones in that cones heated to specified temperatures are used to indicate the softening behaviour of the mixed solids from which they are constructed.

It can, of course, be argued that the strength possessed by the cone material when it exhibits the state considered in this work to show softening is not known, whereas the more usual tests are carried out under known loads. However, knowledge of the stress conditions under which the softening behaviour of the burden is studied does not really assist the application of the results of such studies to blast furnace practice. The physical conditions to which blast furnace burden is subjected during its passage through the furnace are insufficiently well understood.

Observation[25] on experimental and commercial blast furnaces have been taken to indicate that the stack column could be in a state of suspension even under normal conditions. In addition fluidizing phenomena are considered as a factor limiting the blowing rate in today's practice. A safety factor for fluidisation must be applied especially when operating the blast furnace under high top pressure. This safety factor is the pressure drop between the tuyeres and the stock line, calculated from the Ergun equation, divided by the dead load pressure of the burden calculated from its weight and the friction force against the furnace walls. Blast furnaces are normally operated with this factor close to its maximum operating value of 0.8, so that some 20% of the weight of the burden in the stack is exerted on the solid particles in the softening zone.

Thus it could be argued that the stress levels to which iron bearing materials are subjected in the blast furnace are quite low and that the formation of a liquid phase within the material is more important in determining its behaviour in the high temperature zone than mere loss in mechanical strength. The behaviour of iron bearing materials reduced to different degrees under the application of an applied load at temperature can be strongly influenced by the physical strengths of the different materials present at different degrees of reduction. At room temperature, for example, hematite particles have hardnesses in the range

719-1000 Knoop, whereas the average hardnesses of magnetite and wustite particles are 467 and 350 Knoop respectively. Thus the overall hardness of the iron bearing materials is likely to decrease as an increasing degree of reduction increases the proportion of the lower oxides present, even without the formation of a liquid phase. The actual stress levels existing in blast furnaces could be too low for such a decrease to be relevant, although they would not be too low for the presence of a liquid phase in material to have an important effect.

The results of the cone experiments carried out in this work are unlikely, therefore, to be less relevant to blast furnace practice than tests carried out under load. They have the added advantage, however, that they have been obtained in the presence of some of the volatile species present in the gases in the blast furnace stack.

5.2.2 Choice of a Closed Silica Tube

At the start of this work a horizontal tube furnace was used to investigate the softening behaviour of the cone shaped samples, in gases of specified composition being passed through the furnace. The softening points obtained however, were inconsistent with the corresponding theoretical melting points of the tested cones. Some tests indicated a softening temperature of the tested sample higher than its melting point, while in other runs a softening temperature much lower than the theoretical melting temperature was obtained.

In the case of FeO cones, softening occurred at about 1379°C (section 4.1.1), while the theoretical melting temperature of wustite in nitrogen at a pressure of one atmosphere is 1370°C. Figure 5-1 shows that this latter melting point corresponds to an oxygen pressure of 10^{-10} Atm. The nominal purity of the argon used in the open tube experiments was 99.999% so that the oxygen partial pressure around the cone would be in excess of 10^{-10}. Thus the oxygen content of the FeO cones would be expected to increase and consequently their melting point increased as shown in Figure 5-1. The actual increase would depend upon the partial pressure of oxygen in the argon, and upon various unknown kinetic factors controlling interactions between the cone and the gas in the tube.

FeS cones, on the other hand, and cones consisting partially of FeS, showed softening temperatures that were sometimes higher than the expected melting point and some times lower. This variation in the softening temperatures could be attributed to the loss of sulphur from the tested cones, since during the tests sulphur vapour will evaporate from the cones. In the open tube, this vapour was swept away by the argon flow so that the cones would continually lose sulphur. This sulphur loss changed the composition of the tested cone, resulting either in a lowering or a

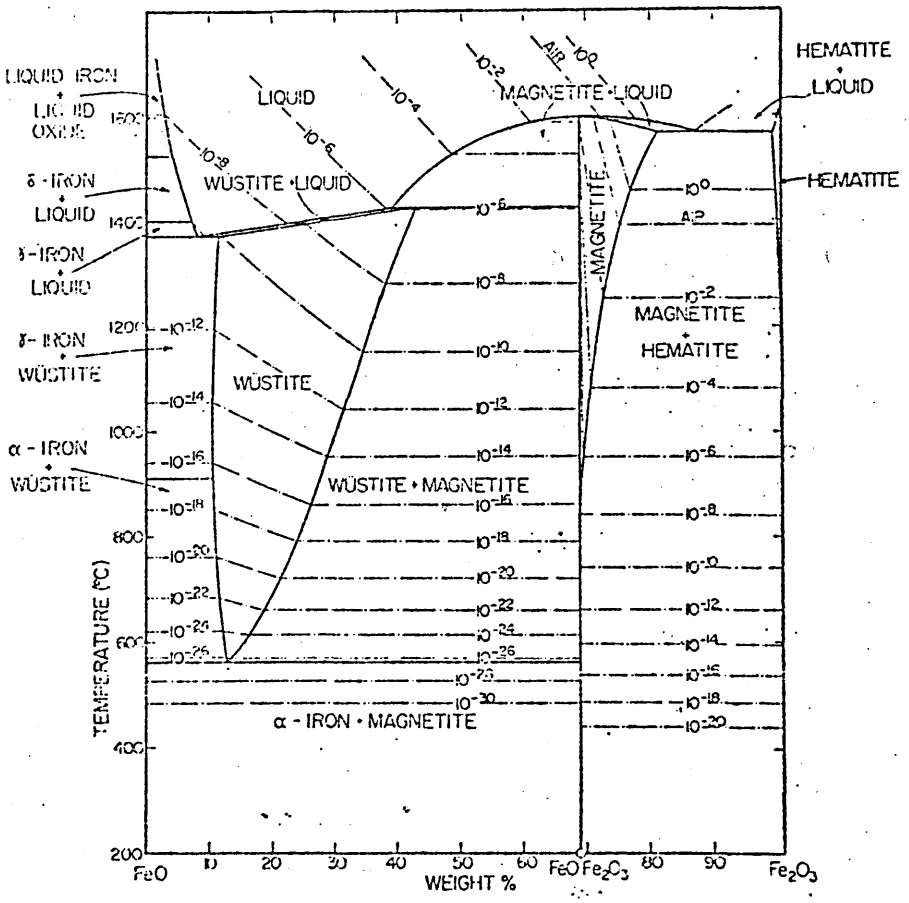

Figure 5-1: $FeO-Fe_2O_3$ phase diagram [14].

raising of the softening temperature as will be shown later. This explanation is in agreement with the results of McCobe et al[58] who measured the vapour pressure of different species above FeS in equilibrium with iron. They reported that neither iron nor FeS are volatile to any appreciable extent but that sulphur only was vaporized quoting a sulphur pressure of 10^{-7} atmosphere at 997°C.

The observed softening point of pure FeS cones was found in this work to be 1023°C, a value much lower than the quoted melting point of 1190°C. During the tests, sulphur was lost from the iron sulphide resulting in the formation of an Fe/FeS mixture. The iron/sulphur phase diagram shown in Figure 5-2 indicates that the liquidus temperature of such a mixture would be below the melting point of pure FeS. The process of sulphur vaporization and liquid formation would continue until the moment when the proportion of the liquid phase present in the cone was sufficient to cause its softening.

On the contrary, the softening point obtained for FeS-FeO cones (Fe:68.2 mass %,S: 24.3 mass % and O: 7.5 mass%) was 982°C (section 4-1-3(c)), while the melting point of this eutectic composition in the Fe-O-S ternary phase diagram shown in Figure 2-8 on page 35 is 915°C. Loss of sulphur from a cone causes its composition to move towards the Fe/O axis so that its liquidus point would move up the liquidus surface giving rise to the higher softening point than was expected.

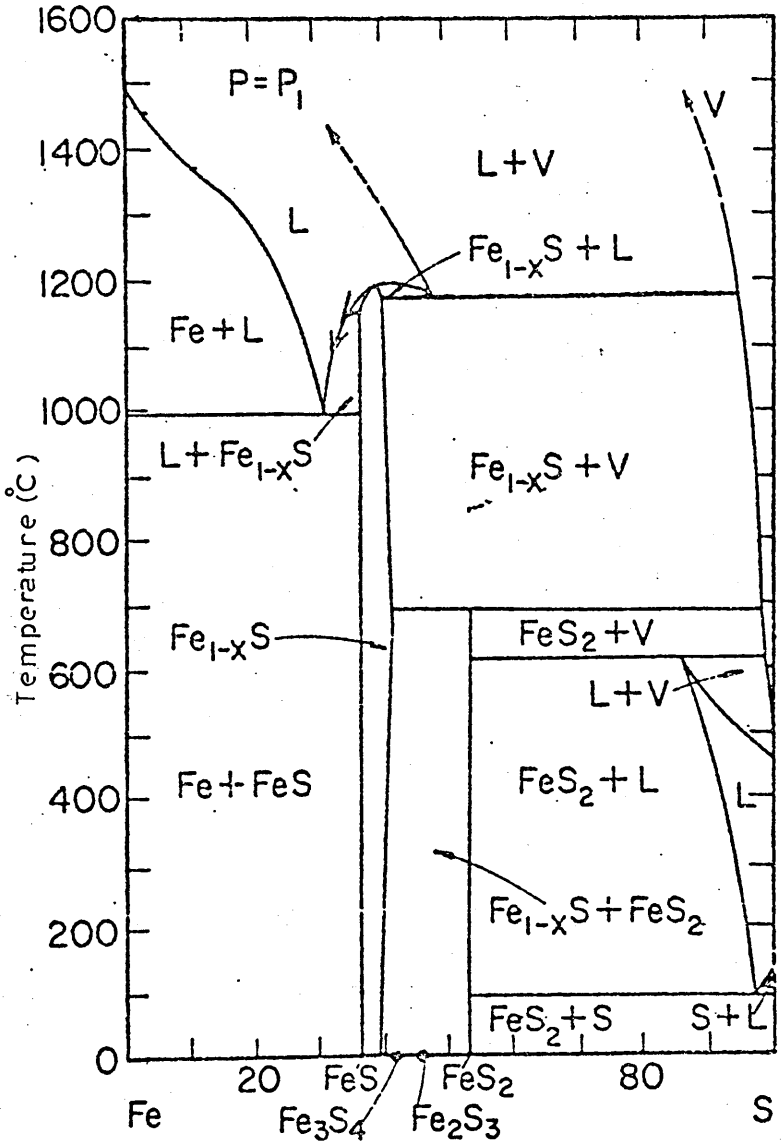

Figure 5-2: Fe-S phase diagram[67].

The results obtained with cones made from Fe/FeS mixtures similarly showed that sulphur was lost from the cones. A cone containing 88.2 mass % Fe and 11.8 mass % S did not soften even when heated to 1387°C although the Fe/S phase diagram in Figure 5-2 shows the liquidus temperature for this composition to be 1370°C. After the experiment, the cone was analysed and shown to contain 2.45 mass % sulphur, this mean composition corresponding to a liquidus temperature of about 1470°C.

The results obtained with Bahira iron ore in the open tube also showed inconsistent behaviour, and this was thought to be due to the uncertain behaviour of the volatile material they contained. It was apparent, then, that the cones exhibited uncertain softening behaviour because of uncertainties of the interactions between the cone and the furnace atmosphere. Thus more control had to be exercised over the gaseous atmosphere surrounding the cones during the determination of their softening temperatures. It was for this reason that the closed silica tube experiments were undertaken.

5.2.3 Precision of Softening Temperature Determination

Considerable care was taken in the experiments, as described in section 3.7.4, to ensure that the temperatures of the cones could be determined with adequate accuracy from the temperatures measured during the experiments. The accuracy of determination was better than ± 2°C, but the precision with which the softening temperatures have been obtained is

somewhat lower. This is because the cones could not be observed at temperature. It was thus necessary to cool each cone down to room temperature after it had been heated to the test temperature and held there for 15 minutes, before its state could be observed. The test temperatures over the softening range were separated by incremental steps of some 10 to 15°C in magnitude. It is the magnitude of these incremental temperature steps that largely determines the precision with which the softening temperatures have been obtained. It is for this reason that a precision of ±5°C is considered to have been achieved. The precision with which Seger cones are taken to indicate the temperatures of high temperature furnaces is also ±5°C[61]. Experiments in this work in which identical cones were separately heated under identical conditions showed agreement that was certainly within the precision of ±5°C.

5.3 Effect of Silica on the Softening of Fe_2O_3 Cones Reduced to Different Degrees

5.3.1 Pure Fe_2O_3 Cones

Table 4-11, on page 133, shows that pure Fe_2O_3 cones reduced to different degrees did not soften within the temperature range of the experiments. A small amount of liquid flowed from the cones reduced 22 and 35%, but the amount was very small.

Figure 5-1, on page 270, shows the iron/oxygen system and demonstrates that the lowest temperatures at which molten

material can exist in this system are in the range 1370-1390°C. The lowest melting temperatures fall within the range of FeO contents from 8 to 30% - and molten wustite (FeO) is the major component in the liquid. The cones that demonstrated the small degree of liquid formation fall within this range of oxygen contents. It would appear that the liquid that forms does so through some interaction between wustite and some minor impurities in the original Fe_2O_3.

5.3.2 Fe_2O_3/SiO_2 Cones

The presence of silica in the cones resulted in their softening within the range of the experimental temperatures achieved. However, Table 4-13, on page 142, shows that the softening only occurred once the reduction of the cones had commenced. The upper experimental points and the upper curve in Figure 5-3 show how the softening temperature of these cones containing silica varies with the degree of reduction. The lowest softening temperatures vary between 1200 and 1220°C and exist for degrees of reduction varying between 20% to 70%. If it is assumed that the reduction process removes oxygen completely from each of the iron oxides in sequence, the cone reduced 20% would contain 19 mass % SiO_2; 50 mass % Fe_3O_4 and 31 mass % FeO. Similarly the cone reduced by 70% would contain 22 mass % SiO_2, 38 mass % Fe and 40 mass% FeO. Cones reduced to intermediate degrees of reduction will contain higher proportions of FeO. As the degree of reduction increases from 20%, the magnetite will be progressively reduced until wustite is the only oxide present, this being the situation when the degree

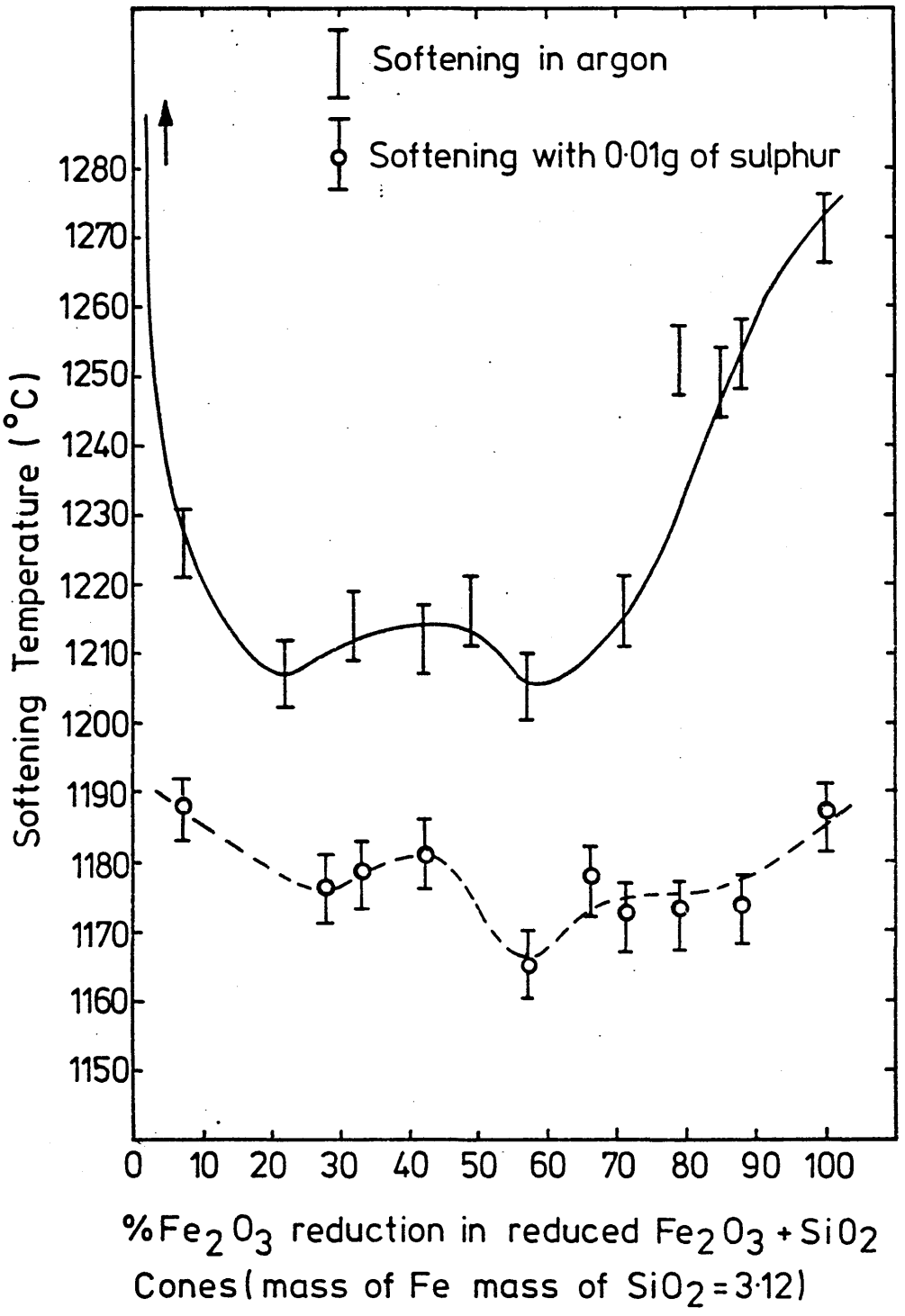

FIG. 5-3 Softening temperature against degree of reduction in cones made from partially reduced $Fe_2O_3+SiO_2$, in both argon and argon + sulphur inside the sealed silica tube

of reduction is 33%. Thereafter, the proportion of wustite will decrease as it is reduced to iron.

The above figures will only be approximate, since each oxide is not completely reduced in sequence but they will not be too much in error. The figures show that wustite is the principal iron containing component involved in the softening process, forming a liquid phase by reaction with the silica.

If we consider the cone reduced 22% and assume that all the silica and wustite it contains reacts to form a liquid phase, this liquid phase would contain 62% FeO. The SiO_2/FeO diagram in Figure 5-4 shows that this is the composition of the eutectic liquid that forms between silica and fayalite (2 FeO.SiO_2). The melting point of this liquid is about 1180°C which corresponds to the measured softening temperature of 1207°C. Similarly, the liquid in the cone reduced 71% will contain 64 mass % FeO, the softening temperature of this cone being 1216°C.

Between these two degrees of reduction, the proportion of FeO in the cone will increase and then decrease again. This will have the effect of moving the composition of the liquid formed towards the fayalite composition (71 mass % FeO) and then away from it again. The phase diagram in Figure 5-4 shows that this change in liquid composition would cause the melting temperature of the liquid to rise up towards 1205°C and then to fall. This change is reflected in the softening temperatures of the cones which rise and then fall again as

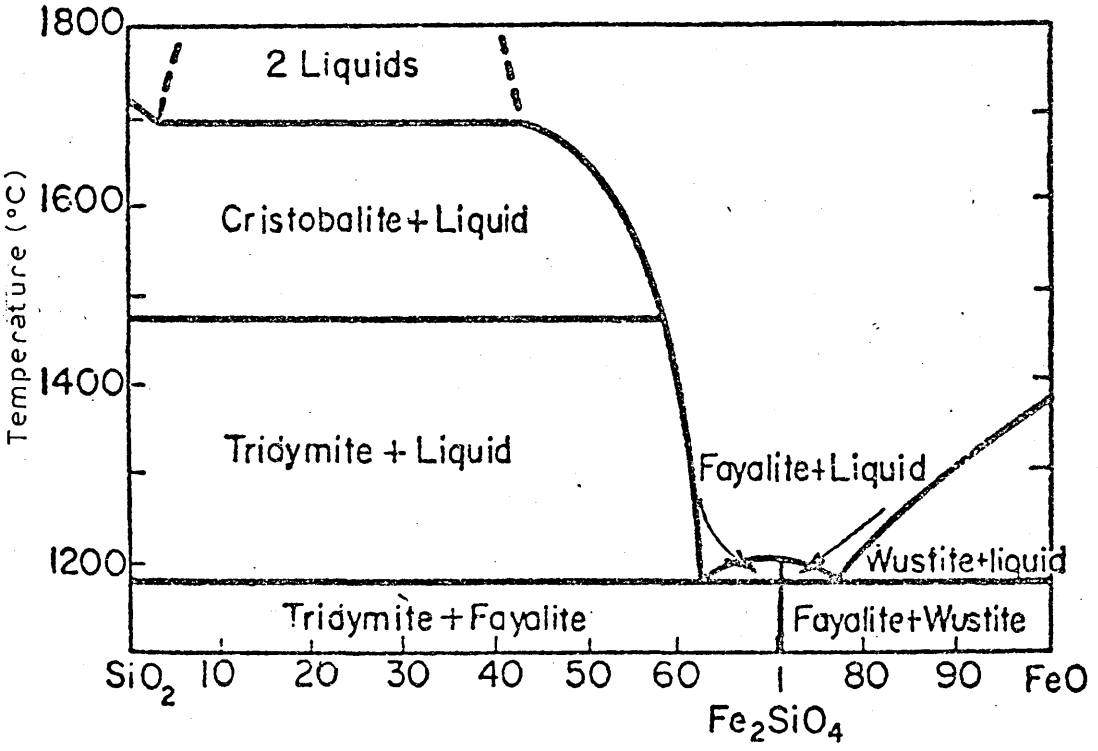

Figure 5-4: SiO_2-FeO phase diagram[14].

the degree of reduction increases from 20 to 70%.

The surprising thing about these figures is the very high mass fractions of liquid that these cones contain when they soften (see below) and the fact that the cones do not soften until their temperature is some 30°C above the melting temperature of that liquid.

Figure 5-5, taken from the work of P.Williams[62] carried out in these laboratories, shows that the viscosity of FeO/SiO_2 melts decreases very rapidly between 1190°C and 1220°C. It is apparent that the melt that forms within the cones is extremely viscous and large volumes of this viscous liquid must form before the cones will soften. Indeed the figure and the measured softening temperatures suggest that the cones containing about 50 mass % liquid will not soften in the experiments until the viscosity of the liquid has fallen to 1.5 Poise.

The important interaction between the viscosity of the liquid that forms and its mass fraction at the softening temperature is also to be seen in the results for degrees of reduction that lie outside the range 20 to 70%. The cone reduced 85.5% will contain 23 mass % SiO_2, 20 mass % FeO and 57 mass % Fe. Since there is an excess of silica in this cone, we can certainly assume that the liquid that forms in the cone will contain 60 mass % FeO and will incorporate all the available FeO. The mass fraction of this liquid in the cone will thus be 33 mass %. Its softening temperature

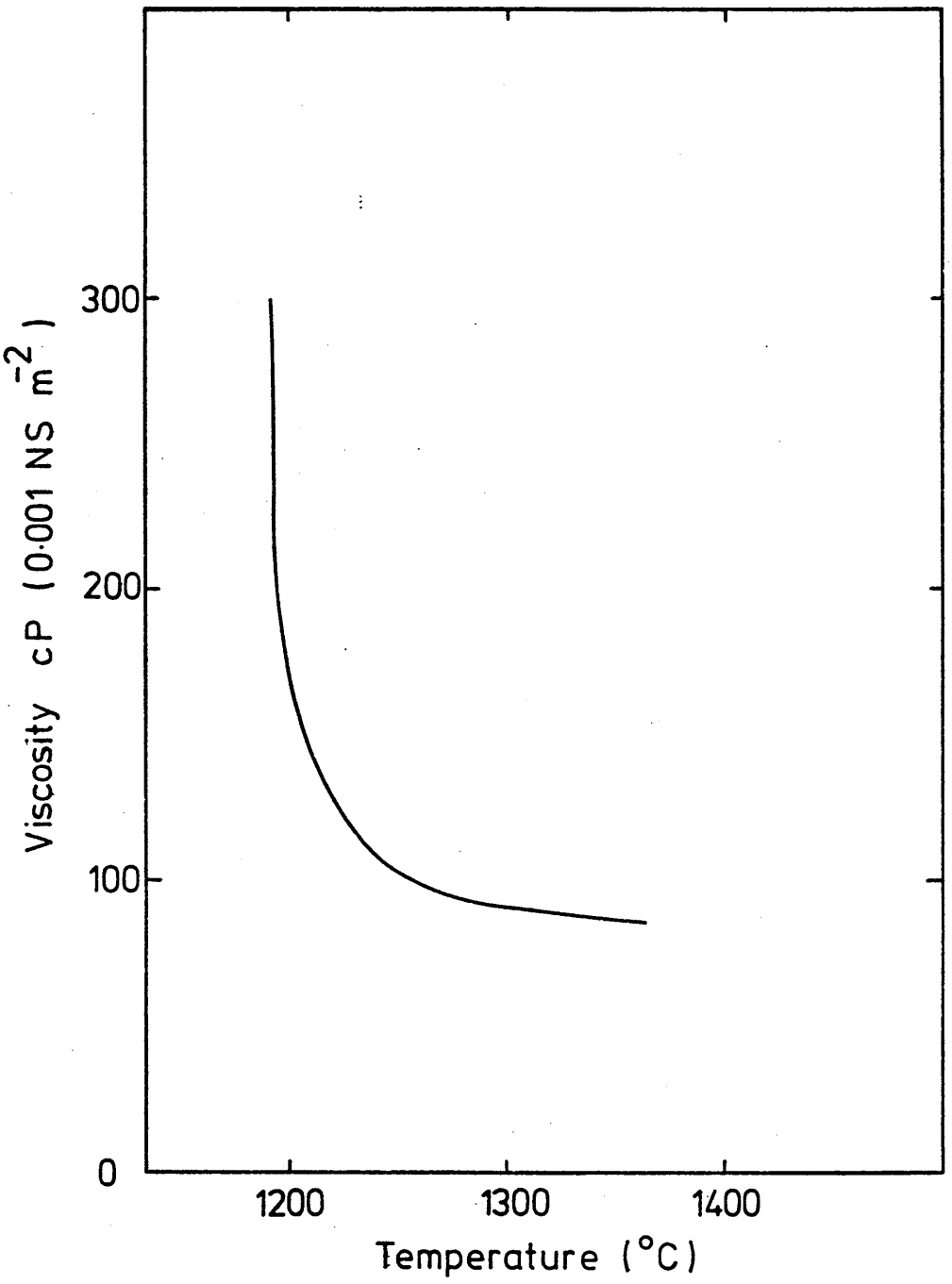

FIG.5-5 Variation with temperature of fayalite viscosity after P.Williams[62]

is 1249°C at which temperature the curve in figure 5-5 shows that the viscosity of the liquid to be 1.0 poise.

The cone reduced 7.3% is very much more difficult to analyse since it will contain FeO, Fe_3O_4 and Fe_2O_3 - its higher degree of oxidation moving the composition of the liquid away from FeO/SiO_2 boundary in the FeO/SiO_2/Fe_2O_3 ternary diagram shown in Figure 5-6.

Assuming that any magnetite that forms exists as a mixture of FeO and Fe_2O_3, we can calculate the composition of this cone to be 19 mass % SiO_2, 18 mass % FeO and 63 mass % Fe_2O_3. Since we have an excess of SiO_2 and Fe_2O_3, we can assume that the composition of the liquid that forms will lie within the eutectic valley running between the Tridymite and Magnetite phase areas. The softening temperature of this cone is 1226°C at which temperature the composition of the liquid will be represented by point $\bar{X}$ on Figure 5-6, that is 13 mass % Fe_2O_3; 51 mass % FeO and 36 mass % SiO_2. Thus the mass fraction of the liquid that forms is 37%. Figure 5-5 shows that viscosity of this liquid at the softening temperature is about 1.2 poise.

The effect of viscosity is further illustrated in the sterogram pictures shown in Plates 4-19 to 4-21 and Plates 4-22 to 4-24, on pages 149 to 151 and 152 to 154. Plate 4-19 shows a cone that has been reduced 33% and which therefore,

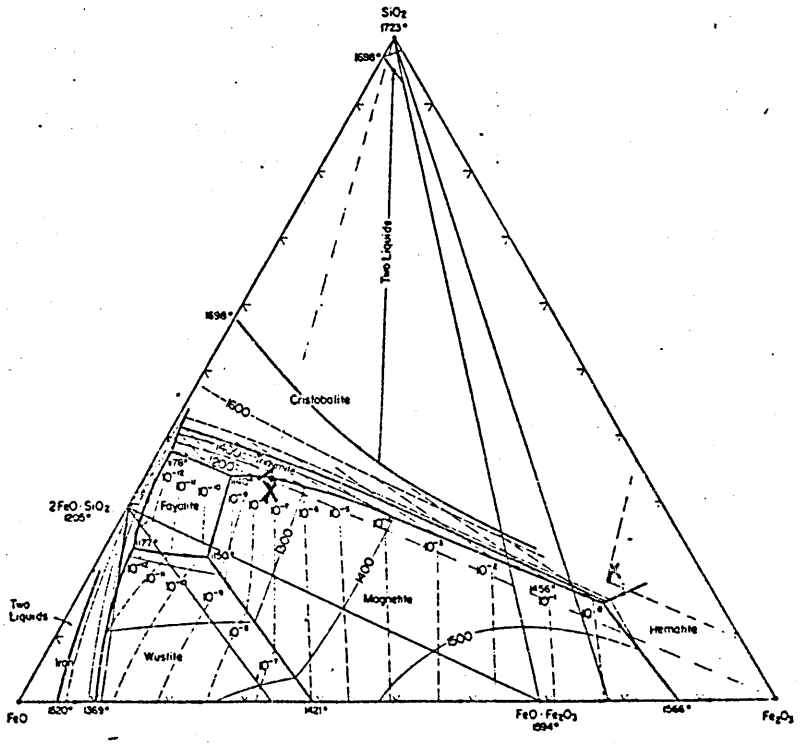

Plate 5-6: Liquid formation during the softening test of 7.3% reduced Fe_2O_3-SiO_2 Cone, $\frac{\text{Fe mass}}{SiO_2 \text{ mass}} = 3.12$, at 1226°C in a sealed silica tube. Point X represents the Cone composition while point $\bar{X}$ represents the liquid composition.

formed a large mass fraction of liquid but softened at 1214°C. The highly viscous nature of the liquid that formed caused it to exist as globules within the porous structure and did not allow it to flow over the surface of the iron particles. Thus the liquid solidified dendritically and left uncovered iron particles, as shown by the coincidence between plate 4-19 and the iron map shown in Plate 4-20. Plate 4-22 shows the cone reduced 85.5% which therefore, contained a lower mass fraction of liquid, but softened at 1249°C. The very much lower viscosity of the liquid allowed it to flow into the pores of the cone and then solidify with a smooth surface showing no evidence of dendrites, but exhibiting shrinkage cracks. The iron particles were then left standing proud of the liquid surface as can be seen by the coincidence between the (Si) and (Fe) maps shown in Plates 4-23 and 4-24 and the actual view of the outer surface of the cone shown in Plate 4-22.

Some inverse relationship is to be expected between the viscosity of the liquid that forms within the cone, and the mass fraction of liquid present at the softening temperature. The actual relationship that has been found from the results here is surprising. Table 5-1 shows that, for the three results presented here, the value of the viscosity divided by the mass fraction of liquid is approximately constant.

Table 5-1: The Relationship Between Viscosity and Mass Fraction of the Formed Liquid in Fe_2O_3/SiO_2 Cones at Softening Temperature

Softening Temperature ^oC	% Reduction	Viscosity (μ) at Softening Temp. (Poise)	Mass Fraction of Liquid (fL) at Softening Temp.	$\frac{\mu}{fL}$ (Poise)
1206	20	1.5	0.5	3.0
1226	7.3	1.2	0.37	3.08
1249	85.5	1.0	0.33	3.03

5.4 Effect of Sulphur Vapour on Fe_2O_3 Cones Reduced Varying Degrees

Table 4-12 on page 134 shows the results of the experiments in which cones of Fe_2O_3 reduced by varying degrees were heated in closed silica tubes in the presence of sulphur vapour. The results show that the cones did not soften although some liquid formed at temperatures in the range 1180°C to 1230°C. In most cases, this liquid flowed from the cones although sometimes it merely formed globules that remained on the surface. The strongest evidence for liquid formation coincided with intermediate degrees of reduction in the range 20 to 80%.

At first glance, it is surprising that these cones did not soften, and indeed, did not soften at lower temperatures. The FeO/FeS phase diagram illustrated in Figure 5-7 shows that the eutectic temperature in this system is 910°C, the eutectic liquid containing about 57% FeS. However, in order to ensure that the sulphur pressure developed inside the silica tubes would not rise to values that might cause the tubes to shatter, the mass of sulphur that they contained was limited to 0.01g. The mass fraction of sulphur in FeS is 0.36 so that its mass fraction in the eutectic liquid is 0.20. Thus the maximum mass of eutectic liquid that could form from the 0.01 g of sulphur that were present is 0.05 g. The total mass of the cones was about 0.5 g so that they could never contain more than 10 mass % liquid. That

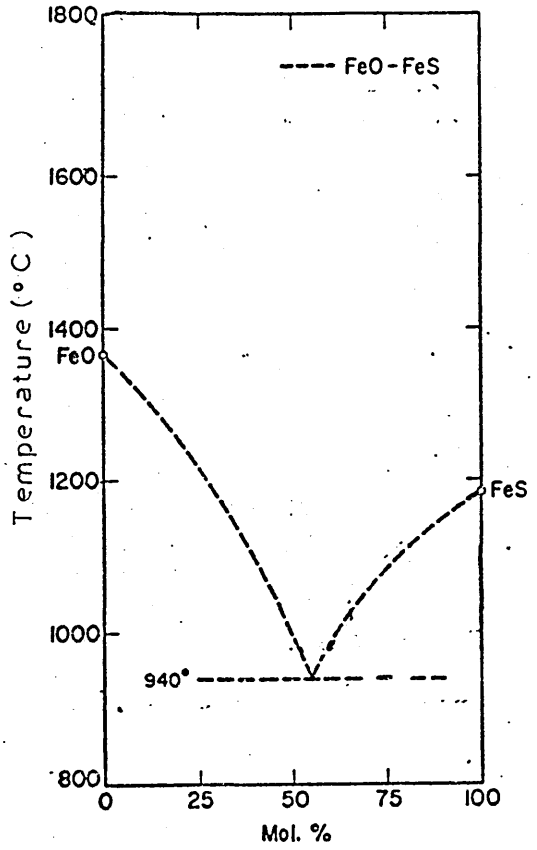

Figure 5-7: FeO-FeS phase diagram [67].

this is so is shown in Plate 4-16, on page 140, which shows the FeS formed on the surface of an Fe_2O_3 cone reduced 78.7% and heated to 1188°C in a sealed silica tube with 0.01 g of sulphur. The iron sulphide appears as a light grey constituent and represents some 8% of area that was not porosity.

Mattes such as liquid FeS have very low viscosities, about the same as liquid metals[60], so that the eutectic liquid that would form at 910°C would initially flow by capillary action to cover the entire surface of the pores within the cone. This is shown in Plate 4-17, on page 141, which is a strereoscan picture of one of these cones. The liquid has spread uniformly over the entire solid surface and the only visible evidence of its presence is the thin neck of liquid that can be seen between two of the iron grains.

Since the mass fraction of the liquid that forms at the eutectic temperature is no more than 10%, this liquid would be retained within the cones, would not cause them to soften and would not flow out.

At temperatures in the region of 1200°C, however, the phase diagram in Figure 5-7 shows that the liquid existing in contact with FeO contains some 25% FeS, the mass fraction of sulphur in this liquid therefore being 0.09. The mass of liquid that would form from the 0.01 g of sulphur present in the silica tube with the cone is thus 0.11 g representing some 22% of the mass of the cone. Whereas this mass fract-

ion of liquid is insufficient to soften the cone by destroying the bonds between the individual grains, it is greater than can be retained within the pores. Hence this liquid either flowed from the cones or formed globules on the outer surface.

The FeO/FeS liquid on which the above calculations have been based can only form in the presence of excess FeO. As the cones are reduced to values above 80%, the amount of FeO decreases. The liquid that forms under these conditions, therefore, contains less FeO and therefore, a higher mass fraction of sulphur. The mass of liquid that can form from the sulphur that is available is thus reduced, as is its mass fraction in the cone. It is for this reason that the highly reduced cones show less and less evidence of liquid formation.

5.5 Effect of Sulphur Vapour on Fe_2O_3/SiO_2 Cones Reduced by Varying Degrees

The lower points and curve in Figure 5-3, on page 276 show the softening temperatures of cones of Fe_2O_3/SiO_2 reduced by varying degrees, the temperatures having been measured in the presence of sulphur vapour. The curve is similar to the curve for Fe_2O_3/SiO_2 cones heated in argon, but lies at temperatures some 30°C lower, thus showing that the presence of sulphur vapour can have a marked effect on the softening behaviour.

As discussed in section 5.4, a liquid containing iron sulphide can form in the presence of sulphur vapour but the amount of this liquid that formed in the experiments involving cones of reduced hematite was never sufficient to cause the cones to soften. Neither did the iron sulphide liquid itself cause the cones containing silica to soften, since the cones did not soften until they reached temperatures some 250°C above the iron-sulphide eutectic temperature. In fact, the cones softened more or less precisely at the liquidus temperature in the FeO/SiO_2 system.

The section of the $FeO/SiO_2/FeS$ phase diagram shown in Figure 5-8 shows that two liquids can exist at these temperatures. One liquid lies close to the FeO/SiO_2 boundary and can conveniently be termed a slag whereas the other liquid lies close to the FeO/FeS boundary and is basically a matte. The existence of this two liquid region is shown on the diagram but the composition tie lines are not indicated. O.L.Shanskii[65] reports that the melt that is present in the FeO-FeS-Fayalite system at temperatures in the region of 1000°C contains more FeO than the melt that forms in the FeO-FeS binary system. In the work carried out here, silica is in excess, so that the compositions of the liquids that form will lie on the right hand side of the eutectic valley that runs from the FeO/FeS eutectic to the Fe/SiO_2 eutectics involving fayalite. Judging by the indicated temperature contours in the phase diagram in Figure 5-8 the composition of the liquid matte in equilibrium with the slag that forms

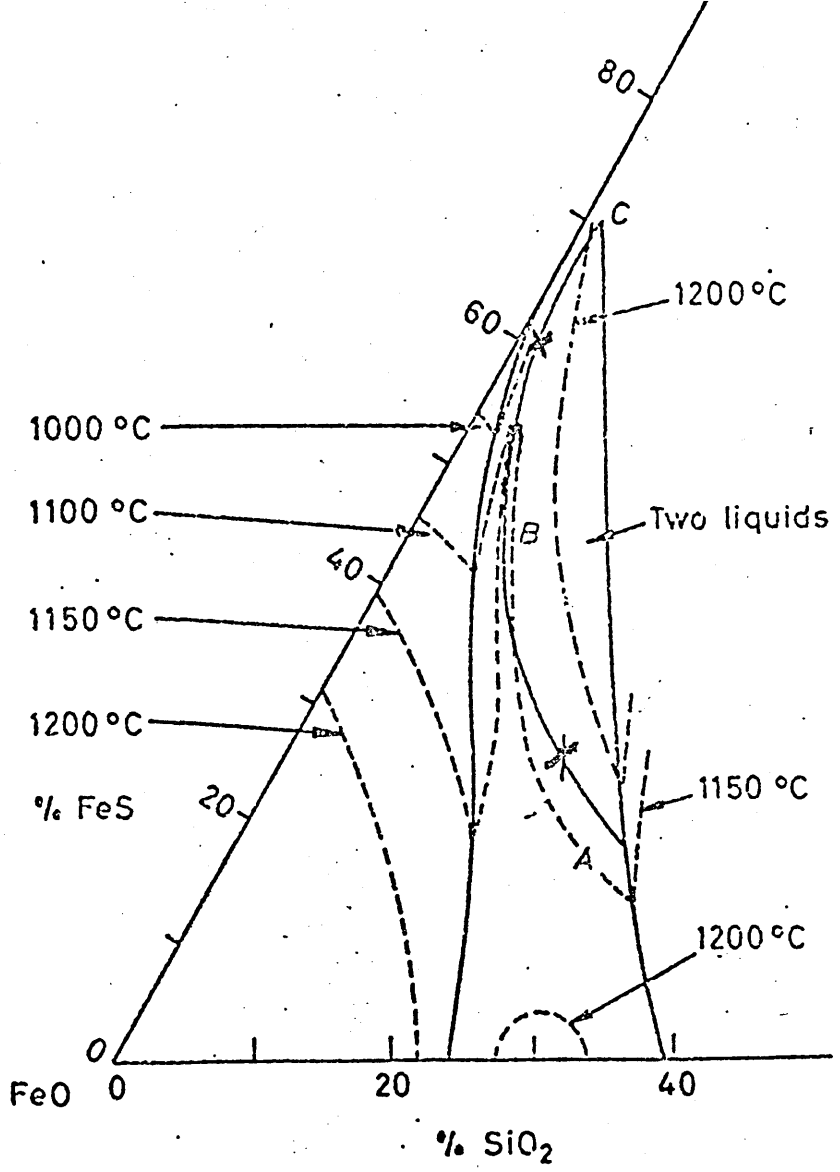

Figure 5-8: Partial liquidus diagram for system FeS-FeO-SiO_2 (after Hills[13]).

at the lower end of the conjugate surface will be represented approximately by point B. Thus we can assume the following approximate equilibrium compositions for the liquid matte and liquid slag that form in the cones at the softening temperatures:-

$$\left[f_{FeO}\right]_{SL} = 0.55 \quad ; \quad \left[f_{FeS}\right]_{SL} = 0.17 \quad ; \quad \left[f_{SiO_2}\right]_{SL} = 0.28$$

$$\left[f_{FeO}\right]_{m} = 0.48 \quad ; \quad \left[f_{FeS}\right]_{m} = 0.44 \quad ; \quad \left[f_{SiO_2}\right]_{m} = 0.08$$

These compositions can be used to calculate the mass fractions of the two liquids that are present in the cones from suitable mass balances on the constituents in the liquids. The constituents that are to be used are those that are in short supply because only for those constituents can their total masses in the liquid phases be known, the amounts of the two liquids formed at equilibrium being such as to dissolve all of these constituents. For low degrees of reduction, the two constituents are sulphur and iron and for high degrees of reduction they are sulphur and oxygen.

Calculations outlined in the Appendix 1 show that for cones reduced 7%, the equilibrium mass fractions of molten matte and molten slags are 7% and 14% respectively, and for cones reduced 85.5%, they are 3% and 26%.

The total volume of liquid in these cones when they soften is thus considerably less than the volume present in the SiO_2/Fe_2O_3 cones that softened in the absence of sulphur vapour. Furthermore, reference to the viscosity data shown in Figure 5-5 demonstrates that at the low softening temperatures found in the presence of sulphur vapour, the viscosity of the principal liquid constituent, the slag, is very much greater. It might thus appear surprising that these cones soften at the temperatures determined in this work. The reason for these lower softening temperatures is indicated, however, by the stereoscan plates shown in section 4.2.2(d).

Plate 4-25, on page 156, shows that a thin network of liquid forms in the cone, and the corresponding sulphur distribution map (plate 4-26) shows this liquid to contain a high concentration of sulphur. Similarly the silicon distribution map in Plate 4-28, on page 159, shows that this network does not contain silicon but surrounds liquid regions that do. The iron distribution map, Plate 4-27, on page 158, shows that iron is present in both liquids and its coincidence with the silicon distribution map indicates the presence of solid particles of silica, supporting the assumption made earlier that silica is present in excess in these cones. Similar picture emerges from the steographic plates obtained for other cones reduced differing degrees and heated in the presence of sulphur, Plates 4-29 to 4-39, on pages 160 to 171.

It appears that the molten matte that forms in these cones together with the highly viscous fayalite slag forms as a thin film around the solid particles. Since the viscosity of the matte is so much lower than the viscosity of the slag, this thin layer of matte acts as a lubricant allowing the highly viscous slag to glide over the solid particles in the cone so that the cones soften and deform immediately the liquid slag is formed. In the absence of sulphur vapour, of course, the highly viscous slag, without the matte as a lubricant, will not cause the cone to soften until its temperature has been increased sufficiently to reduce the slag's viscosity and increase its volume sufficiently for the cone to deform.

That the matte forms as a thin film is confirmed by the work of Statnikov et al[63] in their study of pellet cracking. They report that molten ferrous sulphide forms a thin film that rapidly penetrates between the grains - exactly the behaviour suggested in this work. The films can penetrate very rapidly and Statnikov et al[63] report that the boundary of a 3 μm thick ferrous sulphide film can move across the pellet surface at speeds up to 0.4cm s^{-1}.

It might alternatively be thought possible for the sulphur vapour to affect the softening temperature by reducing the viscosity of the slag, but this appears an unlikely explanation. The British Standard for Harrison (Seger) cones[61] reports

that the softening temperature of the cones is affected by the presence of sulphur in the furnace gases, 0.35% SO_2 in the atmosphere raising the softening temperature of some cones by 35°C. This effect is due to the increase in the viscosity of the molten material in the cone produced by the absorption of sulphur.

Whereas the above mechanism for softening is compatible with the stereoscan plates, the calculated matte volumes are not. The stereoscan plates suggest much greater volumes of matte than indicated by the calculations carried out in appendix 1.

A number of factors could explain these differences. In the first place, the stereoscans are taken on the outer surface where the volume fractions of liquid would very likely be higher than average. Furthermore, it is apparent from the phase diagram in Figure 5-8 that the matte forms at a much lower temperature than the slag, so that it could take some time for the equilibrium mass fractions of the molten slag and matte to be established at the softening temperature. Finally, of course, the calculated mass fractions of liquid depend on the accuracy of the data presented in the phase diagram. This data could be in error, especially in so far as the amount of FeS that can be dissolved in the FeO/SiO_2 slag before the conjugate liquids form. The calculation of the amounts of matte present is particularly sensitive to this composition variable.

However, the work has shown that sulphur influences the softening behaviour of these simulated blast furnace materials, forming a matte which acts as a lubricant and allows the silica containing liquids to flow freely.

5.6 Softening of FeO Cones Containing 5 mass % $CaCO_3$ and 2 mass % K_2CO_3 and 10 mass % Silica in Argon and in a Mixture of Argon and Sulphur Vapour

The softening temperatures of cones made from wustite, with 10 mass % silica, 5 mass % $CaCO_3$ and 2 mass % K_2CO_3 were determined in argon and in argon containing sulphur vapour. The temperatures that were measured are shown in Tables 4-17 and 4-18, on page 182, and Plates 4-47 to 4-50 and 4-51 to 4-55, on page 184 to 187, 188 and 190 to 193 show stereoscan pictures of these cones and the distribution maps of the important elements.

The softening temperatures of these cones in argon was virtually the lowest recorded in this work 1055°C after a 15 minute holding time dropping to 1023°C after a 30 minute holding time. These temperatures are surprising especially since they are some 100°C below the softening temperatures of Fe_2O_3 cones 33% reduced (nominally pure FeO) containing 20 mass % silica and 2 mass % Na_2CO_3. At first sight it might appear that the lower softening temperatures are due to the calcium oxide. However, the potassium, calcium and silicon maps in Plates 4-48 to 50, on page 185, 186 and 187 clearly show that the potassium and silicon are combined together whereas the calcium is not combined with either of them. Moreover, the incidence of the potassium and calcium maps with the stereogram itself in Plate 4-47, on page 184, shows that the regions in which the potassium and

silicon are combined are also the regions in which liquid has appeared to form. The iron map has not been shown since it is virtually featureless, showing that iron is uniformly distributed throughout the entire specimen.

Thus it would appear that liquid that forms in these cones when they soften in argon contains FeO, SiO_2 and K_2O but not CaO, so that the lower softening temperatures obtained are not due to the influence of CaO.

A portion of the $FeO/SiO_2/K_2O$ phase diagram is shown in Figure 5-9. Since there is a predominance of FeO in these cones, the composition of the liquid that forms will lie in the eutectic valley that lies between the Wustite and Fayalite fields. Its composition at temperatures between 1000°C and 1100°C will be such as to contain some 30 mass % K_2O $2SiO_2$. Stoichiometry shows that the mass of K_2O 2 SiO_2 would be 1.62 times the mass of K_2CO_3 present, assuming all the K_2CO_3 reacts. Thus the mass of K_2O 2 SiO_2 in the liquid in the cone is some 3.24 of its total mass. This corresponds to a liquid mass fraction in the cone of about 11%.

This is very much lower than the mass fractions contained in the systems discussed previously. If the relationship between the viscosity and mass fractions of the liquid present at softening that was reported in section 5.3 also applies in this cone material, 11% liquid would correspond to a viscosity of about 0.33 poise. The possibility of a liquid of this viscosity being present is difficult to judge

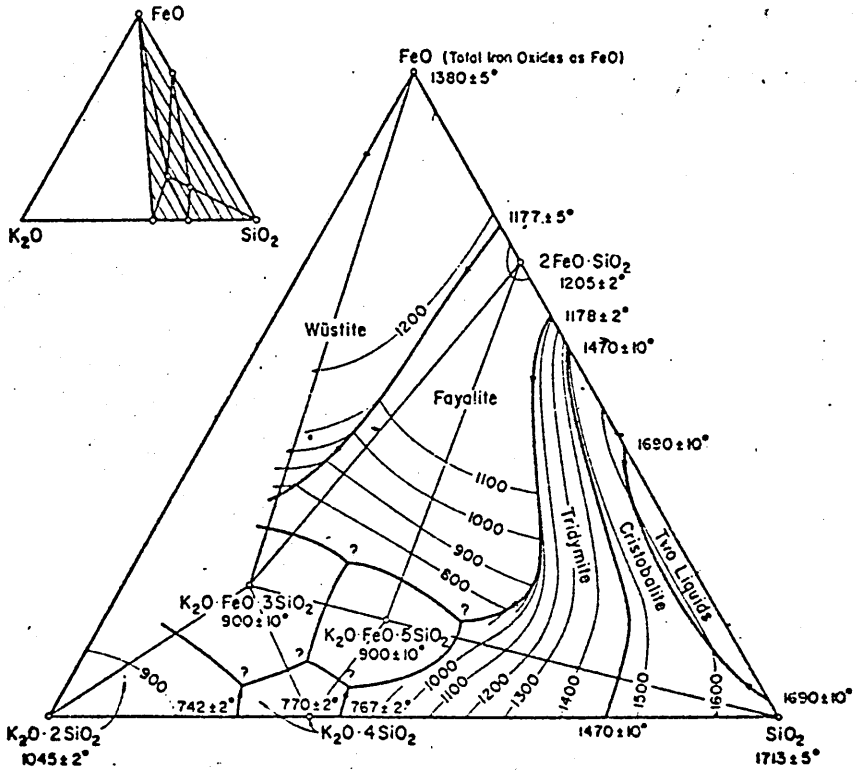

Figure 5-9: $FeO-SiO_2-K_2O$. Phase diagram[67].

because of the lack of data on the effect of alkali oxides on the viscosities of FeO/SiO_2 slags. However, the viscosity of SiO_2/K_2O liquids is very much lower, at the same mass fraction of alkali oxide, than the viscosity of SiO_2/Na_2O, so that it is plausible that the liquid's viscosity is as low as 0.33 poise.

Such a low viscosity would then explain why the liquid fraction is so low at the softening point and, also, why the softening point is lower than that measured for cones of other compositions.

The effect of sulphur vapour on the softening of these cones is most interesting since, as table 4-18, on page 182 shows, it raises the softening temperature some 100°C. A stereoscan picture of a cone that softened in sulphur vapour at 1151°C is shown in Plate 4-51, on page 188, and Plates 4-52 to 4-55, on pages 190 to 193, show the calcium, silicon, sulphur and potassium maps that correspond to this picture. In these plates, the silicon and calcium maps overlap with one another and with the areas in Plate 4-51, on page 188, in which evidence of liquid formation exists. The sulphur and potassium maps, on the other hand, do not overlap with those of silicon and calcium. This suggests that the presence of sulphur prohibits the formation of potassium silicate, presumably because potassium sulphide, sulphite or sulphate form.

The reaction of potassium oxide with the sulphur rather than with the silicate prohibits the formation of any $FeO/SiO_2/K_2O$ liquid. Thus the liquid that does form and thus softens the cone involves CaO, SiO_2, FeO and this liquid can only form at higher temperatures.

Figure 2-7(a), on page 33, shows the $CaO/SiO_2/FeO$ phase diagram. With an excess of FeO present in these cones, the composition of the liquid that forms will lie in the eutectic valley between the wustite and olivine fields. At 1150°C, this composition is about 4 mass % CaO, 26 mass % SiO_2, 70 mass % FeO. These cones contain 10 mass % silica so that, if all this silica were incorporated into the liquid, the mass fraction of liquid in the cone would be about 38%. This figure is closely comparable with the mass fractions of liquid at softening found in the cones containing FeO and SiO_2 only.

5.7 The Effect of Concentrations of Sodium Oxide on the Softening Behaviour of Fe_2O_3/SiO_2 Cones Reduced by Varying Degrees

Softening temperatures were measured for Fe_2O_3/SiO_2 cones reduced by varying degrees and then impregnated with different concentrations of sodium carbonate. As the calculations presented in appendix 2 show, the sodium carbonate decomposed at temperatures within the softening range to form sodium silicate. In effect, then, the measured softening temperatures indicate the influence exerted by sodium oxide on the softening behaviour of the cones.

Figure 5-10 shows how this effect varied with the degree of reduction for cones impregnated with 2 mass % Na_2CO_3, whereas Figure 5-11 shows how the softening temperature varied with the amount of sodium carbonate added for cones reduced by different degrees.

Figure 5-10 shows that the softening temperature of the cones reduced between 20 and 80% is lowered some 50 to 60°C by the addition of the sodium oxide that is produced when the 2 mass % Na_2CO_3 added to the cone decomposes. Figure 5-11 shows that the addition of greater amounts produces no significant further difference, although there appears to be an anomaly for higher degrees of reduction with additions of sodium carbonate round about 1.5 mass %.

The analysis of these results is extremely complicated. Not only can there be four oxides involved in the cones at the lower degrees of reduction - FeO, Fe_3O_4, SiO_2 and Na_2O, but the CO_2 liberated by the decomposition of the carbonate will cause some reoxidation to take place. It is thus somewhat complicated to calculate the composition of liquid phases that exist in the cones.

Stoichiometry shows that the mass of Na_2O introduced into the cones is 0.58 of the mass of Na_2CO_3 that they contain. For cones reduced less than 33%, the reoxidation reaction brought about by the CO_2 can be written as:

$$3\ FeO + CO_2 = Fe_3O_4 + CO$$

For which, at the temperatures involved in the experiments, the equilibrium CO/CO_2 ratio is about 1/5. Thus some sixth

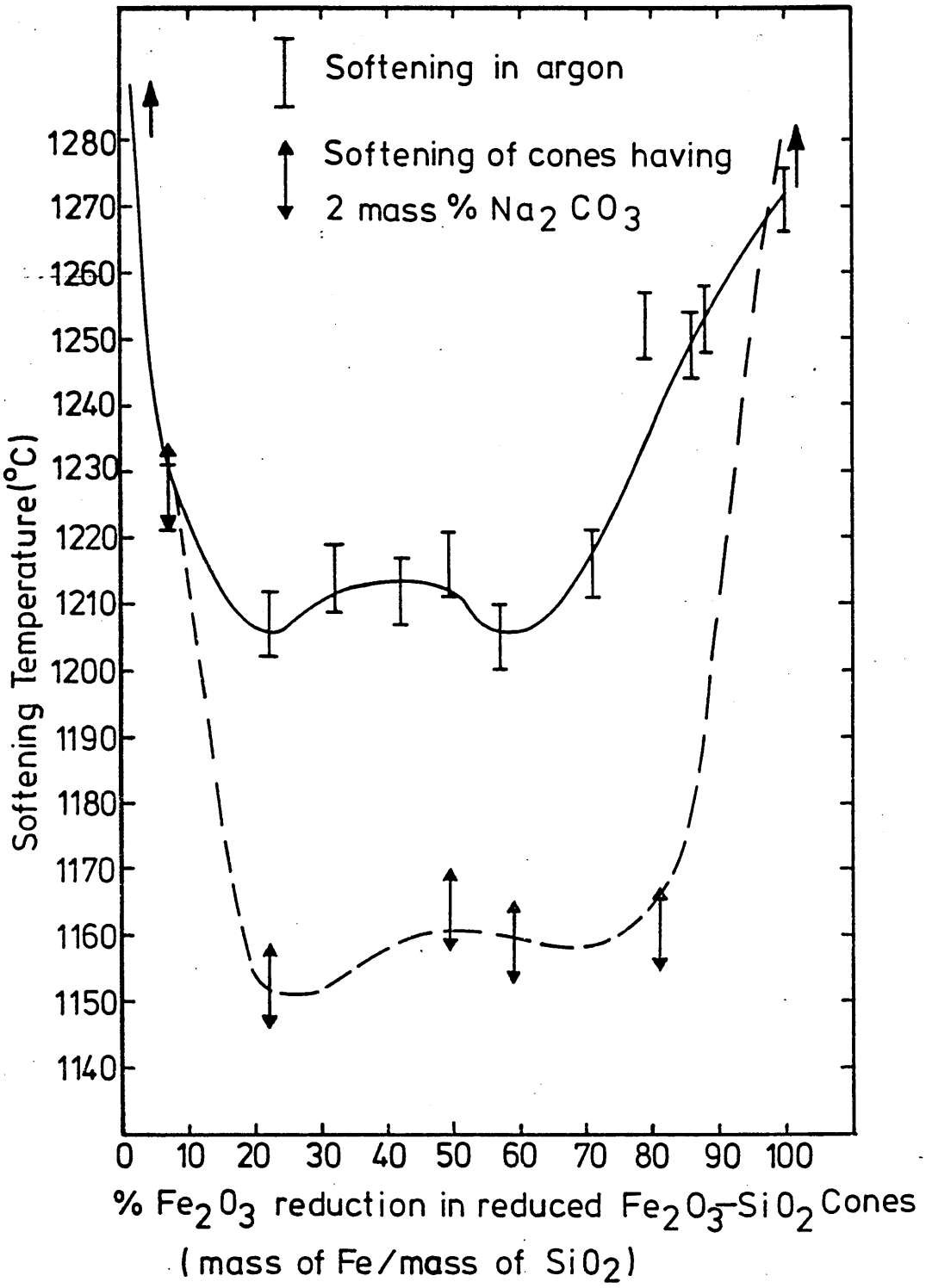

FIG. 5–10 Effect of enrichment-partially reduced Fe_2O_3 and SiO_2 cone with 2 mass % Na_2CO_3 on their softening temperature when tested under argon in sealed silica tubes.

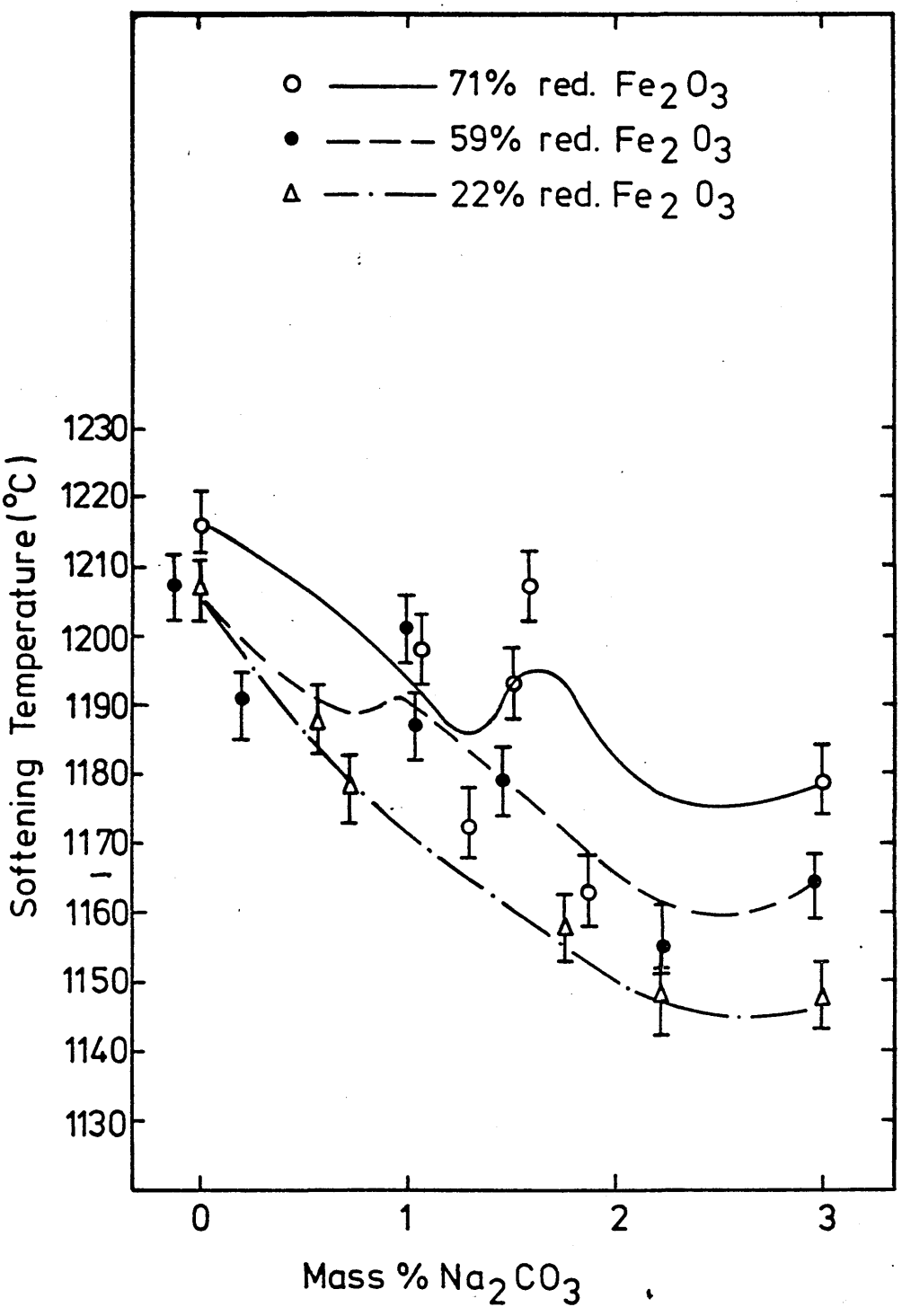

FIG. 5-11 The softening temperature of partially reduced $Fe_2O_3-SiO_2$ cones tested in sealed silica tube with different percentages of Na_2CO_3

of the CO_2 liberated by the decomposition of the carbonate will reoxidise FeO to Fe_3O_4. The ratio between the mass of FeO removed by the reoxidation and the mass of sodium carbonate added is thus 0.34.

However, for cones reduced a greater extent, the reoxidation reaction will be:

$$Fe + CO_2 \rightarrow FeO + CO$$

for which the equilibrium CO/CO_2 ratio is about 3/2 so that some 60% of the CO_2 liberated will be involved in reoxidation. In this case, however, the reoxidation will add FeO to the cone. The ratio of the mass of FeO added in this way to the mass of Na_2CO_3 added to the cone is thus 0.41.

The above stoichiometric considerations show the difficulties that are involved in calculating the composition and the amount of the liquid that is present in these cones. Since the results obtained for the Fe_2O_3/SiO_2 cones in the absence of any other species have indicated the important effect exerted by viscosity, interpretation of the results obtained in the presence of sodium oxide is further complicated by the absence of data on the effect the sodium oxide has on the viscosity of SiO_2/FeO slags. Na_2O lowers the viscosity of silicate glasses very considerably since it breaks up the long polymer chains that exist. However, this is just the mechanism that allows the FeO present in FeO/SiO_2 slags to lower their viscosity to values some two orders

of magnitude smaller than the values of silicate glasses containing up to 40% Na_2O. Alper[66] reports that, after large additions of Na_2O, further additions of Na_2O result in no further breaking of silica chains and thus have no further effect on the viscosity. It seems likely that the small additions of Na_2O to the molten phases existing in the cones will similarly have little effect on the viscosity of the phase since the FeO already there will have reduced the average chain length very considerably. Thus the effect of Na_2O will be considered to be principally exerted through its effects on the melting point of the slag and on the mass fraction of the liquid phase with the cone.

The $Fe_2O_3/SiO_2/Na_2O$ and $FeO/SiO_2/Na_2O$ phase diagrams[67] show that the addition of Na_2O will lower the melting point of the slags. As we have seen in Section 5.3.2, on page 275 the compositions of the liquid phases in the reduced Fe_2O_3/SiO_2 cones lies close to that of Fayalite so that the 2 FeO $SiO_2/Na_2O.2$ SiO_2 join in the $FeO/SiO_2/Na_2O$ ternary diagram, see Figure 5-12, is the most relevant section across the diagram. The slope of the liquidus line on this diagram is about -9^oC (mass % $Na_2O.2$ $SiO_2)^{-1}$. This corresponds to a slope of -26^oC (mass % $Na_2O)^{-1}$ if the diagram were plotted against the mass percentage of Na_2O. For a cone containing 50 mass % liquid, impregnated with 2 mass % Na_2CO_3, the mass fraction of Na_2O in the cone would be 1.16% and in the liquid phase 2.3%. This would correspond to a drop in liquidus temperature, as shown by

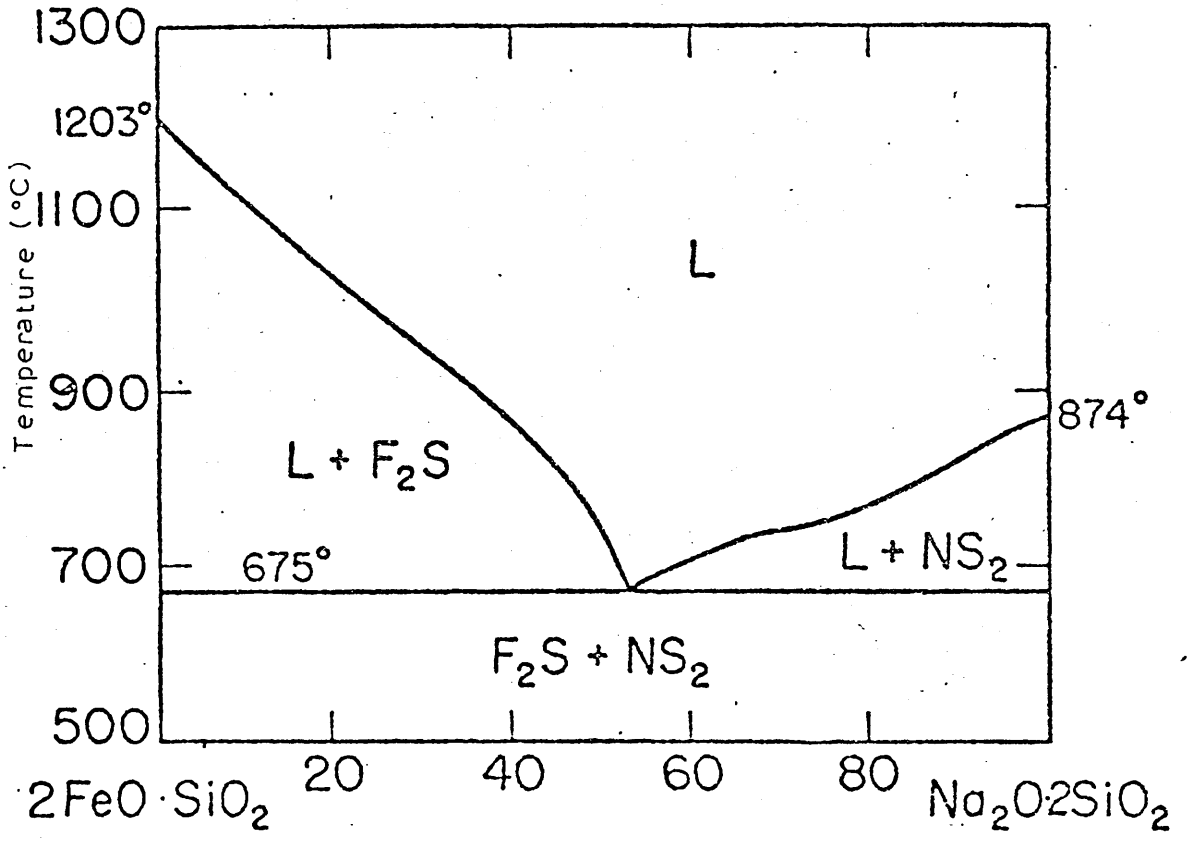

Figure 5-12: $2FeO\ SiO_2$-$Na_2O\ 2SiO_2$ Phase diagram[67].

Figure 5-12 of 60°C. Figure 5-10 shows that this is almost precisely the drop in softening temperature that has been obtained.

Similar drops in softening temperature have been obtained with 2 mass % added sodium carbonate for cones reduced by amounts up to about 90%. Thereafter the softening temperature rapidly rises to the figure obtained in the absence of sodium carbonate. This is only to be expected since the amount of FeO is diminishing rapidly, and there is a smaller and smaller volume fraction of oxide liquid to interact with the sodium oxide.

The effect of the sodium oxide addition at low degrees of reduction is less easy to understand. The results plotted in Figure 5-10 show that the cones made from silica and Fe_2O_3 reduced 7% soften at the same temperature whether or not they contain the added 2 mass % of Na_2CO_3. This is surprising because it means that some other phenomenon is occurring to compensate for the 60°C or so drop in melting temperature that the additional Na_2O would be expected to produce. The discussion in section 5.3.2 on page 275, shows that these cones contain the lowest concentrations of FeO. Thus the reoxidation of these cones by the CO_2 produced when the sodium carbonate decomposes would be expected to have its greatest proportionate effect. The removal of FeO from the liquid phase by reoxidation would reduce the total volume of liquid in the cone and would increase the proportion of the more refractory

Fe_2O_3 that they contain. Both these effects would be expected to increase the softening temperature although it is surprising that they are sufficient to compensate so completely for the effect of the sodium oxide.

It is possible, of course, for the softening temperature of the cone to be increased by some viscosity enhancement effect due to the reoxidation brought about by the CO_2 produced when the sodium carbonate decomposes. Toguri et al[68] have measured the viscosity of $FeO/Fe_2O_3/SiO_2$ slags and shown that their viscosity is relatively little effected by the degree of oxidation throughout the bulk of the composition ranges that they investigated. However, in certain ranges the viscosity does increase with degree of oxidation, and such an effect, were it to occur to the slag phase in the cone reduced 7% could further compensate for the effect that the sodium oxide has in reducing the melting point.

Figure 5-11 showing how the softening temperature changes with increasing additions of Na_2CO_3 for different degrees of reduction is even more difficult to explain since it contains the anomalous results for intermediate degrees of reduction with Na_2CO_3 additions of the order of 1-2 mass %. After an initial drop of softening temperature produced by the addition of 0.5 mass % Na_2CO_3 for all degrees of reduction, the softening temperature rises for cones reduced 59 and 71%. The softening temperature again falls for all

degrees of reduction by the time Na_2CO_3 additions greater than 2 mass % have been made. The reasons for this behaviour are not at all clear. It could be that some critical effect takes place between 1 and 2 mass % additions, perhaps with the reoxidation phenomena and the switch from the FeO/Fe_3O_4 equilibrium to the FeO/Fe equilibrium.

The scanning photomicrograph in Plate 4-61, on page 206, shows a cone treated in this range. The cone was reduced 71% and contained 1.9 mass % Na_2CO_3. Crystals in the form of long shaped needles can be seen whereas normal evidence of liquid formation is shown for all the other scanning photomicrographs in this series. The coincidence of the (Si) and (Na) maps, Plates 4-63 and 4-62 on pages 208 and 207, seems to suggest that the crystals contain sodium but not silica. The crystals are similar in form to crystals found by Komppa[69] on the surface of high alkali glasses after they had been weathered. He found that the crystals dissolved in water and contained sodium oxide but no silica, he concluded that they were sodium carbonate. If sodium carbonate tended to form or reform in these intermediate addition ranges, this would explain why the softening results are somewhat erratic in this range.

Plate 4-72, 73 and 74, on pages 219, 220 and 221, show the cone of material reduced 71% which contained 1.6 mass % Na_2CO_3 and softened at 1204°C. Plate 4-72 shows that extensive areas of the outer surface are covered with liquid that has formed, and a spot analysis of this liquid shows its

Fe/Si ratio to be very close to that of fayalite but that the liquid also contains a small amount of sodium. The high magnification plate, Plate 4-73, on page 220, seems to show one or two craters of the type that might be left by gas bubbles escaping from a highly viscous liquid. This offers a possible explanation for the anomalous results since the existance of gas bubbles within the liquid produced by the decomposing sodium carbonate would clearly cause erratic softening behaviour.

It is interesting to note that Bleifuss[65] in his investigation of the swelling and collapse of pellets during reduction under load also reports anomalous effects produced by Na_2CO_3 additions in the range 1 to 2 mass %. These additions caused the pellets to swell and not to collapse at all, whereas the addition of Na_2CO_3 of 0.5 mass % and the addition of any mass percent up to 2% of NaCl, KCl and K_2CO_3 always caused the pellets to collapse even if an initial swelling occurred. The experiments were carried out at 1000°C under a load and thus would be comparable to the experiments carried out in this work at a higher temperature but without an applied load.

Similarly, Nekrasov et al[56] reported pellets containing from 0.64 to 0.99 mass % Na_2O or K_2O showed the best retention of strength during reduction.

Neither author attempts to advance an explanation.

5.8. Softening of Iron Ore Cones Reduced Different Degrees and Heated in Argon and in Argon and Sulphur Vapour

The softening test carried out on partially reduced iron ore cones in sealed silica tubes under an argon atmosphere showed softening temperature minima at 30-70% reduction, followed by a steep rise in softening temperature as the reduction progresses. Table 4-21, on page 224, and curve A in Figure 5-13 show how the softening temperature of these cones varies with the degree of reduction. The lowest softening temperature is 1122^{o}C and exists for degrees of reduction varying from 33% to 43%. If it is assumed, as before, that the reduction process removes oxygen completely from each of the iron oxides in sequence, 33% reduction corresponds to the ferrous constituent of the cone being entirely wustite. The mass fraction of wustite in the cone is thus a maximum at 33% reduction which explains why the minimum softening temperatures lie in the region of this degree of reduction. FeO is strongly fluxed by both the acid and basic constituents of the gangue in the iron ore. (As shown in Section 5.3, on page 274, softening occurs when a mass fraction of a liquid phase with appropriate viscosity is formed in the sample).

Table 3-2, on page 55, shows the chemical analysis of the iron ore used. The liquid phase in the sample will form from interaction between the gangue and the ferrous

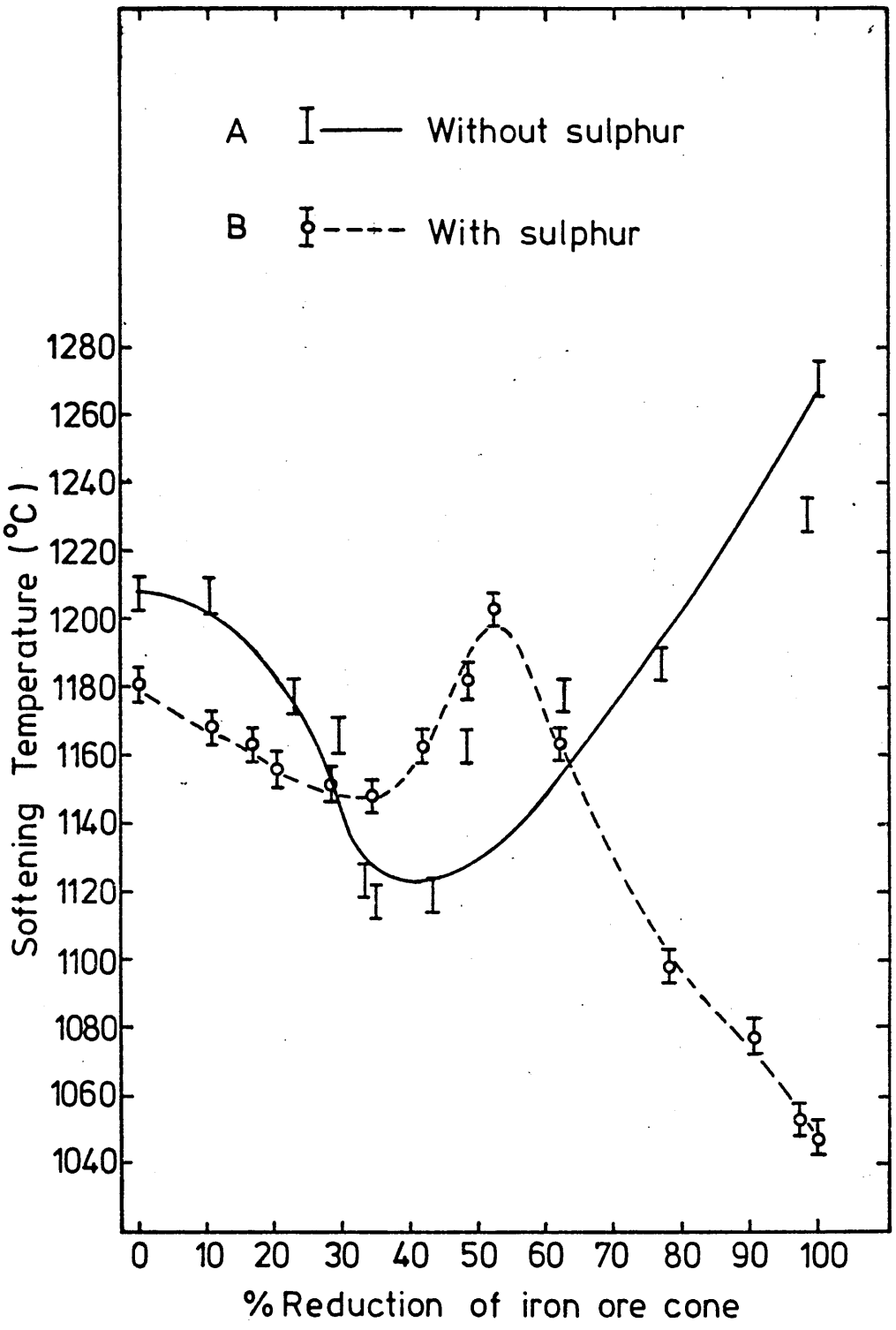

FIG.5-13 Softening temperature against degree of reduction of Bahira iron ore cone with and without sulphur inside sealed silica tube

constituents.

Examination of the composition of the iron ore suggests that the predominant liquid that will form will contain Al_2O_3, SiO_2, FeO and possibly some Na_2O. Figure 5-14 shows the phase diagram involving SiO_2, FeO and Na Al SiO_4 which will give some indication of the basic compositions of the liquids which will form. Since there is an excess of FeO in the cone, the composition of the liquid will lie in the eutectic valley running between wustite and fayalite. The composition of this liquid at 1123°C, the softening temperature of a cone reduced 33%, is 52 mass % FeO, 23 mass % SiO_2, 25 mass % Na Al SiO_4. If we assume that all Si O_2 is used up in forming this liquid, the mass fraction of the liquid present at softening can be calculated from the SiO_2 content of the tested cone. The calculated value is 0.22. This is somewhat lower than the mass fraction of liquid at softening when FeO and SiO_2 alone were involved, but it does lie in with the suggestion made in the previous section that the presence of alkali oxide can lower the viscosity of FeO/SiO_2 liquids and thus decrease the liquid mass fraction at which softening occurs. It must also be borne in mind that there are, several other constituents in the iron ore cone notably CaO, that could also be incorporated into the liquid phase, increasing its mass fraction further.

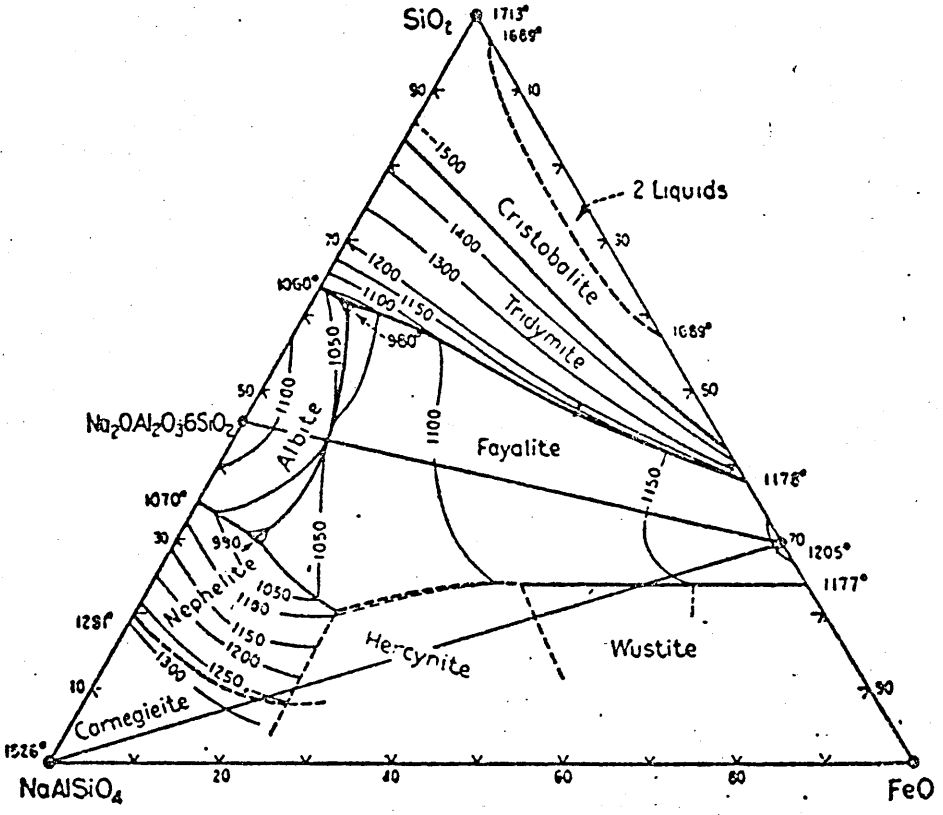

Figure 5-14: SiO_2-FeO-Na Al SiO_4 phase diagram[67].

The unreduced cones softened at about 1204°C which is lower than for unreduced material considered previously in this work. Once again, this softening process is brought about by the interaction of the gangue with the ferrous material, in this case in the form of Fe_2O_3. Figure 5-15 shows the phase diagram between Na_2O 4 SiO_2 and Fe_2O_3. As can be seen, the liquid that forms at 1200°C in this system in contact with Fe_2O_3 would contain some 33 mass % Fe_2O_3. Mass balances based on the amount of sodium oxide in the cone show that the mass fraction of this Na_2O 4 SiO_2/ Fe_2O_3 liquid would be about 5.5%. If we assume that the other constituents in the cone (FeO, Al_2O_3, MnO) also enter this liquid, we can calculate that its mass fraction will rise to about 16%, the composition of this liquid being Fe_2O_3: 11.25 mass %, FeO: 6.25 mass %, Na_2O: 4.6 mass %, SiO_2: 43.4 mass %, Al_2O_3: 11.06 mass % and MnO: 7 mass %, the balance being made up from the other minor gangue constituents.

The iron ore cone 100% reduced softened at 1271°C. Review of Table 3-2, on page 55, shows that the gangue will represent 21 mass % of this cone. In this cone MnO, CaO and Na_2O will work as strong fluxes for the SiO_2 and Al_2O_3. Mass balances based on the amount of Na_2O, CaO and MnO in the cone show the liquid that forms at 1271°C would contain some SiO_2: 46.7 mass %, Al_2O_3: 21.25 mass %, Na_2O: 4.5 mass %,

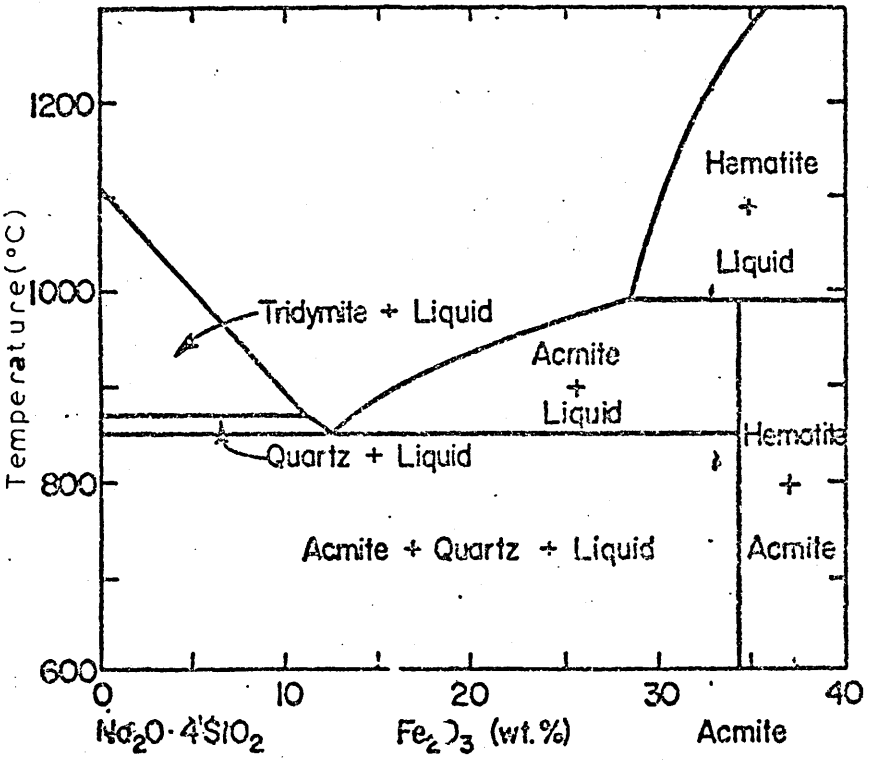

Figure 5-15: $Na_2O \cdot 4SiO_2$-Fe_2O_3 phase diagram[67].

CaO: 7 mass %, MnO: 7.5 mass %, its mass fraction being 0.2. This figure is about the same as the liquid mass fractions at softening for the other systems in which alkali oxides play an important role.

The influence of sulphur on the softening of these iron ore cones is extremely interesting since it gives rise to an increase in the softening temperature in the reduction range 33% to 60%, although it reduces the softening temperature outside this range.

Plate 4-86, on page 239, shows the unreduced cone for which a softening temperature of 1181°C was measured, and Plates 4-87 and 4-88, on pages 240 and 241 show the sulphur and silicon distributions determined for the field of view shown in Plate 4-86. It is apparent that a thin film of iron sulphide has permeated throughout the cone material separating the silica rich liquid regions in the manner observed when the influence of sulphur on the softening of Fe_2O_3/SiO_2 cones was studied. Once again, this highly mobile material will act as a lubricant and thus lower the softening temperature.

Plate 4-96, on page 251, shows a cone reduced 34% for which a softening temperature of 1148°C had been measured. There is no evidence in the figure that a thin continuous film of sulphide has formed. Plates 4-97, 98, 99, 101 and 102

on pages 252, 253, 254, 256 and 257 show, in sequence, the S, Si, Fe, Ca and Mn distributions in this cone and it is apparent that the sulphur has entered the slag phase and not reacted with the iron. The melting point of calcium sulphide is 2525°C[70] and that of manganese sulphide is 1530°C[71] Thus a slag phase containing high quantities of CaS and MnS would certainly be more viscous at about 1200°C than slag formed in the absence of sulphur, even if it might not be solid. The formation of a highly viscous or even semi-solid slag phase containing sulphur is further supported by Plate 4-103 on page 258 which shows a cone reduced 78% and "over softened" at 1130°C Plates 4-104 to 4-108, on pages 259 to 263, show in sequence, the sulphur, sodium, calcium, silicon and manganese distributions for this cone. Once again, it is apparent that the sulphur has reacted with the CaO, MnO and Na_2O to produce a particle which in the field shown by Plate 4-103, on page 258, appears not to have melted or, at least, to have melted only very slightly.

The reason why this hardening influence of sulphur vapour is only to be felt in the reduction range 30% to 65% can be seen from Table 5-2 which shows the equilibrium P_{S_2} / P_{O_2} ratios at 1200°C for the three relevant reactions of the type:-

$$MO + \tfrac{1}{2} S_2 \rightarrow MS + \tfrac{1}{2} O_2$$

TABLE 5-2 Relative Stability of the Oxides and the Sulphides in the Iron Ore Cone Tested at 1200°C for Softening in a Sealed Silica Tube

Reaction	$\frac{P_{S_2}}{P_{O_2}}$	P_{S_2} Atmosphere		
		with $\frac{Fe_2O_3}{Fe_3O_4}$	with $\frac{Fe_3O_4}{FeO}$	with $\frac{FeO}{Fe}$
$CaO + \frac{1}{2} S_2 = CaS + \frac{1}{2} O_2$	10^{+9}	10^{5}	10^{-1}	10^{-4}
$Na_2O + \frac{1}{2} S_2 = Na_2 S + \frac{1}{2} O_2$	10	10^{-3}	10^{-9}	10^{-12}
$MnO + \frac{1}{2} S_2 = MnS + \frac{1}{2} O_2$	10^{11}	10^{7}	10	10^{-2}

The table also shows the resulting sulphur pressures that would cause these reductions to be at equilibrium under the oxygen pressures at which the following iron reduction reactions would be at equilibrium:-

$3\ Fe_2O_3 \rightarrow 2\ Fe_3O_4 + \frac{1}{2}\ O_2$: $\left[P_{O_2}\right]_{eq,\ 1200^oC} = 10^{-4}$ Atm.

$Fe_3O_4 \rightarrow 3\ FeO + \frac{1}{2}\ O_2$: $\left[P_{O_2}\right]_{eq,\ 1200^oC} = 10^{-10}$ Atm.

$FeO \rightarrow Fe + \frac{1}{2}\ O_2$: $\left[P_{O_2}\right]_{eq,\ 1200^oC} = 10^{-13}$ Atm

The sulphur pressures in the table only apply for the oxides at unit activity, but they do show that the sulphur pressure developed in the sample tube, approximately 1 Atm., would be insufficient for CaS or MnS to form when the oxygen partial pressure in the tube was determined by the Fe_2O_3/Fe_3O_4 equilibrium. Under these conditions, it would be expected that FeS or the Fe/S/O ternary eutectic would form. However, when the oxygen partial pressure in the tube is reduced to values in equilibrium with the Fe_3O_4/FeO or FeO/Fe reactions, the sulphur pressure in the tube will exceed that for the formation of CaS and MnS and these sulphides will form in preference to iron sulphide because of their lower free energies of formation.

The formation of these sulphides would remove the oxides CaO and MnO from the cone which would not then be available to flux with the silica. If we assume the sulphur pressure in the tube to be about 1 atmosphere, we can see that the activity of CaO and MnO in the molten phase would need to be substantially below unity if these oxides were also to react with the sulphur vapour in the presence of the Fe_2O_3/Fe_3O_4 equilibrium oxygen pressure.

The situation with regard to sodium is not so clear. It is apparent from Plates 4-104, 105, 106 and 108, on pages 259, 260, 261 and 263, that the sodium has also reacted with the sulphur and is present together with the manganese, calcium and sulphur. Although no evidence of sodium concentration could be found in the other cones. This may be considered suprising in view of the equilibrium sulphur pressures shown in Table 5-2, which indicate an equlibrium sulphur pressure below the actual pressure in the tube at all degrees of reduction, and thus suggest that sulphur would react with the sodium oxide at all degrees of reduction.

This is not compatible with the role suggested for sodium oxide in the softening of cones in the absence of sulphur vapour or with the fact that sulphur lowers the softening temperature at low degrees of reduction. These factors

suggest that the sodium oxide will still react with silica at the higher oxygen potentials, although clearly not at the oxygen potentials in equilibrium with FeO/Fe. That this is likely to be the case can be seen if the equilibrium equation for the reaction between the oxide and sulphur vapour is written in the form:-

$$\frac{P_{S_2}}{P_{O_2}} = \left\{K_{eq} \quad \frac{a_{Na_2S}}{a_{Na_2O}}\right\}^2$$

Whence it can be seen that the reduction in the activity of Na_2O due to reaction with silica will increase the equilibrium sulphur pressure. No values have been found in the literature for the activity of Na_2O in silica melts, but the high degree of bonding known to occur between Na_2O and SiO_2, will certainly give rise to very low Na_2O activities in the presence of silica. A value of $\frac{a_{Na_2S}}{a_{Na_2O}}$ of 10^3 would be sufficient to rise to 10^3 atmosphere the sulphur pressure needed for sulphur to react with sodium oxide in the presence of the Fe_2O_3/Fe_3O_4 equilibrium, but would still allow this reaction to occur at higher degrees of reduction. A value of 10^3 for this ratio is certainly compatible with the known reactions between Na_2O and SiO_2. Indeed, the absence of any discernable concentration of sodium in the cone reduced 34%, where the Fe_3O_4/FeO equilibrium would be dominant, suggests the ratio might be of

the order of 10^4, and that little reaction between Na_2O and the sulphur vapour has occurred in this cone either.

Certainly sodium oxide reacts with silica more readily than with lime[72] and this fact will modify the sulphur pressures in Table 5-2 to allow the sodium oxide to interact with the sulphur vapour in a very similar way to calcium oxide.

However, these reactions do not absorb all the sulphur present so that, as the availability of iron increases after 50% reduction, greater and greater amounts of iron sulphide can form giving rise to the steep drop in softening temperature that occurs after 50% reduction.

Thus the influence of sulphur vapour on the softening of these Bahira iron ores is somewhat complex. At low degrees of reduction, iron sulphide is formed to act as a lubricant allowing the moderately viscous silica based slags of gangue constituents to flow more easily, thus lowering the softening temperature. At intermediate degrees of reduction, the low oxygen pressures present allow the sulphur vapour to form sulphides with the base gangue constituents, thus removing them as fluxes for the silica present. This gives rise to an increase in the softening temperature. At high degrees of reduction, the easy availability of iron allows iron sulphide to form, once again causing the softening temperature to drop very sharply.

5.9 Relevance of the Investigation to Blast Furnace Operation

The investigation has considered the influence of two specific volatile species, sulphur and alkalis, on the softening of actual and simulated blast furnace burden materials. This work is relevant to blast furnace practice because the softening process occurs in the blast furnace in regions where high concentrations of these volatile species can exist.

The burden softens after it has been reduced by about 70%[31, 9] in the temperature range 900°C to 1200°C[13,25,41,26]. Although a liquid phase may form within the burden at lower temperatures higher in the furnace, its low volume fraction and high viscosity will tend to reduce any effect it will have on the plasticity of the material. Thus the bulk of the softening process will take place in the isothermal zone in the furnace in regions where a relatively high concentration of the volatile species can exist. Appendix 3 shows that sulphur liberated from the coke by the solution loss reaction can increase the sulphur vapour pressure to 0.75×10^{-3} atmospheres, and the solution loss reaction too has been reported to be at its most intense round the 1100°C isotherm[74]. The high speed of the furnace gases could cause the sulphur liberated to be carried to higher levels in the furnace.

The existence of alkalis in this region of the furnace has been long reported and discussed in the literature.

In the experiments reported here, the alkalies have been provided by incorporating them into the simulated burden materials or by using an Egyptian iron ore with a very high alkali content. The presence of sulphur has been achieved by enclosing a small amount of sulphur in the silica tubes together with the cones of material investigated. Of course, it could be argued that the high pressure that this sulphur could generate in the atmosphere surrounding the cones (approximately 1 atmospheres at the temperature of investigation) produces conditions that are completely different from those existing in the furnace. However, the actual pressure of sulphur that could be developed in the cones in the absence of any reaction is of somewhat less importance than the actual mass fraction of sulphur incorporated within the cones by the reaction, especially in relation to a sulphur partial pressure in equilibrium with FeS of 10^{-7} atmospheres at 997°C[58].

As stated earlier, appendix 3 suggests that the solution loss reaction could liberate sufficient sulphur to produce a partial pressure of 0.75×10^{-3} atmospheres, where as Tsuchiya et al[46] suggests that the concentration of sulphur in blast furnace gases is $0.65 g/(m^3)_N$ - equivalent to a partial pressure of some 0.5×10^{-3} atmospheres. Both these

figures are significantly greater than the equilibrium partial pressure and, when the mass effect resulting from the large volume of furnace gases is borne in mind, it can be seen that the presence of sulphur in the silica tubes is not noticeably different from its presence in the blast furnace. This is further borne out by the final mass fraction of sulphur in the cones, 0.8%, which is of the same order as mass fraction reported in the softening zone by a number of workers, whose results will be discussed later. As a final point, the kinetic results reported in section 4.2.2 (c), on page 145, show that the full softening effect of sulphur in the cones is achieved in under 60 minutes - a time period that is of the same order as the 2 hour dwell time of blast furnace burden in the isothermal zone.

A number of workers have suggested that alkalies play an important role in the softening and melting processes that occur in the blast furnace. At first sight, it might appear that the present work supports this view but further analysis of the results suggests that alkalis do not play an important part.

The curves presented in Figure 5-11, on page 303, do show a decrease in softening temperature with increasing quantities of sodium carbonate incorporated into the Fe_2O_3/SiO_2 cones.

However, the greatest effect is obtained for the cones reduced 22 and 59% and a much smaller effect is observed for cones reduced 71% (the upper curve in figure 5-11).

Indeed, it is for this curve that the anomaly at about 1.5 mass % of alkali carbonate is most apparent. This anomaly causes a slight drop in softening temperature with carbonate percentage to be followed by a rise so that the softening temperature at 1.5 mass % is very close to the value obtained in the absence of alkali carbonate. The results obtained with completely reduced Fe_2O_3/SiO_2 cones, see Table 4-19, on page 195 , show that cones containing as much as 2.1 mass % sodium carbonate did not soften when heated to the upper limit of the experiments, 1270°C. This result is more or less duplicated by the result shown in Figure 5-13, on page 312, for the Egyptian iron ore. Even though this ore contains a high mass fraction of alkalis , its softening temperature increases as the degree of reduction exceeds 40% and temperatures of 1270°C and 1230°C are obtained for the fully reduced ore.

When those results are viewed in the light of the observation that softening occurs in the blast furnace after 70% reduction has been achieved, they suggest that alkalis play a relatively minor role in the softening process, and this is borne out by the results of recent investigations on

operating furnaces. Saski et al[31] investigated the softening region in a blast furnace after it had been water quenched. They reported the existence of icicles that formed in the later stages of softening and showed them to contain slag in which the alkali content was very low indeed, even though slag at lower levels in the furnace contained up to 2 mass % alkali. Jomato et al[73], furthermore, took samples directly from a blast furnace during the period it was shut down and found the softening material to contain no alkali although fully molten slag from lower down the furnace contained 2.11 mass % K_2O and 0.74 mass % Na_2O.

Rather than alkalis, the results of this work suggest that it is sulphur that plays the major role in the softening process. Once free iron is available in the cones liquid iron sulphide can be formed at temperatures above about 950°C. Even though the mass fraction of sulphur in the experimental cones is low, about 0.8 mass %, the iron sulphide can have a major effect since its low viscosity (less than 0.1 poise) and high penetrating power (see section 5.5) allow it to act as a lubricant. This effect is most clearly shown in Figure 5-3, on page 276, in which it is apparent that the lubricating effect of the small mass fraction of iron sulphide present allows the cones to soften immediately molten fayalite is formed. In the absence of iron sulphide, however, the cones must be heated some further 30°C before the viscosity of the fayalite has been reduced sufficiently for the cones to soften.

Once again, the results of recent investigations on operating furnaces bear out the importance of sulphur. Tsuchiya et al[46] reported a concentration of 0.5 mass % sulphur in the reduced charge just before melting, and Shimomura et al[41] reported a value of 0.3 mass % sulphur in what they termed the lumpy zone. Borts et al[39] observed an iron/oxygen/sulphur eutectic lining surface pores in sinter lumps taken from the softening zone of a quenched blast furnace. Jomato et al[73] took samples of softened materials from a blast furnace during a shut down period and observed that a thin film of molten iron containing 6.15 mass % FeO, 0.041 mass % S existed on the surface of the coke. They also found a slag like substance filling the voids in the coke which they divided for chemical analysis into magnetic, non-magnetic and tail fractions. The magnetic and non-magnetic fractions contained metallic iron: 56 and 41 mass % respectively, wustite 13 and 23 mass % respectively and sulphur: 0.136 and 0.185 mass % respectively. The tail fraction contained 58.05 mass % wustite 0.223 mass % sulphur, 10.82 mass % silica and 9.12 mass % lime. Thus there is a relatively high concentration of sulphur present in the softening zone and indeed, a number of other workers have shown that the sulphur content of the burden reaches its peak value just about the softening point. Many investigators have suggested[13,75,76,46,43,42] this peak value to be due to the recirculation of sulphur liberated when the coke is burnt in

the tuyere zone, and Hills[13] has suggested that this sulphur is involved in the first formation of a liquid phase in the furnace. The results obtained here with the Fe_2O_3/SiO_2 cones bear out this suggestion but do support Hills[13] melting model in which an initial Fe/O/S eutectic is formed and steadily increases in volume as the burden descends by dissolving FeO until the conjugate region is reached on the phase diagram at about 1350°C when distinct iron rich and oxide rich phases separate out. The presence of SiO_2 causes the oxide rich phase to form at a much lower temperature close to the melting point of fayalite. It is vapour borne sulphur, however, that causes these cones to melt immediately the fayalite is formed.

The vital importance of sulphur to the softening region of the blast furnace is further emphasised by the results obtained with the cones of $FeO/SiO_2/CaO/K_2O$ and of Egyptian iron ore. The former correspond to a degree of reduction 30% and an intermediate oxygen potential of about 10^{-13} atmospheres. In the absence of sulphur, these cones soften at 1055°C due to the formation of a $K_2O/SiO_2/FeO$ slag phase. In the presence of sulphur, however, these cones do not soften until 1149°C. This is because the sulphur, at the lower oxygen potential existing, will react with the potassium oxide to form potassium sulphide. The higher melting point of this potassium sulphide virtually

negates the contribution the potassium oxide otherwise makes to the formation of the liquid phase (the observed softening temperature of these cones in the presence of sulphur, 1149°C, is virtually the same as the melting point of fayalite in the presence of small amounts of lime.

Similar behaviour is shown in Figure 5-13, on page 312, for the Egyptian iron ore. Here the softening at intermediate degrees of reduction in the absence of sulphur is due to the formation of a complicated slag containing FeO/SiO_2/Al_2O_3/Na_2O/CaO/MnO. FeO plays an important role in this slag and it is for this region that the minimum softening temperatures in the absence of sulphur occur at a degree of reduction of about 30%. A similar minimum temperature occurs in the presence of sulphur but the lower oxygen potentials corresponding to further reduction cause the sulphur to combine with the calcium oxide, negating its contribution to the liquid slag. Thus the softening temperature rises some 50°C only to fall again as reduction proceeds and the sulphur can react directly with metallic iron to form the lubricating iron sulphide phase.

Undoubtedly, vapour borne sulphur plays a major role in the softening of the cones used in the work reported here, but it could be argued that the experimental conditions used are quite different from those experienced in the blast furnace. The volume fractions of liquid in the cones when they soften is certainly quite large, and the cones are subjected to no

more stress than is exerted by their own weight and by surface tension forces. As indicated in an earlier part of the discussion (section 5.2), some doubt must be expressed about the actual stress levels exerted on ore in the softening zone of actual furnaces, so that no conclusion can be drawn about the similarity of the stress levels existing in the experiments reported here or existing in the blast furnace. What can be said, however, is that the type of phases and compositions of phases found in this work are similar to those found in samples taken from the blast furnace bosh zone. It can also be said that, if the stress levels existing in the blast furnace are higher than those existing in the experiments, the importance of sulphur on softening could be more marked than indicated by the results. This is because the sulphide forms a low temperature liquid phase which has its most pronounced effect on the softening of the cones when other liquids have formed as well. At higher stress levels, the low volume of sulphide liquid formed could be expected to have a more immediate effect on the softening behaviour of the charge because a lower volume fraction of liquid would allow the cones to deform at these higher stress levels.

Thus the work reported in this thesis suggests that the presence of sulphur has an important role to play in the softening of blast furnace burden. Because the sulphur, at certain intermediate oxygen pressure levels, can combine with alkali metal or calcium to form refractory sulphides,

the presence of sulphur can lead to a rise in the softening temperature as well as to a fall. The initial softening and melting process in the blast furnace is thus dependent on the temperature distribution throughout the furnace, on the distribution of oxygen potential and on the distribution of sulphur. For example, material that softens at the bottom of the stack, where the oxygen potentials are high, by the formation of oxide liquids could harden again further down the furnace where the oxygen potentials are lower but where the presence of sulphur is more marked. Such a state of affairs could, for example, explain where high alkali ores are difficult to treat in the blast furnace.

The results attained here certainly suggest that a full understanding of melting and softening in the blast furnace requires a study of the behaviour of sulphur, and that softening tests on blast furnace burden materials should be carried out in the presence of sulphur vapour.

6. CONCLUSIONS

1- The composition of the gas phase in which softening tests are carried out on blast furnace burden materials must be considered, and should be maintained close to that existing in the softening zone of the blast furnace.

2- Vapour borne sulphur plays an important role in the softening process in the blast furnace.

3. Alkalis also play a role in the chemistry of softening in the blast furnace, but appear less important than sulphur. However, they may delay softening under low oxygen potential, or contribute to premature softening followed by hardening.

7. SUGGESTIONS FOR FURTHER WORK

The existing technique has shown that the mechanism of softening of blast furnace burden materials can be investigated using small samples heated with specific atmospheres in closed silica tubes. The technique that has been used is somewhat clumsy and a great improvement would result if the samples could be observed continuously at temperature. The construction of an apparatus that allowed this to be done would thus be a great advance in the technique that has been used.

The partial pressures of the volatile species investigated have varied during the experiments, but more information about the blast furnace process could be obtained if the experiments could be repeated under conditions of constant partial pressure. If a suitable technique could be developed and used together with continuous observation, for example some valuable data could be collected on the kinetics of the softening process.

The cones used in these experiments have contained fairly large volume fractions of liquid phase when they softened. Information about earlier stages in the softening process could be obtained if the technique could be modified to give an indication of softening at a lower volume fraction of liquid.

REFERENCES

1. S. Eketorp, The Future of the World's Steel Industry, ed. Julian Szekely, 1976.

2. A. S. Sarkisyants, Stal; 1937; 1.

3. B. I. Kitaev, Yu.G. Yaroshenko and V. D. Suchkov, Heat Exchange in Shaft Furnaces, Pergamon Press, ed. P. A. Young, 1967.

4. B. L. Lazarev et al, Stal; 1961; 3; pp. 162-167.

5. M. L. Lavrentev, Stal; 1969; 2.

6. A. Poos, Iron Making, AIME, 1973.

7. H. W. Meyer, H. F. Ramstad and W. H. Goodnow, Blast Furnace Theory and Practice, Gordon and Breach Science, ed. J. H. Strassburger, 1969.

8. P. Reichardt, Arch. Eisenhattenwesen, 1927, 1.

9. K. Kanbara et al, Trans. ISIJ; 1977; 7, 17; pp. 371.

10. B. V. Apasin, Stal 1968; pp. 383.

11. J. M. Girard, N. Jusseau and J. Michard, Proceeding ICSTIS; Suppl. Trans. JISI, 1971; 11.

12. V. I. Loginovita, Stal; 1969; 6.

13. A. W. D. Hills, In Process Engineering of Pyrometallurgy; London; IMM, 1974, pp. 81-93.

14. A. Maun and E. F. Osborn, Phase Equilibria Among Iron Oxides in Steel Making, Addison-Wesley Comp. Inc., 1965.

15. F. D. Richardson and J. H. E. Jeffes, JISI; 1949; 113; pp. 397-420.

16. A. Decker and R. Scimon,Metall. Rep. C.N.R.M.; 1967; 9, pp. 37-41.

17. N. Tsuchiya, M. Tokuda and M. Ohtani, Metall. Trans. B; 1976; 9, 7B; pp. 315-320.

18. H. A. Kortmann and O. P. Burghardt, Agglomeration, AIM, ed. K. V. S. Sastry, 1977.

19. O. P. Burghardt and K. Grebe, Stahl Eisen; 1969; 89; pp. 561-573.

20. P. Lecomte et al., C.N.R.M.; 1969; 9, (16).

21. M. NaKamura, U. Seki and S. Kondo, Trans. ISIJ; 1971; 11, pp. 331.

22. Yu. M. Potebnya et al.,Steel in the USSR; 1972; 3, pp. 176-178.

23. P. Lecomte et al, C.N.R.M. 1969; 12, (21).

24. L. M. Tsyien, Isves, Akod. Nauk SSSR. Otd. Teckh Nauk, 1948; 6, pp 889-898.

25. S. Pallella et al, Blast Furnace Aerodynamics, Austrialian Inst. Min. Met; 1975; pp. 75-85.

26. N. Nakamura, Y. Togino and M. Tateoka, Iron Making and Steel Making; 1978; 5, (1).

27. G. Winzer and K. H. Schmitz, Stahl und Eisen, 1967; 8, pp. 432-438.

28. V. D. Kanfer and V. N. Muravev, Steel in the USSR; 1974; 11, pp.864-868.

29. Yu. A. Orlov et al, Steel in the USSR; 1973; 4, pp. 268-273.

30. I. D. Balon et al, Steel in the USSR; 1973, 4, pp. 268-273.

31. M. Sasaki et al., Trans. ISIJ; 1977; 7, 17, pp. 391-399.

32. Z. I. Nekrasov and M. T. Buzoverya, Stal,1969; 2.

33. N. Luganin and I. G. Luganina, Izv. Vuz. Chern Met.; 1971; 6; pp. 43-45, BISI, 9665, 1971, 9.

34. V. N. Muravev et al., Stal, 1970; 10, pp. 768-771.

35. F. S. Manning, Blast Furnace Theory and Practice, Gordon and Breach Science, ed: J. H. Strassburger; 1969.

36. G. A. Volovik, Stal, 1961 11, pp. 794-797.

37. M. G. Benz and J. F. Elliot, Trans. AIME; 1961; 221, pp. 323-330.

38. V. L. Pokryshkin, "Byulleten", TSIINCHM, 1960, 20.

39. Yu. M. Borts et al., Stal; 1968; 6, pp. 462-465.

40. K.Kodama and S.Hashimato, Proceedings ICSTIS, Suppl. Trans. ISIJ, 1971; 11;pp.112-117.

41. Y.Shimomura et al., Trans ISIJ; 1977; 7; 17.

42. C.E.Grip et al., Scand. J. of Metall; 1976; 5; pp.229-247.

43. I.D.Balon, Steel in the USSR; 1975; 2; pp.65-69.

44. G.A.Volovik et al, Steel in the USSR; 1975; 10; pp.532-533.

45. K.Blomster, P.Taskinen and J.Mygrilic, Transaction C, 1977; 9; pp 147-152.

46. N.Tsuchiya,M.Ohtani and K.Okabe, JISIJ; 1973; 1; 59; pp.33-45.

47. E.T.Turkdogan and G.J.W.Kor, Met. Trans; 1971; 2; pp.1561-69.

48. G.J.W.Kor and E.T.Turkdogan, Met. Trans; 1971; 2; 1571-78.

49. T.Leonard and G.St.Pierrex, private communication from reference 51.

50. K.Hauffe and A.Rahmel, Zeit fur Physik Chemie; 1952;199; pp.1673-78.

51. S.McCormick, M.A.Dayanda and R.E.Grace, Met. Trans; 1975; 6B; pp.55-61.

52. H.Neuhaus et al., Arch Eisenhuttenw; 1966; 37, pp.1.

53. I.S.Kulikov, Desulphurization of Pig Iron, Metallurgizdat, 1962.

54. R.Vidal and A.Poos, Blast Furnace Technology, Marcel Dekker INC; New York, ed. Julian Szekely; 1972.

55. JANAF, Thermochemical Tables, 2nd edition, U.S. Government Printing Office, Washington D.C.,1971.

56. Z.I.Nekrasov, N.A.Gladkov and G.M.Drozdov, Steel in the USSR; 1976; 11; pp.973-979.

57. K.P.Abraham and L.T.Staffan, Scand. J. Metall; 1975; 4; 193.

58. C.L.McCobe, C.B.Alcock and R.G.Hudson, J. Metals; 1956; 5.

59. R.A.Meussner, L.E.Richards and C.T.Fujii, Naval Research Laboratory, Washington, D.C., 1965; 12; pp.26-28.

60. R. Schuhmann, Metallurgical Engineering, Vol. 1, Addison Wesley Publishing Company, 1952.

61. British Standard, B.S. 1041, Part 7, 1964, pp.4-9.

62. P. Williams, Sheffield City Polytechnic, Private communication.

63. B.Sh. Statnikov, Steel in the USSR; 1975; 3.

64. Ya. I. OL'shanskii, Doklady Akad. Nauk SSSR; 1948; 3; 59; pp. 513-516.

65. R. L. Bleifuss, Blast Furnace Technology, Marcel Dekker INC. New York, ed. Julian Szekely, 1972.

66. A. M. Alper, High Temperature Oxides, Part IV Refractory Glasses, 1970, pp.230.

67. E. M. Levin, C. R. Robbins and H. F. McMurdie, Phase Diagrams for Ceramists, The American Ceramic Soc., 1964.

68. J. M. Toguri, G. H. Kaiura and G. Marchant, Extractive Metallurgy of Copper, Vol. II, Pyrometallurgy and Electrolytic Refining, 1976, pp. 259-273.

69. V. Komppa, Glass Technology; 1978; 10; 19, (5); pp. 124-126.

70. R. P. Elliott, Constitution of Binary Alloys, McGraw - Hill Inc., 1965, pp.247.

71. J. F. Elliott and M. Gleiser, Thermo-Chemistry for Steel Making, AISI, Addison-Wesley, 1960, pp.248.

72. C.Jorgensen and I.Thorngreen, Thermodynamic Tables for Process Metallurgists, Almqvist Wiksell, Stockholm 1969.

73. Y.Jomoto et al., Nippon Steel Technical Report Over Seas No.1, 1972, 8, pp.8-15.

74. A.W.D.Hills, Physical Chemistry and Steelmaking, Versailles, France, 1978, 10, 3.

75. R.Jon et al., C.N.R.m., 1968; 6, (15).

76. J.J.Bosley, N.B.Melcher and M.M.Harris, J.Metals; 1959, 9, pp. 610-615.

APPENDIX I

Calculation of the Mass Fractions of the Two Liquids Present in the Reduced Fe_2O_3/SiO_2 Cones Heated with Sulphur

Let m^*_{SL} and m^*_m be, respectively, the mass fractions of the $FeO/SiO_2/FeS$ slag and the FeO/FeS matte and $\left[f_{FeO}\right]_{SL}$, $\left[f_{FeS}\right]_{SL}$, $\left[f_{SiO_2}\right]_{SL}$ and $\left[f_{FeO}\right]_m$, $\left[f_{FeS}\right]_m$ and $\left[f_{SiO_2}\right]_m$ the mass fractions of the specified species in these two liquids.

Thus the mass fractions of iron, sulphur and oxygen (other than that combined in the silica) in these two liquids are:-

(a) Slag:-

(i) iron:- $\frac{56}{72}\left[f_{FeO}\right]_{SL} + \frac{56}{88}\left[f_{FeS}\right]_{SL} = \left[f_{Fe}\right]_{SL}$

(ii) oxygen:- $\frac{16}{72}\left[f_{FeO}\right]_{SL} = \left[f_{O}\right]_{SL}$

(iii) sulphur:- $\frac{32}{88}\left[f_{FeS}\right]_{SL} = \left[f_{S}\right]_{SL}$

(b) Matte:

(i) iron:- $\frac{56}{72}\left[f_{FeO}\right]_m + \frac{56}{88}\left[f_{FeS}\right]_m = \left[f_{Fe}\right]_m$

(ii) oxygen:- $\frac{16}{72}\left[f_{FeO}\right]_m = \left[f_{O}\right]_m$

(iii) sulphur:- $\frac{32}{88}\left[f_{FeS}\right]_m = \left[f_{S}\right]_m$

The discussion in section 5.5 on page 288 suggests that:-

$$\left[{}^{f}_{FeO}\right]_{SL} = 0.55, \quad \left[f_{FeS}\right]_{SL} = 0.17; \quad \left[f_{SiO_2}\right]_{SL} = 0.28$$

and

$$\left[f_{FeO}\right]_{m} = 0.48; \quad \left[f_{FeS}\right]_{m} = 0.44; \quad \left[f_{SiO_2}\right]_{m} = 0.08$$

Thus we have:-

$$\left[f_{Fe}\right]_{SL} = 0.52; \quad \left[f_{O}\right]_{SL} = 0.14; \quad \left[f_{S}\right]_{SL} = 0.06$$

and

$$\left[f_{Fe}\right]_{m} = 0.65; \quad \left[f_{O}\right]_{m} = 0.11; \quad \left[f_{S}\right]_{m} = 0.16$$

The mass fractions of the iron, sulphur and oxygen in the cones actually in the liquid phases are thus:-

Iron:- $0.52\ m^{*}_{SL} + 0.65\ m^{*}_{m}$

Sulphur:- $0.06\ m^{*}_{SL} + 0.16\ m^{*}_{m}$

Oxygen:- $0.14\ m^{*}_{SL} + 0.11\ m^{*}_{m}$

The mass fractions of the liquid matte and the liquid slag that forms can thus be determined from mass balances on two of the above three elements. One suitable element throughout the reduction range is sulphur, iron being the second suitable element at low degrees of reduction and oxygen at high degrees of reduction.

(a) 7% reduction:-

Mass of sulphur = 0.01g

If the cone mass is taken as 0.5g , the overall mass fraction of sulphur in the cone is thus 0.02. Since all of this sulphur will be in the liquid phases, the sulphur balance gives:-

$$0.06 \quad m^*_{SL} + 0.16 \quad m^*_m = 0.02 \qquad \text{(A-1)}$$

The iron in the liquid comes from the FeO produced by reduction. The discussion in section 5.3.2. on page 275 shows the mass fraction of FeO to be 0.18 whence the mass fraction of iron will be $\frac{56}{72} \times 0.18 = 0.12$.

Thus the iron balance gives:-

$$0.52 \; m^*_{SL} + 0.65 \quad m^*_m = 0.12 \qquad \text{(A-2)}$$

Solving (A-1) and (A-2) as a pair of simultaneous equations gives:-

$$m^*_{SL} = 0.14; \quad m^*_m = 0.07 \qquad \text{(A-3)}$$

(b) 85.5% reduction

Mass of sulphur = 0.01g

If the cone mass is taken as 0.5g , the overall mass fraction of sulphur in the cone thus is 0.02. Since all of this sulphur will be in the liquid phases, the sulphur balance gives:-

$$0.06 \; m^*_{SL} + 0.16 \quad m^*_m = 0.02 \qquad \text{(A-1)}$$

The oxygen in the liquid (other than in the silica) comes from Fe_2O_3 reduction. The discussion in section 5.3.2. on page 275 shows the mass fraction of oxygen will be 0.04.

The oxygen balance:-

$$0.14\ m^*_{SL} + 0.11\ m^*_m = 0.04 \qquad \text{(A-4)}$$

Solving (A-1) and (A-4) as a pair of simultaneous equations gives:-

$$m^*_m = 0.03 \quad \text{and} \quad m^*_{SL} = 0.26 \qquad \text{(A-5)}$$

APPENDIX 2

The Behaviour of K_2CO_3 in the Container During the Softening Test Carried out on Fe_2O_3/SiO_2-Cones in the Sealed Silica Tube

Potassium carbonate may decompose according to the reaction:-

$$K_2CO_3 \rightarrow K_2O + CO_2 \qquad (1)$$

This may be considered in terms of

$$\tfrac{1}{2}\, O_2 + 2\, K \rightarrow K_2O \qquad (2)$$

$$O_2 + C \rightarrow CO_2 \qquad (3)$$

$$K_2CO_3 \rightarrow 2K + C + \tfrac{3}{2}\, O_2 \qquad (4)$$

At 1500^oK

$$\Delta G_2^o = -97298 \text{ Joules mol}^{-1}$$

$$\Delta G_3^o = -396342 \text{ Joules mol}^{-1}$$

$$\Delta G_4^o = +664151 \text{ Joules mol}^{-1}$$

As $\Delta G_1^o = \Delta G_2^o + \Delta G_3^o + \Delta G_4^o$

$\therefore \Delta G_1^o = 170511 \text{ Joules mol}^{-1}$

$\therefore \Delta G_1^o = - R\, T\, \text{Ln}\, K$

$$\therefore \log K = \frac{-170511}{2.3 \times 1500 \times 8.3114} = -5,944$$

$\therefore K \simeq 10^{-5}$

Again

$$K_2CO_3 \rightarrow K_2O + CO_2 \qquad (1)$$

$$K_1 = \frac{PCO_2 \,.\, {}^aK_2O}{a\, K_2\, CO_3}$$

If $a^*_{K_2O} = 1$ and $a^*_{K_2CO_3} = 1$

$\therefore P_{CO_2} = 10^{-5}$

The oxide resulted from the decomposition of K_2CO_3

From the Gas Laws:-

$PV = n\,RT$

For CO_2

$10^{-5} \times 20 = n \times 82.03 \times 1500$

Number of CO_2 moles $= 10^{-9} \times 1.63$

But $K_2CO_3 \rightarrow K_2O + CO_2$

So the number of moles of K_2O

$$= \frac{10^{-9} \times 1{,}16 \times 94}{44}$$

$$= 10^{-9} \times 3.5$$

But, above 881°C K_2O will decompose to K_2 vapour and O_2.

$\therefore$ The number of moles of $K_2 = 10^{-9} \times 3.5 \times \frac{78}{94}$

$$= 10^{-9} \times 3$$

The pressure of K_2 vapour inside the sealed silica tube when K_2CO_3 was present would be

$$P = n\frac{RT}{V} = 10^{-9} \times \frac{3.00 \times 82.03 \times 1500}{20}$$

$$\cong 0.2 \times 10^{-4} \text{ atmospheres}$$

---

*These values of the activities are not correct as the sodium carbonate and oxide will be in the molten state at 1500°K. Also the possible reaction between the cone constituents and the products of the K_2CO_3 decomposition may effect the equilibrium state of reaction 4). However, this calculation will give an approximate figure for the potassium partial pressure in the sealed silica tube during the test.

The Behaviour of Sodium Carbonates in the Fe_2O_3/SiO_2 Cones During the Softening Test

The stability of Na_2CO_3 with respect to the silica in the Fe_2O_3/SiO_2 cones can be calculated as follows.

The possible reaction is:-

$$Na_2CO_3 + SiO_2 \rightarrow Na_2SiO_3 + CO_2 \qquad (1)$$

This reaction can take place through the following steps:

$$4\ Na + 2\ SiO_2 + O_2 \rightarrow 2\ Na_2SiO_3 \qquad (2)$$

$$\frac{2}{3}\ Na_2CO_3 \rightarrow \frac{4}{3}\ Na + \frac{2}{3}\ C + O_2 \qquad (3)$$

$$C + O_2 \rightarrow CO_2 \qquad (4)$$

$$\therefore \Delta G_1^o = \tfrac{1}{2}\ \Delta G_2^o + \tfrac{3}{2}\ \Delta G_3^o + \Delta G_4^o$$

At 1300^oK

$$\Delta G_2^o = -962320 \text{ Joules mol}^{-1}$$

$$\Delta G_3^o = +543920 \text{ Joules mol}^{-1}$$

$$\Delta G_4^o = -393296 \text{ Joules mol}^{-1}$$

$$\therefore \Delta G_1^o = -58576 \text{ Joules mol}^{-1}$$

Which means reaction (1) will tend to move to the right resulting in the formation of sodium silicate, evolving CO_2 gas inside the sealed silica tube.

APPENDIX 3

Determination of Sulphur Vapour Pressure in Blast Furnace at 1000°C Isothermal Line

Consider as a base for calculation 1 kg of coke to burn in front of the tuyeres. It needs O_2 to burn completely to CO.

$$C + \tfrac{1}{2} O_2 \rightarrow CO$$

If carbon in coke = 0.88 kg

$\therefore$ O_2 required per 1 kg of coke = $0.88 \times \frac{16}{12} = 1.17$ kg.

N_2 in the blast equivalent to 1 kg coke = $1.17 \times \frac{76.8}{23.2} = 3.88$ kg

If we consider that at temperature level 1000°C the blast has 50 mass % N_2 and 50 mass % (CO + CO_2 + Minor vapour species).

$\therefore$ Per 1 kg of coke there will be 7.84 kg of blast.

According to Volovik[36], coke charges to the blast furnace with a sulphur content of 0.58 mass % will reach the tuyeres with a sulphur content of 0.33 mass %.

$\therefore$ The sulphur going to the vapour phase per kg of coke burn in front of the tuyeres = 0.58% - 0.33% = 25×10^{-4} kg.

But 30% of the charged coke in the blast furnace lost in solution reaction[74].

∴ 0.43 kg of coke will be consumed in solution loss reaction for every 1 kg of coke burn in front of the tuyeres.

The sulphur resulted from solution loss reaction:-

$$= \frac{0.43 \times 0.58}{100} = 0.25 \times 10^{-2} \text{ kg}$$

∴ The sulphur in the gas phase at 1000°C isotherm in blast furnace = $0.25 \times 10^{-2} + 0.25 \times 10^{-2} = 50 \times 10^{-4}$ kg

This blast at 1000°C will have 95 mass % CO, 5 mass % CO_2.

Mole of blast per kg of coke burnt in front of the tuyeres

$$= \frac{\text{Mass } N_2}{28} + \frac{\text{Mass CO}}{28} + \frac{\text{Mass } CO_2}{44}$$

$$= \frac{3.9}{28} + \frac{95 \times 3.9}{28 \times 100} + \frac{5 \times 3.9}{44 \times 100} = 0.276 \text{ kg mol (NTP)}$$

Concentration of sulphur in the blast =

$$\frac{50 \times 10^{-4}}{32} \times \frac{1}{0.276} = 5.74 \times 10^{-4}$$

For blast pressure 2.2 atmosphere and top pressure 1 atmosphere. The blast pressure at 1000°C isotherm will be 1000mm Hg.

∴ The sulphur vapour pressure at isotherm 1000°C will be

$= 5.7 \times 10^{-4} \times 1000 = 0.57$mm Hg which represent 0.8g of sulphur per m^3 of blast.

Although the above calculation of the value of sulphur vapour pressure in the blast furnace depends on tentative observations, it is in agreement with the value of 0.65g of sulphur per N m^3 given by Tsuchiya[46].